LEABHARLANN CHOLÁISTE NA TRÍONÓIDE, BAILE ÁTHA CLIATH | TRINITY COLLEGE LIBRARY DUBLIN
Ollscoil Átha Cliath | The University of Dublin

Terms and Conditions of Use of Digitised Theses from Trinity College Library Dublin

Copyright statement

All material supplied by Trinity College Library is protected by copyright (under the Copyright and Related Rights Act, 2000 as amended) and other relevant Intellectual Property Rights. By accessing and using a Digitised Thesis from Trinity College Library you acknowledge that all Intellectual Property Rights in any Works supplied are the sole and exclusive property of the copyright and/or other IPR holder. Specific copyright holders may not be explicitly identified. Use of materials from other sources within a thesis should not be construed as a claim over them.

A non-exclusive, non-transferable licence is hereby granted to those using or reproducing, in whole or in part, the material for valid purposes, providing the copyright owners are acknowledged using the normal conventions. Where specific permission to use material is required, this is identified and such permission must be sought from the copyright holder or agency cited.

Liability statement

By using a Digitised Thesis, I accept that Trinity College Dublin bears no legal responsibility for the accuracy, legality or comprehensiveness of materials contained within the thesis, and that Trinity College Dublin accepts no liability for indirect, consequential, or incidental, damages or losses arising from use of the thesis for whatever reason. Information located in a thesis may be subject to specific use constraints, details of which may not be explicitly described. It is the responsibility of potential and actual users to be aware of such constraints and to abide by them. By making use of material from a digitised thesis, you accept these copyright and disclaimer provisions. Where it is brought to the attention of Trinity College Library that there may be a breach of copyright or other restraint, it is the policy to withdraw or take down access to a thesis while the issue is being resolved.

Access Agreement

By using a Digitised Thesis from Trinity College Library you are bound by the following Terms & Conditions. Please read them carefully.

I have read and I understand the following statement: All material supplied via a Digitised Thesis from Trinity College Library is protected by copyright and other intellectual property rights, and duplication or sale of all or part of any of a thesis is not permitted, except that material may be duplicated by you for your research use or for educational purposes in electronic or print form providing the copyright owners are acknowledged using the normal conventions. You must obtain permission for any other use. Electronic or print copies may not be offered, whether for sale or otherwise to anyone. This copy has been supplied on the understanding that it is copyright material and that no quotation from the thesis may be published without proper acknowledgement.

The pharmacological effects of novel isosorbide-based butyrylcholinesterase inhibitors

Denise Khan M.Sc.

A thesis presented to the University of Dublin
for the degree of Doctor of Philosophy

School of Pharmacy and Pharmaceutical Sciences
Trinity College Dublin

January 2009

TRINITY COLLEGE
10 AUG 2009
LIBRARY DUBLIN
THESIS
8854

This thesis is dedicated to Hakim Muhammad Rafiq Khan and Akther Jehan Begum.

Declaration

I hereby certify that the work embodied in this thesis has not been submitted as an exercise for a degree at this or any other university. I also certify that the work embodied in this thesis is entirely my own work, except where duly acknowledged. I agree that the library may lend or copy this thesis upon request.

Denise Khan.

Denise Khan

Table of Contents

Dedication i

Declaration ii

Table of Contents iii

Table of Figures xi

Table of Tables xx

Abbreviations xxi

Acknowledgements xxv

Summary xxvi

Chapter 1 Introduction 1

1.1 Memory 1

1.1.1 General 1

1.1.1 Types of memory 1

1.1.2 Processing of memory 2

1.1.3 Memory and aging 9

1.2 Alzheimer's Disease 10

1.2.1 History 10

1.2.2 Pathophysiology 12

1.2.2.1 General 12

1.2.2.2 Amyloid Precursor Protein 13

1.2.2.3 Presenilins 16

1.2.2.4 Neurofibrillary tangles 18

1.2.3 Neurochemical changes 23

1.3 Animal Models of Alzheimer's Disease 28

1.4 Butyrylcholinesterase 31

1.4.1 Introduction 31

1.4.2 Molecular forms of BuChE 35

1.4.3 Functions of butyrylcholinesterase 37

1.4.3.1 Introduction 37

1.4.3.2 Distribution of BuChE 37

1.4.3.3 Embryology 39

1.4.3.4 Lipid metabolism 40

1.4.3.5 Genetic polymorphisms of BuChE 42
1.4.3.6 BuChE sequence homology 44
1.5 Drug Treatment in Alzheimer's Disease 45
1.5.1 General 45
1.5.2 Cholinergic precursors 45
1.5.3 Cholinesterase inhibitors 46
1.5.4 Glutaminergic antagonist 48
1.5.5 Anti-inflammatory drugs 49
1.5.6 Oestrogen therapy 49
1.6 Novel isosorbide-based butyrylcholinesterase inhibitors 50
1.7 Aims 53
Chapter 2 *In vitro* studies and behavioural profiling of novel BuChE inhibitors 54
2.1 Introduction 54
2.2 Determination of plasma BuChE activity in animal species 56
2.2.2 The Ellman assay 57
2.2.3 Results 59
2.3 Determination of IC_{50} of the novel compounds using the Ellman assay .. 60
2.3.1 Introduction 60
2.3.2 Preparation of plasma 60
2.3.3 The Ellman assay 60
2.3.4 Results of IC_{50} values 62
2.4 ADMET (Absorption, Distribution, Metabolism, Excretion, Toxicity) and Log P values 70
2.4.1 Introduction 70
2.4.2 Methods 71
2.4.3 Results 74
2.5 Behaviour following administration of novel compounds 73
2.5.1 Introduction 75
2.5.2 Animals 75
2.5.3 Drug preparation 76
2.5.4 Drug administration 77
2.5.5 Behavioural scoring 77
2.5.6 Results 79

2.6 Pharmacodynamic profile of the novel compounds 82
2.6.1 Introduction 82
2.6.2 Animals 82
2.6.3 Drug preparation 83
2.6.4 Drug Administration 83
2.6.5 Blood sampling 84
2.6.6 Isolation of tissue samples 85
2.6.7 Processing of tissues 86
2.6.8 Analysis of BuChE activity 86
2.6.9 Results 88
2.7 Pharmacokinetics 105
2.7.1 Introduction 105
2.7.2 Animals 105
2.7.3 Drug preparation 106
2.7.4 Drug Administration 106
2.7.5 Blood sampling 106
2.7.6 Isolation of tissues 107
2.7.7 Processing of tissues 107
2.7.8 HPLC analysis of drug concentration 107
2.8 Results 109
2.9 Diurnal variation in BuChE activity 109
2.8.1 Introduction 110
2.8.2 Animals 110
2.8.3 Blood sampling 110
2.8.4 Results 112
2.9 Discussion 113
2.9.1 Comparison of plasma BuChE between animal species 113
2.9.2 IC_{50} of the novel compounds using the Ellman assay 114
2.9.3 Behavioural profile of compounds following administration of novel compounds 116
2.9.4 ADMET (Absorption, Distribution, Metabolism, Excretion, Toxicity). 118
2.9.5 Pharmacodynamic profile of novel compounds 120
2.9.6 Pharmacokinetic profile of novel compounds 123
2.9.7 Diurnal variation 124

Chapter 3 Lesion-based model of Alzheimer's disease 125
3.1 Introduction 125
3.2 Animals 125
3.3 Preparation of drugs 126
3.3.1 Compound 51 126
3.3.2 Anaesthesia 126
3.3.3 Analgesia 126
3.3.4 Lesioning agent 127
3.4 Surgery 127
3.4.1 Preparation of animals 127
3.4.2 Injection procedure 128
3.4.3 Drug treatment 129
3.5 The Morris water maze 130
3.5.1 Introduction 130
3.5.2 Apparatus 131
3.5.3 Habituation 134
3.5.4 Training 134
3.5.5 Probe trial 135
3.6 Statistical analyses 135
3.7 Object recognition task 136
3.7.1 Introduction 136
3.7.2 Apparatus 136
3.7.3 Training 137
3.8 Statistical analyses 140
3.9 Verification of lesion 141
3.9.1 Processing of brain tissue 141
3.9.2 Preparation of slides 141
3.9.3 Sectioning of brain tissue 142
3.9.4 Preparation of cresyl violet stain 143
3.9.5 Staining of slides 143
3.9.6 Microscopic examination of slides 144
3.10 Results 145

3.10.1 Histology 145
3.10.2 Results: Morris water maze 148
3.10.3 Results: object recognition task 155
3.11 Discussion 158
3.11.1 Morris water maze 158
3.11.2 Object recognition 160
3.12 Conclusion 162
Chapter 4 Young and middle-aged mice in cognitive studies 163
4.1 Introduction 163
4.2 Animals 164
4.2.1 Comparison of one and two-year old animals 164
4.2.2 Comparison of young and aged animals 164
4.2.3 Housing of animals 165
4.3 Drug preparation 165
4.4 Drug treatment of young and aged animals 165
4.5 Analysis of BuChE activity in young and aged animals 166
4.5.1 Procurement of tissue samples 166
4.5.2 Processing of tissue samples 166
4.6 The Morris Water Maze 167
4.6.1 Habituation 167
4.6.4 Training 167
4.6.5 Probe trial 167
4.7 Statistical analyses 168
4.7.1 One and two year old mice 168
4.7.2 Young and aged mice 168
4.8 Object recognition task 169
4.8.1 Introduction 169
4.8.2 Training 169
4.9 Statistical analyses 170
4.9.1 One and two year old mice 170
4.9.2 Young and aged mice 170
4.10 The modified radial arm maze 171
4.10.1 Introduction 171

4.10.2 Animals 171
4.10.3 Drug preparation 172
4.10.4 Drug treatment 172
4.10.5 Apparatus 172
4.10.6 Training 174
4.11 Results 175
4.11.1 Morris water maze with one and two-year old animals 175
4.11.2 Morris water maze with young and middle-aged animals 181
4.11.3 Object recognition task with one and two-year old mice 191
4.11.4 Object recognition task with young and aged mice 194
4.11.5 Modified radial arm maze 197
4.12 Discussion 200
4.12.1 One and two-year old mice 200
4.12.2 Young and middle-aged mice 202
Chapter 5 Chronic drug treatment study 208
5.1 Introduction 208
5.2 Animals 208
5.3 Drug Treatment 209
5.4 Health monitoring 209
5.4 The Morris Water Maze 210
5.4.1 Habituation 210
5.4.2 Training 210
5.4.4 Probe trial 210
5.5 Object Recognition 211
5.5.1 Apparatus 211
5.5.3 Training 211
5.6 Statistical analyses 211
5.6.1 Morris water maze 211
5.6.2 Object recognition task 212
5.7 Results 213
5.7.1 Morris water maze 213
5.7.2 Object recognition task 222
5.8 Discussion 225

5.8.1 Morris water maze 225
5.8.2 Object recognition task 227
5.9 Conclusion 229
Chapter 6 Toxicology and histology 230
6.1 Introduction 230
6.2 Animals 231
6.3 Drug preparation 231
6.3.1 One-day toxicology study 231
6.3.2 One-year toxicology study 231
6.3.3 Histology study 231
6.4 Drug treatment 232
6.4.1 One-day toxicology study 232
6.4.2 One-year toxicology study 232
6.4.3 Histology study 232
6.5 Isolation and preparation of tissue samples 233
6.5.1 Toxicology studies 233
6.5.2 Histology study 234
6.7 Results 236
6.7.1 One-day toxicology study 236
6.7.2 One-year toxicology study 239
6.8 Discussion 245
Chapter 7 Stability of Novel Compounds *in vitro* 247
7.1 Aims 247
7.2 Procurement of blood 247
7.2.1 Mouse blood 247
7.2.2 Human blood 248
7.3 Sample preparation 248
7.3.1 Phosphate buffered saline 248
7.3.2 Zinc sulphate 248
7.3.3 Drug standards 248
7.3.4 Plasma samples 249
7.3.5 Mouse liver samples 249
7.3.6 Human liver microsomes 249

7.3.7 Human intestinal microsomes 249
7.3.8 BuChE activity 250
7.4 Hydrolysis of compounds 250
7.4.1 Plasma/liver and novel compound 250
7.4.2 Plasma/ liver /BNPP & novel compound 251
7.4.3 Human liver microsomes 251
7.4.4 Human intestinal microsomes 252
7.5 High-Performance Liquid Chromatography 252
7.5.1 Mobile phase 252
7.5.2 HPLC Method 253
7.6 Data analysis 254
7.7 Results 256
7.7.1 Compound 51 256
7.7.2 Compound 30 272
7.7.3 Compound 21 279
7.7.4 Rivastigmine 281
7.8 Discussion 283
7.9 Conclusion 285
Chapter 8 Conclusion and Future work 286
Bibliography 290
Appendix I 320
Appendix II 322
Published articles 328

Table of Figures

Figure 1.1 Atkinson and Shiffrin's model of memory processes 4
Figure 1.2 Wong's circuit model, the hypothetical three-neuron chip. 6
Figure 1.3 Organization of the somatic, auditory and visual association areas..... 8
in the human brain 8
Figure 1.4 Mid-sagittal section of the human brain 12
Figure 1.5 Processing of amyloid precursor protein. 13
Figure 1.6 The amyloid precursor protein pathway.. 14
Figure 1.7 The structure of the transmembrane protein, Presenilin 1 17
Figure 1.8 Tau protein in microtubule stability and in the formation of neurofibrillary tangles 19
Figure 1.9 A. Healthy neurons. B. Neurons containing neurofibrillary tangles and surrounded by β-amyloid deposits 20
Figure 1.10 Progression of AD throughout the brain. 20
Figure 1.11 Gross changes and cortical shrinkage in the brain during AD. 22
Figure 1.12 Acetylcholine synthesis and degradation at the synaptic bouton and cleft of a neuron synapse 24
Figure 1.13 The major cholinergic projections in the brain 26
Figure 1.14 Helical structure of human butyrylcholinesterase 32
Figure 1.15 The catalytic triad of the active site of butyrylcholinesterase. 34
Figure 1.16 The molecular forms of butyrylcholinesterase 36
Figure 1.17 Novel isosorbide-based compounds. 51
Figure 2.1 Reaction pathway of the Ellman assay 57
Figure 2.2 The activity of BuChE in human, mouse and rat plasma 59
Figure 2.3 Inhibition of butyrylcholinesterase by compound 21 in human plasma... 63
Figure 2.4 Inhibition of butyrylcholinesterase by compound 30 in human plasma... 63
Figure 2.5 Inhibition of butyrylcholinesterase by compound 30 in mouse plasma... 64
Figure 2.6 Inhibition of butyrylcholinesterase by compound 33 in human plasma... 64
Figure 2.7 Inhibition of butyrylcholinesterase by compound 33 in mouse plasma... 65
Figure 2.8 Inhibition of butyrylcholinesterase by compound 51 in human plasma... 65
Figure 2.9 Inhibition of butyrylcholinesterase by compound 51 in mouse plasma... 66

Figure 2.10 Inhibition of butyrylcholinesterase by compound 57 in human plasma.66
Figure 2.11 Inhibition of butyrylcholinesterase by compound 57 in mouse plasma. 67
Figure 2.12 Inhibition of butyrylcholinesterase by rivastigmine in human plasma.. 67
Figure 2.13 Inhibition of butyrylcholinesterase by rivastigmine in mouse plasma. . 68
Figure 2.14 Inhibition of butyrylcholinesterase by physostigmine in human plasma. 68
Figure 2.15 Inhibition of butyrylcholinesterase by physostigmine in mouse plasma. 69
Figure 2.16 Venous plexus in the mandible of the mouse for submandibular blood sampling 85
Figure 2.17 Mean mouse plasma BuChE activity (± SEM) over 72 hours following a single dose of 1 mg/kg of compound 51 i.p. or p.o. 88
Figure 2.18 The activity of BuChE in mouse brain 24, 48 and 72 hours following a single dose of 1 mg/kg of compound 51 i.p. and p.o. 89
Figure 2.19 The activity of BuChE in mouse liver 24, 48 and 72 hours following a single dose of 1 mg/kg of compound 51 i.p. or p.o. 90
Figure 2.23 The activity of BuChE in mouse plasma following administration of a single dose of 1 mg/kg of compound 30 i.p. 94
Figure 2.26 The activity of BuChE in mouse brain following administration of a single dose of 5 mg/kg of compound 30 i.p. 97
Figure 2.27 The activity of liver BuChE following administration of a single dose of 5 mg/kg of compound 30 i.p. 98
Figure 2.28 The activity of BuChE in mouse plasma following 1 mg/kg of compound 33 i.p. or 0.1 ml/10 g 0.9% saline 99
Figure 2.31 Mean mouse plasma BuChE activity (± S.E.M.) following a single dose of 1 mg/kg of rivastigmine i.p. 102
Figure 2.32 The activity of BuChE in the mouse brain following administration of a single dose of 1 mg/kg rivastigmine.....103
Figure 2.33 The activity of BuChE in mouse liver following administration of a single dose of 1 mg/kg rivastigmine i.p.....104
Figure 2.34 Chromatogram representing compound 51 and its metabolites benzyl carbamate and benzoic acid.....109
Figure 2.35 Mean mouse plasma BuChE activity (± SEM) from blood samples procured at 8 a.m. and 8 p.m.....112

Figure 3.1 Water maze with platform and visual cues. 132
Figure 3.2 Layout of apparatus in the room for Morris Water maze testing. 133
Figure 3.3 Spatial arrangement of objects in the open field during the habituation sessions (S1 - S3). 137
Figure 3.4 Spatial arrangement of the objects in the open field during the spatial novelty session 5. 138
Figure 3.5 Spatial arrangement of objects in the open field during the object novelty session 7. 139
Figure 3.6 Layout of sections on subbed slide 142
Figure 3.7 Entry point of the needle track into the mouse brain. 145
Figure 3.8 Needle track passing lateral to the lateral ventricle and finishing at the location of the basal nucleus. 146
Figure 3.9 Needle track finishing at the location of the basal nucleus 147
Figure 3.10 Latency to reach the platform (s) during water maze training days 1 - 5. IBO lesioned drug-treated, IBO lesioned saline-treated, sham lesioned drug-treated and sham lesioned saline-treated 2 -3 month old male C57BL/6 mice. 148
Figure 3.11 Path length (cm) of animals to reach the platform during water maze training days 3 – 5. IBO lesioned drug-treated, IBO lesioned saline-treated, sham lesioned drug-treated and sham lesioned saline-treated 2 -3 month old male C57BL/6 mice. 149
Figure 3.12 Swim speed (cm/s) of animals during water maze training days 3 – 5. IBO lesioned drug-treated, IBO lesioned saline-treated, sham lesioned drug-treated and sham lesioned saline-treated 2 -3 month old male C57BL/6 mice. 150
Figure 3.13 % of total time animals spent in thigmotaxis. IBO lesioned drug-treated, IBO lesioned saline-treated, sham lesioned drug-treated and sham lesioned saline-treated 2 -3 month old male C57BL/6 mice. 151
Figure 3.14 % time animals spent swimming in the quadrant containing platform during water maze training days 3 – 5. IBO lesioned drug-treated, IBO lesioned saline-treated, sham lesioned drug-treated and sham lesioned saline-treated 2 -3 month old male C57BL/6 mice. 152
Figure 3.15 % time spent each group spent swimming in the southeast quadrant (formerly occupied by the platform) during the probe trial for IBO lesioned drug-treated, IBO lesioned saline-treated, sham lesioned drug-treated and sham lesioned saline-treated 2 -3 month old male C57BL/6 mice. 153

Figure 3.16 Paths to the platform during water maze training and the probe trial of the best performing animal for each group. Sham saline-treated, sham drug-treated, IBO lesioned saline-treated and IBO lesioned drug-treated 2 – 3 month old male C57BL/6 mice. 154

Figure 3.18 Reactivity to spatial novelty. Mean change in duration of time (± SEM) in contact with the non-displaced (NDOs) and displaced objects (DOs) during sessions 4 – 5. IBO lesioned drug-treated, IBO lesioned saline-treated, sham lesioned drug-treated and sham lesioned saline-treated 2 -3 month old male C57BL/6 mice. 156

Figure 3.19 Reactivity to object novelty. Mean change in duration of time (± SEM) in contact with the non-substituted objects (NSOs) and substituted objects (SOs) during sessions 6 – 7. IBO lesioned drug-treated, IBO lesioned saline-treated, sham lesioned drug-treated and sham lesioned saline-treated 2 -3 month old male C57BL/6 mice. 157

Figure 4.1 The radial arm maze. 173

Figure 4.2 Latency to reach the platform (s) during water maze training days 1 - 5. 12 month old (n = 8) and 24 month old (n = 7) male C57BL/6 mice. 175

Figure 4.3 Path length to the platform (cm) during water maze training days 1 - 5. 12 month old (n = 8) and 24 month old (n = 7) male C57BL/6 mice. 176

Figure 4.4 Swim speed of the animals during water maze training days 1 - 5. 12 month old (n = 8) and 24 month old (n = 7) male C57BL/6 mice. 177

Figure 4.5 % time spent in thigmotaxis during water maze training days 1 - 5. 12 month old (n = 8) and 24 month old (n = 7) male C57BL/6 mice. 178

Figure 4.7 % time spent in the southeast quadrant (previously containing the platform) during the probe trial. 12 month old (n = 8) and 24 month old (n = 7) male C57BL/6 mice. 180

Figure 4.10 Swim speed of animals (cm/s) during water maze training days 1 - 5. Young saline-treated, young drug-treated, aged saline-treated and aged drug-treated 2 -3 month old C57BL/6 mice. 183

Figure 4.14 Swim paths to the platform during training days 2, 4, 6, 8, 10 and the probe trial. The training and probe plots represent the best animal from each group. Young saline-treated, young drug –treated, aged saline-treated and aged drug-treated male C57BL/6 mice..... 187

Figure 4.15 Plasma BuChE activity in young and aged mouse plasma 188

Figure 4.16 Mean activity of BuChE (± SEM) in the plasma of young and aged mice. 189

Figure 4.17 Mean activity of BuChE (± SEM) in the liver of young and aged mouse 190

Figure 4.18 Habituation of object exploration during sessions 1 – 3. Mean duration of contacts with the objects (± SEM) in each session in 12 month old (n = 7) and 24 month old (n = 8) male C57BL/6 mice. 191

Figure 4.19 Reactivity to spatial novelty. Mean duration of of time (s) in contact with the objects (± SEM) during sessions 4 and 5. 12 month old (n = 7) and 24 month (n = 8) old male C57BL/6 mice. 192

Figure 4.20 Change in the duration of time (s) (mean ± SEM) spent by one and two-year old mice exploring non-substituted objects (NSOs) and substituted objects (SO) in sessions 6 and 7. 12 month old (n = 7) and 24 month (n = 8) old male C57BL/6 mice. 193

Figure 4.21 Habituation of object exploration during sessions 1 – 3. Mean duration of contacts with the objects (± SEM) in each session in young saline-treated, young drug-treated, aged saline-treated and aged drug-treated old male C57BL/6 mice. 194

Figure 4.22 Reactivity to spatial novelty. Mean change in duration of time (± SEM) in contact with the non-displaced objects (NDOs) and displaced objects (DOs) during sessions 4 – 5. Young saline-treated, young drug-treated, aged saline-treated and aged drug-treated old male C57BL/6 mice. 195

Figure 4.23 Reactivity to object novelty. Mean change in duration of time (± SEM) in contact with the non-substituted objects (NSOs) and substituted objects (SOs) during sessions 6 – 7. 12 month old (n = 7) and 24 month old (n = 8) male C57BL/6 mice. 196

Figure 4.24 Mean number of completed trials (± SEM) over training days 1 – 6. male C57BL/6 mice. 197

Figure 4.25 Mean number of trials successfully completed (± SEM) during training days 4 – 6. Young saline-treated, young drug-treated, aged saline-treated and aged drug-treated 2 – 3 month old male C57BL/6 mice. 198

Figure 4.26 Mean number of incorrect arm entries (± SEM) during training days 4 – 6. Young saline-treated, young drug-treated, aged saline-treated and aged drug-treated 2 – 3 month old male C57BL/6 mice. 199

Figure 5.1 Latency to reach the platform (s) during water maze training days 1 - 5. 14 month old chronic saline-treated (n = 6) and 14 month old chronic drug-treated (n = 7) male C57BL/6 mice. 213

Figure 5.2 Path length to the platform (cm/s) during water maze training days 1 - 5. 14 month old chronic saline-treated (n = 6) and 14 month old chronic drug-treated (n = 7) male C57BL/6 mice. 214

Figure 5.3 Swim speed of the animals (s) during water maze training days 1 - 5. 14 month old chronic saline-treated (n = 6) and 14 month old chronic drug-treated (n = 7) male C57BL/6 mice. 215

Figure 5.4 % thigmotaxic time during water maze training days 1 - 5. 14 month old chronic saline-treated (n = 6) and 14 month old chronic drug-treated (n = 7) male C57BL/6 mice. 216

Figure 5.5 % time in the southeast quadrant (containing the platform) during water maze training days 1 - 5. 14 month old chronic saline-treated (n = 6) and 14 month old chronic drug-treated (n = 7) male C57BL/6 mice. 217

Figure 5.6 % time in spent in the southeast quadrant (previously containing the platform) during the probe trial. 14 month old chronic saline-treated (n = 6) and 14 month old chronic drug-treated (n = 7) male C57BL/6 mice. 218

Figure 5.7 Swim paths to the platform during training days 1 – 5 and the probe trial. The training and probe plots represent the best and worst performing animals in each group. Saline-treated and drug-treated 14 month old male C57BL/6 mice.219

Figure 5.9 Mean BuChE activity in mouse brain (± SEM). Saline-treated (n = 6) and drug-treated (n = 7) 14 month old male C57BL/6 mice. Chronic treatment with saline (0.1 ml /10 g body weight) or compound 51 (1 mg/kg) for one year..... 221

Figure 5.10 Habituation of object exploration during sessions 1 – 3. Mean duration of contacts with the objects (± SEM) during sessions 1 – 3. Saline-treated (n = 6) and drug-treated (n = 7) 14 month old male C57BL/6 mice. 222

Figure 5.11 Reactivity to spatial novelty. Mean change in duration of of time (s) in contact with the non-displaced objects (NDOs) and displaced (DOs) (± SEM) during sessions 4 and 5. Saline-treated (n = 6) and drug-treated (n = 7) 14 month old male C57BL/6 mice. 223

Figure 5.12 Reactivity to object novelty. Mean change in duration of of time (s) in contact with the non-substituted objects (NSOs) and substituted objects (SOs) (±

SEM) during sessions 6 and 7. Saline-treated (n = 6) and drug-treated (n = 7) 14 month old male C57BL/6 mice. 224

Figure 6.1 The lobes of the mouse liver 233

Figure 6.2 Mean levels of alanine transferase, aspartate transaminase, alkaline phosphatase and albumin (± SEM) in mouse plasma 24 hours oral post administration of 1 mg/kg of compound 51 (n = 3) or 1 mg/kg of compound 30 (n = 3). 2 - 3 month old male C57BL/6 mice. 236

Figure 6.3 Mean levels of alkaline phosphatase and albumin (± SEM) in mouse liver 24 hours post oral administration of 1 mg/kg of compound 51 (n = 3) or 1 mg/kg of compound 30 (n = 3). 2 - 3 month old male C57BL/6 mice. 237

Figure 6.4 Mean levels of alanine transferase and glutamate dehydrogenase (± SEM) in mouse liver 24 hours post oral administration of 1 mg/kg of compound 51 (n = 3) or 1 mg/kg of compound 30 (n = 3). 2 – 3 month old male C57BL/6 mice... 238

Figure 6.5 Mean levels of alanine transferase, alkaline phosphatase, aspartate transaminase, glutamate dehydrogenase and albumin (± SEM) in mouse plasma. One year treatment with 1 mg/kg of compound 51 (n = 7) or saline 0.1 ml/10 g body weight (n = 6). 14 month old male C57BL/6 mice. 239

Figure 6.6 Mean levels of alkaline phosphatase, glutamate dehydrogenase and albumin (± SEM) in mouse liver. One year treatment with 1 mg/kg of compound 51 (n = 7) or 0.1 ml/10 g body weight of saline (n = 6). 14 month old male C57BL/6 mice. 240

Figure 6.7 Mean levels of total bilirubin, alanine transferase, aspartate transaminase and gamma glutamyl transpeptidase (± SEM) in mouse liver. One year treatment with 1 mg/kg of compound 51 (n = 7) or 0.1 ml/10 g body weight of saline (n = 6). 14 month old male C57BL/6 mice. 241

Figure 6.8 Area of necrosis in mouse liver tissue 24 hours post administration of a single oral dose of 10 mg/kg of compound 51. Haematoxylin and eosin staining. 243

Figure 6.9 Area of necrosis in mouse liver tissue 24 hours post administration of a single oral dose of 10 mg/kg of compound 51. Haematoxylin and eosin staining. 244

Figure 7.1 Pathway of hydrolysis for compound 51 (isosorbide 2-benzylcarbamate 5-benzoate) by butyrylcholinesterase. 255

Figure 7.2 Hydrolysis of compound 51 in a 33% mouse plasma solution. Metabolites benzyl carbamate and benzoic acid.. 256
Figure 7.3 Overlay of chromatograms from hydrolysis of compound 51 in mouse plasma.. 257
Figure 7.4 Hydrolysis of compound 51 in a 33% mouse plasma solution in the presence of 100 μM BNPP. 258
Figure 7.5 Overlay of chromatograms for compound 51 in a 33% mouse plasma solution with BNPP. 259
Figure 7.6 Hydrolysis of compound 51 in a 0.5% mouse liver solution. Metabolites benzoic acid and benzyl carbamate.. 260
Figure 7.7 Overlay of chromatograms of hydrolysis of compound 51 in mouse liver...261
Figure 7.8 Hydrolysis of compound 51 in a 0.5% mouse liver solution in the presence of 100 μM BNPP 262
Figure 7.9 Overlay of chromatograms from hydrolysis of compound 51 in mouse liver in the presence of BNPP. 263
Figure 7.10 Hydrolysis of compound 51 in a 0.5% mouse liver solution in the presence of 100 μM BNPP and 100 μM rivastigmine 264
Figure 7.11 Overlay of chromatograms from hydrolysis study of compound 51 in the presence of BNPP and rivastigmine.. 265
Figure 7.12 Stability of compound 51 in a 33% human plasma solution. 266
Figure 7.13 Overlay of chromatograms from stability of compound 51 in human plasma. 267
Figure 7.14 Hydrolysis of compound 51 in human intestinal microsomes. 268
Figure 7.15 Overlay of chromatograms for the hydrolysis of compound 51 in human intestinal microsomes. 269
Figure 7.16 Hydrolysis of compound 51 in human liver microsomes.. 270
Figure 7.17 Overlay of chromatograms from hydrolysis of compound 51 in human liver microsomes. 271
Figure 7.18 Stability of compound 30 in a 33% mouse plasma solution.. 272
Figure 7.19 Overlay of chromatograms for compound 30 in mouse plasma. 273
Figure 7.20 Stability of compound 30 in a 0.5% mouse liver solution.. 274
Figure 7.21 Overlay of chromatograms for compound 30 in mouse liver. 275
Figure 7.22 Stability of compound 30 in a 33% human plasma solution.. 276

Figure 7.23 Overlay of chromatograms at various time points for compound 30 in human plasma. 277
Figure 7.24 Stability of compound 30 in a 50% human plasma solution..... 278
Figure 7.25 Stability of compound 21 in a 0.5% mouse liver solution.. 279
Figure 7.26 Stability of compound 21 in a 33% human plasma solution..... 280
Figure 7.27 Stability of rivastigmine in a 33% mouse plasma solution 281
Figure 7.28 Stability of rivastigmine in a 33% human plasma solution..... 282

Table of Tables

Table 1.1 Stages of Alzheimer's disease 11

Table 1.2 Transgenic mouse models of Alzheimer's disease..... 30

Table 1.3 Conditions causing alteration in serum cholinesterase levels 41

Table 2.1 IC_{50} values for the novel BuChE inhibitors. 62

Table 2.2 Results of behavioural scoring of animals following administration of the novel compounds..... 80

Table 2.3 Protocol for submandibular blood sampling..... 84

Table 2.4 Gradient HPLC method for hydrolysis studies on novel compounds.... 108

Table 7.1 Gradient HPLC method for hydrolysis studies on novel BuChE compounds. 253

Abbreviations

°C	degrees Celsius
ACh	acetylcholine
AChE	acetylcholinesterase
AChEI	acetylcholinesterase inhibitor
AD	Alzheimer's disease
Adas-Cog	Alzheimer's Disease Assessment Scale – cognitive subscale
ADL	activities of daily living
ADMET	absorption, distribution, metabolism, excretion, toxicity
Alk phos	alkaline phosphatase
ALT	alanine transaminase
AMPA	α-amino-3-hydroxy-5-methyl-4-isoxazole propionic acid
ANOVA	analysis of variance
ApoE4	apolipoprotein E4
APP	amyloid precursor protein
AST	aspartate transaminase
Aβ	amyloid β
BACE	β-site APP cleaving enzyme
BBB	blood-brain barrier
BN	basal nucleus
BNPP	bis (p-nitrophenyl) phosphate
BTCI	butyrylthiocholine iodide
BuChE	butyrylcholinesterase
BuChEI	butyrylcholinesterase inhibitor
cDNA	complementary deoxyribonucleic acid
CDP-choline	cytidine 5′-diphosphocholine
CDR	clinical dementia rating
CE	carboxylesterase
CGIC	clinical global impression change
CH_3CN	acetonitrile
ChAT	choline acetyltransferase
cm	centimetre(s)

CNS	central nervous system
ColQ	collagen Q
COX-2	cyclo-oxygenase 2
CR	controlled release
CYP450	cytochrome P_{450}
DO	displaced object
DPX	distyrene, a plasticizer and xylene
DSM-IV	Diagnostic and Statistical Manual of Mental Disorders, 4th edition
DTNB	5,5′-dithio-bis(2-nitrobenzoic acid)
EAD	early-onset Alzheimer's disease
ER	endoplasmic reticulum
FAD	familial Alzheimer's disease
FTDP-17	frontotemporal dementia and Parkinsonism linked to chromosome 17
g	gram(s)
GGT	γ-glutamyl transpeptidase
GLDH	glutamate dehydrogenase
GMT	Greenwich mean time
hBuChE	human butyrylcholinesterase
HIA	human intestinal absorption
HPLC	high-performance liquid chromatography
HRT	hormone replacement therapy
IBO	ibotenic acid
i.p.	intraperitoneal
IC50	median inhibition concentration
ICV	intracerebroventricular
Iso-OMPA	tetraisopropylpyrophosphoramide
kg	kilogram(s)
l	litre(s)
LAD	late-onset Alzheimer's disease
LH	lateral hypothalamus
LogBB	log of brain/blood partition coefficient
LSD	least significant difference

LTM	long-term memory
LTP	long-term potentiation
LTS	long-term store
LV	lateral ventricle
MAO	monoamine oxidase
MAP	microtubule associated protein
MCI	mild cognitive impairment
mg	miligram(s)
ml	millilitre(s)
µg	microgram(s)
µl	microlitre(s)
MMSE	mini-mental state examination
MRI	magnetic resonance imaging
mRNA	messenger ribonucleic acid
MT	microtubule
MWM	Morris water maze
nACh	nicotinic acetylcholine
nBM	nucleus basalis magnocellularis
NDO	non-displaced object
NFT	neurofibrillary tangle
NMDA	N-methyl-D-aspartate
NSAID	non-steroidal anti-inflammatory drug
NSO	non-substituted object
NT	neurofibrillary tangle
OCT	optimum cutting temperature
p.o.	per os
PBS	phosphate buffered saline
PD-APP	platelet-derived growth factor promoter controlling expression of human amyloid precursor protein
PDGF	platelet-derived growth factor
PRAD	proline-rich attachment domain
PrCh	propionylcholine
PRIMA	proline-rich membrane anchor
PrP	prion protein

PS	presenilin
RCT	randomized controlled trial
RNA	ribonucleic acid
RSD	relative standard deviation
s	second(s)
S1	session 1
S2	session 2
S3	session 3
S4	session 4
S5	session 5
S6	session 6
S7	session 7
SEM	standard error of mean
SO	substituted object
SP	senile plaque
SPF	specific pathogen free
STM	short-term memory
STS	short-term store
TCIN	Trinity College Institute of Neuroscience
TG	triacylglycerol
TgAD	Alzheimer's disease transgenic mice
Tukey's HSD	Tukey's honestly significant differences
WFI	water for injection

Acknowledgements

I would firstly like to extend my gratitude to Sheila Ryder and Dr. John Gilmer for the opportunity to undertake this research, for their continued guidance and advice over the past three years.

A special thanks to Dr. Joanne Gaynor for all her help, support and good humour during this research and also to Dr. Gerry Dillon for his ideas. To Breda Walsh, thank you so much for cheering me up on those long experimental days in the 'mad house', and I am so grateful for your support, humour and friendship over the past three years. Thanks to Brian for making behavioural studies so amusing and for his expert opinions. Thanks to the Bioresources team, Peter, Anne and Tom, for all their much appreciated help and advice, and to Dr Colm Cunningham and Dr Silvia Middei for their guidance on cognitive testing. Thanks to Lesley Penney for all of her help with histology and for being so kind to me – you made histology so easy for me. I would also like to thank Dr. Peter O'Brien in UCD for assisting me with toxicology and for answering all my questions. Thank you to Professor Brian Sheahan in UCD for kindly analysing histology samples for me. I am also grateful to Laura Gleeson for her help with photomicroscopy.

To my wonderful husband, Hamid, I cannot thank you enough for your continuous love and support. Bhut shukria to Arshad bacha for his support, good fun and du'as. To papa and aami and all their family bhut bhut shukria apka du'as ke liye, I could not have completed this work without you. To my parents, Christopher and Elizabeth, and my family thank you for your kindness and for supporting me throughout everything I have chosen to do.

I would like to especially thank Valerie and Atieh for their help with this thesis and their hours of endless proof-reading, I know you had fun! To Doaa and Raya thank you both for your support and good humour. Thanks to Ciaran for his pleasant company in the lab and on coffee breaks. Also a special thanks to Juan, Paul, Miriam and Jenny and to all the other postgrads for their support and friendship.

Summary

This study sought to determine the pharmacological effects of novel isosorbide-based butyrylcholinesterase inhibitors (BuChEI's) *in vitro* and *in vivo*. The potency of the novel compounds 2-benzylcarbamate 5-nicotinate (compound 21), 2-benzylcarbamate 5-salicylate (compound 30), mono-ethyl carbamate 5-salicylate (compound 33), isosorbide-2-benzylcarbmate 5 benzoate (compound 51) and isosorbide-2-butylcarbamate 5-benzoate (compound 57) were assessed in human and mouse plasma using the Ellman assay.

The most potent compounds were then profiled *in vivo* in a mouse model using a protocol based upon the Shirpa profile. Administration of the novel compounds did not reveal any abnormalities.

In vivo toxicology studies did not reveal any signs of hepatoxicity with 1 mg/kg of compound 51. However, 10 mg/kg of compound 51 and 2 mg/kg of compound 30 revealed gross changes in the liver. Histological evidence confirmed hepatoxicity secondary to necrosis.

Following preliminary dose-ranging studies *in vivo,* the pharmacodynamics of compound 51 and compound 30 were assessed in male C57BL/6 mice by various routes of administration. Administration of 1 mg/kg of compound 51 intraperitoneally (i.p.) and orally (p.o.) produced 40% and 60% inhibition of plasma BuChE respectively. This peripheral inhibition was relatively short-lived with recovery of plasma BuChE levels 30 minutes following i.p. and 1 hour following oral administration. 2 mg/kg of compound 30 i.p. produced approximately 25% inhibition of plasma BuChE 30 minutes following administration, with plasma BuChE levels recovering thereafter.

Compound 51 was further tested in cognitive studies. Male C57BL/6 mice were stereotaxically injected with 0.9% saline or ibotenic acid (IBO) into the nucleus basalis magnocellularis (nBM). IBO lesioned and sham lesioned mice were treated with 1 mg/kg of compound 51 i.p. or 0.9% saline. Mice were trained in the Morris water maze (MWM) and in an object recognition task. Lesioned mice treated with the novel compound located the platform faster than the lesioned animals treated with 0.9% saline; $P < 0.05$ using a two-way ANOVA for repeated measures. Contrary to this, the

sham lesioned animals treated with compound 51 performed significantly worse than the sham lesioned mice treated with saline, $P < 0.05$.

The object recognition trial again showed that IBO lesioned mice treated with compound 51 performed better than IBO lesioned mice treated with saline. On this task the sham-lesioned animals treated with saline performed significantly better than the sham-lesioned animals treated with compound 51 ($P < 0.05$).

The effect of young (2 - 3 month old) and middle-aged (1 year old) mice pre-treated with 1 mg/kg compound 51 p.o. for two weeks was also assessed in both the MWM and an object recognition task. A statistically significant difference was found between the aged mice treated with saline and those treated with 1 mg/kg compound 51 in the MWM; $P < 0.05$. A significant difference was found between the aged and the young mice in the object recognition trial ($P < 0.05$) with the aged mice performing better in this task.

A chronic drug treatment study with mice treated with 1 mg/kg of compound 51 twice weekly for one-year did not reveal any significant difference in terms of cognitive improvement when compared with control saline-treated animals.

Hydrolysis studies were performed, on compound 51, in human plasma, human liver and intestinal microsomes, mouse plasma and mouse liver to find a rationale for the short half-life *in vivo*. It was found that compound 51 was also acting as a substrate for carboxylesterase along with BuChE.

These findings suggest that perhaps these novel BuChE inhibitors could improve cognition or spatial learning in IBO lesioned mice and aged mice where cholinergic deficits exist.

Chapter 1

Introduction

Chapter 1 Introduction

1.1 Memory

1.1.1 General

Memory is defined as the ability to retain and recall prior learning (information and events). It is a very complex process and includes different types of memory such as episodic memory, semantic memory, short-term memory and long-term memory [1]. Traditionally it was thought that memory was unitary. However, it is now known that different types of memory systems exist. Short-term memory (also known as working memory) is considered to be a primary memory while long-term memory is referred to as secondary memory. Long-term memory can further be divided into episodic and semantic memory [2].

1.1.1 Types of memory

Short-term memory (STM) is thought to be extremely fragile, lasting only a few seconds. Working memory holds information that is currently used. Once this information is no longer needed it is removed from the STM and rapidly decays [3].

Long-term memory is known as the permanent store of information. It arises from consolidation of STM through repetition of information [4]. It is principally divided into two subtypes, namely episodic memory and semantic memory.

Episodic memory is a specialized type of memory associated with past experiences or events. This type of memory is unique in that it is linked to the past and it is the only memory system that allows conscious re-experience of past events [5]. It is most likely that this type of memory is unique to humans and it is also more vulnerable to neuronal dysfunction than other memory systems. It is thought that the right pre-frontal cortex plays a primary role in episodic memory both in terms of its processing and retrieval [6, 7]. However, recent studies using neuroimaging have also implicated the parietal cortex in episodic memory retrieval [8, 9]. The prefrontal cortex is thought to play a role in

higher orders of memory and conscious awareness, hence the reason this region of the brain differs between humans and non-human animals [10]. It has been suggested that episodic memory develops in early childhood as children younger than four years of age do not possess the ability to encode previously experienced events [11]. Episodic memory is dependent upon the hippocampus and the fornix [2]. It is thought that episodic memory is derived from semantic memory.

Semantic memory is a type of memory used to describe general facts [2]. This non-episodic memory lies in the present as there is no conscious awareness of any past or future to utilize these memories [10]. Impersonal factual knowledge can be encoded, stored and retrieved through semantic memory [10]. Learning and memory can occur at the semantic level and can be processed there without having to reach the episodic memory. This type of memory is highly dependent upon the perirhinal cortex and the medial dorsal nucleus of the thalamus [2]. Semantic memory and episodic memory are closely related and are similar in that they are both conscious, declarative types of memory that guide behaviour [10].

1.1.2 Processing of memory

For decades there has been much speculation about learning and memory. Charles Darwin's theory of biological evolution described human learning as an adaptive mechanism that evolved over millions of years throughout the animal kingdom. Learning was thought to result from particular situations which subsequently caused a change in an organism's behavioural disposition. Ebbinghaus (1885) introduced many important concepts in learning including the idea of measurable 'degrees of learning'. His conclusions were based on measuring the difficulty of learning a list of words using himself as the sole subject. He noted that the number of errors decreased with multiple re-learnings and that over learning prompted retention [10].

In 1968 Atkinson and Shiffrin proposed a system for human memory and its control processes (Figure 1.1), which has proved popular. They divided memory into three components: the sensory register, the short-term store (STS) and the long-term store (LTS). The sensory register was thought of as an area where incoming sensory information briefly resides. This sensory information in the sensory registry then

decays and is lost. The STS was described as working memory, which receives specific information from the sensory register and additionally from the long-term store. The STS does not have the ability to store the information for prolonged periods of time and it therefore decays completely and is lost within 30 seconds. However, the STS has a control process known as rehearsal and this can retain a limited amount of information in this store as long as is desired. Information is more likely to be transferred from the STM to the permanent store following rehearsal. The permanent storage of information occurs in the LTS. It is thought that information from the STS is transferred or copied to the LTS without removing this information from the original store. Atkinson and Shiffrin proposed that all information from the sensory register and STS are eventually lost but the LTS is different in that information does not decay and become lost in the same manner [12].

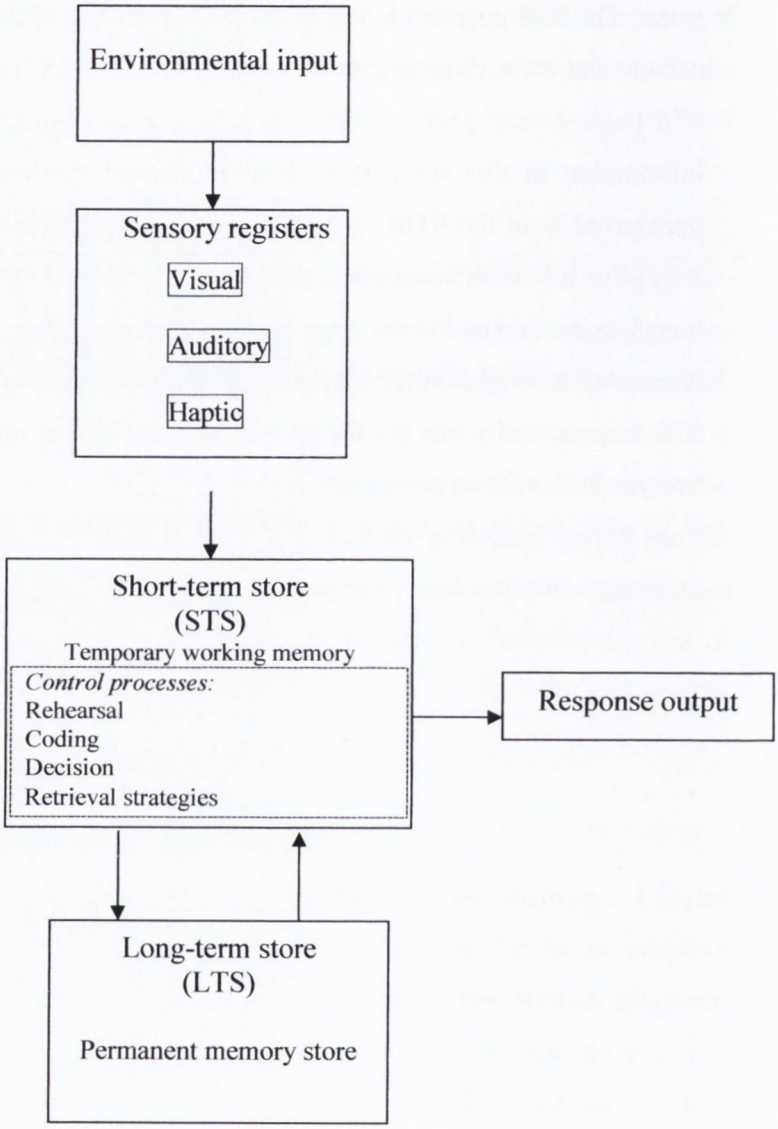

Figure 1.1 Atkinson and Shiffrin's model of memory processes [12].

In 1997, Wong devised a circuit model for the conversion of short-term memory into long-term memory. Wong described a loop of memory-conversion of the axons connecting the perceptive cortices, mesotemporal lobes, dorsomedial nuclei of the thalamus and the prefrontal lobes. The three-neuron chip refers to a simple brain model of memory based upon a circuit containing three neurons namely n_1, n_2 and n_3. The interneurons n_1 and n_2 receive encoding synapses from first order neurons. This encoded information travels along the collateral axons, e_1 and e_2, of interneurons n_1 and n_2 to reach the effector neuron, n_3. The axons of the effector neuron, e_3, then send the signals out of the neuronal chip (*Figure 1.2*).

The brain model consists of a neuron sending out an axonal output of either 'on' or 'off' every time it receives a presynaptic input. The sequence of presynaptic axonal 'on-off' codes over a period of time represents a number of different data. These first-order neurons connect to second-order neurons conveying the data and thus influence the output of the second-order neurons. The presynaptic axonal 'on-off' pattern of short-term memory is consolidated into long-term memory, and retrieval of long-term memory requires re-activation of the same presynaptic axons. The decay of long-term memory is due to disuse or synaptic failure at a biochemical, axonal or neuronal level [13].

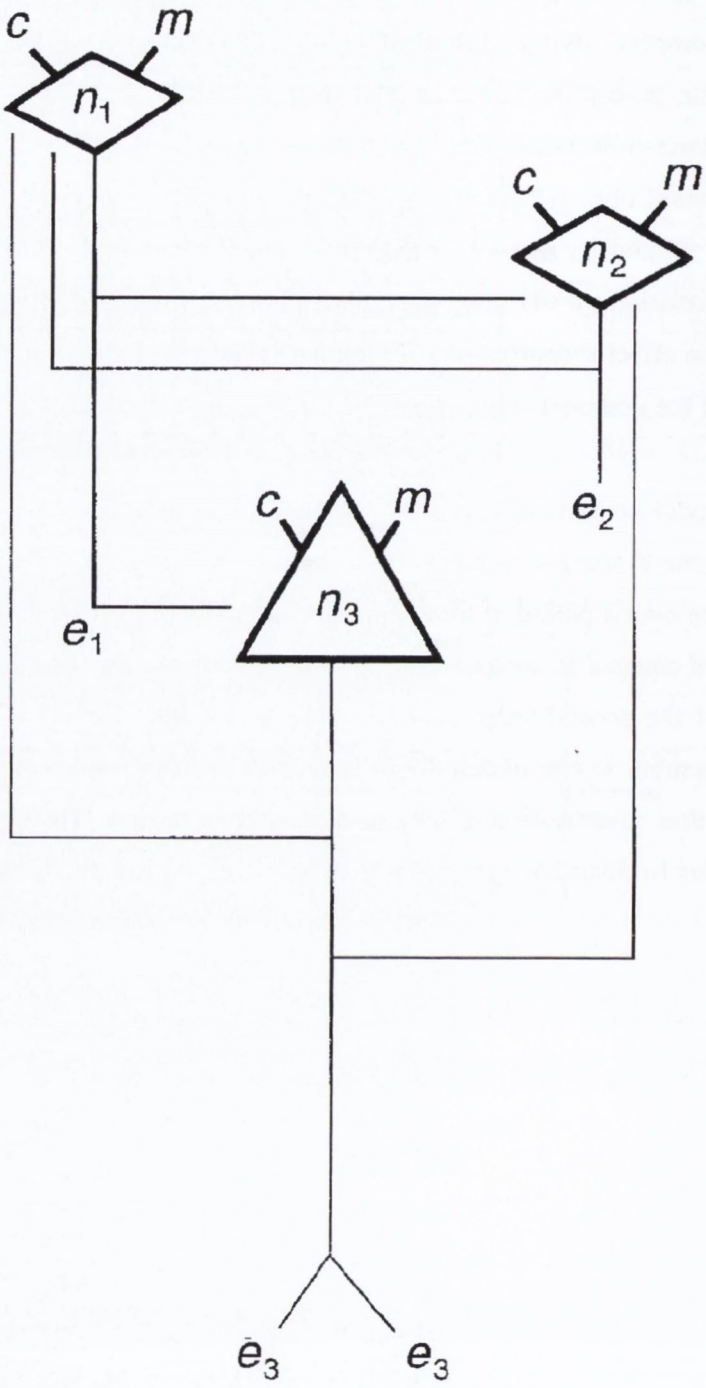

Figure 1.2 *Wong's circuit model, the hypothetical three-neuron chip.*

From Wong, C, 1997 [13]

c: encoding synapse. m: modulating synapse. n_1, n_2: interneurons. n_3: effector neuron. e_1,e_2, e_3: collateral axons from n_1, n_2 and n_3.

Short-term memory is thought to be caused by continual neuronal activity so that nerve signals travel around in a temporary memory trace through a circuit of reverberating neurons [4].

Long-term memory is believed to be a consequence of actual structural changes at the synapses instead of chemical changes alone. True long-term memory depends on physical restructuring of the neurons themselves. There is an increase in the number of vesicles and vesicle release sites for transmitter secretion. Sometimes there is upregulation with more than double the normal number of pre-synaptic terminals. Additionally there is an increase in the size of the dendritic neck thus producing stronger signals [4].

For STM to be converted into LTM it must be consolidated so that it can be retrieved at a later time. If short-term memory is repeatedly activated by frequent rehearsal of the same information it will produce chemical, physical and anatomical changes in the synapses responsible for long-term memory. The consolidation of newly acquired information is crucial for the establishment of long-lasting memories as initial memory traces are fragile and sensitive to disruption. Following reactivation of memory, an additional process called reconsolidation is required for the memory trace to remain in long-term memory. When the memory trace is permanent, it is then stored in the cortical regions and is insensitive to hippocampal disruption [14].

Many areas of the brain are involved in the memory process. The hippocampus, the most medial part of the temporal cortex, promotes storage of memories. Damage or removal of the hippocampi results in an inability to store verbal or symbolic memories for longer than a few minutes [4]. As the hippocampi are important in the storage of memory it is the frontal cortex that is involved in the organizational aspects of memory such as encoding and retrieval [15]. The hippocampi are the most important output pathways from the "reward" and "punishment" areas of the limbic system. The limbic system is the entire neuronal circuitry that controls emotional behaviour and motivational drives. The somatic, visual and auditory association areas all meet each other in the posterior part of the superior temporal cortex. This area of divergence is particularly highly developed in the dominant hemisphere of the brain. Its role is in the higher comprehensive levels of brain function known as intelligence and is named

Wernicke's area. Wernicke's area is closely associated with Broca's area, in the frontal cortex, the centre for word formation (Figure 1.3). The prefrontal cortex also plays a role in higher intellect in human beings. It is involved in the solving of complex problems, ambition, elaboration of thoughts and control of behaviour [4].

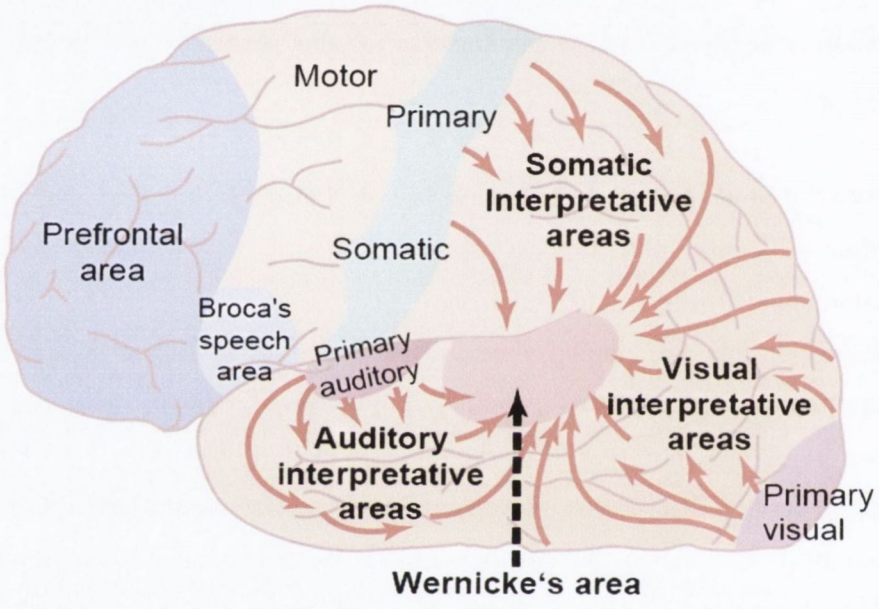

Figure 1.3 *Organization of the somatic, auditory and visual association areas in the human brain [4].*

1.1.3 Memory and aging

It is known that memory declines with increasing age [15]. Studies have shown that older adults perform more poorly than younger adults in tests of memory [16, 17]. These age-related cognitive deficits are also evident in animals [18]. The Maastricht aging study found that education did not offer any protective effects against normal cognitive aging [19]. Aged adults also show a deficit in face recognition memory when compared with young adults [20, 21]. In addition there is evidence to suggest that aged adults are more easily distracted during reading tasks than younger adults [22].

1.2 Alzheimer's Disease

1.2.1 History

Alzheimer's disease (AD) was first described by the Bavarian neuropsychiatrist Alois Alzheimer in 1901. He described the behavioural changes in a 51 year-old mentally ill patient, Auguste D, over a five year period. The neuropsychological changes he observed were deteriorating memory, disorientation and occasional hallucinations. In 1907, upon post-mortem examination of this patient, Alzheimer described two pathological lesions in the brain, namely 'miliary foci' accumulating extracellularly which are known as *senile plaques* and 'dense bundles of fibrils' occurring intracellularly which are now known as *neurofibrillary tangles*. Emil Kraepelin officially named the disorder after Alzheimer in 1910 because of his thorough description of the disease [23].

Alzheimer's disease is the most common dementing disease with over 40,000 people in Ireland suffering from this condition [24]. In the United States there are approximately 5 million sufferers with 4.9 million over 65 years of age and 200,000-500,000 under the age of 65. It is estimated that every 72 seconds someone in the United States develops Alzheimer's disease and by the mid-century someone will develop Alzheimer's disease every 33 seconds [25].

The primary manifestations of brain dysfunction in Alzheimer's disease include cognitive impairment, neuropsychiatric disturbances and neurological abnormalities. Cognition refers to higher brain skills including arousal, attention, concentration, learning, memory, concept formation, problem-solving and language skills. Neurological abnormalities include loss of the ability to walk and talk, incontinence, and emergence of the primary reflexes such as the grasp and suck reflexes. The neurological impairments generally occur in the late stage of the disease. Secondary effects of AD comprise inability to perform activities of daily living (ADL). The stages of AD are summarised in *Table 1.1* [23].

Table 1.1 Stages of Alzheimer's disease [23].

Stages	Behavioural changes
1	Decrease in energy and spontaneity, minor memory loss and mood swings, slowed reaction and learning.
2	Slowing of speech and comprehension, loss of train of thought in mid-sentence. Depression and irritability at awareness of loss of control.
3	Short-term memory loss, disorientation of time, place and person, paraphasic speech.
4	Behavioural disturbances, loss of ability to perform ADL, increasing need for care.
5	Loss of ability to chew and swallow; vulnerability to pneumonia and other illnesses. Coma and death.

Dementia is difficult to diagnose in its early stages and very often goes unrecognised and misdiagnosed as deficits are attributed to normal aging [23]. A diagnostic evaluation for dementia includes a complete history, neuropsychological evaluation (Mini-Mental State Examination (MMSE)), physical examination and neuroimaging studies [26]. DSM-IV (Diagnostic and Statistical Manual of Mental Disorders, 4th Edition) states that the essential feature of dementia is impairment in short- and long-term memory, associated with impairment in abstract thinking, impaired judgement, other disturbances of higher cortical function, or personality change. The disturbance is severe enough to interfere significantly with work or usual social activities or relationships with others [27].

1.2.2 Pathophysiology

1.2.2.1 General

The pathological hallmarks of AD are senile plaques and neurofibrillary tangles. The senile plaques (SPs) are large and located within the neuropil throughout the neocortex and hippocampus. Neurofibrillary tangles (NFTs) are predominantly found in the hippocampus, amygdala, nucleus basalis and the hypothalamus (*Figure 1.4)* [28]. The general consensus among neuropathologists with regard to post-mortem diagnosis of AD is the presence of neuritic plaques and neurofibrillary tangles in the neocortex [29]. Although these features are found in patients with AD they are not exclusive to the disease as they are also found in patients with Down's syndrome (trisomy 21) and they frequently occur in elderly persons with normal brain function [30].

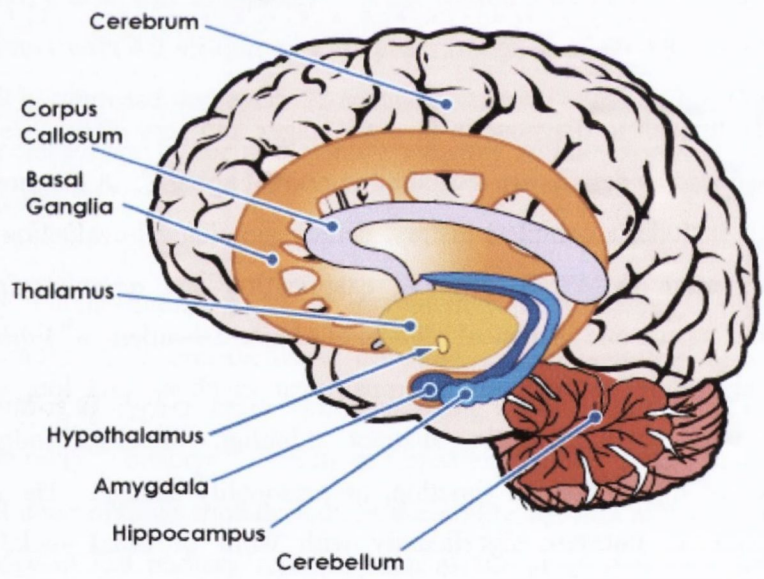

Figure 1.4 Mid-sagittal section of the human brain [31].

1.2.2.2 Amyloid Precursor Protein

SPs are extracellular accumulations of the β-amyloid (Aβ) peptide in the form of insoluble amyloid plaques [30]. This extracellular amyloid is gradually deposited in the brain parenchyma and meningocerebral blood vessel walls [32]. The levels of Aβ increase in early dementia and there is a strong correlation between high levels of Aβ and cognitive decline [33]. The Aβ peptide originates from a much larger membrane-spanning amyloid precursor protein (APP). The APP gene encodes APP. APP functions as a membrane-anchored receptor-like molecule [34]. This protein is located in many tissues and organs including the brain and spinal cord (the central nervous system) [35]. APP has a short half-life and is metabolized by protease action along two pathways, a non-amyloidogenic and an amyloidogenic pathway (*Figure 1.5)* [36].

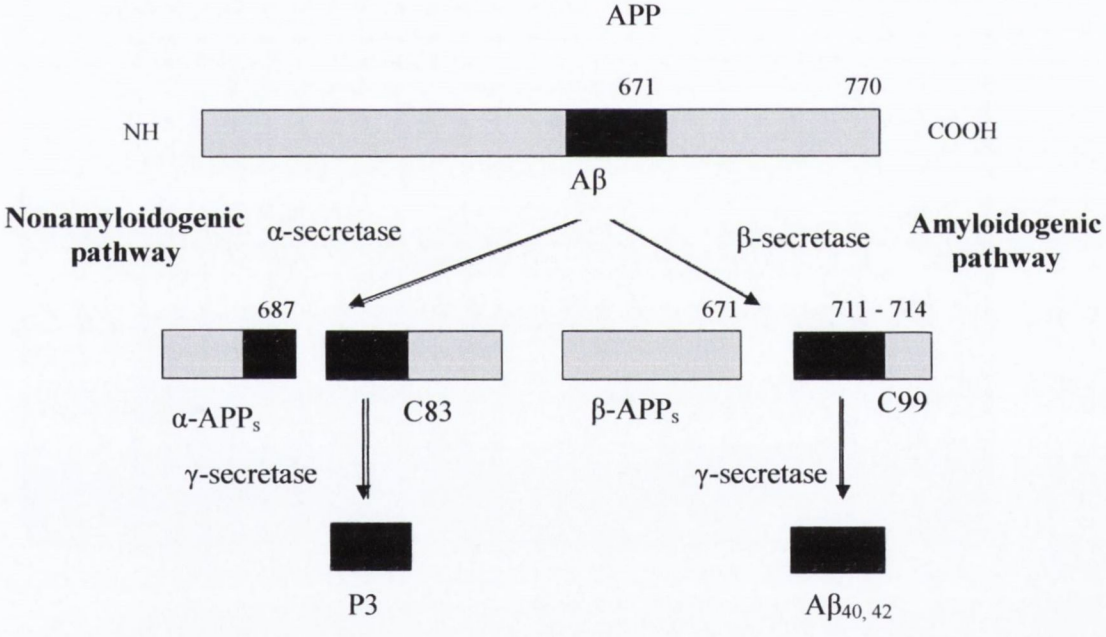

Figure 1.5 *Processing of amyloid precursor protein.*

Adapted from Richardson et al. 2002 [36].

The membrane-anchored protease, α-secretase, initiates the non-amyloidogenic pathway by cleaving APP between extracellular residues 687 and 688 within the Aβ domain resulting in the release of a large soluble ectodomain αAPP_s *(Figure 1.6)* [36, 37]. The principal cleavage takes place at the cell surface but is now also known to occur in endoplasmic reticulum (ER) Golgi and trans-Golgi networks [34]. Endoproteolytic cleavage of the C-terminal fragment by γ-secretase produces a short fragment, p3. P3 is released by APP-expressing cells during normal metabolism [36].

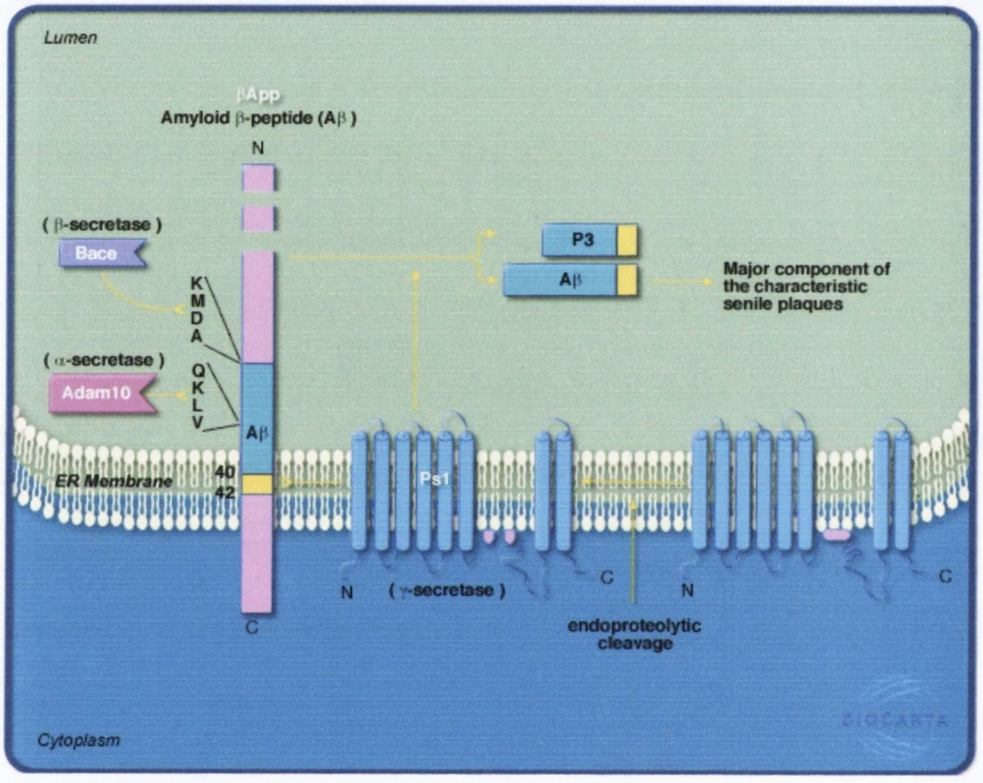

Figure 1.6 *The amyloid precursor protein pathway. Cleavage of amyloid precursor protein by the secretase enzymes to form Aβ and P3* [38].

The amyloidogenic pathway is by β-secretase cleaving APP after amino acid 671 producing an N-terminal fragment, β-APP_s. However if the C-terminal fragment is cleaved by γ-secretase it produces Aβ. Cleavage at amino acid residues 712 and 713 produces $Aβ_{42}$. However, if it is cut at amino acid 714 $Aβ_{40}$ is produced. The majority of the secreted Aβ peptides are the short, soluble $Aβ_{40}$. However, approximately 10% of the secreted Aβ peptides are the insoluble $Aβ_{42}$, which aggregate to form extracellular fibrils [33, 36]. There are two β-secretase enzymes which have been identified, namely β-site APP cleaving enzymes BACE1 and BACE2. BACE1 is highly expressed in the brain and it is the major β-secretase involved in the generation of Aβ peptides in neurons [39]. Additional research has now found that integrins and extracellular signal-regulated kinases 1 and 2 are involved in inducing beta-amyloid cell-cycle activation and neuronal death [40]. BACE1 knockout mice exhibit a normal phenotype, have no behavioural abnormalities and are fertile. They survive into middle and old age with no obvious abnormalities. The $BACE1^{-/-}$ mice lack brain β-amyloid and therefore BACE1 inhibitors may be feasible as a therapeutic strategy in AD [41].

SPs are hydrophobic self-aggregating Aβ peptides. Genetic mutations of the APP gene on chromosome 21 are common in dominantly inherited forms of AD, also known as familial AD (FAD). Amyloid plaques are not exclusive to AD as they are also found in patients with trisomy 21 (Down's syndrome) who possess an extra copy of chromosome 21 encoding the APP gene [34]. Older Down's syndrome patients express neuropathological phenotypes that resemble AD. $Aβ_{42}$ is the first form of Aβ to appear in the diffuse plaques in the brains of Down's syndrome patients and it has been shown to be present in greater abundance in the cortex than $Aβ_{40}$. Moreover, a substantial $Aβ_{42}$ plaque burden has been found in post-mortem brains of Down's syndrome patients as young as 12 years of age but there were no significant $Aβ_{40}$ plaques before 29 years of age [32]. Although APP is expressed in many cells and tissues throughout the body it remains unclear why Aβ deposition only occurs in the brain [34].

The precise function of APP is unknown but due to its predominant neuronal location it is thought to be involved in cell adhesion and neurite outgrowth [42], to function as a growth factor in cell culture and to regulate intraneuronal calcium levels [43]. APP knockout mice display decreased locomotor activity and forelimb grip strength perhaps as a result of impaired neuronal function. They also have a lower body weight, 15-20%

lower than that of age-matched controls. The absence of APP does not appear to be lethal as $APP^{-/-}$ mice were viable and fertile [44]. Although a deficiency of APP is not fatal, 4 and 10 month old $APP^{-/-}$ mice performed poorly in cognitive testing in the Morris water maze and a conditioned avoidance test, compared to wild-type controls. The APP knockouts also displayed impaired long-term potentiation (LTP) and showed reactive gliosis in the cortex and hippocampus [45]. It is therefore evident that APP is crucial for normal neuronal function. Ring *et al.* showed that mice expressing only the N-terminal domain of APP were rescued from impairments in spatial learning and LTP [46]. These results may indicate that the N-terminal of APP plays a greater role in neuronal function than the C-terminal domain and that perhaps the C-terminal is dispensable.

1.2.2.3 Presenilins

The presenilin genes 1 and 2 are also thought to play a fundamental role in AD pathogenesis. The gene for presenilin 1 is expressed on chromosome 14 while the presenilin 2 gene is located on chromosome 1 [47-49]. Presenilin 1 (PS1) and presenilin 2 (PS2) are ubiquitously expressed transmembrane proteins with six to nine transmembrane domains and are principally localized in the endoplasmic reticulum and Golgi apparatus (*Figure 1.7)* [36].

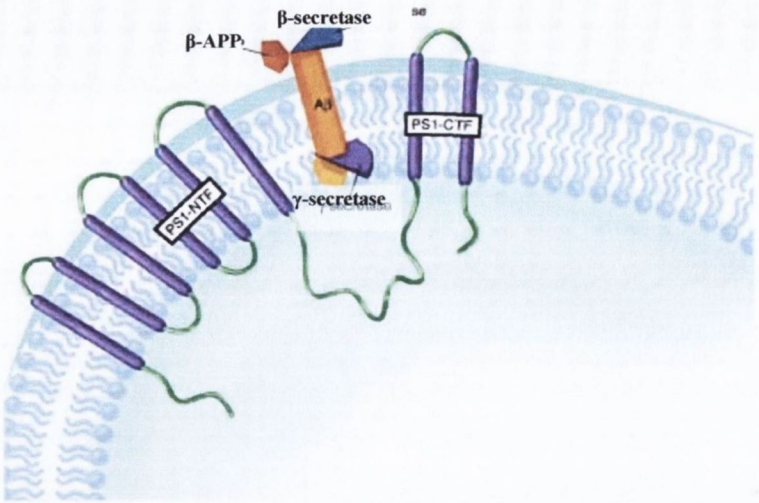

Figure 1.7 *The structure of the transmembrane protein, Presenilin 1* [50].

PS1-NTF: Presenilin 1 N-terminal fragment; PS1-CTF: Presenilin 1 C-terminal fragment

Both PS1 and PS2 are both expressed at comparable levels in human and mouse tissues however, PS1 messenger ribonucleic acid (mRNA) is found in higher levels in the developing brain than PS2. This may indicate different biological functions among the presenilins. Both PS1 and PS2 exhibit marked expression in neurons but they are also present in glial white matter [51]. Mutations in the presenilin genes, in particular PS1, account for a significant proportion of cases of FAD, hence the reason the focus of presenilin research lies with PS1 [35, 36].

Presenilin 1 is involved in an array of cellular functions including cleavage of the receptor protein Notch [52], the multifunctional cell surface receptor, low-density lipoprotein receptor-related protein and the cell adhesion receptors E- and N-cadherins [53, 54]. It is thought that the presenilins are necessary for the proteolytic activity of γ-secretase, which cleaves APP [55]. PS1 facilitates the proteolytic activity that cleaves the integral domain of APP [56]. Vetrivel *et al.* suggested that the presenilins function as the catalytic subunits of γ-secretase [57]. It is the α- and β-secretases that first act upon APP generating C-terminal transmembrane fragments which γ-secretase then cleaves with

the involvement of PS1 [56]. Further evidence suggests that γ-secretase contains a presenilin dimer in its catalytic core and the substrate binds at a site separate from the active site. The substrate is then cleaved at the interface of two presenilin molecules [58]. In the absence of PS1, cleavage of the APP extracellular domain by α- and β-secretases can take place but intramembraneous cleavage by γ-secretase is prevented [56]. This suggests that PS1 and γ-secretase are dependent upon each other in order to cleave APP.

Although the exact function of presenilin-1 is still unknown, it has been determined that PS1 plays a crucial role in neuronal differentiation in murine neurogenesis [59]. Unlike $APP^{-/-}$ mice, presenilin-1-deficient mice have a high neonatal mortality rate. Growth of the embryo is severely retarded [56]. Neonatally the skeletons of the mice exhibit gross deformations and there is evidence of neuronal degeneration in the lateral ventricle. The reason for the large number of neonatal $PS1^{-/-}$ mice deaths is thought to be due to failure of respiratory mechanisms due to marked deformities in the ribcage with hypoinflation of the alveoli. It is therefore evident that PS1 is essential for proper formation of the axial skeleton and normal neuronal development [60]. Neurogenesis also persists throughout life and occurs in the adult brain [61, 62]. Presenilin 1 inhibitors would therefore not be a viable therapeutic strategy in AD as they may interfere with adult neurogenesis.

1.2.2.4 Neurofibrillary tangles

Neurofibrillary tangles consist of paired helical filaments that are abnormal aggregates of hyperphosphorylated forms of the microtubule (MT) associated tau protein [30]. Tau protein is a soluble hydrophilic neuronal microtubule associated protein (MAP) [36]. MAPs bind to the microtubules and stabilize them, but they may have other functions such as cross-linking to other elements of the cytoskeleton or providing docking sites for enzymes. MAPs and their phosphorylation are thought to be important regulators of microtubule dynamics [63]. In AD, tau loses its ability to stabilize the MTs due to its hyperphosphorylation [64]. Instability of the MTs leads to the formation of neurofibillary tangles (*Figure 1.8).*

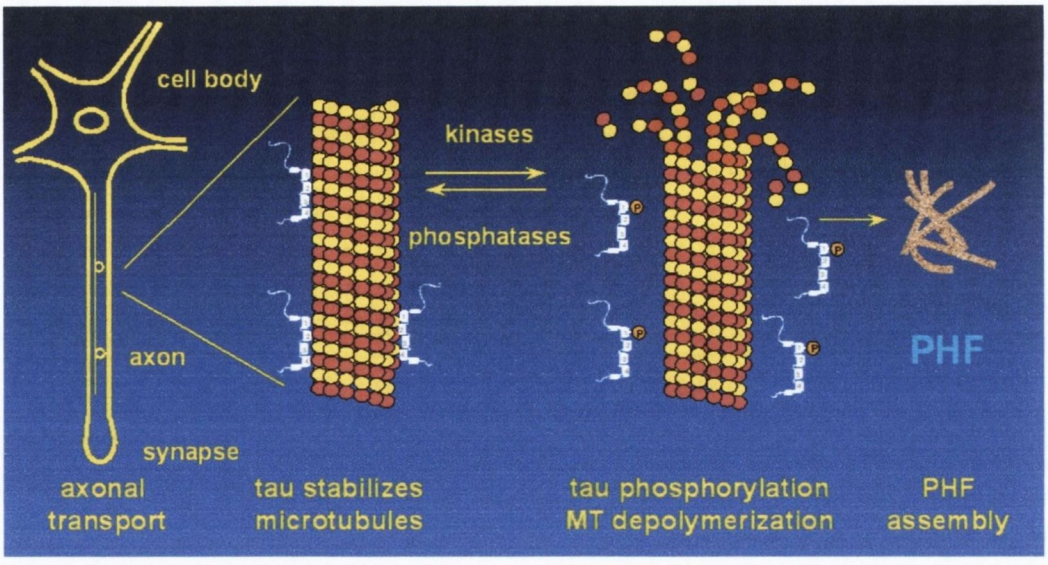

Figure 1.8 *Tau protein in microtubule stability and in the formation of neurofibrillary tangles* [65].

MT = microtubule, PHF = paired helical filament.

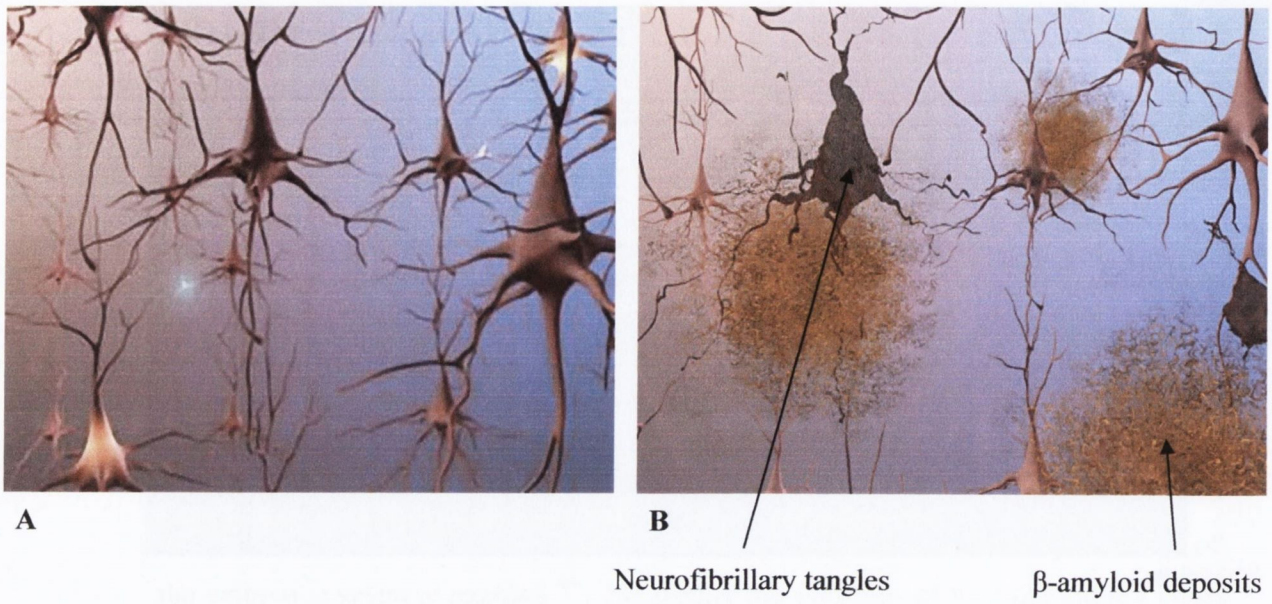

Figure 1.9 *A. Healthy neurons. B. Neurons containing neurofibrillary tangles and surrounded by β-amyloid deposits* [66].

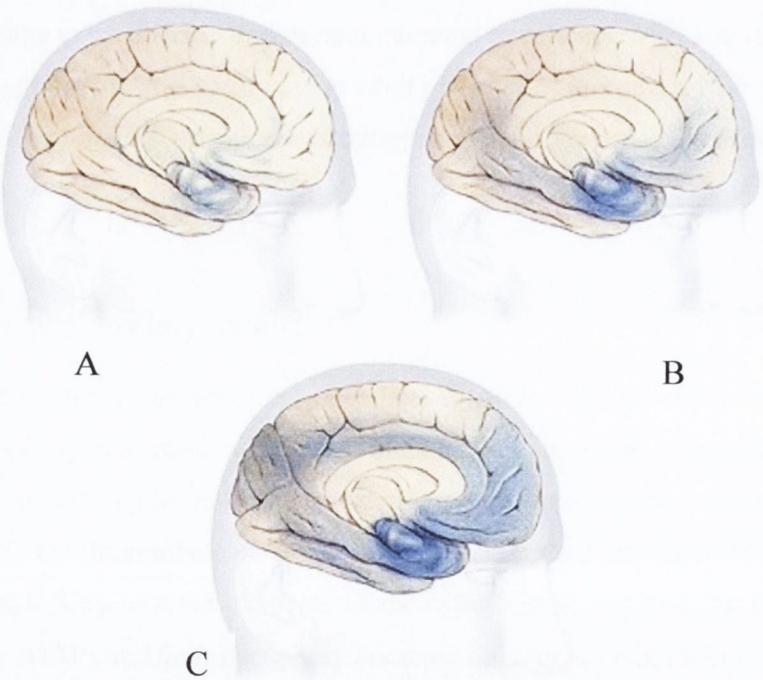

Figure 1.10 *Progression of AD throughout the brain. A. The hypothalamus. B. Spread from the hypothalamus to the frontal and temporal cortices. C. Involvement of the entire cortex. (Plaques and tangles represented by the blue-shaded areas.)* [67]

Both senile plaques and NFTs spread throughout the cortex in a predictable pattern as AD progresses (*Figure 1.9)* [68]. NFTs first appear in the entorrhinal cortex followed by the hippocampus, spreading to the frontal, temporal, parietal and occipital cortices [30, 68] (*Figure 1.10)*.

Gross changes in the brain also occur during AD. There is a reduction in brain weight compared with age- and sex-matched non-demented individuals. There is also a degree of lateral and third ventricle dilatation due to cortical shrinkage and the loss of underlying white matter [30] (*Figure 1.11)*. Cortical thinning has been observed in patients with mild cognitive impairment (MCI) and AD with the greatest lobar thickness difference in the temporal cortex in AD subjects [69]. The overall cortical thickness reduces with the severity of the disease [70]. Cortical atrophy in early-onset (EAD) or familial AD (FAD) patients appears to have a predilection for the precuneus bilaterally while late-onset AD (LAD) patients have significant atrophy of the temporal cortex [71]. The precuneus is located on the posteromedial portion of the parietal lobe and functions in visuospatial imagery [72]. Visuospatial functioning is marginally less in EAD patients compared to LAD patients [71]. In FAD the genetic defect is present from birth and yet the symptom onset is at least 30 years later. Cognitive decline may precede dementia by several years [73] .

A. The brain of a normal elderly person

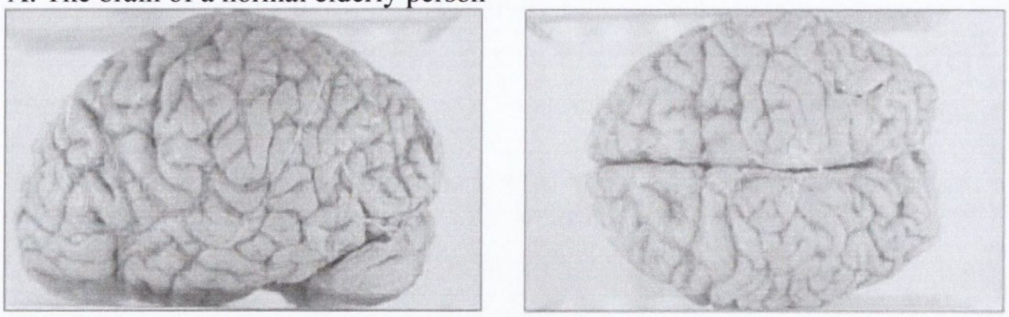

B. The brain of a person with Alzheimer's disease

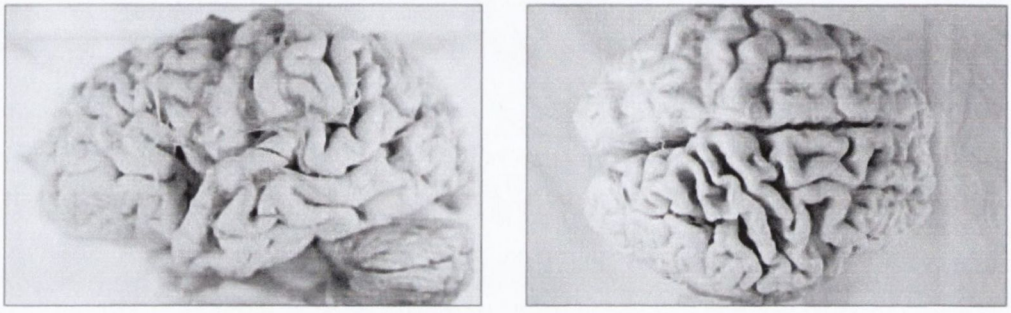

Figure 1.11 Gross changes and cortical shrinkage in the brain during AD [74].

In patients with AD it has been shown that they have a significant gray matter deficit in the bilateral temporal and parietal cortices on high-resolution magnetic resonance imaging (MRI) scanning. These structural differences in AD patients correlated functionally with a decline in cognitive performance, as quantified by MMSE scores. In longitudinal studies repeat scanning enabled rates of tissue loss to be determined in both healthy and AD patients. Control groups showed attrition of gray matter with aging at an annual rate of 0.91% and this mimics that seen in adolescents [75]. However, significant loss of gray matter was observed in AD patients and this rate was more rapid than in control subjects with a total gray matter loss of 5.03% per year. The regions exhibiting the most prominent gray matter loss include the right cingulate, temporal and frontal cortices bilaterally. There was however a trend for faster gray matter loss in the left hemisphere in both control and AD groups. The left hemisphere was generally more severely affected both metabolically and structurally in AD, however this study used right hand dominant subjects [76, 77]. It may be the case that hand dominance affects

which hemisphere will functionally decline more severely as the dominant hemisphere contra-laterally corresponds with the dominant handedness.

1.2.3 Neurochemical changes

There is a loss of cholinesterase and cholinergic neurons during AD. It had initially been surmised that there was no significant decrease in the cerebral cortex with normal aging [78]. However, studies have found substantial decreases in cortical acetylcholinesterase (AChE) activity with a 20-25% loss in AChE-rich axons in the temporal lobe in normal aging patients [79, 80]. In the cortex of AD patients, AChE activity decreases progressively from mild to severe stages of the disease to reach only 10-15% of normal values, while BuChE activity remains unchanged or even increases by 20% [81, 82].

Deposition of β-amyloid and the formation of NFTs inevitably leads to neurotransmitter dysfunction. The most renowned neurotransmitter system targeted in AD is the cholinergic system. Deficits in the biogenic amines noradrenaline and serotonin are also thought to exist [83]. In the cholinergic deficit hypothesis it has been found that there is a decrease in the ACh synthesising enzyme, choline acetyltransferase, and the degrading enzyme acetylcholinesterase (E.C. 3.1.1.7) [30].

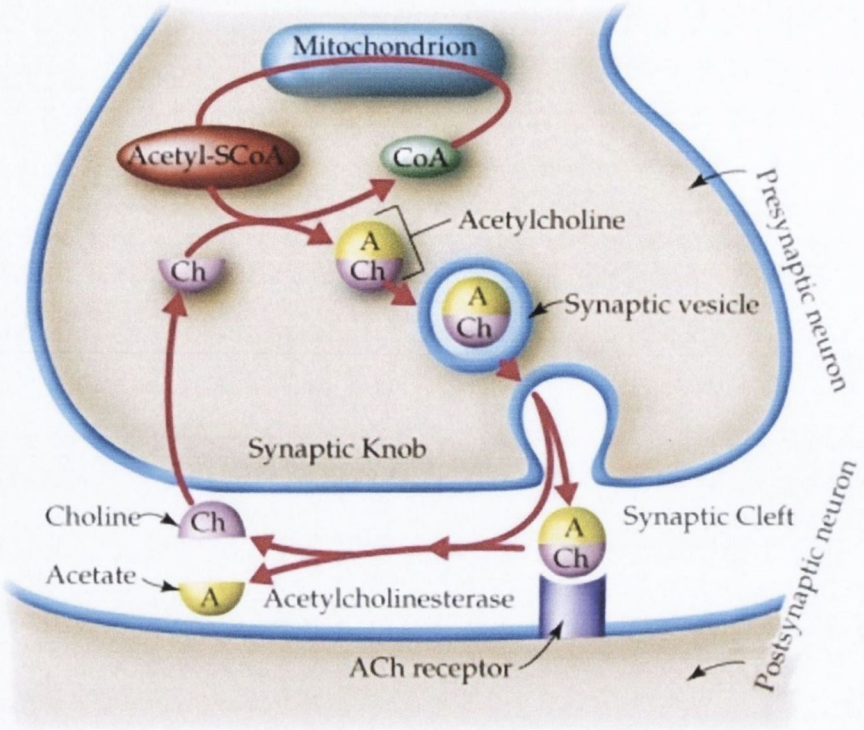

Figure 1.12 *Acetylcholine synthesis and degradation at the synaptic bouton and cleft of a neuron synapse* [84].

Acetylcholine (ACh) is a chemical transmitter of the central and peripheral nervous systems exerting agonist effects on muscarinic and nicotinic receptors [23]. It is synthesized within the nerve terminal from choline and acetate, whose acetylation is mediated by acetyl coenzyme A [30] (*Figure 1.12)*. It is rapidly hydrolyzed at cholinergic synapses, primarily by the enzyme acetylcholinesterase (AChE). AChE belongs to the cholinesterase family of enzymes and it constitutes the most abundant cholinesterase in the nervous system [85].

There are two major groups of cholinergic neurons in the brain, namely the basal forebrain and the pontine cholinergic systems (*Figure 1.13)*. Firstly the basal forebrain cholinergic systems constitutes the medial septal nucleus, the vertical and horizontal limb nuclei of the diagonal band of Broca, and the nucleus basalis of Meynert. This cholinergic system innervates the cingulate cortex, hippocampus, basolateral amygdalae and the olfactory bulb [86].

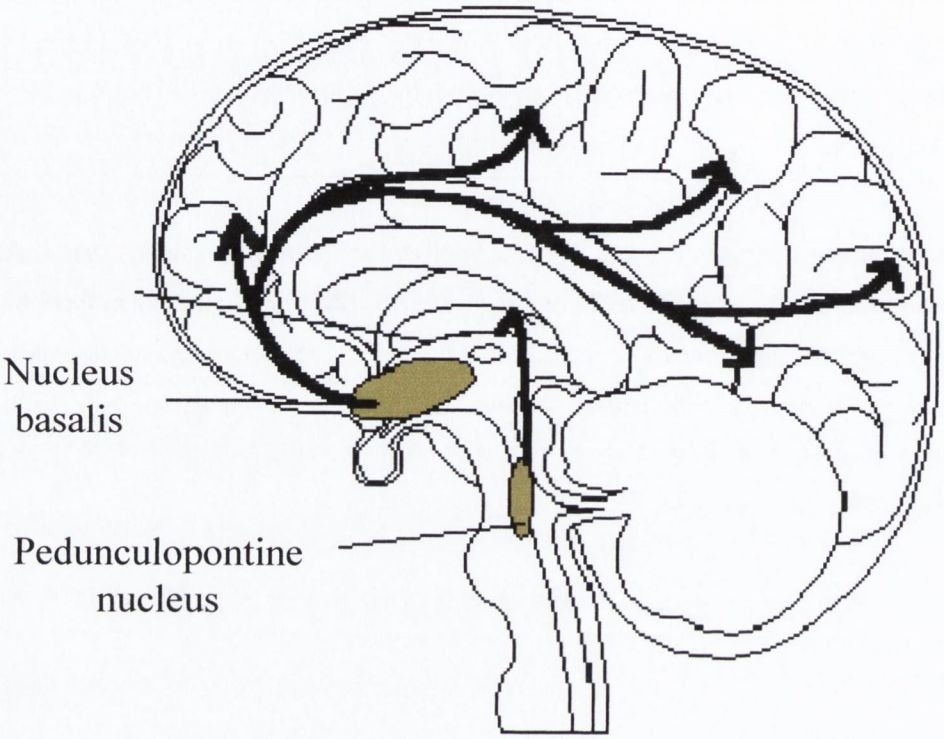

Figure 1.13 *The major cholinergic projections in the brain. Nucleus basalis projections to the neocortex; Pedunculopontine nucleus projections to the thalamus* [87].

Furthermore evidence of choline acetyltransferase (ChAT) positive axons is found in the striatum, globus pallidus, subthalamic nucleus, red nucleus and the substantia nigra indicating substantial cholinergic innervation [88]. Functionally the basal cholinergic neurons have been implicated in learning and memory in all mammals [30]. The second group of cholinergic neurons lie in the pedunculopontine nucleus and are implicated in arousal and the sleep/wake cycle [86].

The loss of the basal forebrain cholinergic system is one of the most significant aspects of neurodegeneration in the brains of AD patients and it is thought to play a central role in producing cognitive impairments. ChAT and AChE activities have been shown to decrease significantly as the mean plaque count rises and a reduction in ChAT activity correlates with the extent of intellectual impairment in memory information tests [82].

1.3 Animal Models of Alzheimer's Disease

Mice share many physiological, anatomical and genomic similarities with humans and are therefore useful as models to understand human diseases [89]. However, animal models only partially represent a diseased state and focus on a limited aspect of a disease [90]. An important aspect in modelling neurological diseases in mice is the genetic strain of the mouse. It is preferable to study the effect of mutations on pure inbred strains to avoid any confounding background effects [89].

Normal aging is known to produce progressive cognitive decline in humans, non-human primates and rodents [91-93]. Animal models of aging are used extensively in tests of cognition. Pathophysiologically aging is associated with cholinergic hypofunction and morphological alterations in the brain. Although rodents exhibit cognitive decline and behavioural changes during normal aging they do not exhibit pathological hallmarks of AD [93]. Aged mice are useful in determining the cognitive effects of aging but they are ambiguous in determining the underlying pathology of AD.

Lesion models in rodents are used to mimic the cholinergic hypofunction associated with AD. This type of model chemically induces an aspect of the disease but it is limited in its ability to express the symptoms of AD in that it only mimics cholinergic loss and there is no evidence of disease progression. Scopolamine, an anti-cholinergic agent, produces cognitive deficits in humans [94, 95] and rodents [96, 97]. Central stereotaxic administration of the excitotoxic lesioning agent ibotenic acid produces cognitive impairment secondary to neuronal loss [98, 99]. The animal model of AD involves injection of ibotenic acid into the nucleus basalis magnocellularis (nBM) producing a loss of cholinergic neurons in this region. It is estimated that the highest dose of ibotenic acid can produce approximately 75% loss of cholinergic neurons [100]. However, ibotenic acid is a non-specific lesioning agent and thus produces additional non-cholinergic neuron loss [101]. The loss of cholinergic neurons in the brain resembles AD correlating with a loss of cognitive function.

The complexity of Alzheimer's disease means it is difficult to produce a mouse model of AD that replicates the disease in its entirety. Single, double or triple transgenics have been used to create a single pathological marker or an overlay of several

pathological markers (*Table 1.2*). The majority of mouse models of AD involve APP, presenilin or tau transgenic mice [102]. APP and presenilin transgenic mice display remarkable similarities in the anatomical pattern of plaque formation with that seen in human AD. However, the APP model does not display any features of neurofibrillary tangles, neurodegeneration or cortical atrophy. The JNPL3 tau transgenic mouse models develop congophilic neurofibrillary tangles in the amygdala, septal nuclei, preoptic nuclei, hypothalamus, midbrain, pons, medulla and spinal cord. These tangles are associated with neuronal degeneration especially in the spinal cord [103]. This model shows signs of human taupathies rather than mimicking AD itself.

Table 1.2 Transgenic mouse models of Alzheimer's disease.

Transgenic line	**Mouse strain**	**Mutation**	**Promoter**	**Pathology**
PD-APP	Swiss Webster-B6D2F1	V717F	PDGF-β	Aβ deposits, neuritic plaques, synaptic loss [104].
PS1	Swiss Webster-B6D2F1	M146V or M146L	PDGF	Elevated amyloidogenic Aβ42(43), neuronal loss [105].
TgCRND-8	C57BL/6-CH3	K670M/N67IL & V7171	Hamster PrP	Aβ deposits, neuritic plaques, learning impairments [106].
FTDP-17	$PS1_{M146V}$	Tg25-76 & VLW	Hamster PrP	Neuritic plaques and phophorylated tau [107, 108].
3xTgAD	$PS1_{M146V}$	βAPP_{SWE}, $PS1_{M146V}$, tau_{301L}	Human APP, Human Tau	Aβ deposition and tau pathology in hippocampus [109, 110].

1.4 Butyrylcholinesterase

1.4.1 Introduction

Dale first differentiated between muscarinic and nicotinic actions of esters in 1914. He also noted that an esterase contributed to the removal of ACh *in vivo* [111]. In 1932 Stedman isolated an ACh-splitting enzyme from horse serum and named it 'choline-esterase'. Mendel and Rudney (1943) later showed that serum contained two enzymes which were capable of hydrolyzing AChE. They found that one of the enzymes was non-specific in the sense that it could split not only choline esters but also non-choline esters such as tributyrin. The second enzyme acted exclusively on esters of choline. They named the former non-specific enzyme 'pseudocholinesterase' and the latter specific enzyme was called 'cholinesterase' or 'true cholinesterase' [112, 113].

Cholinesterases are among the oldest, fastest-acting and most ubiquitous enzymes in all of nature [114, 115]. Acetylcholinesterase and butyrylcholinesterase both hydrolyze the neurotransmitter acetylcholine [115]. Despite being products of two different genes located on chromosome 7 (AChE; 3.1.1.7) and chromosome 3 (BuChE; 3.1.1.8), the two enzymes share a 65% amino acid homology [116]. Both AChE and BuChE exist as water-soluble forms secreted into body fluids [117]. AChE is found in cholinergic synapses in the brain, neuromuscular junction and autonomic ganglia, platelets and erythrocyte membranes [118, 119].

BuChE or pseudocholinesterase is synthesized in the liver and secreted into the blood [120]. BuChE is found in serum, haemopoietic cells, lung, heart, glial cells, astrocytes and cholinergic synapses in the central nervous system (CNS) [121]. This enzyme has no clear physiological function or exclusive biological substrate. However, it is known to hydrolyze esters of choline, including succinylcholine and ACh at high concentrations [117, 122].

BuChE belongs to the α/β-fold family of proteins as it contains a central β-sheet that is surrounded by α-helices (*Figure 1.14)* [123]. This family includes proteins with a broad range of functions such as lipases, peptidases, dehalogenases and adhesion proteins such as neuroligin and neurotactin [116].

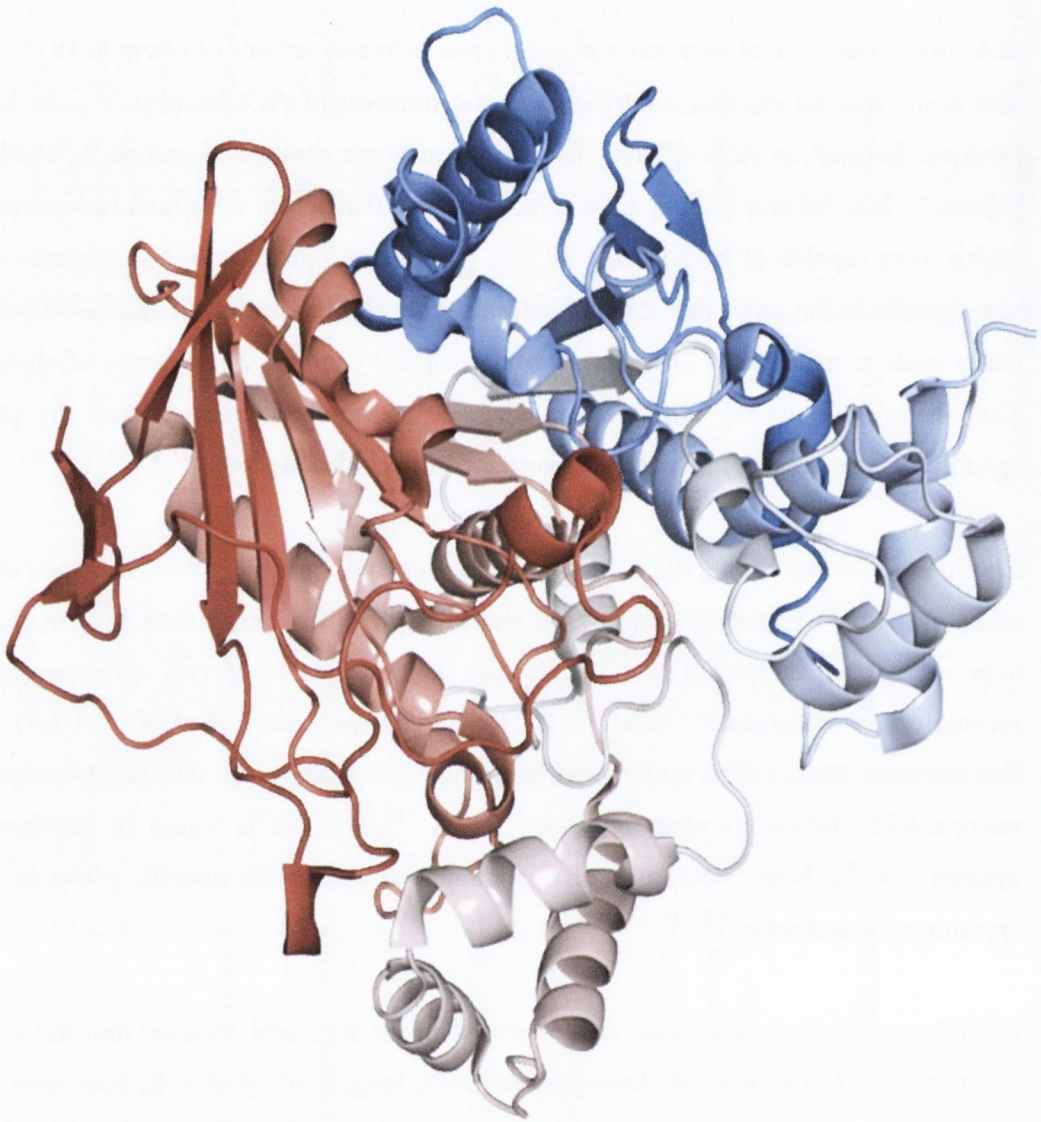

Figure 1.14 Helical structure of human butyrylcholinesterase [124].

The complete sequence of BuChE contains 574 amino acids. BuChE contains a catalytic triad comprising serine 226, histidine 466 and glutamic acid 353 [125]. The catalytic triad is found at the bottom of a 20Å gorge that is lined by six aromatic amino acid residues (*Figure 1.15)* [126]. The active site gorge contains an 'anionic site', which can bind to the cationic quaternary nitrogen of choline, and the aromatic amino acid tryptophan 82. Positively charged substrates are guided down the gorge by interaction with aspartic acid 70 and tyrosine 332, which are located at the lip of the active site gorge. Residues in the peripheral site control binding, are involved in substrate activation and can affect the catalytic rate [127]. Also within the active site gorge is an acyl pocket where the group of acyl esters are held in place during catalysis; lysine 286 and valine 288 line this pocket [128]. Due to the large size of the active site BuChE can accommodate larger substrates such as the four carbon group of butyrylcholine or the aromatic ring of benzylcholine [122].

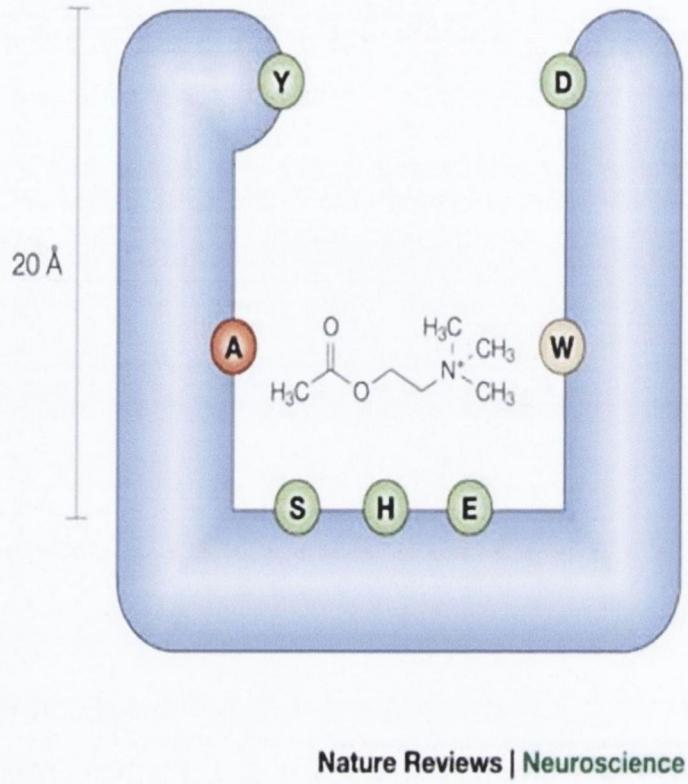

Figure 1.15 The catalytic triad of the active site of butyrylcholinesterase.

The active site consists of the amino acids serine (S), histidine (H), and glutamic acid (E). The acyl group of the substrate (acetylcholine is shown here) fits in the acyl pocket (A), whereas the quaternary nitrogen interacts with the anionic site that is formed by the amino acid tryptophan (W). Substrates are guided down the active site gorge by interaction with aspartic acid 70 (D) and tyrosine 332 (Y) residues found at the lip of the active site gorge [122].

1.4.2 Molecular forms of BuChE

BuChE exists in different molecular forms, including monomers and oligomers that consist of identical catalytic subunits. The molecular forms of BuChE exist as hydrophilic or membrane-bound forms [117].

The globular forms exist as G_1, G_2 and G_4 containing one, two or four subunits respectively. The globular forms of the enzyme are hydrophilic with the exception that the G_4 form of BuChE may be membrane-bound. G_1 is the symmetric monomeric form [117]. G_2 consists of two monomers that are joined by a disulphide bridge formed between the cysteine 571 residues of each monomer [129]. Two G_2 forms can be held together by hydrophobic interactions to form a tetramer, the G_4 globular form [87]. Globular BuChE also occurs in asymmetric membrane-bound forms that are amphiphilic and consist of tetramers (G_4) that are anchored to membranes by a protein anchor, known as proline-rich membrane anchor (PRIMA). PRIMA is a 20 kDa (p-subunit) integral membrane protein that possesses a proline-rich attachment domain (PRAD). PRIMA organises BuChE tetramers and anchors them to plasma membranes. 95% of the BuChE activity found in human plasma is due to the G_4 form. The breakdown of the G_4 form in plasma leads to the formation of by-products such as dimers and polymers [117, 129, 130].

The asymmetric forms of BuChE have an elongated shape and are bound to the extracellular matrix [87]. They contain one to three tetramers of subunits linked by disulphide bonds that are attached to membranes by a triple helical non-catalytic collagen anchor. The tetramer in the collagen-tailed form is called A_4 and two A_4 tetramers constitute the A_8 form. Three A_4 forms make up the complex A_{12} form. Collagen Q (ColQ), like PRIMA, also contains a PRAD in its subunit. ColQ attaches the asymmetric molecular forms to the extracellular domain (*Figure 1.16).* ColQ is required for assembly and accumulation of asymmetric BuChE at the synaptic cleft. The ColQ gene appears to encode the collagenous tails of BuChE as asymmetric BuChE is not detectable in ColQ-deficient mutant mice while the globular form is retained [117, 131, 132].

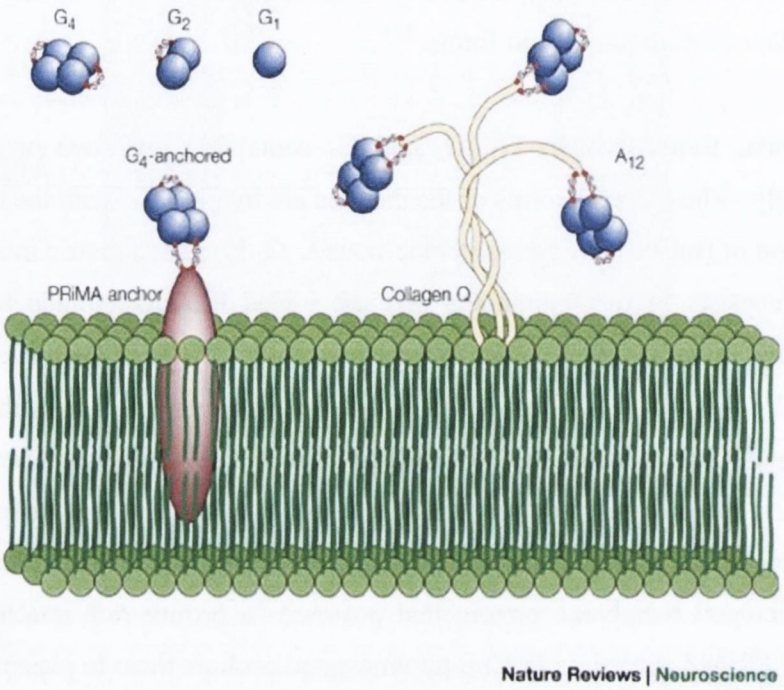

Figure 1.16 The molecular forms of butyrylcholinesterase [122] *.*

Globular forms G1, G2 and G4; asymmetric form A12.

1.4.3 Functions of butyrylcholinesterase

1.4.3.1 Introduction

BuChE has no clear physiological function or exclusive substrate. It was therefore named non-specific or pseudocholinesterase. It was regarded as the single troublesome enzyme, which unless inhibited, upset the results of studies on AChE. BuChE hydrolyzes higher esters of choline, such as butyrylcholine (BuCh) and propionylcholine (PrCh) more rapidly than it hydrolyzes ACh. This is the reverse of the pattern shown by AChE [117, 120]. Moreover, BuChE exhibits its maximum enzymatic activity at high concentrations of acetylcholine but it shows slight activity at low substrate concentrations; the opposite is true for AChE. Excess ACh will inhibit AChE but not BuChE. Additionally, the K_m values of BuChE exceed those of AChE for choline esters [113, 120]. The neuromuscular blocker suxamethonium competes with ACh for cholinergic receptors at the neuromuscular junction. Suxamethonium is not hydrolyzed by AChE and its action persists until it has been hydrolyzed by BuChE [133]. Pseudocholinesterase in the plasma and liver metabolizes alkaloids such as cocaine as well as local anaesthetic derivatives procaine, chlorprocaine and tetracaine [116]. Human BuChE expressed sequence tags are found in complementary deoxyribonucleic acid (cDNA) libraries from many different tissues, including germ cells, foetal and adult tissue cells and malignant tumours. This indicates a multifunctional role of BuChE [78].

1.4.3.2 Distribution of BuChE

In the human CNS, AChE is present in much greater quantities than BuChE and displays a much more consistent association with the pre- and post-synaptic components of the cholinergic pathways [116]. BuChE is thought to have a more restricted neuronal distribution in the CNS. The number of BuChE rich neurons in the human cerebral cortex is approximately two orders of magnitude less than the number of AChE-rich neurons. BuChE is present in many populations of neurons in the human amygdala and hippocampal formation. In the amygdala, the distribution of BuChE is different from that of AChE in that BuChE is found predominantly in the neurons and their processes, whereas AChE is found predominantly in the neuropil. In the hippocampal formation, BuChE and AChE are found in neurons and their processes

with an overlap in their distribution, shapes and relative numbers of neurons, but only AChE is found in the neuropil [134]. In the superior cervical ganglion of rats BuChE active sites are approximately equal to the number of AChE sites. Both enzymes are also structurally similar which may imply that BuChE possesses a precise physiological role similar to that of AChE. It has been suggested that BuChE may play a role in cholinergic neurotransmission because it catalyses the hydrolysis of acetylcholine [135]. Burgen and Chipman (1951) measured the activity of AChE and BuChE in the nervous system of the dog and found that BuChE was present in relatively large amounts in the fibre tracts, exceeding the activity of AChE in these areas [136]. In wild-type mouse brain BuChE activity is 10% of AChE activity [78]. Human BuChE is clearly synthesized in the brain, and not derived from plasma, since cDNA clones have not been found in brain cell cDNA libraries [137]. BuChE is present throughout the thalamus with neurons widespread in the anteroventral, mediodorsal, ventral, lateral and pulvinar thalamic nuclei. These thalamic nuclei are related to cognitive and behavioural functions suggesting that BuChE may play an important role in cognition [138].

BuChE may act to hydrolyze ACh in the absence of AChE. However, it is an inadequate substitute for AChE based on the phenotype of $AChE^{-/-}$ mice. AChE knockout mice have severe abnormalities and many do not survive until adulthood. The level of BuChE activity in the serum of $AChE^{-/-}$ mice is not increased in the absence of AChE [78, 139]. When 0.05 mg/kg bambuterol, an inhibitor of BuChE, is administered to $AChE^{-/-}$ mice BuChE activity decreases peripherally but not in the brain. Induced apnea and death occur in the adult and neonate $AChE^{-/-}$ mice without affecting littermate $AChE^{+/+}$ and $^{+/-}$ animals, suggesting that BuChE is essential for survival peripherally, particularly in respiratory movements in AChE knockout mice [140].

$BuChE^{-/-}$ mice are healthy and indistinguishable from wild-type mice under normal conditions. However, they are unusually sensitive to succinylcholine and in a study by Li *et al.* $BuChE^{-/-}$ mice treated with 1 mg/kg of succinylcholine intraperitoneally (i.p.) died of respiratory failure within 11 minutes. Additionally, nicotinic acetylcholine receptor function seems to be normal in $BuChE^{-/-}$ mice but muscarinic M_2 and M_4 receptor function seems to be altered in BuChE knockouts [141].

BuChE is found peripherally at the neuromuscular junction and asymmetric and globular forms of BuChE are detectable in muscle. In $ColQ^{-/-}$ mice membrane associated BuChE persists in the absence of ColQ; this is likely to be associated with nerve terminals or terminal Schwann cells [117, 131]. BuChE is present in the peripheral nerve but it is associated with the Schwann cells rather than the axons [120].

1.4.3.3 Embryology

BuChE and AChE mRNA expression have been found in placental RNA. Early cultured cytotrophoblasts show very faint AChE mRNA signals suggesting that the gene for BuChE might be the primary cholinesterase gene expressed in the early placenta perhaps to protect against and metabolize poisons and drugs. Early syncytiotrophoblast cells produce mainly BuChE, whereas term placenta cells produce primarily AChE. BuChE has also been found in the chorionic villi indicating that some of the enzyme might have originated from serum [142].

In cultivated retinal neurons the expression of cholinesterases appears to be time-regulated in that BuChE expression precedes AChE expression. Cholinesterases display a co-regulation with each other so that when BuChE is down-regulated the expression of AChE is increased. However, BuChE apparently cannot completely replace the function of AChE as development of the retina in $AChE^{-/-}$ mice is drastically disturbed [143].

A large proportion of live births in AChE knockout mice indicate that AChE is not essential during embryogenesis and foetal development or that a compensatory mechanism exists. Maternal AChE may cross the placenta to support survival of the growing foetus or BuChE may replace AChE during development [144].

However, during embryogenesis at embryonic day 9 the neural tube stains heavily for BuChE activity. During formation of the dorsal root ganglion BuChE activity is prominent while that of AChE is barely evident. At later stages BuChE disappears from the neurons but becomes highly expressed in the glial cells of the surrounding

neuropil and ganglionic roots. BuChE is thought to be involved in sensory neuron cell proliferation and is replaced by AChE in post-mitotic differentiation [145].

Zebrafish do not possess functional BuChE activity. AChE knockout zebrafish exhibited paralysis, severe defects of the neuromuscular apparatus and lethality at the early larval stage. Yet AChE knockout mice survive for months after birth indicating that perhaps BuChE can partially compensate for the loss of AChE activity [146].

1.4.3.4 Lipid metabolism

BuChE is thought to play a role in lipid metabolism. In fact hyperlipidaemic patients were found to have significantly higher serum levels of BuChE when compared to a control group. Kalman *et al.* suggested that expression of the BuChE gene is upregulated by hyperlipidaemia [147]. It has also been shown that serum BuChE activity is elevated in patients with both type I and type II diabetes mellitus and there is a positive correlation between BuChE activity and triacylglycerol (TG) concentrations [148]. Furthermore, in a study of insulin-treated patients with type II diabetes mellitus a positive correlation was found between BuChE activity and serum TG concentrations. Low BuChE activity might be associated with low TG synthesis, whereas high activities of BuChE might be associated with high rates of very-low density lipoprotein-triglyceride synthesis [149]. This may indicate a relationship between lipid metabolism and BuChE. However, a study by Sridhar *et al.* found a negative correlation between serum BuChE and serum total cholesterol in patients with type II diabetes mellitus [150]. Metabolic syndrome comprises a series of conditions such as increased blood pressure, excess body weight and elevated insulin levels that increase the risk of a person developing heart disease, stroke or diabetes. In patients with metabolic syndrome it has been found that there is an increase in the level of serum BuChE. Waist circumference and triglyceride levels have shown a positive correlation with BuChE levels. This may indicate a link between BuChE activity and obesity [151, 152].

Table 1.3 Conditions causing alteration in serum cholinesterase levels [133].

Type	Condition
Decrease	
Inherited	Rare cholinesterase variant.
Physiological	Last trimester of pregnancy. Newborn infants.
Acquired	Liver disease (acute hepatitis). Myocardial infarction. Collagen diseases (progressive muscular dystrophy, congenital myotonia). Hyperpyrexia. Malnutrition. Tuberculosis. Acute infections. Carcinomas. Chronic anaemias. Uraemia.
Iatrogenic	X-ray therapy. Anti-cancer drugs. Monoamine oxidase inhibitors. Contraceptive pills. Chlorpromazine chloride.
Increase	
Inherited	Electrophorectic variants (Cynthiana variant).
Acquired	Obesity. Nodular goitre. Psoriasis. Thyrotoxicosis. Nephrosis. Asthma. Anxiety states. Alcoholism. Schizophrenia.

1.4.3.5 Genetic polymorphisms of BuChE

The BuChE gene is present in a single copy on chromosome 3 and it is 73kb long containing four exons. Over 40 mutations of BuChE have been identified, but not all of them have been fully investigated [153]. The most common variant of BuChE is called the atypical variant of BuChE. A mutation at codon 70 causes the substitution of aspartic acid for a glycine residue (D70G). There is approximately 20% inhibition of the atypical BuChE with dibucaine [154]. The atypical variant is less sensitive to dibucaine inhibition and has approximately 30% lower enzymatic activity than wild-type BuChE. Since the atypical enzyme is characterized by a reduced affinity for positively charged substrates and inhibitors, this mutation identifies aspartate 70 as a key component of the anionic site. Patients with the atypical variant experience prolonged apnoea after a normal dose of succinylcholine [155, 156]. 90% of atypical variants also carry the K-variant [157] (see below).

Another genetic variant, the K-variant, has a mutation at codon 539 whereby an alanine residue is replaced by a threonine residue. This variant was first discovered by Rubinstein in 1978. He found a new allele with unusual results for dibucaine inhibition. The K-variant has approximately 33% less activity than normal BuChE activity [158]. The K-variant is a common variant and Evans and Wardell calculated that one person in 76 could be a KK homozygote [159], while Bartels *et al.* estimated that 1 in 63 people could be homozygous for this variant. In any case this variant of BuChE does not cause a clinically significant long-lasting response to a normal dose of the muscle relaxant succinylcholine [160]. In late-onset AD there is a suggestion that a synergy exists between the K-variant and apolipoprotein E4 (ApoE4) and patients with this variant are at a greater risk of developing AD [161].

The J-variant (E_1^J) was discovered by Garry in 1976. He found a family (H-J pedigree) with altered BuChE activity that did not fit into any previously known phenotype. They exhibited dibucaine inhibitions between the normal and atypical variant values thus resulting in approximately a 66% reduction in the normal BuChE molecules [162]. The J-variant occurs as a result of a mutation at codon 497 that changes a glutamic acid to a valine residue altering the expression of BuChE [160]. Patients with the J-variant are at an increased risk of sensitivity to succinylcholine. Immunological testing suggests

that the E_1^j allele has reduced numbers of immunologically active cholinesterase molecules [163]. This variant is rare in the population and in a study of 795 patients only 3 were found to possess the J-variant [159].

In 1987 Whittaker discovered another allele at cholinesterase locus 1 called the H-variant. The H-variant is caused by a single point mutation, a guanine to adenine transition at nucleotide 424 changing amino acid valine at codon 142 to methionine [164]. The E_1^h gene appears to be associated with a much more drastic reduction in enzymatic activity such as that found in some of the silent genes [165]. There is approximately 90% less BuChE activity in patients with the H-variant [122]. The frequency of the H-variant in the population is unknown as it is difficult to identify and in many cases is misclassified as the 'silent' variant (see below) [164].

Some individuals express no BuChE activity and therefore cannot hydrolyze choline esters. This variant is known as the 'silent' variant. This variant is unusual as it is less effective against a wide range of substrates and it is more resistant to dibucaine inhibition resulting in approximately 20% inhibition compared to 80% in the usual enzyme [166]. 'Silent' BuChE has a prevalence of 1:100,000 in European and American populations, but 1:24 in the Vysya community in Coimbatore, India. Patients with 'silent' BuChE are extremely sensitive to succinylcholine as there is no plasma BuChE activity to hydrolyze this anaesthetic. Cognitive testing proved a difference between 'silent' and wild-type individuals, perhaps suggestive of a role of BuChE in cognition[167].

At least twelve silent alleles of human BuChE (hBuChE) have been detected in 17 unrelated patients. All of these alleles are the result of single nucleotide substitutions or deletions which cause changes in the structure of the BuChE enzyme. Three of these variants, BChE*33C, BChE*198G and BChE201T produce normal amounts of BuChE but the enzyme is enzymatically inactive in the plasma. The six other amino acid substitutions, BChE*37S, BChE*125F, BChE*170E, BChE *471R and BChE*518L, cause reduced expression of the BuChE protein. Finally the other four silent alleles, BChE*271STOP, BChE*500STOP, BChE*FS6 and BChE*I1E3-8G, encode BuChE truncated at the C-terminus because of premature stop codons [168].

1.4.3.6 BuChE sequence homology

The BuChE gene is present in a single copy in most vertebrates [155]. Of the four exons that comprise the BuChE gene, it is exon 2 that contains 83% of the coding sequence for the mature protein [155].

The sequence homology of the BuChE gene differs between species. A study of the homology of the BuChE gene in a number of species namely man, monkey, cow, sheep, pig, rabbit, dog, rat, mouse, guinea pig, and chicken found homology between the species [169]. Human and monkey showed the highest identity with 100% homology. The lowest identity was found between human and mouse with 91.5% homology. In fact the sequence of BuChE in mouse had a greatest number of amino acid changes when compared to the human BuChE gene. However, the sequence around the active site, serine 198, and the anionic site, aspartate 70, were preserved in human, monkey, sheep, cow, rabbit, pig, dog and mouse [169]. There is 89.3% homology between human and horse BuChE. Differences in the metabolism of drugs between species may be due to differences in the homology of the BuChE gene [170]. Moreover, preservation of the active site and the anionic site between species suggests a similar functional role of BuChE among species. Within the mouse species it has been found that the BuChE gene shares 52% homology with the mouse AChE gene [171].

The evolutionary retention of the BuChE gene suggests it the enzyme has an important function. It is estimated that it would take 2.2 million years for an evolutionary change in one amino acid in the BuChE sequence [169].

1.5 Drug Treatment in Alzheimer's Disease

1.5.1 General

Since the cholinergic hypothesis in the 1970s there has been an attempt to augment cholinergic function in the expectation that enhancement of the cholinergic system would improve AD. Anti-inflammatory agents, neurotrophic growth factors and oestrogen replacement therapy have all been tested in an attempt to improve AD symptomology.

1.5.2 Cholinergic precursors

The use of drugs to enhance cholinergic function is based on the idea that low levels of ACh lead to cognitive decline. Various strategies have been tested such as the use of precursors, choline and lecithin (phosphatidylcholine), to increase ACh production. Administration of egg lecithin to mice with dementia revealed cognitive improvement in passive avoidance performance and an increase in choline concentrations in the cortex and hippocampus compared to control animals [172]. However, studies by Jope [135] and Domino *et al.* [136] showed an increase in the level of choline in the brains of rats and mice but the level of ACh in the cortex and hippocampus remained unchanged. The use of choline and lecithin as a precursor strategy failed to show any significant cognitive improvements in controlled clinical trials. Twelve randomised trials involving 265 AD patients failed to show any clear cognitive or behavioural benefits of lecithin [173].

Cytidine 5'-diphosphocholine (CDP-choline or citicoline) is an endogenous precursor of phosphatidylcholine, an essential component of cell membranes. Phosphatidylcholine breaks down into free fatty acids and free radicals during ischaemia. CDP-choline is thought to suppress the release of free fatty acids and enhances resynthesis of phospholipids in the cell membrane [174]. Analysis of fourteen double-blind, placebo-controlled randomized controlled trials (RCTs) for cognitive impairment using CDP-choline found that there is some evidence to suggest that CDP-choline has a positive effect on memory and behaviour in the short to medium term in elderly patients with cognitive deficits associated with chronic cerebral disorders. The

benefit of CDP-choline from a global impression was strong but the limitation was the short duration of the studies [174].

Choline alphoscerate (alpha-glycerylphosphorylcholine) is a phospholipid that enters nerve cell membranes. Dosing of choline alphoscerate in rats resulted in choline incorporation into brain phospholipids in increasing amounts within 24 hours of dosing [175]. Four controlled clinical trials in patients with degenerative dementia disorders administered a daily dose of 1000 mg choline alphoscerate orally for six months showed improvement in memory and attention impairments. MMSE scores increased in these patients indicating a marked improvement in cognitive function [176].

1.5.3 Cholinesterase inhibitors

Another approach in the treatment of AD is the use of cholinesterase inhibitors that preserve acetylcholine at the synaptic cleft. These inhibitors include tacrine, donepezil, rivastigmine and galantamine. The inhibition of cholinesterase may be reversible, pseudo-irreversible or pseudo-reversible. These inhibitors may be selective for AChE or BuChE or they may inhibit both enzymes [30].

Tacrine (Cognex®) is a non-competitive, irreversible inhibitor of both AChE and BuChE, with a greater potency for BuChE [30]. Additionally tacrine has been found to block potassium channels, inhibit neuronal monoamine uptake processes and inhibit monoamine oxidase (MAO) [177]. Tacrine was the first anticholinesterase licensed for the treatment of AD in the United States in 1993. Results of a 30-week randomized, double-blind, placebo-controlled, parallel group trial revealed dose-related improvements in cognitive function in patients with probable AD [178]. Wong *et al.* found cognitive improvement in MMSE scores in patients with AD treated daily with varying daily doses of tacrine (30-120 mg) over a period of 30 weeks. However, 52% of the patients were withdrawn from this study due to side-effects of the drug such as asymptomatic increased alanine transaminase (ALT) levels, anorexia and nausea [179]. Contrary to the positive cognitive findings with tacrine use, a double-blind controlled trial conducted by Maltby *et al.* did not find any positive improvement in cognition in patients treated with an initial dose of 25 mg escalating to 100 mg of tacrine daily for 36 weeks when compared to placebo-controlled groups and in fact only half of the

patients could tolerate the highest dose of tacrine at 100 mg [180]. A serious side-effect of tacrine is significant hepatotoxicity with an elevation in the level of transamines. For this reason there is a high dropout rate from clinical trials, providing less consistent data on cognitive improvement. The hepatotoxicity is reversible upon discontinuation of the drug. Because of its hepatotoxic effects tacrine is not widely prescribed [23].

Donepezil is a reversible inhibitor of AChE with a long elimination half-life and 100% bioavailability. Unlike tacrine it does not produce liver toxicity; it does however frequently cause nausea, vomiting and diarrhoea [23, 30]. A one-year placebo controlled study demonstrated that AD patients continue to exhibit disease progression, as measured by the AD Functional Assessment and Change Scale, MMSE and clinical dementia rating scale, over time. However, treatment with donepezil for one year resulted in a 38% reduction in the risk of functional decline compared to the control group [181]. Setlzer *et al.* also showed that donepezil improves Alzheimer's disease Assessment Scale – cognitive subscale scores in patients with early AD treated for one year with daily dose of 5-10 mg in a placebo-controlled study [182]. Additionally, donepezil is found to improve and preserve cognitive function in patients with severe AD treated for 6 months with an initial dose of 5 mg for one month increasing to 10 mg for the remainder of the study [183]. On the basis of 34 reports (from 24 distinct studies), there is consistent evidence that donepezil, at both 5 and 10 mg per day, improves cognition and global function assessment for patients with AD and vascular dementia [184].

Rivastigmine (Exelon®) is a pseudo-irreversible inhibitor of both AChE and BuChE. It initially blocks the enzymes but it is metabolized by them, giving the drug a short half-life. However, cholinesterase inhibition in the CNS lasts an average of ten hours [23]. Patients with mild-moderate AD treated with 10 mg/day of rivastigmine showed enhanced cognitive ability on memory tests and in fact a twice daily dose showed greater improvement than three times daily dose of the drug [185]. Figiel *et al.* found that AD patients treated with daily doses of 3-12 mg of rivastigmine exhibited improved global functioning as assessed on the Clinical Global Impression Change scale. Initially these patients were non-responders to treatment with donepezil; however, treatment with rivastigmine enhanced cognitive function in these patients [186]. A review of clinical nine relevant studies comparing Rivastigmine and placebo revealed

consistent significant improvement in cognition and global assessment in patients treated with Rivastigmine [184].

Galantamine (Reminyl®) is a reversible competitive inhibitor of AChE. Galantamine is derived from the alkaloids from the daffodil and snowdrop family. It is an agonist at nicotinic ACh (nACh) receptor sites thus potentiating cholinergic nicotinic neurotransmission [23, 30]. At least eight clinical trials to date have shown significant cognitive enhancement and a positive effect on global assessment in AD patients [184]. A six month randomized placebo-controlled clinical trial showed a significant improvement in cognition and global function in AD patients with maintenance of function for 12 months with a daily dose of 24 mg [187]. Galantamine was found to slow the progression of cognitive decline with sustained cognitive benefits over a 36-month period when compared to untreated AD patients [188].

Physostigmine is a reversible inhibitor of AChE. Controlled release physostigmine salicylate (CR physostigmine) proved effective in an objective test of cognitive function in a group of 850 patients with mild to moderate AD; however nausea and vomiting was experienced by 47% of the group [189]. Similar cognitive enhancement was also found in a 24-week RCT with CR physostigmine. Moreover, there were mild to moderate gastrointestinal side-effects which may have reduced any positive response of the drug with respect to ADL [190].

1.5.4 Glutaminergic antagonist

Disturbance in the glutamatergic system has also been implicated in contributing to cognitive deficits in AD with biochemical evidence suggesting pre- and post-synaptic glutamatergic hypoactivity [191]. Memantine is an NMDA (N-methyl-D-aspartic acid) antagonist. Treatment with memantine was found to reduce clinical deterioration in moderate to severe AD [192]. Patients with mild to moderate vascular dementia showed improved cognitive MMSE scores with daily treatment of memantine at 10 mg twice daily [193]. Six distinct studies consistently indicate an improvement in cognition and global assessment with memantine treatment with less frequent agitation when compared to placebo groups [184].

1.5.5 Anti-inflammatory drugs

Inflammation is associated with AD. It appears that cyclo-oxygenase 2 (COX-2) plays a vital role in the inflammatory process and is expressed in inflammatory cells such as monocytes and macrophages. It has a primary role in the synthesis of prostanoids involved in pathological processes such as acute and chronic inflammation [23]. It is induced at sites of inflammation rather than being expressed [194]. There is an increase in COX-2 in the brains of AD patients with an increased expression of COX-2 mRNA in the frontal cortex and also in the temporal cortex [195, 196]. The use of NSAIDs (non-steroidal anti-inflammatory drugs) for two years was found to be associated with an 80% reduction in AD [197]. The Rotterdam study which investigated NSAID use over a ten year period also reported that long-term use of NSAIDs reduces the risk of developing AD [198].

1.5.6 Oestrogen therapy

Evidence for a protective effect on AD is strongest for NSAIDs and hormone replacement therapy (HRT) [197]. A study by Schmideskamp *et al.* found that oestrogen replacement in the postmenopausal period reduced the risk of women developing AD by half. It is thought that oestrogen may prevent AD by directly influencing nerve cells in the brain [199]. Results from a population-based study also suggested that oestrogen replacement therapy is associated with a reduced risk of AD in postmenopausal women [200]. However, a one-year randomized, placebo-controlled double-blind study involving women with mild to moderate AD and hysterectomies failed to show any cognitive improvement following oestrogen therapy [201]. The investigational drugs neurestrol and ABPI-124 underwent testing to prevent AD; they were thought to be useful in preventing brain cell damage without producing the feminizing effects of oestrogen [202]. However, no further information has been found on these investigational drugs since 2000.

1.6 Novel isosorbide-based butyrylcholinesterase inhibitors

This purpose of this thesis was to determine the pharmacological effects of a novel class of isosorbide-based BuChE inhibitors. These novel and highly selective BuChE inhibitors were developed in the School of Pharmacy and Pharmaceutical Sciences in Trinity College Dublin. Initial studies found that these compounds are approximately 1,000-fold more selective for BuChE than tetraisopropylpyrophosphoramide (iso-OMPA) and they possessed the additional advantage of 1,000-fold greater potency [203].

The compounds are potent and selective inhibitors of human BuChE and they use the simple sugar, isosorbide, as a building block. It was initially discovered that 2-ester derivatives of isosorbide were rapidly hydrolyzed by BuChE [204]. It was then surmised that replacement of the 2-ester group with a carbamate or reversed carbamate at the 2' position of the isosorbide would produce more selective and potent inhibitors of BuChE. The 5'-position possessed an ester [203, 205].

The novel compounds explored here are isosorbide 2-benzylcarbamate 5-nicotinate (compound 21), isosorbide 2-benzylcarbamate 5-salicylate (compound 30), isosorbide mono-ethyl carbamate 5-salicylate (compound 33), isosorbide 2-benzylcarbamate 5-benzoate (compound 51) and isosorbide 2-butylcarbamate 5-benzoate (compound 57) *(Figure 1.17)*. These compounds were firstly tested *in vitro* to determine their potency against BuChE in different species. The most potent BuChE inhibitors were then brought forward for *in vivo* testing in the mouse. The work of the thesis primarily focuses on one of the novel BuChE inhibitors, isosorbide 2-benzylcarbamate 5-benzoate (compound 51).

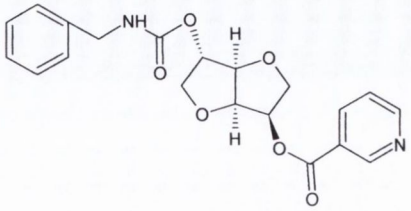

Compound 21

isosorbide 2-benzylcarbamate 5-nicotinate

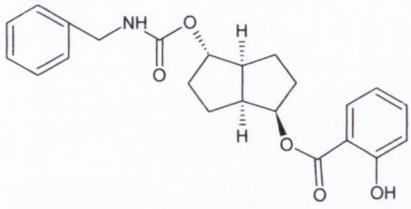

Compound 30

isosorbide 2-benzylcarbamate 5-salicylate

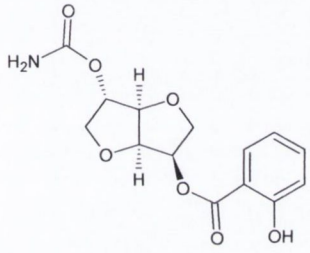

Compound 33

isosorbide mono-ethyl carbamate 5-salicylate

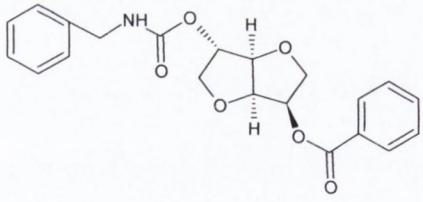

Compound 51

isosorbide 2-benzylcarbamate 5-benzoate

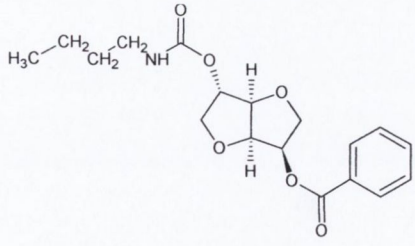

Compound 57

isosorbide 2-butylcarbamate 5-benzoate

Figure 1.17 Novel isosorbide-based compounds.

As the precise function and pathological role of BuChE have not yet been established it was thought that these novel compounds would provide a unique opportunity to explore the physiological and pathological roles of BuChE. Additionally it was desirable to explore whether inhibition of BuChE by such compounds could be a viable therapeutic strategy in AD based on animal models. The majority of current AD drug treatments are AChE inhibitors or inhibitors of both AChE and BuChE; none is a specific BuChE inhibitor.

1.7 Aims

- To determine the potency of the novel isosorbide-based butyrylcholinesterase inhibitors *in vitro.*

- To assess the toxicological profile of the novel drugs using ADMET predictor toxicity software, *in vitro* and *in vivo* studies.

- To produce pharmacodynamic profiles of the novel compounds *in vivo.*

- To produce a lesion-based model of AD and determine whether acute treatment with a novel BuChE inhibitor could reverse the cognitive impairments associated with the lesion-induced cholinergic deficit, using the Morris water maze and an object recognition task.

- To determine the effects of BuChE inhibition on cognitive function in young versus aged mice in the Morris water maze, an object recognition task and the radial arm maze, with a view to establishing whether BuChE inhibition might be helpful in reversing age-related cognitive decline.

- To assess the effects of chronic dosing of mice with a novel BuChE inhibitor over a one-year period and thereafter to determine cognitive function using the Morris water maze and an object recognition task, thereby exploring whether BuChE inhibition might be a useful preventative strategy in combating age-related cognitive decline.

- To assess the rates of hydrolysis of the compounds in biological fluids *in vitro* using high performance liquid chromatography (HPLC).

Chapter 2

In vitro studies and behavioural profiling of novel BuChE inhibitors

Chapter 2 *In vitro* studies and behavioural profiling of novel BuChE inhibitors

2.1 Introduction

This aim of this study was firstly to find a good animal model on which to test the novel compounds. It was important that the chosen species had plasma BuChE activity comparable to humans as the level of BuChE is known to differ between species [206]. Once the mouse was chosen as the animal model on which to test the novel drugs, their potency was assessed *in vitro* in mouse plasma. The potency of the novel compounds had previously been determined *in vitro* in human plasma and they were found to be highly selective and potent for human BuChE [203, 205]. Having established the relative potency of the novel compounds *in vitro* they were administered to mice to determine the effect of different drug doses on the behaviour of the animals using a scoring system based upon modification of the SHIRPA profile [207].

Determination of the potency of the compounds *in vitro* yielded information regarding the potential ability of the drugs to inhibit BuChE *in vivo*. In addition to this a computer-based programme, Pipeline Pilot (Accelrys, California, USA), was used to predict the activity of the novel compounds *in vivo* in terms of their aqueous solubility, absorption across the human intestine, their ability to penetrate the blood-brain barrier (BBB) and their potential to cause hepatotoxicity. The log P values of the drugs were also calculated using Chemsketch (ACD labs, Toronto, Canada) to determine the lipophilicity of the compounds and the likelihood that they would partition into the adipose tissue following peripheral administration. Based on these results the compounds which were potentially more likely to penetrate the BBB and demonstrated lowest probability of causing hepatotoxicity would be brought forward for animal testing.

The pharmacodynamic profiles of the compounds were assessed *in vivo* over a total period of 72 hours. The purpose of this part of the study was to find a suitable dose that

could be used for future behavioural studies and to determine whether at this chosen dose the novel compounds would have the potential to treat cognitive deficits such as those found in Alzheimer's disease.

As the majority of drug withdrawals from the market are due to problems associated with hepatotoxicity [208] it was next decided to determine whether a single acute dose of the novel compounds had any adverse effects on the liver. A 24-hour toxicity study was carried out and the plasma and livers of the animals were tested for any signs of hepatotoxicity using measurements of biomarkers in plasma and liver compared to the same of control animals. Additionally the liver tissues of animals were histologically examined 24 hours following a single dose of the novel compounds to determine if there were any gross changes in the liver ultrastructure.

It is thought that enzymes naturally fluctuate diurnally [209, 210]. For this reason it was decided to assess whether any diurnal variation existed in the BuChE activity within the mouse by analysis of peripheral BuChE activity.

2.2 Determination of plasma BuChE activity in animal species

In order to develop a good animal model for testing the novel butyrylcholinesterase inhibitors (BuChEIs) it was important to choose an animal species with plasma levels of butyrylcholinesterase similar to that of humans, as the initial pharmacodynamic studies would be based on peripheral BuChE inhibition. It is known that the activity of BuChE varies within [211, 212] and between species [213]. The level of plasma BuChE in male rats and mice were tested and compared with that of humans.

2.2.1 Procurement of blood

2.2.1.1 Mouse and rat blood

Blood was procured from three healthy experimentally naïve male CD-1 mice (25-35 g) and two healthy naïve male Wistar rats (200-250 g) via cardiac puncture. The animals were anaesthetized using halothane gas. A 25 gauge needle containing a small amount of lithium heparin (25,000 Units/ml) (Leo laboratories, Dublin) in its base was attached to a 1 ml syringe (Brand, UK). The needle was inserted beneath the xiphisternum and passed superiolaterally through the pericardium into the ventricles of the heart. The blood was slowly procured from the heart and subsequently transferred from the syringe into a clean 10 ml glass vial.

2.2.1.2 Human blood

10 ml of venous blood were procured from healthy male volunteers by a nurse in the Health Centre in Trinity College Dublin. A volunteer information leaflet (Appendix I) was given to the volunteer and the nature of the research was explained. A consent form was signed by the volunteer (see Appendix I). A sterile 21 gauge needle (21 G x 1½ inches) (Greiner Bio-one, UK) was inserted into the cubital vein in the cubital fossa of the forearm and the venous blood was collected in a 4 ml lithium heparinized vacuette vial (Greiner Bio-one, UK).

2.2.2 The Ellman assay

2.2.2.1 Introduction

The Ellman assay is a sensitive colourimetric assay used to determine cholinesterase activity in blood or tissue samples. It was developed in 1961 by George Ellman [214]. The enzyme activity is measured from the interaction of the substrate butyrylthiocholine iodide (BTCI) with BuChE to form thiocholine and acetate. The thiocholine subsequently interacts with 5,5'-dithio-bis(2-nitrobenzoic acid) (DTNB) to produce a yellow colour. The higher the level of enzyme in the sample the greater the production of thiocholine that is available to react with DNTB thus producing a greater colour change. It is based upon the coupling of the following reactions:

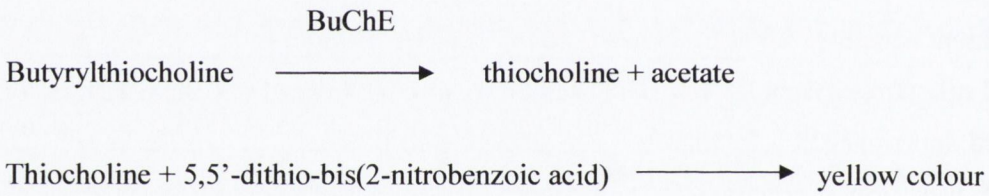

Figure 2.1 Reaction pathway of the Ellman assay

2.2.2.2 Preparation of plasma

Heparinized venous human, rat and mouse cardiac blood were centrifuged at 3,000 rpm (Sorvall RT6000B) for 10 minutes at 4°C. The plasma was removed and 1 ml aliquots were transferred to labelled 1.5 ml Eppendorfs (Brand, Germany). Plasma samples for near-immediate use were stored on ice until tested for BuChE activity in the Ellman assay. The remaining aliquots of plasma were frozen at -80°C until use. Storage of plasma samples for up to 14 months at -20°C has previously shown no detrimental effects on cholinesterase activity [215].

2.2.2.3 Determination of BuChE activity

2 µl of human plasma were incubated with 198 µl of 0.1 M phosphate buffered saline (PBS) pH 8.0 in the presence of 25 µl of 3 mM 5,5'-dithio-bis(2-nitrobenzoic acid) (DTNB) (Sigma-Aldrich, Germany) for 30 minutes at 37°C in a 96-well plate (Cellstar, Lennox, Dublin). 3 µl of rat and mouse plasma were incubated under the same conditions as human plasma, with the quantity of PBS pH 7.4 adjusted accordingly. Following incubation, 25 µl of 5 mM butyrylthiocholine iodide (BTCI) (Sigma-Aldrich, Dublin) was added to the plate. The final assay volume for all samples was 250 µl per well. Eight replicates of three blood samples from three of each species were used (n = 3). The absorbance was measured at 405 nm using a spectrophotometer (Anthos Labtec Instruments, Austria). The BuChE activity (µmol/min/ml) was calculated by dividing the average absorbance by the extinction coefficient for nitrothiobenzoate, 1.36×10^4.

2.2.3 Results

It was found that BuChE activity in plasma was different between the species. The activity of BuChE in human plasma was considerably higher than that of mouse and rat plasma. Rat plasma showed the lowest level of BuChE activity. A one-way ANOVA revealed a significant difference between the groups, $F(2, 23) = 1615.074$, $P < 0.001$. Post-hoc analysis using Tukey's HSD found the differences were between human and mouse ($P < 0.05$), human and rat ($P < 0.05$), and mouse and rat ($P < 0.05$).

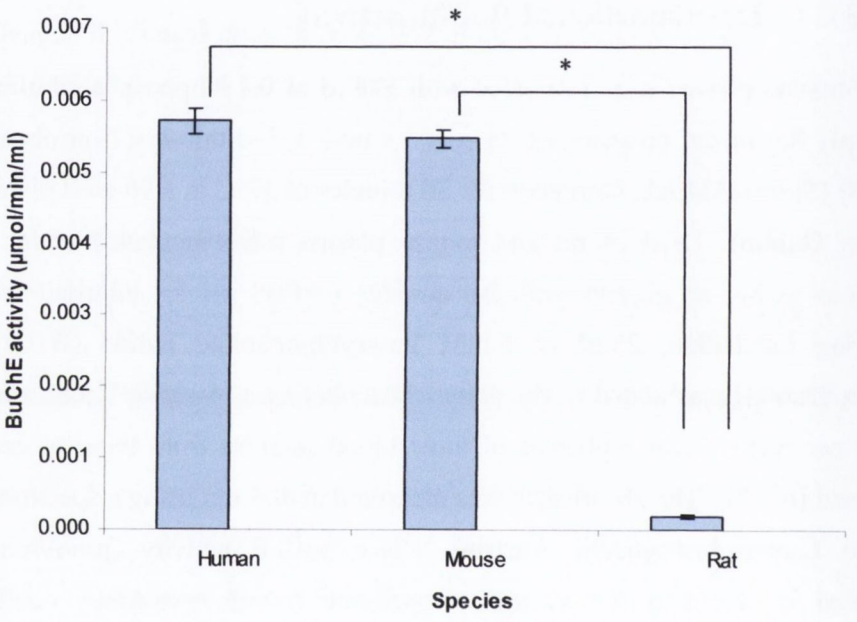

Figure 2.2 *The activity of BuChE in human, mouse and rat plasma (Mean ± SEM). n = 3 per group. * P < 0.05.*

2.3 Determination of IC_{50} of the novel compounds using the Ellman assay

2.3.1 Introduction

Assessment of the IC_{50} values of the novel compounds *in vitro* was used to determine and compare the potency of the novel compounds against BuChE in human and mouse plasma. As it was previously found that the rat had low plasma BuChE levels the mouse was chosen as the species for further pharmacodynamic, pharmacokinetic and behavioural profiling of the compounds. The potencies of the novel compounds were assessed *in vitro* to help determine which compounds would be most suitable to bring forward to *in vivo* testing in the mouse model.

2.3.2 Preparation of plasma

Human and mouse plasma were prepared in the same manner as described in section 2.2.2.2.

2.3.3 The Ellman assay

A stock solution of 1 mM of compounds 21, 30, 33, 51, 57, physostigmine and rivastigmine was individually dissolved in 1:3 acetonitrile (CH_3CN): 0.1 M phosphate buffered saline (PBS) pH 8.0 in a 10 ml volumetric flask. Eight serial dilutions were made from the 1 mM stock solution of each compound to reach a final concentration of 1 nM.

2 µl of human plasma were added to a 96-well plate containing 173 µl of PBS pH 8.0 and 25 µl of 3 mM DTNB. 25 µl of the inhibitor were added and the plate was incubated at 37ºC for 30 minutes [214]. Eight replicates of each sample were used. Following the 30 minute incubation period 25 µl of 5 mM BTCI were added, to reach a final volume of 250 µl. 3 µl of mouse plasma were used in the assay and the volume of PBS pH 8.0 was adjusted to reach a final volume of 250 µl.
The absorbance was read at 405 nm using a spectrophotometer (Anthos Labtec Instruments, Austria). The absorbance values were plotted as a function of inhibitor

concentration using Graphpad Prism version 4.0. Non-linear regression was used to determine the IC_{50} value for each compound.

2.3.4 Results of IC_{50} values

The novel isosorbide-based BuChE inhibitors displayed good IC_{50} values *in vitro (Table 2.1)*. However, there are apparent differences in the level of enzyme inhibition by the novel compounds and rivastigmine between the species. These compounds appear to display greater in vitro potency for human BuChE than mouse BuChE. This may be due to structural differences in the active site of the enzyme between the human and mouse.

Table 2.1 IC_{50} values for the novel BuChE inhibitors.

	IC_{50} values (nM)	
	Human plasma	**Mouse plasma**
Compound 21	0.3329	N/A
Compound 30	0.01	2.731
Compound 33	6.844	14.57
Compound 51	30.00	1090
Compound 57	75.77	458.8
Physostigmine	22.00	99.00
Rivastigmine	42.14	2864

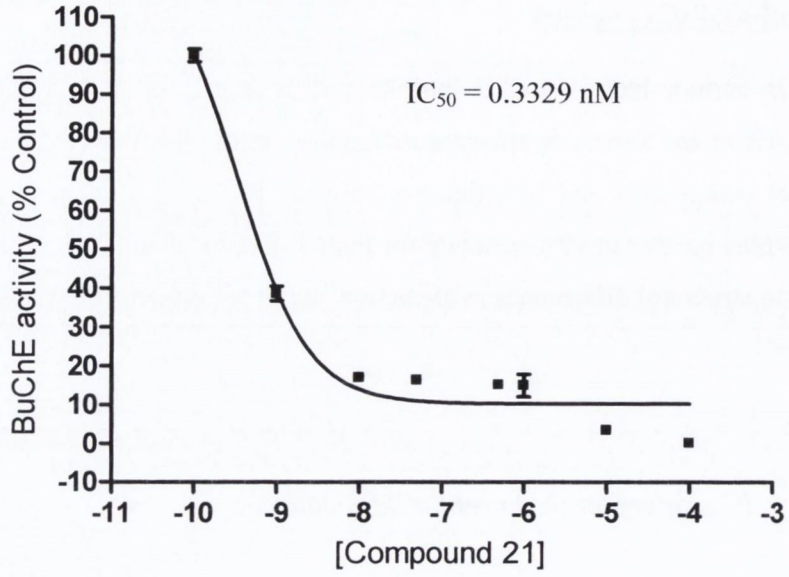

Figure 2.3 Inhibition of butyrylcholinesterase by compound 21 in human plasma.

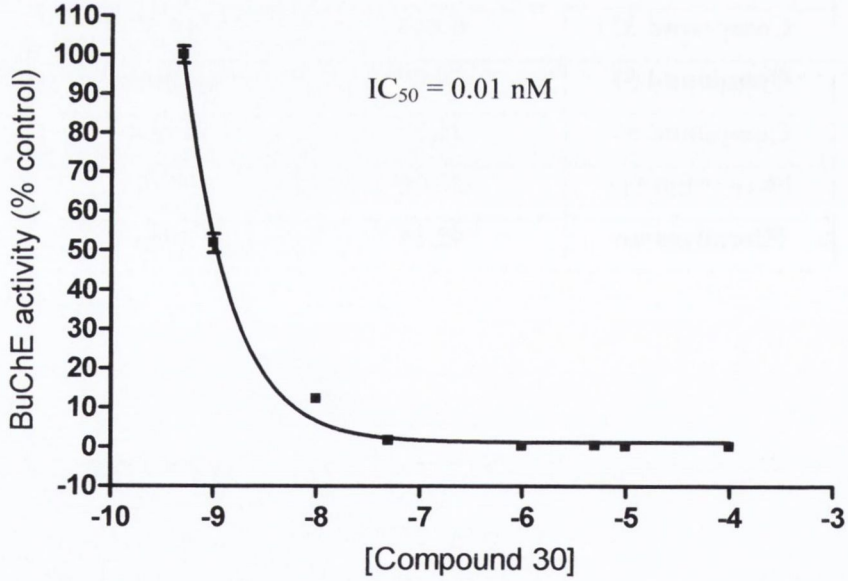

Figure 2.4 Inhibition of butyrylcholinesterase by compound 30 in human plasma.

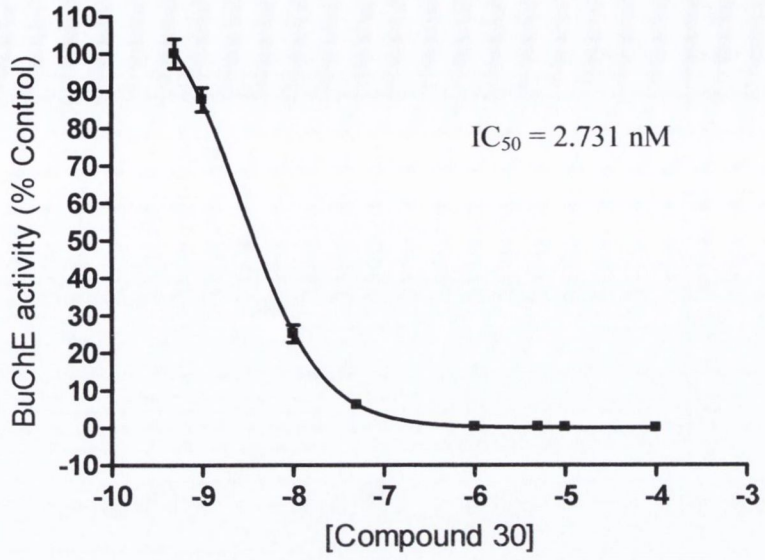

Figure 2.5 *Inhibition of butyrylcholinesterase by compound 30 in mouse plasma.*

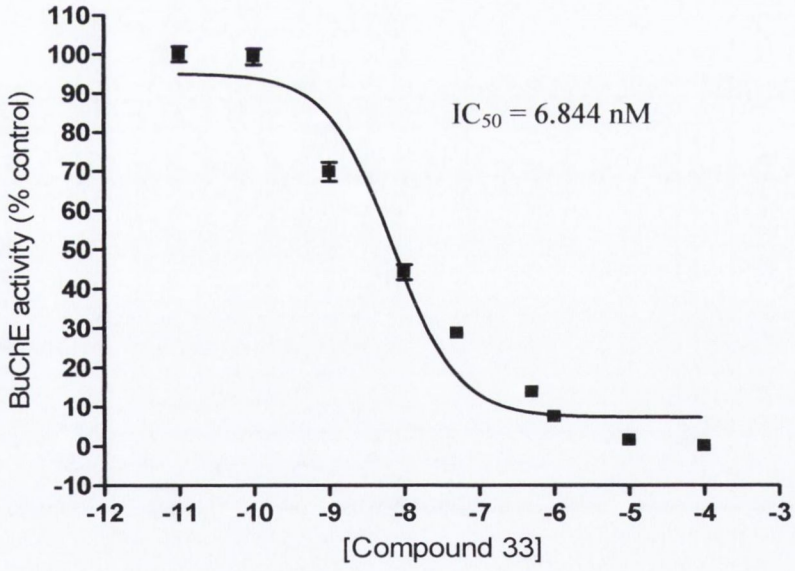

Figure 2.6 *Inhibition of butyrylcholinesterase by compound 33 in human plasma.*

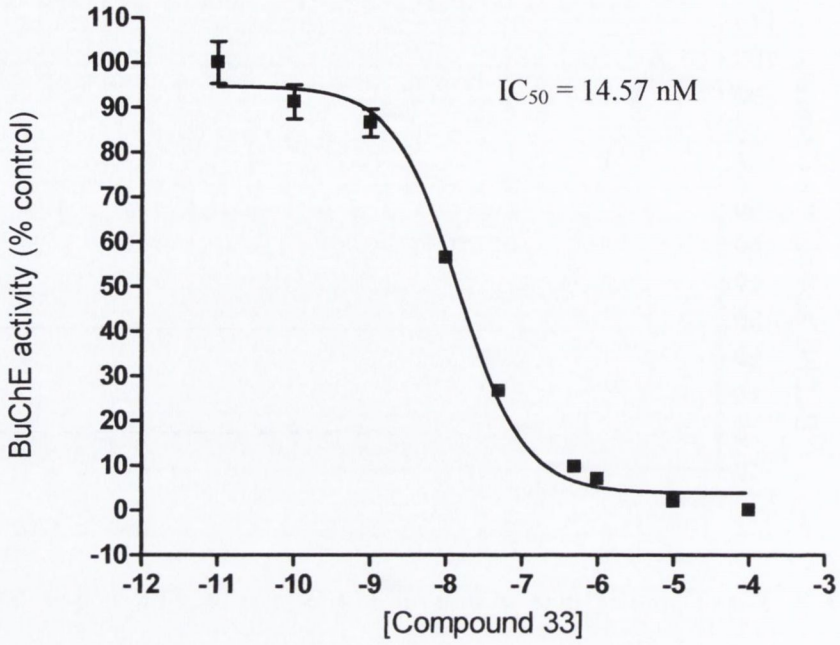

Figure 2.7 *Inhibition of butyrylcholinesterase by compound 33 in mouse plasma.*

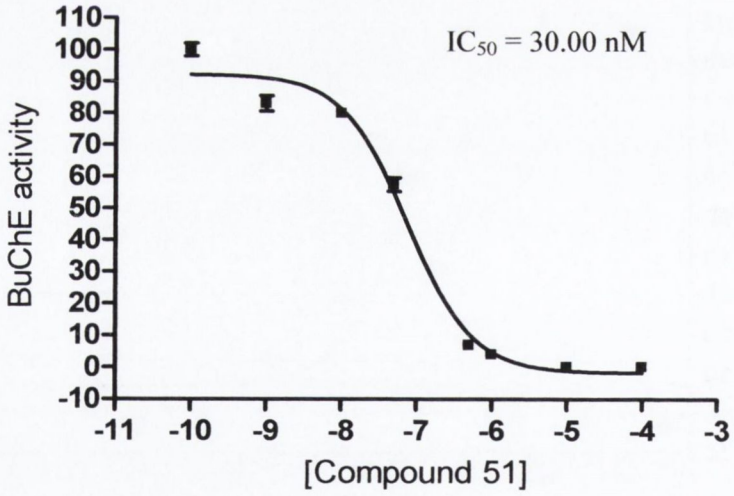

Figure 2.8 *Inhibition of butyrylcholinesterase by compound 51 in human plasma.*

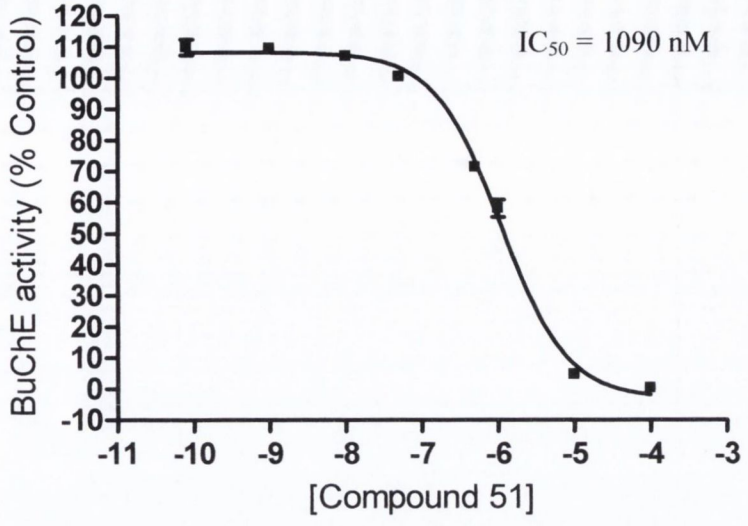

Figure 2.9 *Inhibition of butyrylcholinesterase by compound 51 in mouse plasma.*

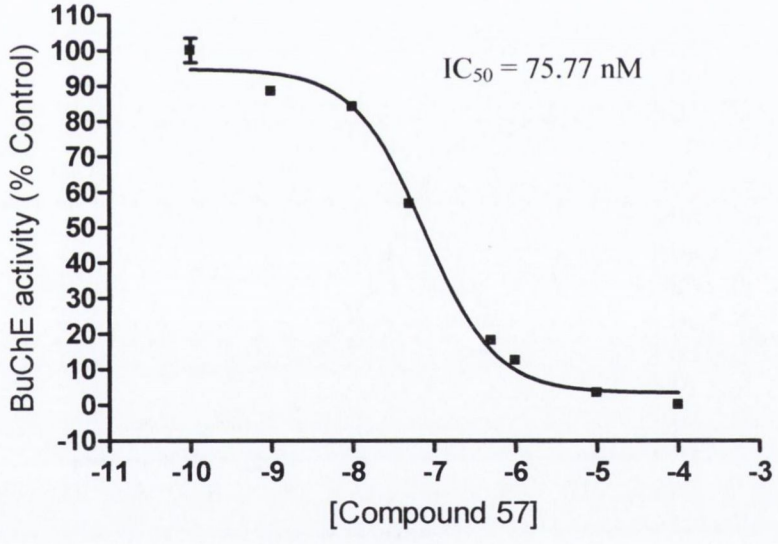

Figure 2.10 *Inhibition of butyrylcholinesterase by compound 57 in human plasma.*

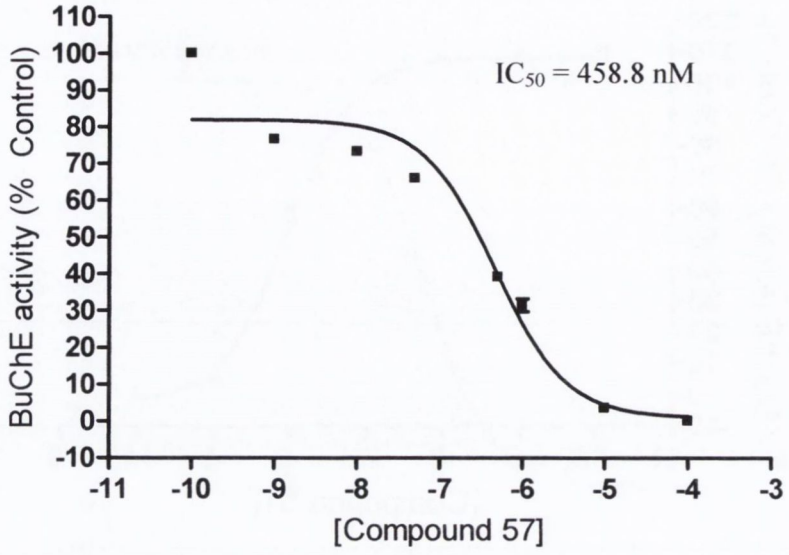

Figure 2.11 Inhibition of butyrylcholinesterase by compound 57 in mouse plasma.

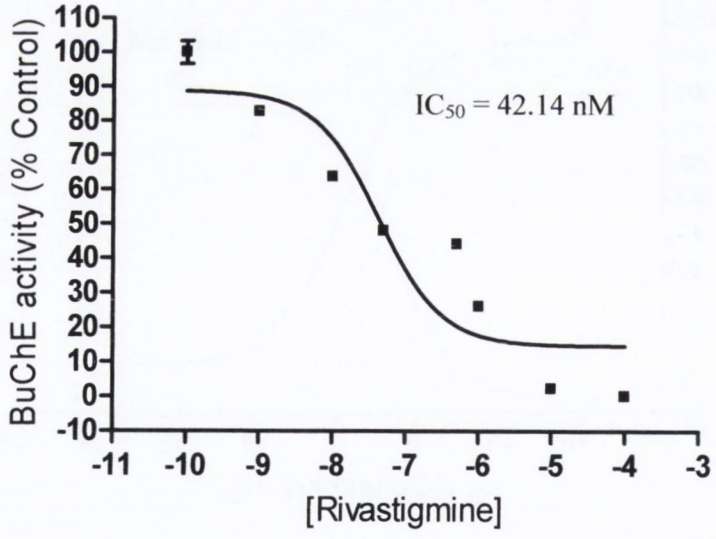

Figure 2.12 Inhibition of butyrylcholinesterase by rivastigmine in human plasma.

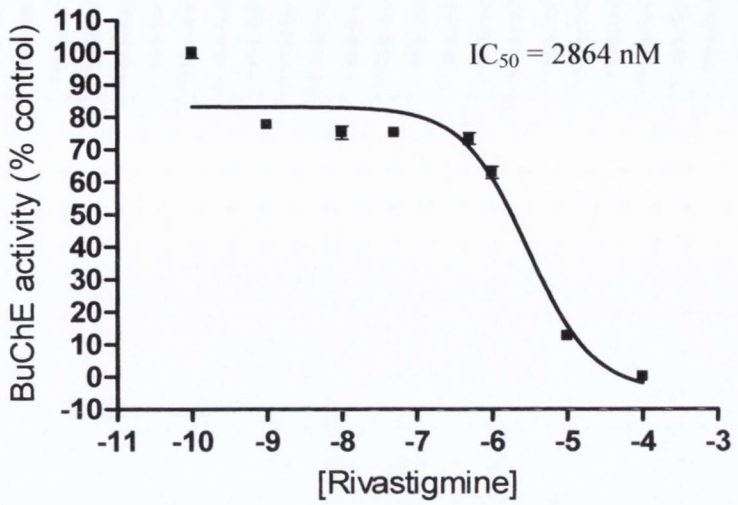

Figure 2.13 Inhibition of butyrylcholinesterase by rivastigmine in mouse plasma.

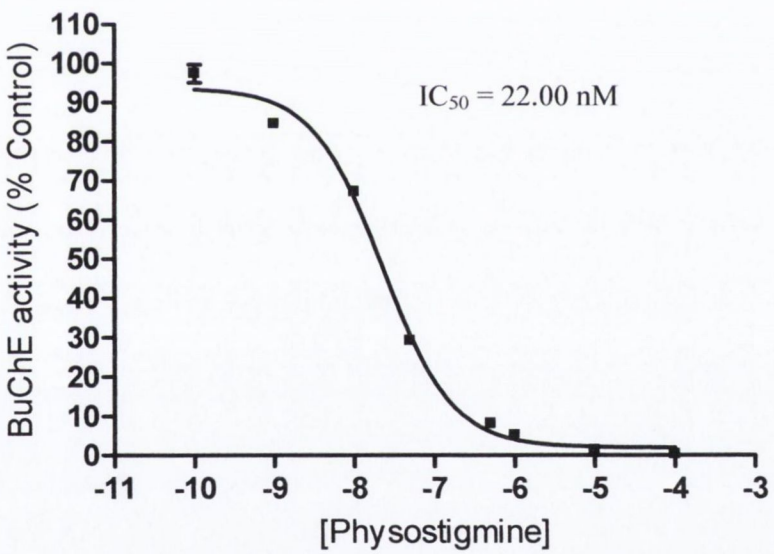

Figure 2.14 Inhibition of butyrylcholinesterase by physostigmine in human plasma.

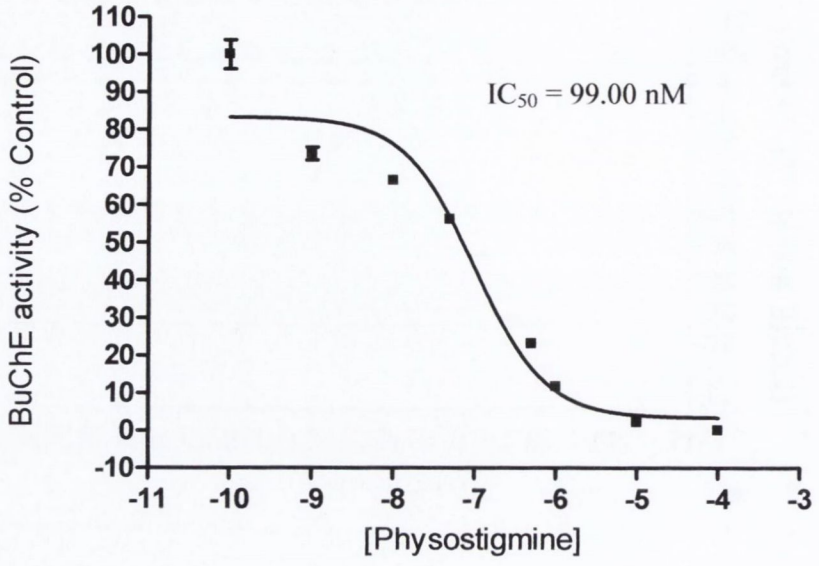

Figure 2.15 Inhibition of butyrylcholinesterase by physostigmine in mouse plasma.

2.4 ADMET (Absorption, Distribution, Metabolism, Excretion, Toxicity) and Log P values

2.4.1 Introduction

Pipeline Pilot version 6.0 (Accelrys, California, USA) was used to predict the ability of the most potent novel compounds to cross the blood-brain barrier (BBB) and the likelihood of their causing any adverse effects such as hepatotoxicity based upon their chemical structure. This programme filters the compounds on the basis of published models. The ADMET component of the programme determines aqueous solubility (based on a dataset of 775 compounds), human intestinal absorption (based on a dataset of 182 compounds), BBB penetration (model validated against 881 compounds) and hepatotoxicity (based on 382 compounds known to exhibit liver toxicity).

As these novel compounds would be administered in sterile water for injection it was necessary to explore their aqueous solubility. As oral administration would be used along with intraperitoneal injection, estimation of the level of absorption across the intestine would be valuable. As these compounds essentially target central BuChE, it was also necessary to evaluate their ability to cross the BBB. Penetration of the BBB requires that the compounds have some degree of lipophilicity but it is also desirable for them to be somewhat water soluble for administration purposes. Evaluation of the compounds' ability to cause liver damage was also assessed based upon the ADMET programme. The log P values were calculated in Chemsketch (ACD labs, Toronto, Canada) to determine the lipophilicity of the compounds with respect to their potential to partition from the blood into the adipose tissue following administration.

2.4.2 Methods

Compounds 21, 30, 33 and 51 were drawn in ADME software (Pharma Algorithms, USA) and exported as a multi mol2 file. The BBB and ADMET properties of the molecules were subsequently calculated using the BBB and ADMET modules of the Pipeline Pilot computer application (Accelrys, California, USA). This involved fragmenting the molecules and calculating descriptor properties (solubility, molecular weight and hydrophobicity) for each of the fragments followed by the prediction of an overall score for each of the whole molecules. The scoring is ranked as outlined below in 2.4.2.1 – 2.4.2.4.

2.4.2.1 Key to aqueous solubility levels

This descriptor uses linear regression to predict the aqueous solubility of each compound in water at 25°C. The calculable properties of the component are:

ADMET solubility: The base 10 logarithm of the molar solubility as predicted by the regression.

ADMET solubility level: Assigns the molecule to one of seven solubility classes based on the value of ADMET solubility. The classes define the solubility relative to a compendium of known drugs.

Level	Value	Description
0	< -8.0	Extremely low solubility, lower than 95% of drugs.
1	-8.0 to -6.0	Very low solubility, at borderline of 95% of drugs.
2	-6.0 to -4.0	Low solubility, at lower end of 95% of drugs.
3	-4.0 to -2.0	Good, slightly soluble to soluble.
4	-2.0 to 0.0	Optimal solubility.
5	> 0.0	Very soluble, perhaps too soluble.
6	1000	Warning; molecules with one or more unknown AlogP98 types.

2.4.2.2 Human intestinal absorption

This model predicts human intestinal absorption (HIA) after oral administration. Intestinal absorption is defined as a percentage absorbed rather than as a ratio of concentrations (cf. blood-brain penetration); a well-absorbed compound is one that is absorbed at least 90% into the bloodstream in humans.

The calculable property of the component is:

ADMET Absorption level: The predicted level of absorption. The levels are defined as:

0 = Good

1 = Moderate

2 = Low

3 = Very low

2.4.2.3 Blood-Brain Barrier Penetration

Accelrys blood-brain barrier penetration model can calculate two properties:

ADMET_BBB: Log of Brain/Blood partition coefficient (LogBB).

ADMET_BBB_Level: Ranking of the LogBB values into one of the following levels:

0 : Very high; brain-blood ratio greater than 5:1.

1 : High; brain-blood ratio between 1:1 and 5:1.

2 : Medium; brain-blood ratio between 0.3:1 and 1:1.

3 : Low; brain-blood ratio less than 0.3:1.

4 : Undefined. Molecule is outside the confidence area of the regression model used to calculate LogBB.

2.4.2.4 Hepatotoxicity

The hepatotoxicity model predicts potential organ toxicity for a wide range of structurally diverse compounds.

The calculable properties of the model are:

ADMET hepatotoxicity: Binary prediction of whether or not the molecule is likely to cause dose-dependent liver injuries. Values are:

0 = Non-toxic

1 = Toxic

2.4.2.5 Log P values

ACD/LogP database calculates the partition co-efficient, log P, for any organic structure. This database contains 18,412 chemical structures with references to experimental log P values.

The calculable properties are:

Low log P (below 0) – injectable

Medium (0 - 3) – oral

High (3 - 4) – transdermal

Very high (4 - 7) – toxic build up in fatty tissues

2.4.3 Results

	Solubility	Absorption	BBB level	Hepatotoxicity	Log P
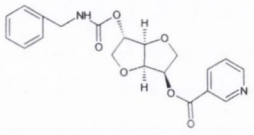	3	0	3	1	3.87 ± 0.28
Compound 21					
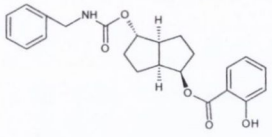	3	0	3	0	5.22 ± 0.31
Compound 30					
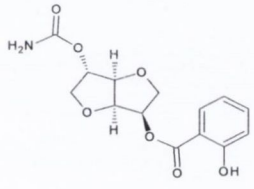	3	0	3	0	1.06 ± 0.64
Compound 33					
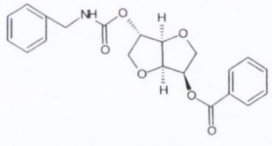	3	0	3	1	3.37 ± 0.62
Compound 51					
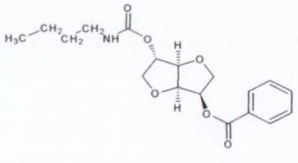	3	0	3	0	3.19 ± 0.60
Compound 57					

Solubility: 3 = good, slightly soluble to soluble.

Absorption: 0 = good.

BBB level: 3 = low; blood-brain ratio less than 0.3 - 1.

Hepatotoxicity: 0 = non-toxic.

1 = toxic.

Log P values: Low log P (below 0) – injectable

Medium (0 - 3) – oral

High (3 - 4) – transdermal

Very high (4 - 7) – toxic build up in fatty tissues

2.5 Behaviour following administration of novel compounds

2.5.1 Introduction

Having established IC_{50} values for the compounds, it was decided to determine the behavioural effects of compounds 30, 33 and compound 51. Compound 30 was chosen as it displayed good potency for mouse BuChE *in vitro* and it was predicted to be highly lipophilic and thus might penetrate the BBB. Although compound 51 had a lower potency for mouse BuChE *in vitro*, it showed reasonable solubility. Despite a prediction that this compound could be a hepatotoxic agent it was also interesting to test the accuracy of the Pipeline pilot programme. Although neither compound was predicted to have high BBB penetration it was decided to test both to determine whether their lipophilic nature gave adequate BBB penetration. Single doses of the novel compounds were administered to mice and their behaviour was monitored. A behavioural scoresheet based upon modification of the SHIRPA profile was used in this dose-ranging study to explore the primary effects on behaviour and physiological functions in parallel with monitoring the enzyme inhibitory activity [216]. The study included observation for signs of neurotoxicity such as convulsions or tremors, CNS stimulation such as excitation or aggression, and CNS depression such as loss of motor coordination or sedation. Autonomic functions such as respiration and salivation were also monitored. The purpose of this study was not to create a definitive picture of the compounds' behavioural effects, which would have entailed more extensive testing and greater numbers of animals, but merely to give guidance on their short-term safety at doses eliciting significant enzyme inhibition.

2.5.2 Animals

Nine healthy experimentally naïve male CD-1 mice (35 – 40 g) were obtained from the Bioresources Unit, Trinity College Dublin. The animals were housed in a specific pathogen free (SPF) environment with controlled temperature and humidity in individual cages with isopad bedding (Harlan, UK). The mice had *ad libitum* access to food and water. A twelve hour light/dark cycle (lights on 7 a.m. – 7 p.m. GMT) was in operation. All experiments were performed during the light cycle and carried out in a

sound-proof room. All experiments were carried out in accordance with the European (Amendment of Cruelty to Animals Act 1876) Regulations 2002.

2.5.3 Drug preparation

1 mg and 5 mg of isosorbide-2-benzylcarbamate 5-benzoate (compound 51) were dissolved in sterile water for injection (WFI) (Braun, Germany) to a final volume of 10 ml to produce concentrations suitable for delivery of 1 mg/kg and 5 mg/kg in a dosage volume of 0.1 ml/10 g. 1 mg of compound 51 was dissolved in WFI to a final volume of 1 ml to produce a concentration suitable for delivery of 10 mg/kg. The compound had a pH of ~ 6. The drug was initially insoluble in sterile WFI so the preparations were sonicated for 20 minutes at 30°C using a Branson Sonicator Model 3510 (Branson, Netherlands); thereafter it formed a solution.

1 mg and 5 mg of isosorbide 2-benzyl-carbamate 5-salicylate (compound 30) was dissolved in sterile WFI to a final volume of 10 ml. 1 mg of compound 30 was dissolved in sterile WFI to a final volume of 1 ml to produce a concentration suitable for delivery of 1 mg/kg. The pH of the compound 30 solutions was ~ 6. As the drug was not immediately soluble in the sterile WFI it was sonicated for 20 minutes at 30°C and it formed a solution thereafter.

1 mg and 5 mg of isosorbide mono-ethyl carbamate 5-salicylate (compound 33) was dissolved in sterile WFI to a final volume of 10 ml. 1 mg of compound 33 was dissolved in sterile WFI to a final volume of 1 ml to produce a concentration suitable for delivery of 1 mg/kg. The pH of compound 33 was ~ 6. As the drug was not immediately soluble in the sterile WFI it was sonicated for 20 minutes at 30°C. The compound then formed solutions in sterile WFI.

2.5.4 Drug administration

A single dose of one of the novel drugs, compound 30, 33 or 51, (1 mg/kg, 5 mg/kg or 10 mg/kg) was administered to each mouse respectively (n = 1 per group) in a dosage volume of 0.1 ml per 10 g of body weight. The novel compounds were injected intraperitoneally (i.p.) into the left lower quadrant of the abdomen using a sterile 21 gauge needle (BD Microlance, UK). The mice were observed over eight hours immediately following administration of the compounds and on the following day.

2.5.5 Behavioural scoring

Behavioural profiles following drug administration were assessed over a period of ten hours using a score sheet based upon modification of the SHIRPA profile (Appendix II). The behaviour of the animals was scored manually by the experimenter.

Undisturbed behaviour was scored while the animal was in the home cage. Undisturbed behaviour included the animal's body position, spontaneous activity, respiration rate, urination, defaecation and any signs of tremor following drug administration.

Active behaviour was monitored when the animal was placed in a new environment. During active behaviour the gait, pelvic and tail elevation of the animal were monitored. The startle response was assessed by clapping loudly next to the animal eliciting a startle response and the Preyer reflex (backward flip of the pinnae). The touch escape was measured by stroking the animal on the back to assess whether the animal tried to mildly, moderately or vigorously escape when touched. The passivity of the animal was determined by holding the animals by the tail and subsequently by the neck.

While the animal was held firmly in supine restraint, the body and limb tone of the animal were assessed by gently pressing the abdomen or pushing against the dorsum of the foot respectively. The response of the animal to toe pinch was also assessed. The absence or presence of the pinnae and corneal reflexes were noted following a gentle

stroke of the external meatus or cornea with a fine bristle from a paint brush. Grip strength was measured by holding the animal by the tail and lowering it towards the cage lid (ensuring they gripped it in the horizontal plane) and pulling the animal back by the tail. Trunk curl was assessed while the animal was held by the tail; the mouse should bring the upper body up by stooping on the ventral side and showing a sit-up movement (trunk curl). The righting reflex was determined by holding the animal by the tail and turning it over onto its back.

Manipulated behaviour such as provoked biting and aggression were assessed by placing a pencil in the animal's mouth while it was restrained. Lacrimation and salivation were also assessed as well as the skin colour. Negative geotaxis was determined by placing the animal on the lid of a cage, and raising the lid in the vertical position with the animal facing the floor. The body temperature was measured rectally using a Physitemp BAT-12 microprobe thermometer (Harvard Apparatus, UK).

2.5.6 Results

All animals were monitored following administration of the novel compounds. Continuous monitoring over a period of ten hours did not reveal any drug-induced abnormalities in the appearance or behaviour of the animals. No cholinergic side-effects were noted following administration of any of the drug doses.

Undisturbed behaviour of the animals was monitored following drug administration. The body position was normal in all cases and there was normal spontaneous activity such as self-grooming following handling. The respiration rate was noted to be normal following all drug doses. No tremors were evident. There was no palpebral closure. Piloerection was present at 10 mg/kg of compound 51 suggesting that this dosage produced a decrease in basal body temperature. Subsequent measurement of the body temperature found a decrease of 0.5°C in the basal body temperature.

Analysis of active behaviour found that all animals moved immediately when placed on the floor of a new environment and exhibited exploratory behaviour. A startle response to a loud clap elicited the Preyer reflex in all the animals. The gait was normal with the body elevated to approximately 3 mm above the ground with the tail held in the normal horizontal position. All mice exhibited a mild escape when stroked and struggled when held by the neck by the experimenter.

A positive trunk curl was observed in all the animals. The body tone was assessed by gently pressing the abdomen, while the animal was in supine restraint, and this revealed slight resistance. There was active reflex retraction of the pinna and presence of the corneal reflex when a fine paint brush bristle was gently passed over the pinna and the cornea. The skin was pink and healthy indicating normal blood circulation.

Salivation and lacrimation were both normal. There was no impairment of the righting reflex. When the animals were placed on their back they immediately turned over to lie in the prone position. Negative geotaxis was assessed and all animals immediately turned around and climbed up onto the grid. No aggressive or bizarre behaviour was observed in any of the animals at any of the drug doses.

Table 2.2 Results of behavioural scoring of animals following administration of the novel compounds.

	Compound 30	**Compound 33**	**Compound 51**
Body position	3 (normal)	3 (normal)	3 (normal)
Spontaneous activity	1 (casual grooming)	1 (casual grooming)	1 (casual grooming)
Respiration rate	2 (normal)	2 (normal)	2 (normal)
Transfer arousal	3 (brief freeze)	3 (brief freeze)	3 (brief freeze)
Piloerection	0 (absent)	0 (absent)	1 (present) at10 mg/kg only
Palpebral closure	0 (wide open)	0 (wide open)	0 (wide open)
Startle response	1 (Preyer reflex)	1 (Preyer reflex)	1 (Preyer reflex)
Gait	0 (normal)	0 (normal)	0 (normal)
Pelvic elevation	2 (normal 3 mm elevation)	2 (normal 3 mm elevation)	2 (normal 3 mm elevation)
Tail elevation	1 (horizontally extended)	1 (horizontally extended)	1 (horizontally extended)
Touch escape	1 (mild)	1 (mild)	1 (mild)
Positional passivity	1 (struggles when held by neck)	1 (struggles when held by neck)	1 (struggles when held by neck)
Trunk curl	1 (present)	1 (present)	1 (present)
Limb grasping	1 (present)	1 (present)	1 (present)
Grip strength	2 (moderate grip, effective)	2 (moderate grip, effective)	2 (moderate grip, effective)
Body tone	1 (slight resistance)	1 (slight resistance)	1 (slight resistance)
Pinna reflex	1 (active)	1 (active)	1 (active)
Corneal reflex	1 (active)	1 (active)	1 (active)
Lacrimation	1 (present)	1 (present)	1 (present)
Provoked biting	1 (present)	1 (present)	1 (present)
Salivation	1 (normal)	1 (normal)	1 (normal)
Abdominal tone	1 (slight resistance)	1 (slight resistance)	1 (slight resistance)

Skin colour	1 (pink)	1 (pink)	1 (pink)
Limb tone	1 (slight resistance)	1 (slight resistance)	1 (slight resistance)
Toe pinch	1 (moderate withdrawal)	1 (moderate withdrawal)	1 (moderate withdrawal)
Righting reflex	0 (no impairment)	0 (no impairment)	0 (no impairment)
Negative geotaxis	0 (turns & climbs on grid)	0 (turns & climbs on grid)	0 (turns & climbs on grid)
Aggression	0 (none)	0 (none)	0 (none)

2.6 Pharmacodynamic profile of the novel compounds

2.6.1 Introduction

Pharmacodynamics is described as how a drug acts on the body and how it alters cell metabolism to exert its effect [1]. Pharmacodynamic profiles of the novel compounds, 30, 33 and 51 were analysed. Compounds were administered to male C57BL/6 mice and peripheral BuChE activity was analysed from plasma samples. A pharmacodynamic profile of rivastigmine was also established and used to compare the pharmacodynamic profiles of the novel compounds. Central BuChE inhibition was assessed 24, 48 and 72 hours following administration of the compounds. The degree of central inhibition was also determined one hour following oral and intraperitoneal administration of compound 51. Additionally the central BuChE effect of direct intracerebroventricular administration of compound 51 was determined. Based on this study one of the compounds would be chosen on the basis of their pharmacodynamic profile and level of peripheral and central BuChE inhibition for further testing in cognitive studies.

2.6.2 Animals

45 healthy experimentally naïve male C57BL/6 mice were obtained from Harlan, UK for pharmacodynamic profiling. Nine healthy naïve 2-3 month old male CD-1 mice were obtained from the Bioresources Unit, Trinity College, Dublin for intracerebroventricular (ICV) studies. Animals were housed in single cages with isopad bedding (Harlan, UK) in a SPF environment with controlled temperature and humidity. All animals had access to food and water *ad libutum*. A 12 hour light/dark cycle (lights on 7 a.m. – 7 p.m. GMT) was in operation. Experiments were carried out during the light cycle. All experiments were carried out in accordance with the European Communities (Amendment of Cruelty to Animals Act 1876) Regulations 2002.

2.6.3 Drug preparation

1 mg of compound 51 (isosorbide 2-benzylcarbamate 5-benzoate), 1 mg or 5 mg of compound 30 (isosorbide 2-benzylcarbamate 5-salicylate), 1 mg of compound 33 (isosorbide mono-ethyl carbamate 5-salicylate), and 1 mg of rivastigmine were weighed and transferred to 10 ml volumetric flasks. Sterile water for injection (Braun, UK) was added to make a final volume of 10 ml. The isosorbide compounds were not immediately soluble in the sterile WFI and were each sonicated for 20 minutes at 30°C in a sonicator (Branson, Netherlands). Following sonication the compounds formed solutions. A pH of approximately 6 was achieved.

2.6.4 Drug Administration

2.6.4.1 Intraperitoneal injection

A single dose of 1 mg/kg or 5 mg/kg of compound 30, 1 mg/kg of compound 33, 1 mg/kg of compound 51, or 1 mg/kg of rivastigmine (each in a volume of 0.1 ml per 10 g body weight), was administered to mice (n = 9 per group) via intraperitoneal (i.p.) injection into the left lower quadrant of the abdomen using a sterile 21 gauge needle (BD Microlance, UK).

2.6.4.2 Oral administration

A single dose of 1 mg/kg of compound 51 (0.1 ml per 10 g of body weight) was given orally to mice (n = 9 per group) by gentle insertion of a 20 gauge (20G x 1½") sterile gavage needle (Popper, New York) down the oesophagus to ensure the drug reached the stomach.

2.6.4.3 Intracerebroventricular administration

0.5 µg compound 51 in a volume of 20µl of sterile WFI was administered directly into the cerebral ventricles of male CD-1 mice (n = 9). ICV injections were made using a 100 µl Hamilton syringe (Hamilton, Switzerland) attached to a retort clamp and stand. The animal was scruffed, held supine and positioned beneath the Hamilton syringe.

Injections were made 2 mm rostral to a line joining the ears' anterior bases and 1 mm lateral to the midline. A polythene tube was fitted onto the needle so that the needle only penetrated through the skull to a depth of 3.2 mm (1/8 inch) [217, 218]. Animals were sacrificed 24, 48 and 72 hours following drug administration. No blood samples were obtained from this study.

2.6.5 Blood sampling

Following a single i.p. or oral dose of 1 mg/kg of compound 51, compound 30, compound 33 or rivastigmine, or a single dose of 5 mg/kg of compound 30 i.p. the animals were returned to their home cages. Submandibular blood samples were then taken at various time points to obtain a pharmacodynamic profile from time zero to 72 hours following a single dose of the compounds (*Table 2.4)*. Mice were divided into groups A, B and C for sample collection, with three mice per group. The protocol for blood sampling was devised to maximise the intervals between blood samples. Additionally 2 - 3 month old healthy naïve male C57BL/6 mice were administered 1 mg/kg of compound 51 via oral and intraperitoneal routes and sacrificed one hour following drug administration.

Table 2.3 Protocol for submandibular blood sampling for groups A, B and C; (n=3 per group).

T0	**10min**	**20min**	**30min**	**1hr**	**2hr**	**3hr**	**4hr**	**6hr**	**8hr**	**24hr**	**48hr**	**72hr**
A	A			A			A			A		
B		B			B			B			B	
C			C			C			C			C

Submandibular blood samples were procured while the mouse was held by the neck (to occlude the jugular vessels thus providing an adequate blood supply) and held in supine restraint. A sterile 18 gauge needle (Sherwood Medical, UK) was used to puncture the skin.

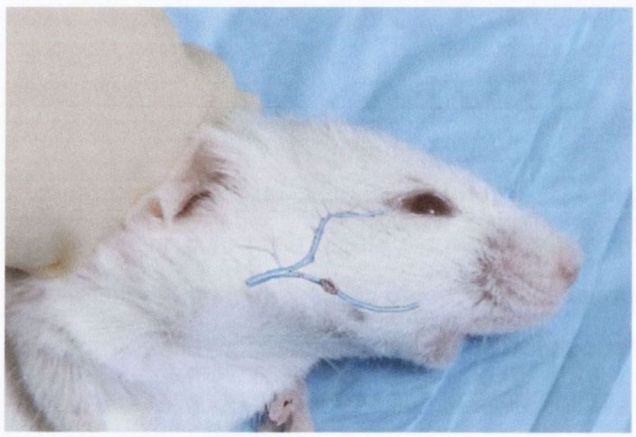

Figure 2.16 Venous plexus in the mandible of the mouse for submandibular blood sampling [219].

Approximately 50 µl of venous blood was collected in 200 µl lithium heparinized Microvette capillary tubes (Sarstedt, Germany) and placed on ice. Following blood sampling the mice were returned to their home cages. Prior to terminal blood sampling mice were anaesthetized by administration of ketamine/xylazine i.p. in a volume of 0.1 ml/10 g [220]. Terminal blood samples were obtained via cardiac puncture using a lithium heparinized sterile 25 gauge needle (Sterican, Braun, Germany).

2.6.6 Isolation of tissue samples

Following terminal blood sampling the anaesthetized animals were sacrificed by cervical dislocation. The head was removed from the axial skeleton using scissors. The scalp was cut through using sharp scissors and then retracted. The skull was carefully cut on each side using sharp scissors held in a lateral direction. Once the skull was cut through it was retracted and the brain was carefully removed using fine

forceps. Care was taken to ensure that the brain remained intact and it was placed in a labelled container on dry ice. The liver was next removed by cutting through the sternum down to the abdomen. The abdominal contents were exposed and the liver was identified. The gall bladder was removed from the liver by excision of the cystic duct from the porta hepatis. The liver was carefully removed ensuring all the lobes were intact and placed in a labelled container on dry ice. The tissues were subsequently frozen at -80°C until they were processed and analysed.

2.6.7 Processing of tissues

2.6.7.1 Blood samples

Upon procurement of the blood samples from the mice, the blood was centrifuged for 10 minutes at 4°C and 3,000 rpm using a Sorvall centrifuge RT6000B (GMI, USA). The plasma was removed using a Pasteur pipette and pipetted into labelled 1.5 ml Eppendorfs (Braun, Germany).

2.6.7.2 Brain and liver samples

Brain and liver samples were homogenised on ice in 10 volumes of 0.1 M phosphate buffered saline (PBS) pH 7.4 using an Ultraturrax T10 Basic (IKA-Werke, Germany). The brain samples were homogenised on ice for two 5 second bursts and liver samples were homogenised on ice for three 5 second bursts. The samples were transferred to labelled 15 ml glass test tubes, parafilmed and centrifuged for 10 minutes at 4°C at 10,000 rpm.

2.6.8 Analysis of BuChE activity

The Ellman assay was carried out as previously described in section 2.2.2.3. The activity of butyrylcholinesterase was determined in each plasma sample and the supernatant of the brain and liver tissues using butyrylthiocholine as a substrate [214]. Eight replicates were used and the average absorbances were recorded for each of the three samples. The absorbance values were converted to units of activity using the extinction coefficient for nitrothiobenzoate, 1.36×10^4. The values were plotted in

Graphpad Prism v 4.0 as percentages of the control (each mouse acted as its own control) using non-linear regression creating a pharmacokinetic profile.

2.6.9 Results

2.6.9.1 Plasma BuChE activity following administration of 1 mg /kg of compound 51 i.p. and p.o.

Administration of a single dose of sterile saline did not produce any changes in plasma BuChE activity over a period of 72 hours. However, a single dose of compound 51 via both i.p. and p.o. routes caused a short-lived decrease in the level of plasma BuChE activity. Twenty minutes following administration of compound 51 i.p. the activity of BuChE was decreased by 60% but the enzyme activity recovered thereafter with an overshoot at 24 and 48 hours. A single dose of compound 51 p.o. produced a less dramatic effect on plasma BuChE as the maximum inhibition was seen one-hour post administration with approximately 40% reduction in the enzyme level with a subsequent spontaneous recovery.

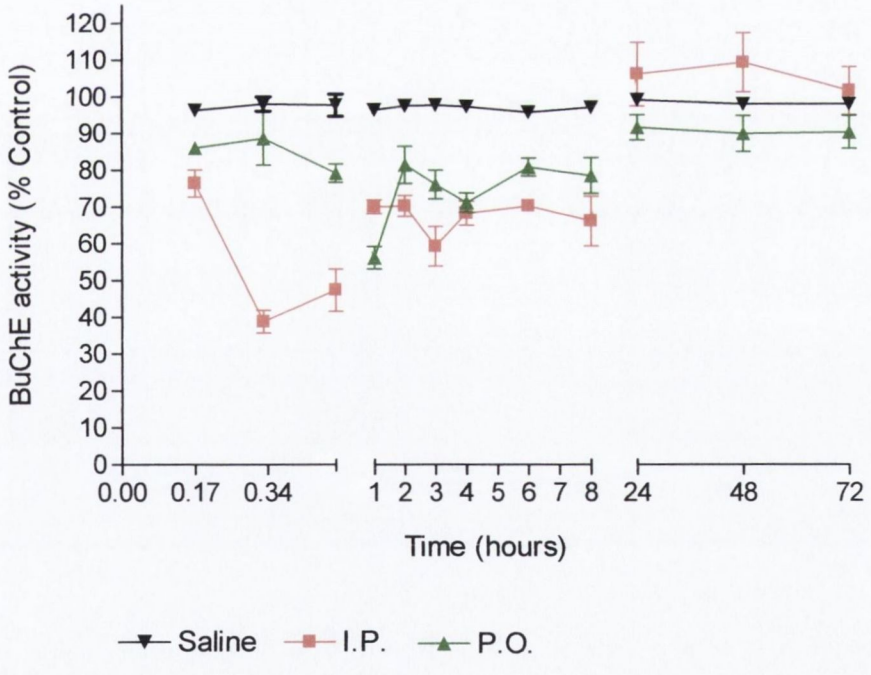

Figure 2.17 *Mean mouse plasma BuChE activity (± SEM) over 72 hours following a single dose of 1 mg/kg of compound 51 i.p. or p.o. (n = 3 per group).*

2.6.9.2 Brain BuChE activity following administration of 1 mg/ kg of compound 51 i.p. or p.o.

Administration of compound 51 via i.p. injection produced a greater decrease in brain BuChE activity compared to administration via the oral route, although the difference was not statistically significant. The BuChE activity in the brain remained below the control levels for at least 48 hours. The decrease in BuChE activity for each route of administration was significant from control activity $F(1, 21) = 4.247$, $P < 0.001$ (two-way ANOVA for repeated measures). Independent t-tests showed differences in brain BuChE levels between the control group and i.p. group at 24 hours post administration of the novel compound, $P < 0.05$. Additionally there were differences in brain BuChE activity between the control and i.p. ($P < 0.05$) and control and p.o. groups ($P < 0.05$) at 48 hours following drug administration. There were no differences in the BuChE levels between the groups at 72 hours, $P > 0.05$

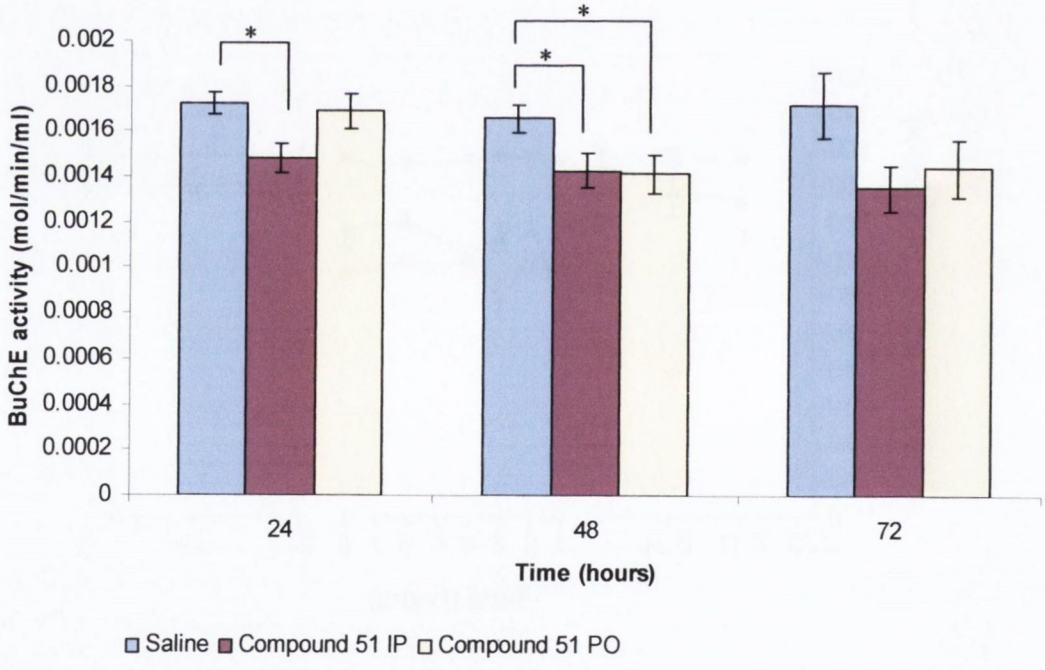

Figure 2.18 *The activity of BuChE in mouse brain 24, 48 and 72 hours following a single dose of 1 mg/kg of compound 51 i.p. and p.o. (n = 3 per group) (Mean ± SEM). * $P < 0.05$.*

2.6.9.3 Liver BuChE activity following administration of 1 mg/kg of compound 51 i.p. or p.o.

The liver BuChE activity was higher than the control values following administration of 1 mg/kg of compound 51 both i.p. and p.o. The enzyme level decreased continuously over the 72 hour period to eventually reach control levels. There were statistically significant differences between the groups, $F(1, 21) = 14.269$, $P < 0.001$ (two-way ANOVA for repeated measures). Post-hoc analysis found significant differences between the control and i.p. ($P < 0.05$) and control and p.o. groups ($P < 0.05$) 24 hours post administration of compound 51. The route of drug administration did not produce any significant differences in the liver BuChE activity, $P > 0.05$.

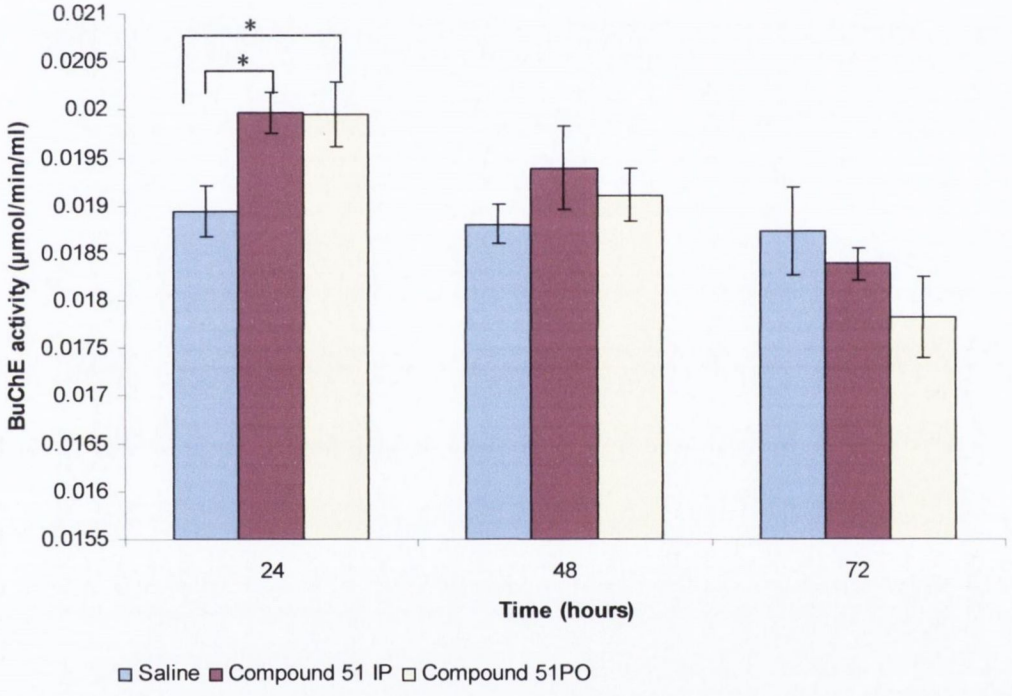

*Figure 2.19 The activity of BuChE in mouse liver 24, 48 and 72 hours following a single dose of 1 mg/kg of compound 51 i.p. or p.o. (n = 3 per group (Mean ± SEM)). * $P < 0.05$.*

2.6.9.4 Brain BuChE activity one hour following administration of 1 mg/kg of compound 51 i.p. or p.o.

Following a single oral or i.p. dose of compound 51 the level of BuChE in the brain of the drug-treated animals was lower than that of the saline-treated groups. A two-way ANOVA found a statistically significant difference between the groups, $F(1, 14) = 3.689$, $P < 0.05$. Post-hoc analyses revealed differences between the saline i.p group and the drug i.p. group ($P < 0.05$), and the saline p.o. group and the drug p.o. group ($P < 0.05$).

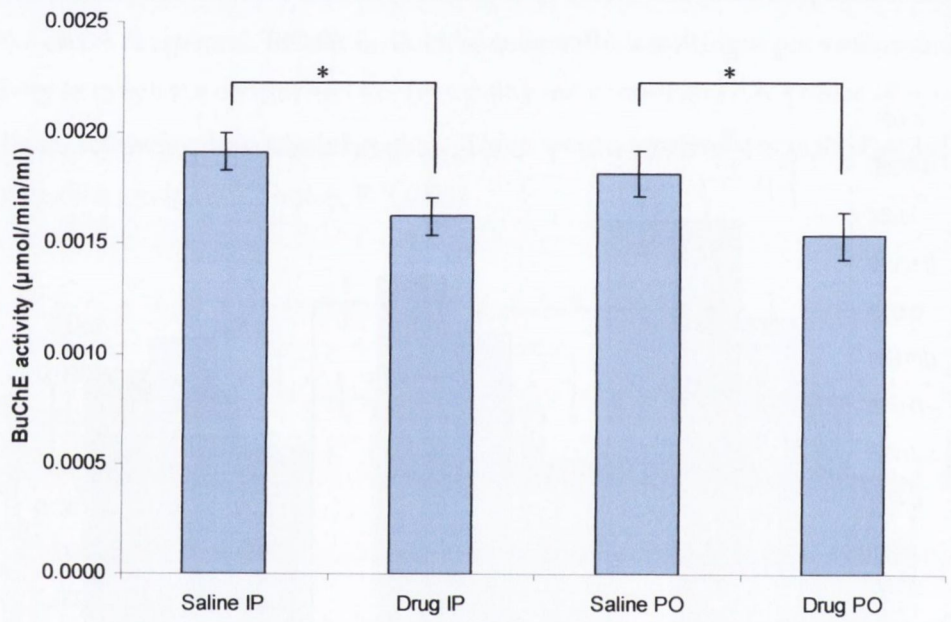

Figure 2.20 *The activity of BuChE in mouse brain one hour following a single dose of 1 mg/kg of compound 51 i.p. or p.o. (n = 3 per group) (Mean ± SEM). * $P < 0.05$.*

2.6.9.5 Liver BuChE activity one hour following administration of 1 mg/kg of compound 51 i.p. and p.o.

Liver BuChE activity decreased 6-fold following oral administration of a single dose of 1 mg/kg of compound 51 and 4-fold via intraperitoneal injection with the same dose as compared to control animals. Both routes of administration decreased the liver BuChE activity compared to that of the saline-treated animals, $F(1, 14) = 272.951$, $P < 0.001$ (two-way ANOVA). Post-hoc analyses showed the differences were between the saline i.p. and drug i.p. groups ($P < 0.05$), the saline p.o. and drug p.o. groups ($P < 0.05$) and between the drug i.p. and drug p.o. groups ($P < 0.05$).

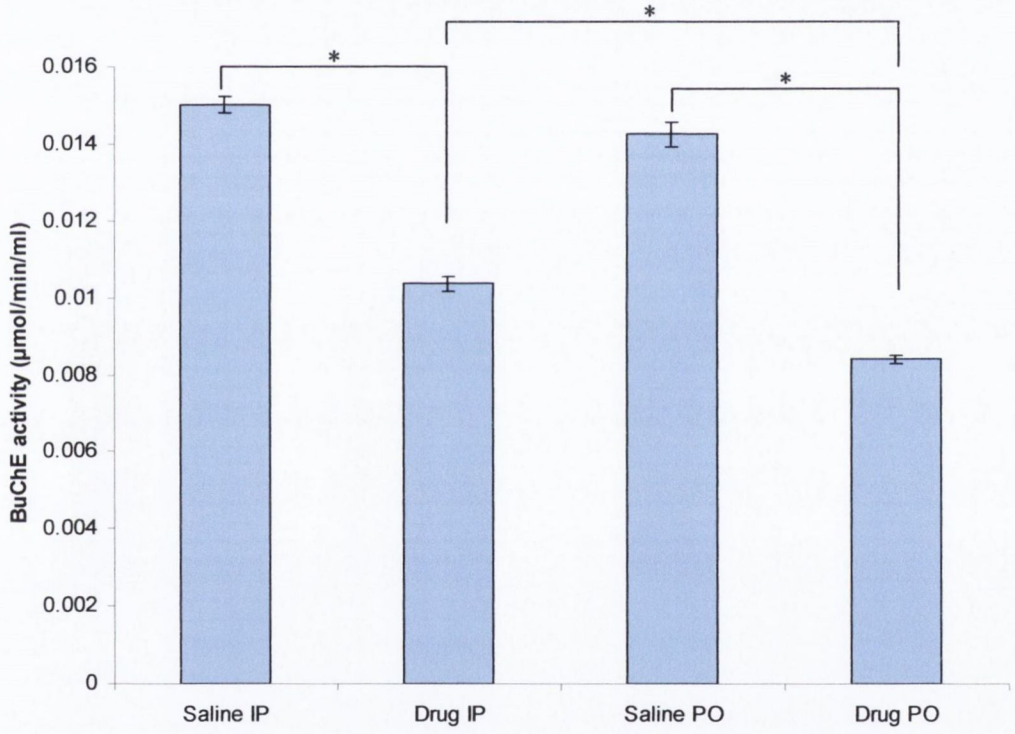

Figure 2.21 The activity of BuChE in mouse liver one hour following a single dose of 1 mg/kg of compound 51 i.p. or p.o. (n = 3 per group) (Mean ± SEM).

** $P < 0.05$.*

2.6.9.6 Brain BuChE activity following ICV administration of compound 51

A reduction in BuChE activity was seen 24 hours following administration of a single dose of compound 51 via ICV injection. The level of BuChE activity in the brain recovered continually over a period of 72 hours following administration of compound 51. A two-way ANOVA for repeated measures revealed a statistically significant difference between the groups, $F(2, 23) = 6.727$, $P < 0.001$. Post-hoc analyses showed differences between the level of BuChE activity in the drug-treated animals at 24 hours and 72 hours ($P < 0.05$), also differences in BuChE activity between the drug-treated animals at 48 hours and 72 hours ($P < 0.05$). Additionally, at 24 hours post drug administration the level of BuChE activity in the drug-treated animals was significantly lower than that of the saline-treated animals, $P < 0.001$.

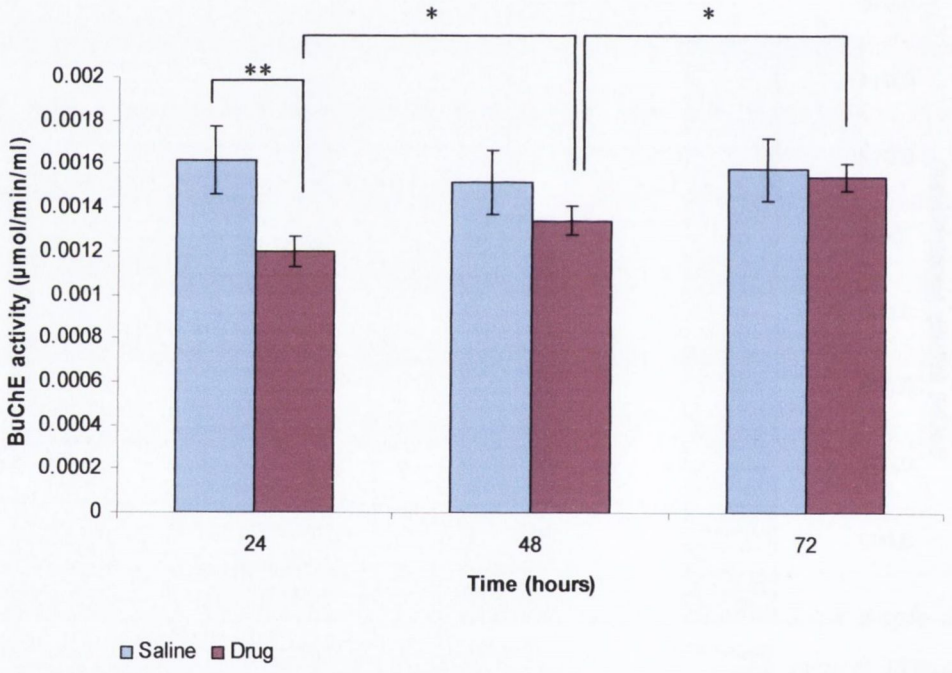

Figure 2.22 *The activity of BuChE in mouse brain following at 24, 48 and 72 hours following ICV administration of 0.5 µg of compound 51 in 20 µl WFI or 20 µl of 0.9% saline (n = 3 per group). (Mean ± SEM). * $P < 0.05$. ** $P < 0.001$.*

2.6.9.7 Plasma BuChE activity following administration of 1 mg/kg of compound 30 i.p.

Administration of a single dose of 1 mg/kg of compound 30 via i.p. injection resulted in inhibition of plasma BuChE activity. The maximum decrease of approximately 25% was observed following administration of the compound. Following inhibition the level of plasma BuChE increased thereafter but with fluctuations in the level of BuChE in the plasma. The level of BuChE rose 24 hours following administration of the compound. However, the initial pre-dose levels of BuChE activity in the plasma were not reached even 72 hours following drug administration.

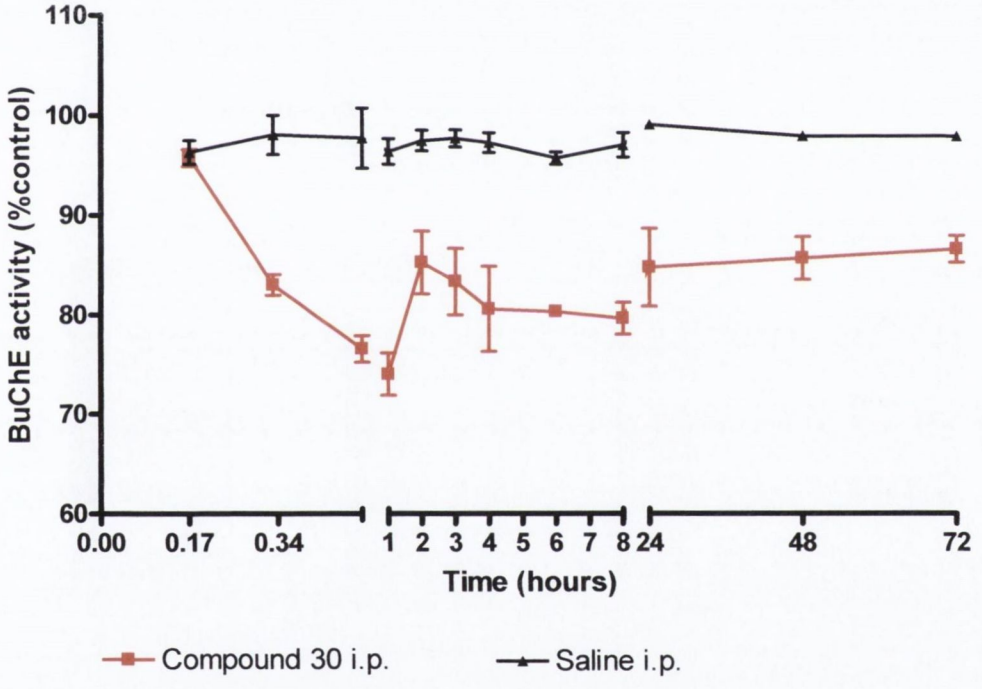

Figure 2.23 *The activity of BuChE in mouse plasma following administration of a single dose of 1 mg/kg of compound 30 i.p. (n = 3 per group) (Mean ± SEM).*

2.6.9.8 Brain BuChE activity following administration of 1 mg/kg of compound 30 i.p.

A single i.p. dose of 1 mg/kg of compound 30 did not produce any apparent reduction in BuChE activity in the brain; rather there was a slight increase when compared to the control levels of brain BuChE activity, which was insignificant except at the 48 hour timepoint. The level of BuChE activity in the brain decreased again by 72 hours post drug administration. There was a statistically significant difference in the BuChE activity in the brain between the control group and the drug-treated group 48 hours following administration of the novel compound, $F(1, 14) = 5.564$; $P < 0.05$ (two-way ANOVA for repeated measures). There was no significant difference between the groups at 24 and 72 hours $P > 0.05$.

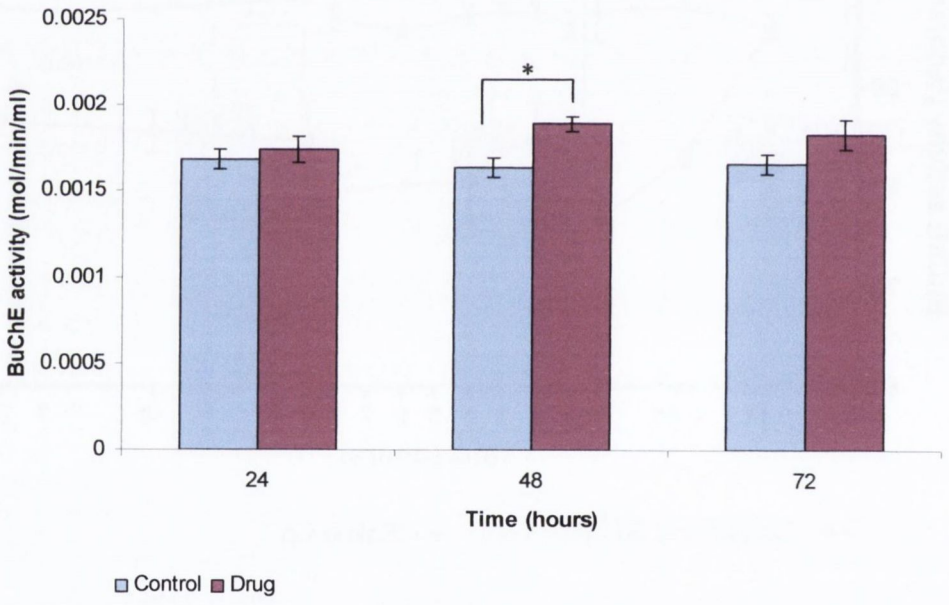

*Figure 2.24 The activity of BuChE in mouse brain following administration of a single dose of 1 mg/kg of compound 30 i.p. (n = 3 per group). (Mean ± SEM). * P < 0.05.*

2.6.9.9 Liver BuChE activity following administration of 1 mg/kg of compound 30 i.p.

The BuChE activity in the liver had increased 24 hours following a single intraperitoneal administration of 1 mg/kg of compound 30. However, this started to gradually decrease over 48 hours with a continual decrease seen at 72 hours. A two-way ANOVA for repeated measures found a statistically significant difference between the time points and the control group, $F(1, 14) = 0.316$; $P < 0.001$. Post-hoc analysis, using a Tukey's HSD test, revealed statistically significant differences in BuChE activity at 24 and 48 hours ($P < 0.05$), 24 and 72 hours ($P < 0.05$), and finally at 48 and 72 hours ($P < 0.05$). The drug groups at each time point were significantly different from the control animals at each time point, $P < 0.05$.

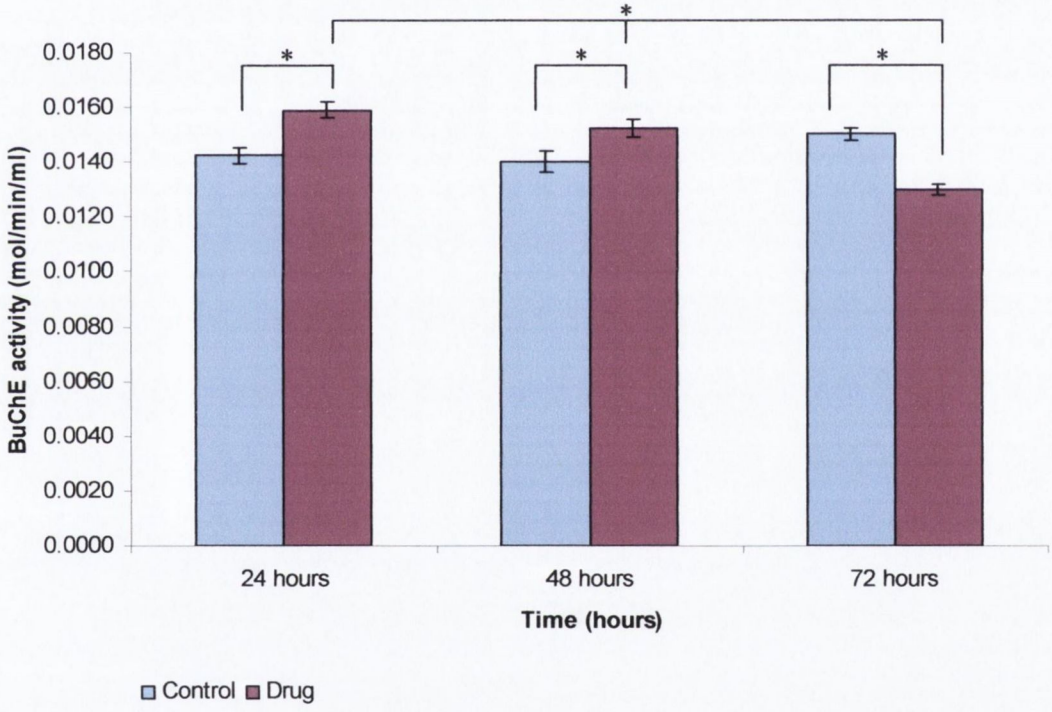

*Figure 2.25 The activity of BuChE in mouse liver following a single dose of 1 mg/kg of compound 30 i.p. (n = 3 per group). (Mean ± SEM) * P < 0.05.*

2.6.9.10 Brain BuChE activity following administration of 5 mg/kg of compound 30 i.p

Following i.p. administration of 5 mg/kg of compound 30 the level of BuChE in the brain decreased from 24 to 48 hours. This was then followed by an increase or overshoot in the enzyme concentration in the brain at 72 hours. However, the differences observed were not statistically significant ($P > 0.05$, two-way ANOVA for repeated measures).

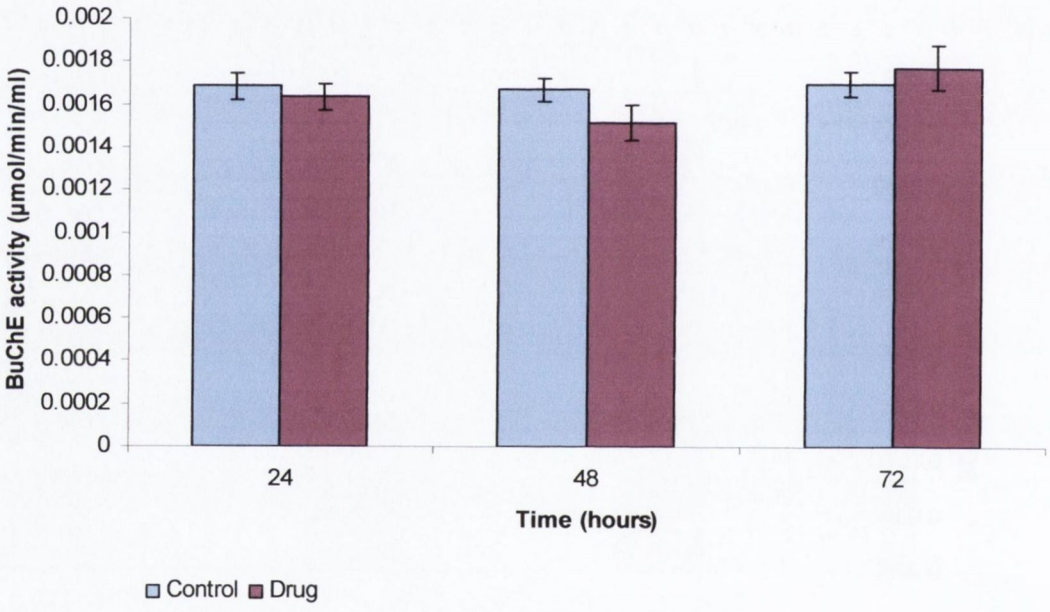

Figure 2.26 *The activity of BuChE in mouse brain following administration of a single dose of 5 mg/kg of compound 30 i.p. (Mean ± SEM). (n = 3 per group).*

2.6.9.11 Liver BuChE activity following administration of 5 mg/kg of compound 30 i.p.

There was a trend in BuChE activity following i.p. administration of compound 30 at 5 mg/kg as there was initially an overshoot at 24 hours followed by a steady reduction in the level of the enzyme activity at 48 and 72 hours. A two-way ANOVA for repeated measures revealed a statistically significant difference in the level of BuChE activity in the liver following administration of 5 mg/kg of compound 30 between the control group and the drug-treated animals, $F(1, 14) = 248.462$; $P < 0.001$. Independent t-tests showed that following drug administration the level of BuChE at 24 hours was greater than that at 48 and 72 hours, $P < 0.05$. At 48 hours BuChE activity was significantly different from that at 24 and 72 hours, $P < 0.05$. And finally the activity of BuChE at 72 hours differed significantly from that at 24 and 48 hours, $P < 0.05$. Additionally the level of BuChE in the liver was significantly different from control values at 24 hours and 48 hours post administration of the novel drug, $P < 0.05$.

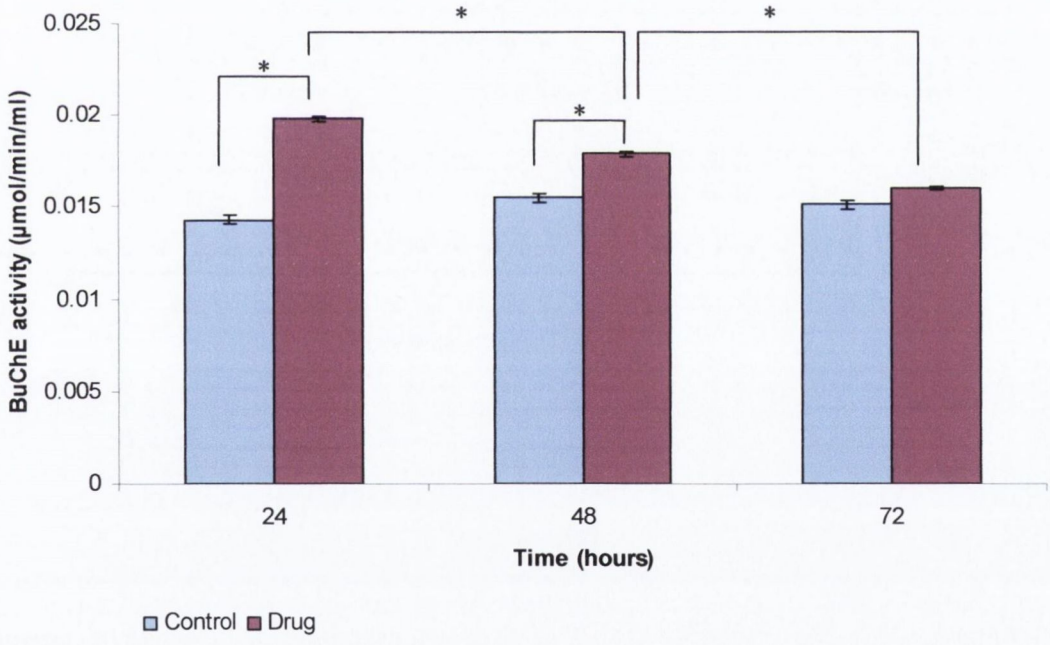

Figure 2.27 *The activity of liver BuChE following administration of a single dose of 5 mg/kg of compound 30 i.p. (Mean ± SEM) (n = 3 per group). * $P < 0.05$.*

2.6.9.12 Plasma BuChE activity following administration of 1 mg/kg of compound 33 p.o.

Plasma BuChE activity showed inhibition of the enzyme by approximately 25% following a single oral dose of compound 33. This maximum inhibition was achieved one hour post administration of the compound. There was a subsequent recovery in the enzyme activity followed by a large increase 48 hours following drug administration with a subsequent decrease to normal levels.

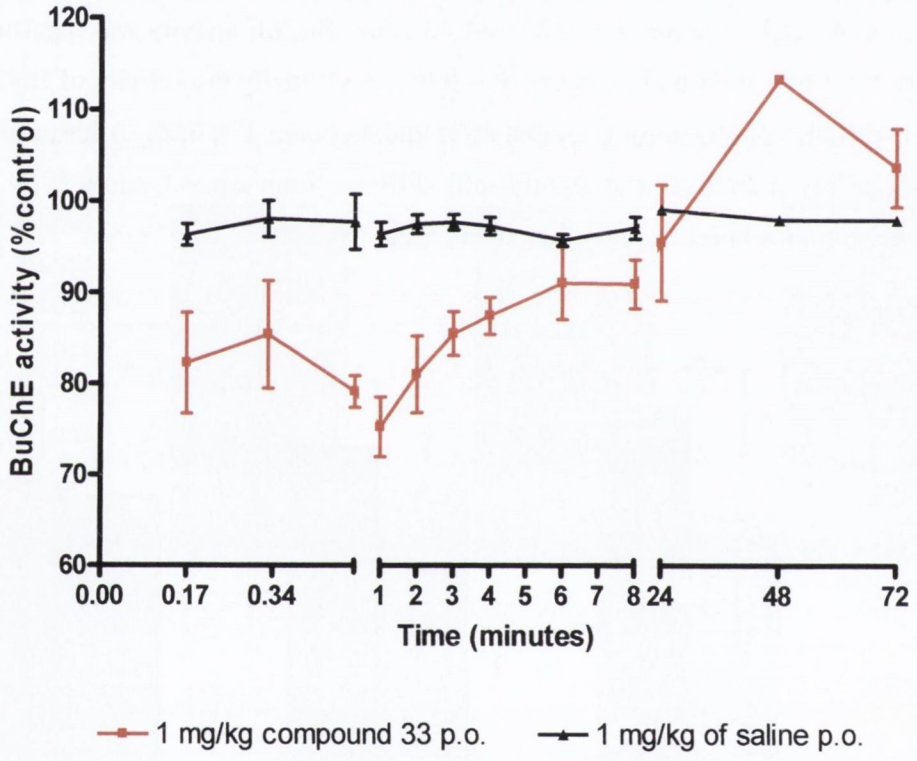

Figure 2.28 *The activity of BuChE in mouse plasma following 1 mg/kg of compound 33 i.p. or 0.1 ml/10 g 0.9% saline (n = 3 per group).*

2.6.9.13 Brain BuChE activity following administration of 1 mg/kg of compound 33 p.o.

Treatment of mice with a single dose of compound 33 p.o. reduced brain BuChE activity. There was a decrease in the level of BuChE activity in the brain 24 hours following administration of the novel compound compared to the control animals. However, the activity of BuChE in the brain increased over the remaining 48 hours. Although an increase was noted in treated animals at 72 hours compared to the control values, there was substantial variation and this difference was not statistically significant. A two-way ANOVA for repeated measures revealed a significant difference between the groups ($F(1, 14) = 23.893$, $P < 0.001$). Independent t-tests comparing the level of BuChE at each time point compared to control values revealed that the BuChE activity at 24 hours showed a highly significant difference, $P < 0.001$, from that of control animals.

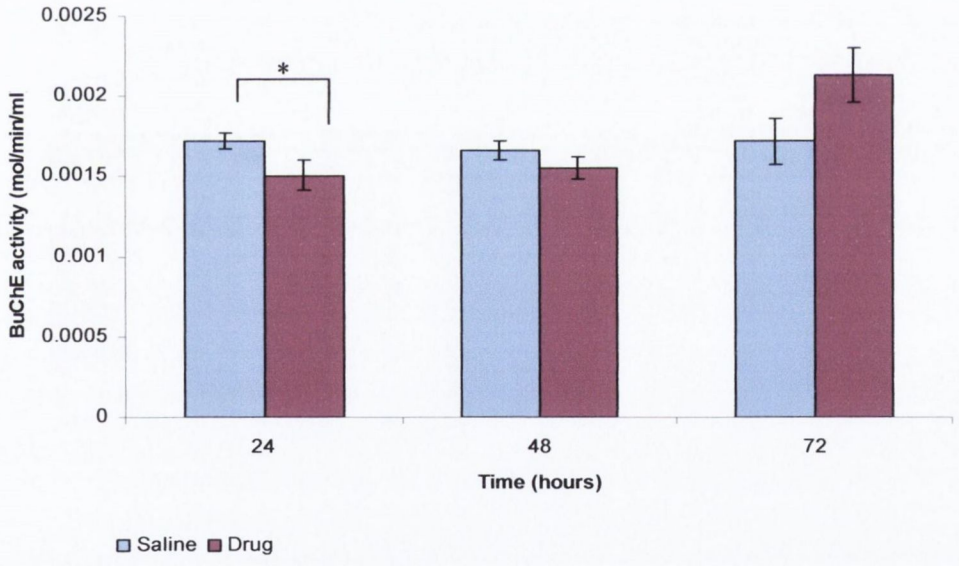

Figure 2.29 The activity of BuChE in mouse brain following a single administration of 1 mg/kg of compound 33 p.o. (n = 3 per group). (Mean ± SEM)

** P < 0.001.*

2.6.9.14 BuChE liver activity following 1 mg/kg of compound 33 p.o.

A single oral dose of 1 mg/kg of compound 33 caused a decrease in the level of liver BuChE activity when compared to the saline-treated control animals. However, the level of BuChE activity increased over a period of 72 hours following administration of the compound. A two-way ANOVA for repeated measures revealed a statistically significant difference within the drug-treated group for the level of BuChE across 24, 48 and 72 hours, $F(1, 14) = 159.391$, $P < 0.001$. Independent t-tests revealed highly significant differences in the liver BuChE activity between the control and drug-treated animals across each time point, $P < 0.001$, the treated animals showing reduced BuChE activity in each case.

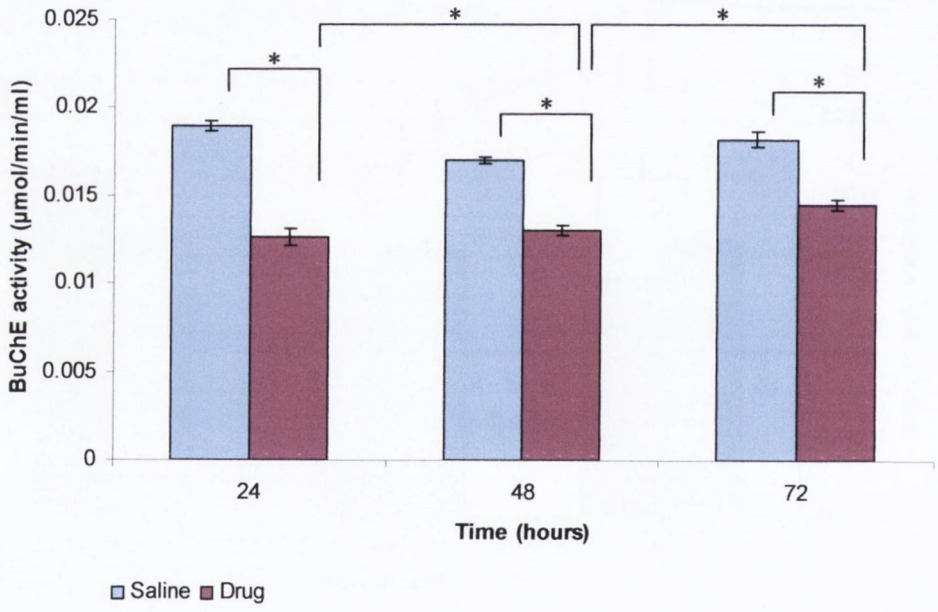

*Figure 2.30 The activity of BuChE in mouse liver following administration of 1 mg/kg of compound 33 p.o. (n = 3 per group). (Mean ± SEM). * $P < 0.001$.*

2.6.9.15 Plasma BuChE activity following 1 mg/kg of rivastigmine i.p.

1 mg/kg of rivastigmine i.p. shows a maximal plasma BuChE inhibition of approximately 35%. There is a gradual but slow recovery in the activity of the enzyme 1 hour following administration with a return to normal activity at 24 hours.

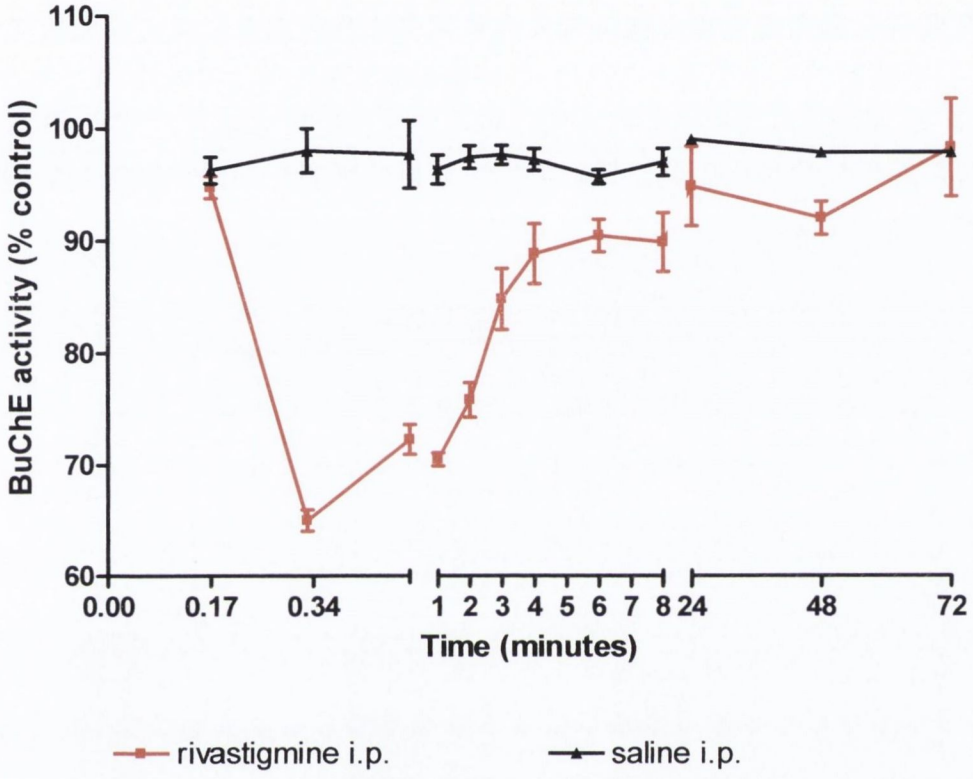

Figure 2.31 *Mean mouse plasma BuChE activity (± S.E.M.) following a single dose of 1 mg/kg of rivastigmine i.p. (n = 3 per group).*

2.6.9.16 Brain BuChE activity following 1 mg/kg of rivastigmine i.p.

The activity of BuChE in the brain of animals following a single i.p. dose of 1 mg/kg of rivastigmine increases 48 hours following drug administration. This is followed by a subsequent decrease in the activity of BuChE in the brain returning to normal levels. A two-way ANOVA revealed a statistically significant difference between the level of BuChE activity in the drug-treated animals over the time points, $F(1, 14) = 20.048$, $P < 0.001$. Independent t-tests also reveal differences in the level of BuChE activity in the brains of saline and drug-treated animals at 24 hour and 48 hours, $P < 0.05$. There was no significant difference in BuChE activity in the brains of control and drug-treated animals at 72 hours post drug administration, $P > 0.05$.

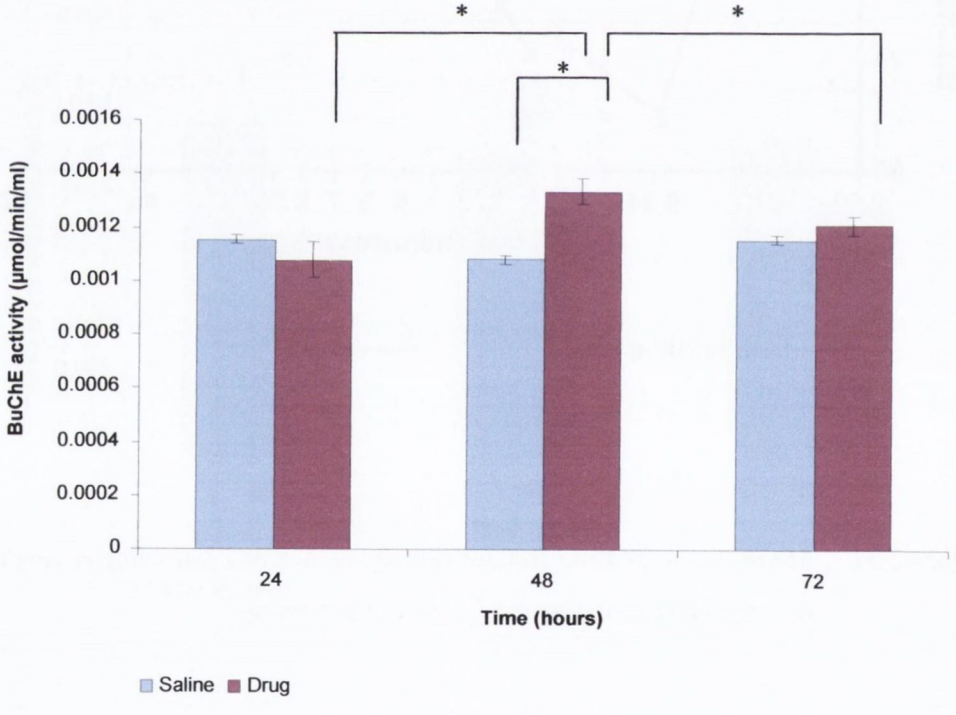

Figure 2.32 *The activity of BuChE in mouse brain following administration of a single dose of 1 mg/kg of rivastigmine i.p. (n = 3 per group). (Mean ± SEM). * $P < 0.05$.*

2.6.9.17 Liver BuChE activity following 1 mg/kg of rivastigmine i.p.

The liver BuChE activity shows a slight decrease 24 hours following administration of 1 mg/kg of rivastigmine i.p. This is followed by an increase in the level of BuChE activity 48 hours post administration of rivastigmine and at 72 hours there is a decrease in the activity of liver BuChE. This pattern is similar to that seen in the brain following administration of 1 mg/kg of rivastigmine i.p. A two-way ANOVA revealed a significant difference in the level of BuChE in the liver of the drug treated animals over the time periods, $F(1, 14) = 33.336$, $P < 0.001$. Additionally independent t-tests showed differences in the BuChE activities between the control and drug-treated animals at 48 and 72 hours, $P < 0.05$.

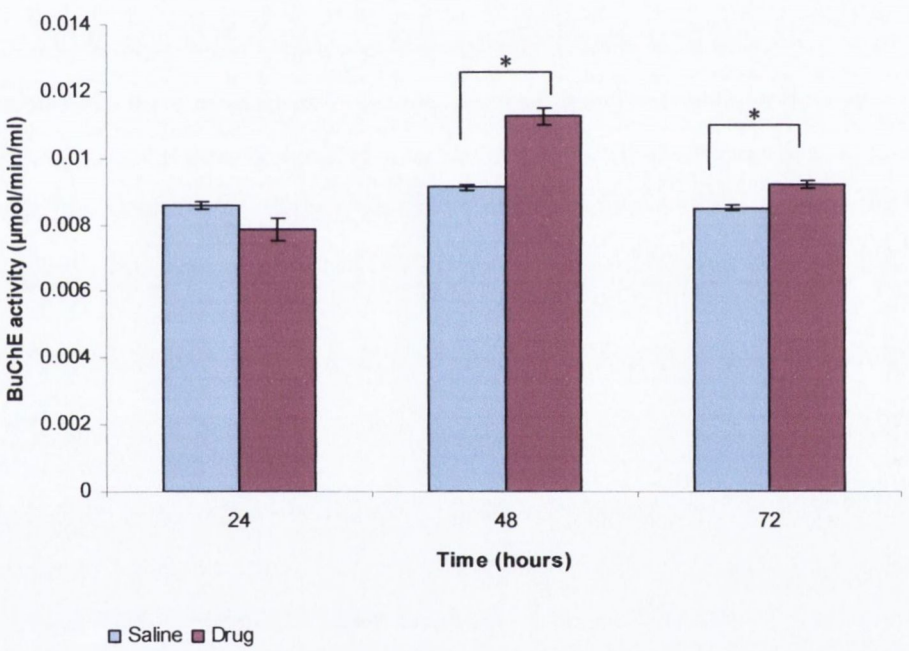

*Figure 2.33 The activity of BuChE in mouse liver following administration of a single dose of 1 mg/kg of rivastigmine i.p. (n = 3 per group). Mean ± SEM. * $P < 0.05$.*

2.7 Pharmacokinetics

2.7.1 Introduction

Pharmacokinetics is the science of the relationships between the movement of drugs through the body and the processes affecting it [221]. As compound 51 produced greater peripheral BuChE inhibition than compounds 30 and 33 *in vivo* based on pharmacodynamic studies it was therefore decided to complete a pharmacokinetic profile on this compound to gain a broader perspective of its *in vivo* activity. Furthermore this study sought to evaluate the quantity of the compound in the plasma, liver and brain tissue over the course of the time points, following both intraperitoneal and oral routes of administration, thus determining the half-life of the novel compound *in vivo*.

Animals were administered the novel isosorbide-based compound and blood samples were taken at fixed time points and the plasma was analysed by high-performance liquid chromatography (HPLC). Terminal blood samples were taken at 24, 48 and 72 hours post drug administration and at these time points the brains and livers were removed from the animals to determine the quantity of drug, if any, remaining.

2.7.2 Animals

Healthy experimentally naïve male 3 – 4 month old C57BL/6 mice were obtained from Harlan, UK for pharmacokinetic profiling. Animals were housed in single cages with Isopad bedding (Harlan, UK) in a SPF environment with controlled temperature and humidity. All animals had access to food and water *ad libitum*. A 12 hour light/dark cycle (lights on 7 a.m.-7 p.m. GMT) was in operation. Experiments were carried out during the light cycle. All experiments were carried out in accordance with the European Communities (Amendment of Cruelty to Animals Act 1876) Regulations 2002.

2.7.3 Drug preparation

1 mg of compound 51 (isosorbide 2-benzylcarbamate 5-benzoate) was weighed and transferred to a 10 ml volumetric flask. Sterile WFI (Braun, UK) was added to make a final volume of 10 ml. The compound was not immediately soluble in the sterile WFI and was therefore sonicated for 20 minutes at 30°C in a sonicator (Branson, Netherlands). Following sonication the compound formed a solution in the sterile WFI. A pH of approximately 6 was achieved.

2.7.4 Drug Administration

2.7.4.1 Intraperitoneal injection

A single dose of 1 mg/kg of the drug (in a volume of 0.1 ml per 10 g body weight) was administered to mice (n = 9) via intraperitoneal injection into the left lower quadrant of the abdomen using a sterile 21 gauge needle (BD Microlance, England).

2.7.4.2 Oral administration

A single dose of 1 mg/kg of compound 51 (in 0.1 ml per 10 g of body weight) was given orally to mice (n = 9) by gentle insertion of a 20 gauge (20G x 1½") sterile gavage needle (Popper, New York) down the oesophagus to ensure the drug reached the stomach.

2.7.5 Blood sampling

Submandibular blood sampling was carried out as previously described in section 2.6.5. An initial blood sample was taken prior to administration of the compound and subsequent blood samples were taken as per the protocol in *Table 2.4.* Blood samples were collected in 200 µl lithium heparinized Microvette capillary tubes (Sarstedt, Germany) and placed on ice. Terminal blood samples were procured via cardiac puncture. Prior to terminal blood sampling mice were anaesthetized using a ketamine/xylazine solution in a volume of 0.1 ml/10 g of body weight [220]. Terminal blood samples were obtained via cardiac puncture using a sterile 25 gauge needle

(Sterican, Braun, Germany) attached to a 1 ml syringe containing a small amount of lithium heparin in its base.

2.7.6 Isolation of tissues

The tissues were isolated as previously described in section 2.6.6.

2.7.7 Processing of tissues

The tissue samples were processed as previously described in section 2.6.7.

2.7.8 HPLC analysis of drug concentration

2.7.8.1 Preparation of samples

50 µl of plasma from each time point was added to a 1.5 ml Eppendorf (Brand, Germany) containing 50 µl of phosphate buffered saline pH 7.4 and vortexed. 50 µl of the plasma/buffer solution was then transferred to an Eppendorf containing 2% zinc sulphate : acetonitrile 1:1 to stop the enzymatic reactions.

100 µl of brain or liver homogenate from each time point was added to a 1.5 ml Eppendorf containing 50 µl of phosphate buffered saline pH 7.4 and vortexed. 100 µl of the brain/buffer solution or liver/buffer solution was then transferred to an Eppendorf containing 2% zinc sulphate : acetonitrile 1:1 to stop enzymatic reactions.

The samples were then centrifuged at 10,000 rpm for 7 minutes. The homogenate was removed and transferred to 1 ml HPLC vials (ABG Scientific Ltd, Dublin).

2.7.8.2 HPLC method

A 16 mM phosphate buffer was prepared from disodium hydrogen phosphate and sodium dihydrogen phosphate salts (Fluka Biochemika, Germany). The salts were dissolved in 1 L of Millipore water and the pH was determined using a pH meter (IKA,

Labortechnik, Germany). The buffer was brought to pH 2.5 using ortho-phosphoric acid (Riedel de Haen, Germany) or sodium hydroxide (Sigma-Aldrich, Dublin). The phosphate buffer was filtered using a 0.22 μm Steritop vacuum driven disposable filter (Millipore, Ireland). The phosphate buffer was passed through line B, separate from the acetonitrile.

1 L of gradient grade acetonitrile (Sigma-Aldrich, Dublin) was used and passed through line A, separate from the phosphate buffer.

HPLC was performed using a system consisting of a Waters 600 pump and controller, Waters autosampler 717 plus, and a Waters 2996 photodiode-array (PDA) detector controlled by Empower software (Waters). A Hichrom Nucleosil C18 column 4.0 x 250 mm was used for both the plasma and liver samples. A gradient method was employed using a mobile phase of 16 mM phosphate buffer (pH 2.5) : acetonitrile 80:20 for the first 10 minutes grading to 20:80 to 15 minutes, grading to 60:40 to 17 minutes and returning to 80:20 until the end of the 20 minute run (*Table 2.3*). The flow rate was 1 ml per minute. The mobile phase was sparged with helium gas at a rate of 20 ml per minute. The eluent was monitored at 210.5 nm and 230 nm. Quantitation was measured by comparison of the drug peaks to external standards run under the same conditions. The relative standard deviation (RSD) on six injections was < 1%. The method was validated for precision, linearity, sensitivity and specificity. External standards of compound 51 and its metabolites, benzoic acid and benzyl carbamate, at a concentration of 100 μM were used.

Table 2.4 *Gradient HPLC method for hydrolysis studies on novel compounds.*

Time (mins)	**% Phosphate Buffer (16mM, pH 2.5)**	**% Acetonitrile**
0	80	20
10	20	80
15	60	40
17	80	20
20	80	20

2.8 Results

HPLC analysis of the plasma, brain and liver samples did not result in the identification of any peaks for compound 51 or its metabolites. The external standards, compound 51, benzoic acid and benzyl carbamate, were detected at 210.5 nm. The samples did not show the appearance of metabolites benzyl carbamate and benzoic acid coinciding with the disappearance of compound 51 as is the case with metabolism of compound 51 in mouse tissues (*Figure 2.34)*. The limit of detection for this particular HPLC machine was in the micromolar range therefore if the drug was present below this concentration it could not be detected.

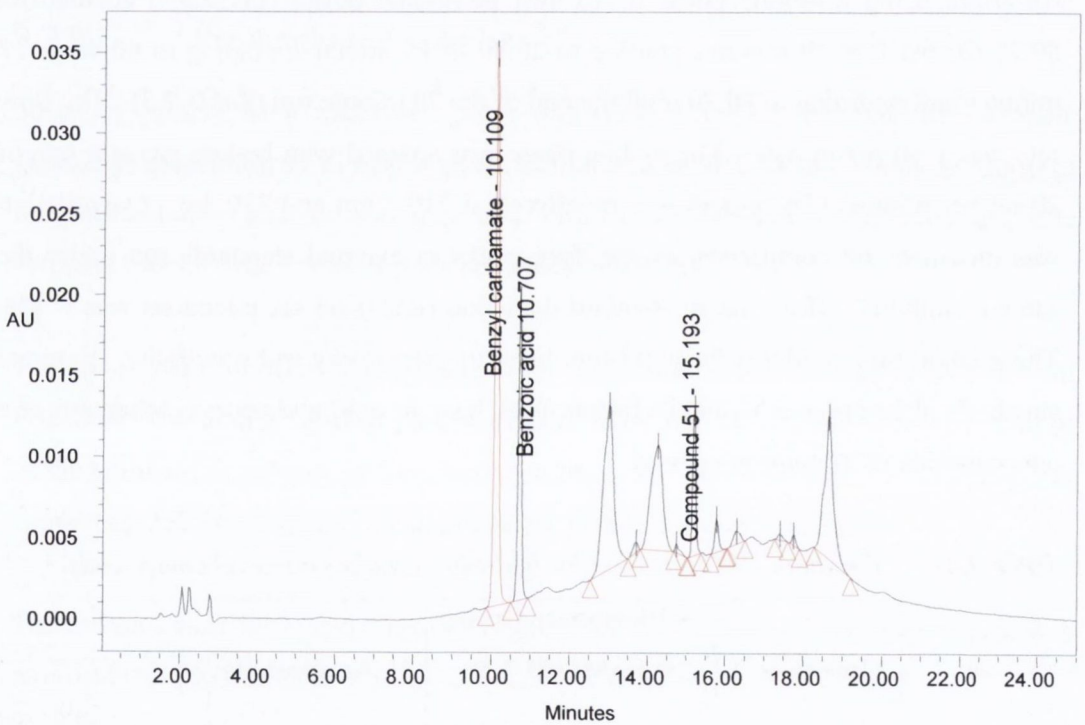

Figure 2.34 Chromatogram representing compound 51 and its metabolites, benzyl carbamate and benzoic acid. Retention times: benzyl carbamate 10.109 minutes; benzoic acid 10.707 minutes and compound 51 15.193 minutes.

2.9 Diurnal variation in BuChE activity

2.8.1 Introduction

2.8.1.1 Background

It is known that diurnal variation in the levels of certain enzymes exists [210]. Circadian variation has been found in the levels of the enzymes alanine aminopeptidase, gamma-glutamyltransferase and beta-glucosaminidase in healthy humans with the highest levels found in the morning time and low levels of the enzymes detected in the evening time [222]. It has also been suggested that diurnal variations exist with respect to the levels of lipoprotein lipase activity [223].

2.8.1.2 Aims

The purpose of this study was to determine whether any circadian variation in the peripheral enzymatic activity of BuChE in mice using the Ellman assay to measure BuChE activity.

2.8.2 Animals

Nine healthy experimentally naïve male 3 – 4 month old C57BL/6 mice were obtained from Harlan, UK for this study. Animals were housed in single cages with isopad bedding (Harlan, UK) in a SPF environment with controlled temperature and humidity. All animals had access to food and water *ad libitum*. A 12 hour light/dark cycle (lights on 7 a.m. – 7 p.m. GMT) was in operation. Experiments were carried out during the light cycle. All experiments were carried out in accordance with the European Communities (Amendment of Cruelty to Animals Act 1876) Regulations 2002.

2.8.3 Blood sampling

Submandibular blood samples were taken from the animals twice a day at 8 a.m. and 8 p.m. over a period of three days. A sterile 18 gauge needle (Sherwood Medical, UK)

was used to pierce a vein in the venous plexus in the cheek pouch (*Figure 2.16*). The venous blood was collected in 200 µl lithium heparinized Microvette capillary tubes (Sarstedt, Germany) and placed on ice. The blood was then centrifuged at 3,000 rpm for 10 minutes at 4°C. The plasma was removed and tested for BuChE activity using the Ellman assay as previously described in section 2.2.2.3.

2.8.4 Results

The results indicate that there is a variation in the level of BuChE activity in the plasma of mice in the morning and the evening. Independent t-tests were used to analyse the BuChE activity at the different time points and showed a statistically significant difference between the enzyme activity in the morning and evening on days 1, 2 and 3, $P < 0.05$.

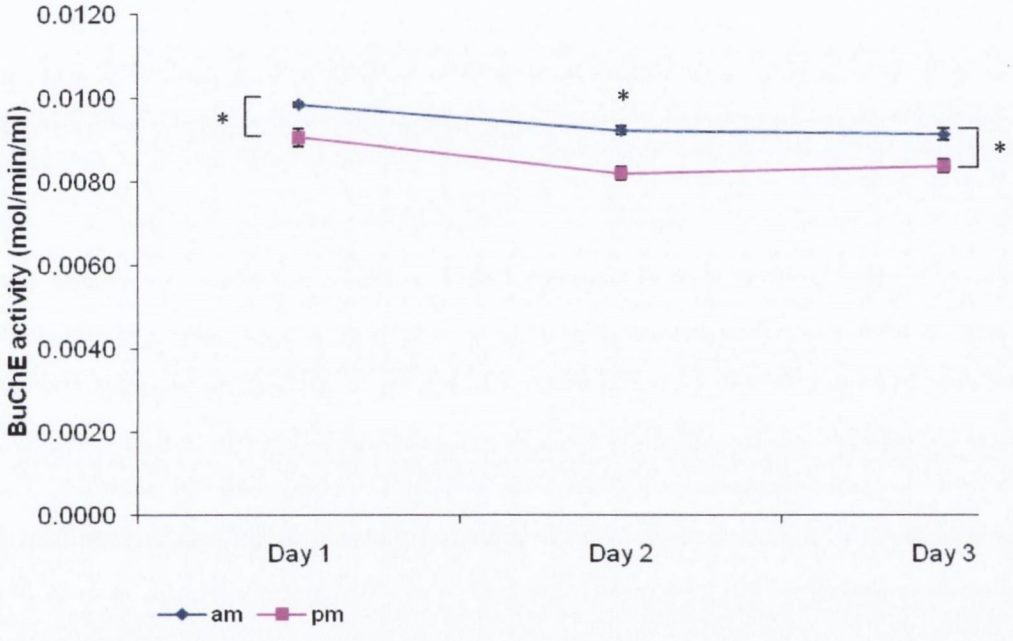

*Figure 2.35 Mean mouse plasma BuChE activity (± SEM) from blood samples procured at 8 a.m. and 8 p.m. 3 – 4 month old male C57BL/6 mice. n = 9. * P < 0.05.*

2.9 Discussion

2.9.1 Comparison of plasma BuChE between animal species

This study sought to determine the plasma BuChE activity in different animal species in order to find a good animal model with a BuChE level comparable to that of humans on which to test the novel BuChE inhibitors.

There were differences in the plasma BuChE levels in human, mouse and rat. Human plasma had the highest level of BuChE activity while mouse plasma had a slightly lower activity than that of human plasma. The volume of human and mouse plasma used in this experiment were adjusted to achieve similar absorbance levels. Rat plasma has low levels of BuChE compared with human and mouse plasma when the same volume of plasma was used.

Human cholinesterase was previously found to show a greater preference for the substrate butyrylcholinesterase whereas rat cholinesterase reacts well with the substrate propionylcholinesterase [224]. The levels of BuChE in the plasma of man and mouse were found to be the highest levels recorded among eleven different species namely, horse, man, mouse, guinea pig, dog, cat, rat, rabbit, swine, goat and hamster. The rat was found to have one of the lowest levels of plasma BuChE activity with activity similar to that of rabbit, goat and hamster [213]. Although plasma BuChE activity in man and mouse is remarkably higher than that of rat, the plasma BuChE activity in man is almost double that of mouse [225]. Just as there are interspecies differences in the activity of BuChE, intraspecies differences are also known to exist. In humans, females naturally exhibit lower plasma BuChE activity than men of the same age [226]. These are accounted for by hormonal differences as lower levels of BuChE activity are known to occur during pregnancy when the level of the hormone oestrogen is high [133]. Furthermore, the hormonal status of women and the use of oral contraceptive pills also cause a decrease in the plasma BuChE activity [211, 227, 228]. However, post-menopausal women show higher BuChE activity than pre-menopausal women [211]. Redderson *et al.* suggested that the female sex steroids depress hepatic synthesis or release of BuChE [229].

Based on the results obtained in this study it was decided that the rat would not act as a good model for testing BuChE inhibitors given the low levels of plasma BuChE activity. Male mice were therefore chosen as the animal model to test the novel BuChE inhibitors.

2.9.2 IC_{50} of the novel compounds using the Ellman assay

This study sought to determine the IC_{50} values or potency of the novel compounds *in vitro* in human and mouse plasma. The compounds proved to be quite potent with values in the low micromolar to nanomolar range. There were however discrepancies in the values between the species, the values in human plasma differing significantly from those in mouse plasma. It appears the novel compounds are more potent in human plasma than in mouse plasma. A likely explanation for the differences seen in the potency of the novel compounds towards human and mouse BuChE is that there are structural and functional differences in this enzyme between humans and mice. Additionally, rivastigmine exhibited greater potency against human BuChE than mouse BuChE while physostigmine showed a similar potency towards both human and mouse BuChE. As physostigmine is an AChE inhibitor while rivastigmine is a dual inhibitor of both AChE and BuChE, this may indicate that AChE exhibits greater structural or functional similarities among the species than BuChE. However, Worek *et al.* found differences between humans and rodents in the reactivation kinetics for AChE using organophosphates as inhibitors [230] suggesting differences in the affinities of AChE for inhibitors among different species. As the esterase enzymes exhibit different catalytic efficiencies and affinites for drugs it seems possible that both human and mouse AChE have similar affinities for physostigmine. Wiesner *et al.* suggested that the tertiary structure of AChE in rats and humans has greater similarities that that of mice and humans [231]. Similarly there may also be differences in the active sites of human and mouse BuChE thus accounting for the different enzyme affinities towards the novel compounds.

These novel compounds were initially designed as inhibitors of human BuChE and were found to be highly selective for BuChE over AChE. However, the affinity of these compounds for other plasma esterases such as carboxylesterase (CE) (EC 3.1.1.1),

which is not found in plasma [225], was not established. Mouse plasma contains CE, and it is possible that CE1 in mouse plasma [232] possesses some affinity for the novel compounds thus accounting for the discrepancies detected. This is explored further in chapter 7.

Despite the species differences in the potencies of the novel compounds they were worth pursuing for *in vivo* testing to determine the level of BuChE inhibition.

2.9.3 Behavioural profile of compounds following administration of novel compounds

The idea of this experiment was merely to determine a dose that was safe to administer for subsequent cognitive testing, hence only a small number of animals were used.

As the compounds are novel BuChE inhibitors this study mainly focused on determination of any cholinergic side-effects that might be observed from the use of such drugs. As none were evident it was considered that inhibition of BuChE does not play a significant role in normal peripheral cholinergic function.

Additionally, as the compounds were isosorbide-based compounds side-effects such as passivity or inactive behaviour were monitored in the animals. This could be a result of dizziness secondary to a reduced blood flow to the brain as this is a side-effect of use of isosorbide dinitrate [233]. As a carbamate moiety is also attached to the compounds it was thought that perhaps side-effects such as diarrhoea, dizziness and agitation might be observed in the animals; however, no such signs were observed post administration of the compounds even at higher doses of 5 mg/kg and 10 mg/kg.

Administration of 1 mg/kg, 5 mg/kg and 10 mg/kg of the novel BuChE inhibitors did not produce any behavioural abnormalities in mice. Inhibition of BuChE at higher doses of the compounds did not produce any cholinergic abnormalities indicating that inhibition of BuChE is not detrimental, and this is evident in the BuChE knockout mouse [141]. However, 10 mg/kg of compound 51 caused a slight reduction in basal body temperature in mice and piloerection was noted shortly after administration of this dose. This may have been indicative of slight CNS depression.

As no obvious cholinergic side-effects were found following administration of these compounds at 1 mg/kg it was decided to first determine the pharmacodynamic effects of a dose of 1 mg/kg of the compounds for potential further investigation in cognitive studies. The higher dose was not used as the reduction in body temperature elicited made it unsuitable for subsequent animal studies.

All animals had normal undisturbed behaviour and the absence of tremors, convulsions or aggressive behaviour indicated that the novel BuChE inhibitors do not produce CNS stimulation. Active behaviour in all the animals was normal with mice exhibiting exploratory behaviour when placed in a new environment. No sedative effects were noted following administration of the compounds to the animals. 24 hours following drug administration all animals were healthy and there were no signs of any physical or behavioural abnormalities.

2.9.4 ADMET (Absorption, Distribution, Metabolism, Excretion, Toxicity)

The purpose of this study was to use a computer programme, Pipeline Pilot (Accelrys, California, USA) to determine the probable solubility, intestinal absorption, BBB penetration and potential hepatotoxicity of the novel compounds.

All of the novel compounds exhibited the same potential solubility in water at 25°C. Although the compounds were found to be poorly soluble when added to sterile water for injection, sonication at 30°C did result in the formation of a solution with all compounds. The solubility of the novel compounds in water was as predicted. Experimentally the compounds had a solubility of 40 millimoles/L and were in the middle of the range of the predicted value of 10^{-4} moles/L to 10^{-2} moles/L.
The ability of the novel BuChE inhibitors to be absorbed across the human intestine was predicted as good for all the compounds indicating that oral administration would result in good absorption and thus good passage of the inhibitors into the bloodstream. The liver and the intestine are involved in first-pass metabolism due to the presence of the cytochrome P_{450} (CYP450) system. Intestinal absorption regulates the bioavailability of orally administered drugs and the presence of the villi and microvilli of the small intestine increase the surface area available for drug absorption. Drugs that are absorbed from the intestine may undergo significant metabolism in the liver before being delivered elsewhere around the body, as the majority of the rich intestinal blood supply goes towards the liver [234, 235].

BBB penetration is paramount in the use of these novel inhibitors to target central BuChE. None of the compounds was predicted to show high BBB penetration *(Table 2.2)*, and therefore it was important to establish the extent of central BuChE inhibition following peripheral drug administration *in vivo*. Compound 33 1 mg/kg and compound 51 1 mg/kg elicited significant inhibition of brain BuChE, while compound 30 (1 mg/kg and 5 mg/kg) did not. The rates of metabolism, excretion and plasma binding affect the concentration of compounds available to cross the BBB. Furthremore, it has been suggested that the ability of a compound to penetrate the BBB may be increased by decreasing the overall hydrogen-bonding ability of a compound [236]. Centrally acting drugs must also possess some hydrophilic properties as a balance

must be struck between gastrointestinal absorption and BBB penetration. Poor BBB penetration of a drug may necessitate a higher dose which may create a greater potential for peripheral side-effects.

The potential toxicity of the compounds was reported as non-toxic for compounds 30, 33 and 57. However, compounds 21 and 51 were predicted to have hepatotoxic potential. In general carbamate-based compounds are known to pose a hepatotoxic risk; for example, a study of vinyl carbamate in rats resulted in centrilobular necrosis in the liver [237]. However, this does not necessarily preclude a role as a successful anti-Alzheimer's drug: For example, rivastigmine (Exelon®) has a carbamate moiety in its structure.

2.9.5 Pharmacodynamic profile of novel compounds

This study sought to evaluate the pharmacodynamic profile of compounds 51, 30, 33 and rivastigmine in mice, and to determine an efficacious dose for behavioural testing.

Compound 51 at 1 mg/kg showed a decrease in plasma BuChE activity when administered both i.p. and p.o.; however i.p. administration produced a greater decrease in mouse plasma BuChE. This may be due to the fact that some of the compound underwent first pass metabolism or it was not highly cleared across the intestinal wall after oral administration [234]. The level of brain BuChE activity was lower following i.p. administration than after the same dose p.o. However, there was a consistent decrease in the level of BuChE inhibition in the brain over a period of 72 hours. On the other hand liver BuChE activity increased above control levels following both routes of administration; this subsequently decreased on progression to 48 and 72 hours post-administration. The brain and liver levels of BuChE were also assessed one hour after administration of 1 mg/kg of compound 51. This revealed a decrease in brain BuChE which was more pronounced following i.p. administration than the oral route. The liver also showed a decrease in BuChE but this was greater following oral administration than i.p. injection. To determine the direct effect of compound 51 on brain BuChE activity bypassing the BBB, a dose of compound 51 was injected directly into the lateral ventricles. This resulted in a decrease in brain BuChE at 24 hours which was subsequently reversed by 72 hours after drug administration. The lower level of BuChE activity in the brain at the 24 hour time point suggests that compound 51 is metabolised slowly by this enzyme in the brain contrary to the results obtained from pharmacodynamic studies. The differences between these studies may be accounted for by the presence of different concentrations of esterases in the brain and blood.

Compound 30 proved to be potent *in vitro*; however this compound did not produce a substantial decrease in BuChE activity *in vivo*. 1 mg/kg of compound 30 via i.p. administration produced a decrease in plasma BuChE activity. The lack of correlation between the *in vitro* and *in vivo* potencies exhibited by compound 30 may be explained by its high log P value. The compound may have partitioned into the adipose tissue thus leaving less drug in the blood to inhibit plasma BuChE. Brain BuChE activity increased at 24 and 48 hours followed by a decrease at 72 hours. The level of BuChE

activity in the liver showed an increase 24 hours following administration of the compound but this decreased on progression to the 48 and 72 hour timepoints. Administration of 5 mg/kg did not produce any significant changes in brain BuChE activity. The level of enzyme in the liver increased 24 hours following administration of the compound with reversal upon progression to the 48 and 72 hour timepoints.

A single dose of 1 mg/kg of compound 33 i.p. reduced plasma BuChE in the mouse by approximately 30%. In the brain the level of BuChE activity significantly decreased at 24 hours and 48 hours compared to control values. The level of BuChE activity did recover over the 72 hour period. The novel compound also reduced the activity of BuChE in the liver of the drug-treated animals with the activity significantly lower than that of saline-treated control animals, although this began to recover during the 72 hour observation period.

Rivastigmine produced approximately a 40% decrease in mouse plasma BuChE activity following a single i.p. dose at 1 mg/kg. In the brain the activity of BuChE varied following administration of rivastigmine; there was a slight decrease 24 hours post-administration but this was not significantly different from the control BuChE activity. The activity of BuChE then rose 48 hours following administration of the drug followed by a subsequent decrease 24 hours later. There was no significant decrease in the liver BuChE activity compared to the control BuChE activity 24 hours following administration of the compound. This was followed by an increase at 48 hours and apparent recovery towards normal BuChE levels at 72 hours post administration.

The differences observed in the pharmacodynamic profiles of the novel compounds and rivastigmine may represent different substrate affinities for the enzyme BuChE in the mouse. Mouse BuChE may have different catalytic affinities for each of the compounds. The potency values observed *in vitro* differed from those seen *in vivo*. It was anticipated that the compounds that exhibited the greatest potency *in vitro* would also show a similar level of potency against BuChE *in vivo*; however, this was not the case. This may be due to individual differences in drug absorption, as the multi-compartmental system of the body is very different from that of a one-compartment model *in vitro*.

The profile of BuChE activity seen after rivastigmine administration may be indicative of homoeostatic control of cholinesterase activity, with BuChE compensating for reduced AChE activity. Although rivastigmine is a dual inhibitor of AChE and BuCE, it shows approximately 5-fold selectivity for AChE [238]. Potent inhibition of AChE might prompt BuChE to assume a greater role temporarily. A similar compensatory action is believed to come into play in AD: As the disease progresses, AChE activity may fall to 55-67% of normal levels in the affected cholinergic regions but simultaneously there may be an increase of 40-90% in BuChE activity [239].

Based on these investigations it was decided to use compound 51 at a dose of 1 mg/kg for cognitive studies. This dose gave significant BuChE inhibition not only peripherally but also centrally, and it also showed no apparent toxicity after acute administration.

2.9.6 Pharmacokinetic profile of novel compounds

The aim of this study was to determine a pharmacokinetic profile for the novel BuChE inhibitor, compound 51, following both oral and intraperitoneal routes of administration. However, the levels of the novel compound in the plasma, brain and liver samples were below the level of detection for the HPLC analysis system. It was not merely the case that rapid hydrolysis had led to such low levels of the compound *in vivo* since the compounds' metabolites were not detectable either. It was concluded that the concentration of the compound in the animals' tissues was below the micromolar limit of detection for HPLC.

2.9.7 Diurnal variation

It is known that a normal circadian variation in a number of enzymes is present in the body [222, 240]. This study showed that there is also diurnal variation in plasma butyrylcholinesterase activity in healthy male mice. It appears that the highest activity for this enzyme is in the morning time and a lower activity is observed in the evening. Studies have shown that the neurotransmitter acetylcholine (ACh) exhibits diurnal variation [209, 241]. It has also been shown that the activity of BuChE in the walls of capillaries in the medulla oblongata and mesencephalon show maximum activity during the day and a decreased activity at night in rodents [242]. However, there had been no previous investigation of circadian variation in BuChE activity in the plasma of mice thus very little literature is available on this topic.

The variation in the enzymatic activity of BuChE in mouse plasma may be linked to the possible lipid metabolizing function that has been attributed to BuChE [243]. As rodents are active at night and sleep during the day, their food consumption would tend to be greatest during the night. It could be possible that the higher levels of BuChE enzyme activity observed during the morning may be associated with post-prandial metabolism. The lower evening enzyme level might be accounted for by the lack of activity and food consumption during the daylight hours.

Chapter 3

Lesion-based model of Alzheimer's disease

Chapter 3 Lesion-based model of Alzheimer's disease

3.1 Introduction

3.1.1 Background

It is known that the nucleus basalis of Meynert provides a large cholinergic input into the neocortex [244]. In AD it is has been established that there is a significant reduction in the cholinergic neurons of the basal nucleus [245]. In the rodent brain, AChE-rich basal forebrain neuronal fibres have been found to enter the anterior and lateral cortex and branch in a complex organized pattern [246]. Disruption or lesioning of the basal nucleus magnocellularis in rodents has shown a decrease in cholinergic neuron numbers as well as an impairment of spatial learning [247-251]. The lesioning agent ibotenic acid (IBO) was chosen as in most cases it produces more behavioural impairments than other lesioning agents such as AMPA (α-amino-3-hydroxy-5-methyl-4-isoxazole proprionic acid) or quisqualic acid [252]. Ibotenic acid has been shown to cause a 30% reduction in extracellular ACh levels and a loss of ChAT-immunopositive neurons [253]. Higher doses of ibotenic acid can cause approximately 75% loss of cholinergic neurons [100]. Injections of ibotenic acid into the nucleus basalis magnocellularis (nBM) can cause substantial impairments in spatial learning acquisition and performance in rodents in a water maze task [98, 252, 254].

3.1.2 Aims

This experiment sought to determine whether acute treatment with a novel BuChE inhibitor could reverse any spatial learning impairment associated with a cholinergic deficit caused by ibotenic acid lesions of the nBM in mice.

3.2 Animals

Thirty two 2 - 3 month old healthy experimentally naïve male C57BL/6 mice (24 – 29 g) were obtained from Harlan, UK. Animals were housed in single cages with

isopad bedding (Harlan, UK) in a specific pathogen free (SPF) environment with controlled temperature and humidity. All animals had *ad libitum* access to food and water. A twelve hour light/dark cycle was in operation (lights on 7 a.m. – 7 p.m. GMT). All experiments were carried out in accordance with the European Communities (Amendment of Cruelty to Animals Act 1876) Regulations 2002. All animals were allowed an acclimatization period of one week upon arrival to the Bioresources Unit in the Trinity College Institute of Neuroscience (TCIN) prior to any treatment. The animals were handled daily for five minutes by the experimenter.

3.3 Preparation of drugs

3.3.1 Compound 51

1 mg of compound 51 was transferred to a 10 ml volumetric flask to which sterile WFI (Braun, UK) was added to produce a concentration suitable for delivery. The compound was not initially soluble in the WFI so it was placed in a sonicator (Branson, Netherlands) for 20 minutes at 30°C. Following sonication and heating the compound formed a solution in the sterile WFI.

3.3.2 Anaesthesia

0.5 ml of ketamine (Vetalar) (50 mg) (Pharmacia Animal Health Ltd., UK) and 0.25 ml of xylazine (Rompun) (5 mg) (Bayer Health Care, UK) were diluted in 4.25 ml of sterile WFI in a sterile 10 ml container [220]. The ketamine/xylazine solution was administered at 0.1 ml per 10 g of body weight to each animal (100 mg ketamine and 10 mg xylamine per kg body weight) via i.p. injection into the left lower quadrant of the abdomen.

3.3.3 Analgesia

1 ml of Rimadyl (0.5 mg/100 g) (Pfizer, Dublin) was diluted in 20 ml of sterile WFI in a sterile 30 ml plastic container. A dose of 0.1 ml per 50 g of body weight was administered to each animal via i.p. injection into the left lower quadrant of the abdomen [255].

3.3.4 Lesioning agent

100 µl of 0.1 M PBS pH 7.4 was added to 1 mg of ibotenic acid (Sigma-Aldrich, Dublin) to form a 1 mg/100 µl solution [256]. 0.1 µl of ibotenic acid was injected into the basal nucleus bilaterally.

3.4 Surgery

3.4.1 Preparation of animals

Stereotaxic surgery was performed on the animals. The mice were anaesthetized with 100 mg ketamine and 10 mg xylazine per kg of body weight [220]. Once sedated the animal was gently placed on a stereotaxic frame (Kopf, Germany). The side of the head was supported with the aid of earbars while the front of the head was supported using a tooth bar adapted for a mouse. The earbars with earbar adaptors were gently inserted into the animal's ear and rested in the external auditory meatus. The upper teeth of the mouse were inserted into the tooth bar of the head holder and locked into position. A heating pack (Mediheat, UK) was heated in warm water and placed underneath the animal on the stereotaxic frame to maintain its body temperature during surgery. Vaseline (Unilever, Norway) was gently applied to the animal's eyes with the aid of a clean cotton bud to prevent them drying out. The hair on the head of the animal was carefully cut using a sharp scissors. A sterile carbon steel surgical blade (size 11) (Swan Morton, England) was used to make an incision down the middle of the scalp. The skin was then retracted. Bregma was identified and the area was cleaned using a sterile cotton bud. It was ensured that bregma and lambda were in the same horizontal plane. The coordinates for the basal nucleus were determined using a stereotaxic atlas for the mouse brain [257]. The coordinates for the basal nucleus were measured from bregma: 0.198 cm lateral, -0.082 cm rostral and 0.39 cm dorsoventral.

3.4.2 Injection procedure

A 0.5 µl Hamilton syringe (Hamilton, Switzerland) fitted with a 25 gauge needle containing the ibotenic acid solution or 0.9% sterile saline (Baxter, UK) was mounted on the stereotaxic frame. The syringe was moved superficially over the lateral and rostral locations of the basal nucleus above the skull using the horizontal vernier scales on the stereotaxic frame. Once located superficially the area was marked with a fine marker. A fine stereotaxic drill (Kopf Model 1471, Kopf, Germany) was used to create entry points bilaterally for the syringe to pass through the skull ensuring the meninges were not damaged. The needle was carefully lowered 0.39 cm into the brain using the vertical vernier scale bar on the stereotaxic frame. Once the location of the basal nucleus was reached, 0.1 µl of ibotenic acid solution or 0.9% sterile saline was slowly injected over 5 minutes manually with the aid of a syringe plunger driver with a control knob and handle. The needle remained in the brain for a further five minutes to ensure absorption of the ibotenic acid or 0.9% saline into the brain. The needle was then carefully and slowly withdrawn from the brain and cleaned with a sterile cotton swab containing ethanol (Sigma-Aldrich, Germany). The same injection procedure was carried out on the ipsilateral side. Rimadyl (Pfizer, Dublin) was administered i.p. to each animal following surgery. Animals were then placed in a heated cage (Mediheat V1200 veterinary recovery chamber, Harvard Apparatus, UK) set at 25°C until the effect of the anaesthetic had worn off and they were subsequently returned to their home cage. All animals were given a period of one week to recover from surgery during which their health was continually monitored by the experimenter and the animal technician. A few hours following surgical treatment all animals were awake and feeding and drinking as normal.

3.4.3 Drug treatment

The animals were randomly assigned to one of four groups with 8 animals per group:

- lesioned and treated with 0.1 ml/10 g of 0.9% sterile saline i.p.
- lesioned and treated with 1 mg/kg of compound 51 i.p.
- sham-lesion treated with 0.1 ml /10 g of 0.9% sterile saline i.p.
- sham-lesion treated with 1 mg/kg of compound 51 i.p.

Mice were acutely dosed with 0.9% sterile saline or 1 mg/kg of compound 51 0.1 ml/10 g 30 minutes prior to commencing the maze, via i.p. injection into the left lower quadrant of the abdomen using a sterile 21 gauge needle (BD Microlance, England).

3.5 The Morris water maze

3.5.1 Introduction

The Morris Water Maze (MWM) was first described in 1981 by Richard Morris. This maze was used to investigate spatial learning and memory in the rat using a swimming task whereby animals had to learn to locate a platform using visible proximal or distal visual cues [258]. It is now one of the most widely used tests to assess spatial learning and memory in rodents [259]. It is used to validate neurocognitive disorders and possible neurocognitive treatments [260]. It is an escape task in which the animal must learn to escape from the adverse environment of the water to the safety of the platform. The platform represents the reward for completing the maze. The MWM relies on the use of proximal or distal visual cues to learn the maze and spatial mapping of the visual cues relative to the platform. In general, the visual strategy dominates performance of mice in the water maze; however in the absence of visual cues olfactory cues prevail [261]. Albino animals are not as proficient in learning the MWM as other strains with no visual defects [262]. Studies have shown that C57BL/6 mice are adept at solving the MWM [263-265] and for this reason this strain of mice was chosen for this experiment. Differences in spatial learning occur between male and female rodents with males outperforming females. The sex hormones are thought to play a role in this as gonadally intact female rats perform more poorly than ovariectomized females. Strain differences also account for differences in ability to learn the MWM [260]. The melanic C57BL/6 mouse strain is recommended for visual tasks and they show better performance over other mouse strains [265].

The pool diameter also influences the difficulty of the maze. Smaller mazes are less stressful for animals and make the task easier. Different maze diameters have been used: 75 cm, 90 cm, 120 cm and 150 cm. However, superior performance has been found using a 120 cm pool in combination with a 15 cm diameter platform in particular in the C57BL/6 strain of mice [266], hence the reason these dimensions were chosen.

3.5.2 Apparatus

The Morris water maze was set up in a sound proof room with adequate fluorescent lighting. The water maze consisted of a white circular tank 120 cm in diameter and 60 cm in height. It was filled with water at 20 - 22°C. The water was made opaque by the addition of powered milk. A Perspex platform, 15 cm in diameter and 23 cm in height, was submerged 1.5 cm below the water surface and 13 cm from the edge of the pool wall in the southeast quadrant. A fine nylon cloth was secured over the top of the platform to ensure that the animals could grip onto the platform once it was found. Two white walls and two white screens (110 cm in height by 120 cm in width) surrounded the water maze at an equal distance of 30 cm and each bore a distinct visual cue card (30 cm x 30 cm). The visual cues were cut from coloured art paper and consisted of a blue circle, a square box bearing a white and black diagonal striped pattern, a red cross and a green triangle (*Figure 3.1)*. A camera was fixed to the ceiling above the water maze and connected to the computer-based tracking programme Water 2020 (HVS Image, UK). The pool was divided into four quadrants, namely north, south, east and west, by the aid of an imaginary line using the Water 2020 software. The main parameters recorded were latency to the platform (s), path length (cm), swim speed (cm/s), thigmotaxis i.e. swimming close to the wall of the pool (% time) and time spent in the platform containing quadrant (% time).

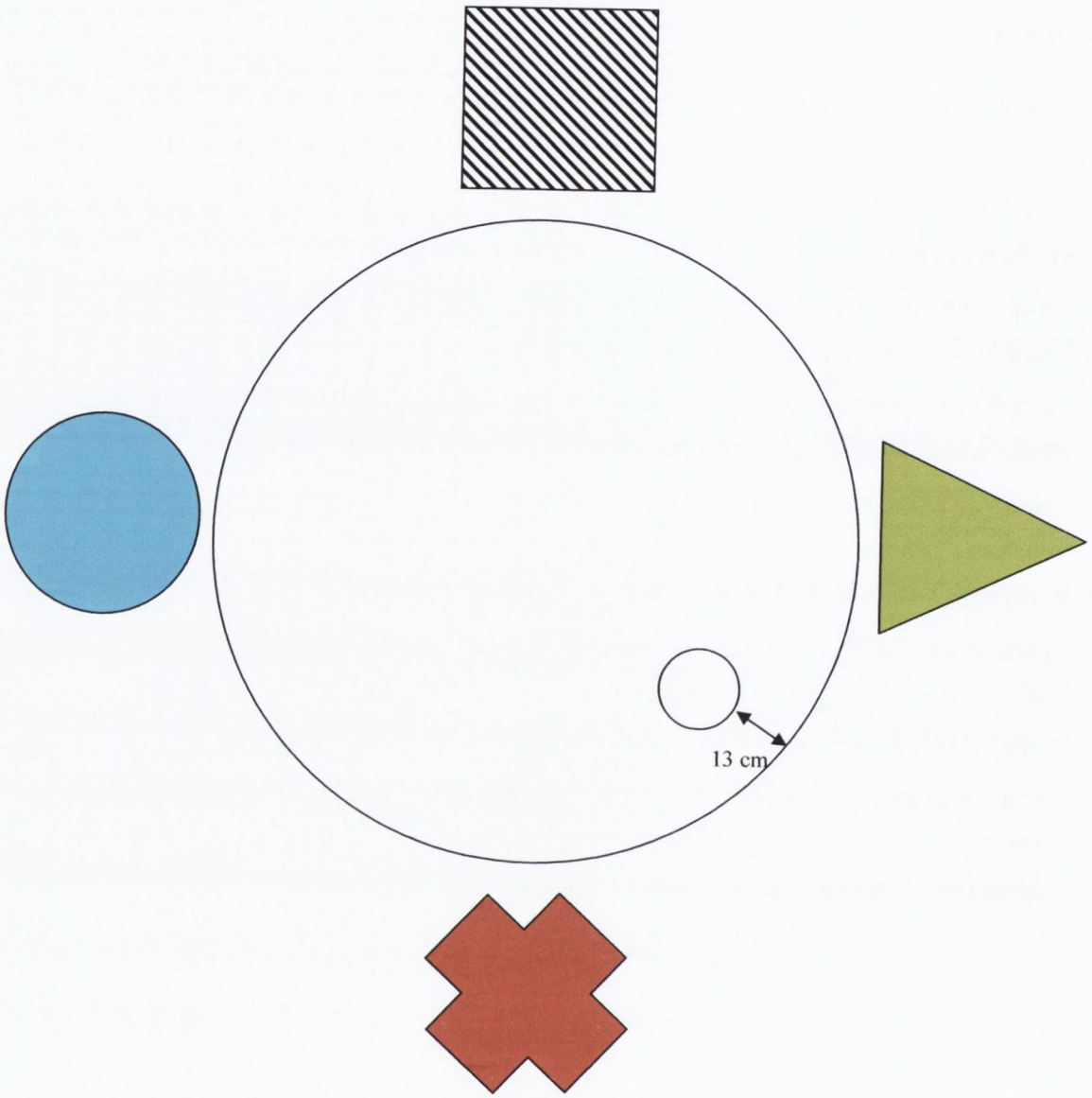

Figure 3.1 *Water maze with platform and visual cues.*

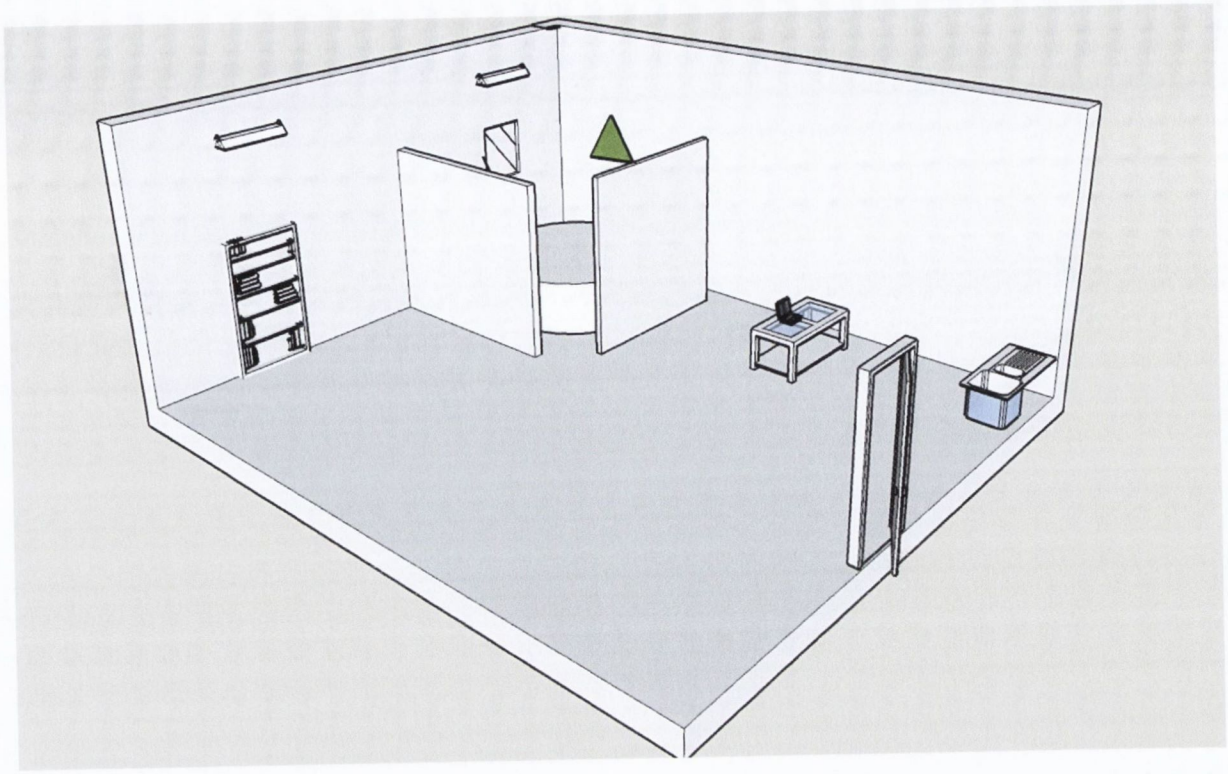

Figure 3.2 *Layout of apparatus in the room for Morris Water maze testing.*

3.5.3 Habituation

Animals were first subjected to a single habituation session during which the animal learned that a safe area existed onto which they could escape from the water. During the habituation session the platform was visible above the water level and marked with a red flag. No visual cues were used during the habituation session. Each animal was placed randomly into the pool facing the pool wall and guided to the platform by the experimenter using a plastic rod. All animals found the platform within 2 minutes and then remained on it for one minute to become familiar with the trial objective and the surrounding area.

3.5.4 Training

Training was commenced the following day and was carried out for 5 consecutive days. During the training sessions the platform was submerged 1.5 cm below the water and the visual cues were put in place. The water was made opaque by the addition of powdered milk. Each training day consisted of four one minute trials with an inter-trial interval of 3 minutes during which the animal was returned to its home cage. The home cage was heated to 25°C by means of a hot water bottle placed underneath the base of the cage. During each trial each animal was placed in a small plastic box (13 x 10 cm) and gently lowered into the pool facing the pool wall. During each trial all animals were released from random start points (*i.e.* north, south, east or west) and these start points were randomized daily by means of a random sequence generator programme [267]. Each trial consisted of a fixed time period of 60 seconds in which each animal had to locate the platform; failure of an animal to find the platform within this time period resulted in the animal being placed on the platform by the experimenter. Following each trial, regardless of success or failure to locate the position of the platform, each animal was placed on the platform for 20 seconds to become familiar with the location of the platform relative to the proximal visual cues.

3.5.5 Probe trial

The probe trial was carried out on day 6 following the training days. This consisted of a single one minute trial in which the platform was removed from the water maze. The probe trial is a measure of an animal's spatial learning ability and ability to retain and access previously learned information. Each animal was gently lowered into the centre of the pool facing away from the experimenter. The percentage of time each animal spent swimming in the quadrant previously containing the platform (*i.e.* southeast quadrant) was measured.

3.6 Statistical analyses

Differences in latency, path length and swim speed were assessed by a two-way ANOVA for repeated measures using SPSS version 14.0 with latency, path length, swim speed, thigmotaxis, and time spent in the platform-containing quadrant as within-subject factors and surgery and treatment as between-subject factors. Post-hoc pair comparisons, Tukey's HSD test, were calculated where appropriate.

3.7 Object recognition task

3.7.1 Introduction

In 1988 Enaceur and Delacour described a new memory test based on animals' exploration of familiar and new objects. It was a one-test trial that assessed 'pure' working memory and did not involve any reward or punishment reinforcements [268]. Known today as the object recognition trial this task takes advantage of an animal's natural tendency to explore novelty. It is a popular task due to the lack of stress it places upon the animal, the fact that relatively little training is required, and the absence of requirement for external motivation [269, 270]. This paradigm was chosen as another means by which to assess the spatial memory of the animals in a less aversive environment than the MWM.

3.7.2 Apparatus

The apparatus consists of a white circular open arena (120 cm in diameter and 60 cm in height) in a sound proof room with optimal fluorescent lighting. The arena was screened by two white walls and two large white boards (110 cm in height x 120 cm in width). Five of six plastic objects were introduced into the maze. The six objects consisted of: A a rectangular wall (12.5 x 3 x 15.5 cm); B a cone-shaped object with a wheel on top (11.5 x 5.5 x 6 cm); C a small block with a triangle on top (6 x 6 x 11 cm); D a cuboidal Lego brick (6.5 x 6.5 x 17 cm); E an irregular-shaped block (9.5 x 6 x 12.5 cm); and F an irregular heptagon shaped block (10 x 2.5 x 10 cm). The initial arrangement of the objects was square with one central object *(Figure 3.3)* with the objects placed at a distance of 15 cm from the maze wall. This protocol was adapted from Middei *et al*, 2006 [271]. This paradigm was manually recorded by the experimenter.

3.7.3 Training

3.7.3.1 Habituation

Animals were first introduced to the open arena on day 1 in the absence of the objects to become familiar with the open field thus reducing anxiety and stress-related behaviours such as thigmotaxis.

On day 2 the animals were given three consecutive 5 minute sessions (sessions 1 - 3) to explore the objects with an inter-trial interval of 3 minutes. Object exploration was measured as the total duration of contacts with the five objects. A contact was defined as the animal's snout touching the object. All the objects, the floor and the walls of the maze were cleaned with a 1% Tego solution following completion of each animal's session to remove any olfactory cues that might interfere with the next animal's exploration.

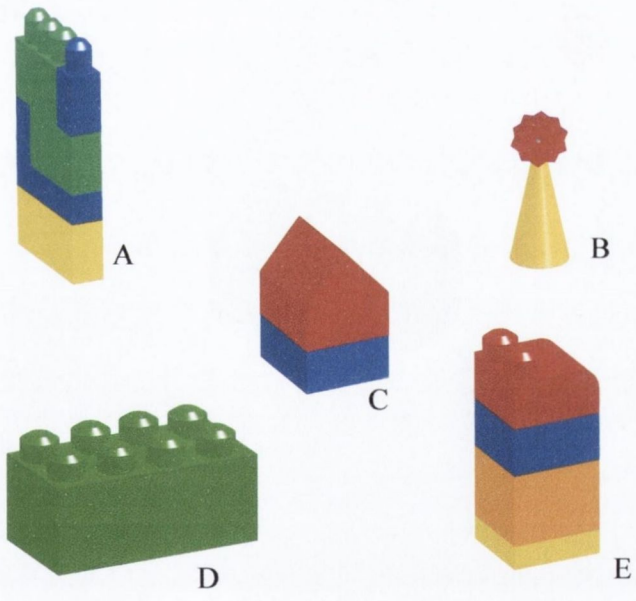

Figure 3.3 *Spatial arrangement of objects in the open field during the habituation sessions (S1 - S3).*

3.7.3.2 Reactivity to spatial novelty

On day 3 during sessions 4 and 5, the spatial configuration of the objects was initially (session 4) the same as that in the habituation sessions S1-S3 on the previous day (*Figure 3.3*). The configuration was then changed (session 5) by displacing objects B and C (*Figure 3.4*). Mice were allowed to explore the configurations during two consecutive 5 minute periods with an inter-trial interval of 3 minutes. Reactivity to spatial novelty was estimated by comparing the mean duration of contacts with the displaced objects (DOs) and the non-displaced objects (NDOs) in session 5 subtracting the mean duration of contacts with the same object in session 4, *i.e.* before the change.

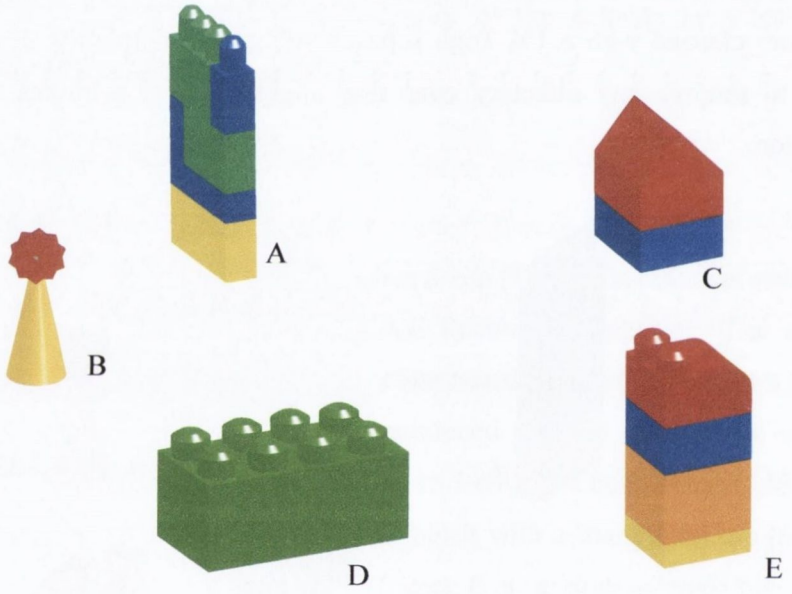

Figure 3.4 *Spatial arrangement of the objects in the open field during the spatial novelty session 5.*

3.7.3.3 Reactivity to object novelty

In session 6 on day 3, the non-displaced object E was substituted with the novel object F. Mice were given a final 5 minute session in which to explore both the displaced objects and the novel object. Reactivity to object novelty was estimated by comparing the mean duration of contacts with the substituted object (SO) and the non-substituted objects (NSOs) subtracting time spent with the objects that were at the same location in session 5, *i.e.* before the substitution of object E by object F.

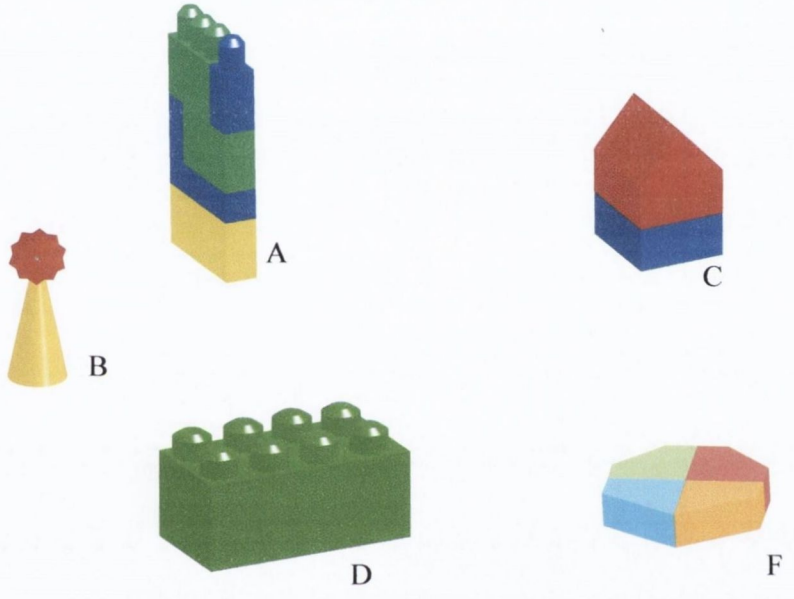

Figure 3.5 *Spatial arrangement of objects in the open field during the object novelty session (session 7).*

3.8 Statistical analyses

Habituation to the objects (sessions 1 - 3) were analysed by a two-way ANOVA for repeated measures using SPSS version 14.0 with age and treatment as between-subject factors and sessions as the within-subject factor. Reactivity to spatial and object novelty was evaluated using a two-way ANOVA for repeated measures with surgery and treatment as between-subject factors and object category as the within-subject factor. T-tests were used to compare the activity of each animal between sessions. Post-hoc pair comparisons, Tukey's HSD test, were calculated where appropriate.

3.9 Verification of lesion

3.9.1 Processing of brain tissue

Following evaluation in the two paradigms all animals were sacrificed using carbon dioxide asphyxiation. When there was no response from the animal to the paw pinch reflex the animal's head was carefully removed from the neck with a sharp scissors. The scalp was cut down the centre and retracted revealing the skull. The skull was then gently incised inferolaterally on both sides and carefully retracted superiorly using a fine forceps. The skull was removed and the brain was exposed. The meningeal connection to the skull on the under surface of the brain was detached using a fine scissors. The brain was carefully removed.

The body and skull of each animal was disposed of according to the health and safety guidelines in the Bioresources Unit in TCIN. The brain was placed on top of a glass box with a lid containing ice to keep the tissue cool. The olfactory bulbs and cerebellum were removed using a sterile carbon steel surgical blade (Swan Morton, England). The cortex was fixed to a cork disk (20 mm diameter and 3 mm thick) (Raymond A. Lamb, USA) using OCT (optimum cutting temperature) compound (Sakura Finetek Europe, NL) with the occipital cortex facing downwards. The cork disk and brain were immersed into a beaker containing isopentane which lay over a flask of liquid nitrogen at -120°C. Once removed the brain was completely covered with OCT and again dipped into the isopentane over liquid nitrogen. The frozen brain tissue in OCT was wrapped in a labelled piece of tinfoil and stored at -80°C until sectioned.

3.9.2 Preparation of slides

A subbing solution was prepared for the slides. 2.5 g of gelatin (Fluka, Germany) and 0.25 g of chromium (III) potassium sulphate dodecahydrate (Sigma-Aldrich, Dublin) were weighed and transferred to a 500 ml conical flask to which 500 ml of distilled water was added. The solution was heated to 150°C and stirred using a magnetic stir bar on a heated plate stirrer (IKA Labortechnik, Germany) for one hour. The slides were then dipped in the subbing solution approximately five times each for 3 seconds at

each time. The slides were then placed on a slide rack, covered and left to dry overnight.

3.9.3 Sectioning of brain tissue

The brain sections were removed from the -80°C freezer and placed on ice. Each brain sample fixed to a cork disk was placed onto a metal key using a drop of water to freeze the cork disk to the metal key. Each brain sample was then placed in the -20°C cryostat (Leica, Laboratory Instruments, Ashbourne, Co. Meath) for one hour for the sample to adjust to the new temperature. The key was mounted to a chuck on the cryostat and the disposable microtome blade (Laboratory Instruments, Ashbourne, Co. Meath) and the anti-rolling plate were set in place. The dial was set to cut the initial sections at 50 µm. 50 µm sections were removed from the brain sample for the first 2000 µm. Thereafter the dial was adjusted to cut 20 µm sections.

Each 20 µm section was carefully cut using a sharp disposable microtome blade. The cut section then went under the anti-rolling plate. The anti-rolling plate was lifted up and the section was carefully rolled out using a fine tipped paint brush. The subbed slide was lowered over the section and the brain section then stuck to the slide which was maintained at room temperature. The brain sections were placed on the slide in a specific pattern as shown in *Figure 3.6* and they remained in the cryostat at -20°C until stained.

140µm	100µm	60µm	20µm	
160µm	120µm	80µm	40µm	

Figure 3.6 Layout of sections on subbed slide.

3.9.4 Preparation of cresyl violet stain

2 g of cresyl violet (Sigma Aldrich, Germany) were weighed and transferred to a 500 ml conical flask. 500 ml of distilled water was added to the conical flask. (For more intense staining a double concentration cresyl violet solution was made: 4 g in 500 ml of distilled water. The solution was stirred using a magnetic stir bar on a stir plate (IKA Labortechnik, Germany). The cresyl violet solution was filtered using a 0.22 µm disposable Steritop filter (Millipore, Ireland) driven by a vacuum pump (KNF, Germany). The solution was stored at room temperature until use.

3.9.5 Staining of slides

The slides with the brain sections were placed in a glass slide rack and defrosted at room temperature for 1 minute. Glass troughs were set up each containing a separate solution of either cresyl violet, 70% ethanol, 90% ethanol, 100% ethanol or xylene. The slides were first placed in the cresyl violet solution for two minutes. The slides were next placed under tap water at a slow flow for 20 seconds to remove the excess cresyl violet. The slides were subsequently immersed through a series of graded ethanol baths to dehydrate the tissue. Firstly the slides were gently dipped three times into a glass trough containing 70 % ethanol followed by 90% ethanol and finally 100% ethanol. Finally the slides were placed in xylene for up to 2 hours to clear the tissue of ethanol. The slides were removed from the xylene and a drop of the mounting medium DPX (distyrene, a plasticizer, and xylene) (DBH VWR International Limited, Poole, England) was placed on the centre of the slide. A coverslip was gently lowered onto the slide with the aid of a forceps. Any air bubbles were expelled by applying gentle pressure to the coverslip. The slides were left to dry in a fume hood overnight or until the DPX had completely dried.

3.9.6 Microscopic examination of slides

The slides from each animal were viewed under a Nikon Eclipse E200 microscope (Nikon, Japan) at magnifications of 40 X and 100 X. Photographs of the needle tracks were taken by photomicroscopy using a Nikon Coolpix 4500 4.0 megapixel camera (Nikon, Japan) attached to the microscope. The needle tracks were identified by a disrupted pattern in the arrangement of the cells. The lateral ventricles containing the choroid plexi were identified and lateral to these passed the needle track to reach the basal nucleus inferiorly.

3.10 Results

3.10.1 Histology

Photomicroscopy of the slides showed that the needle tracks were not continuous on one section of the brain tissue; rather there was continuity of the needle tracks over a series of brain sections. This may indicate that when the brains were glued to the cork disks they were not placed perfectly straight on them once the cerebellum was removed. Nevertheless the needle tracks were identified following cresyl violet staining of the brain tissue. 20 µm coronal sections were taken of the mouse brains. The approximate diameter of the basal nucleus is 280 µm in the mouse brain [257].

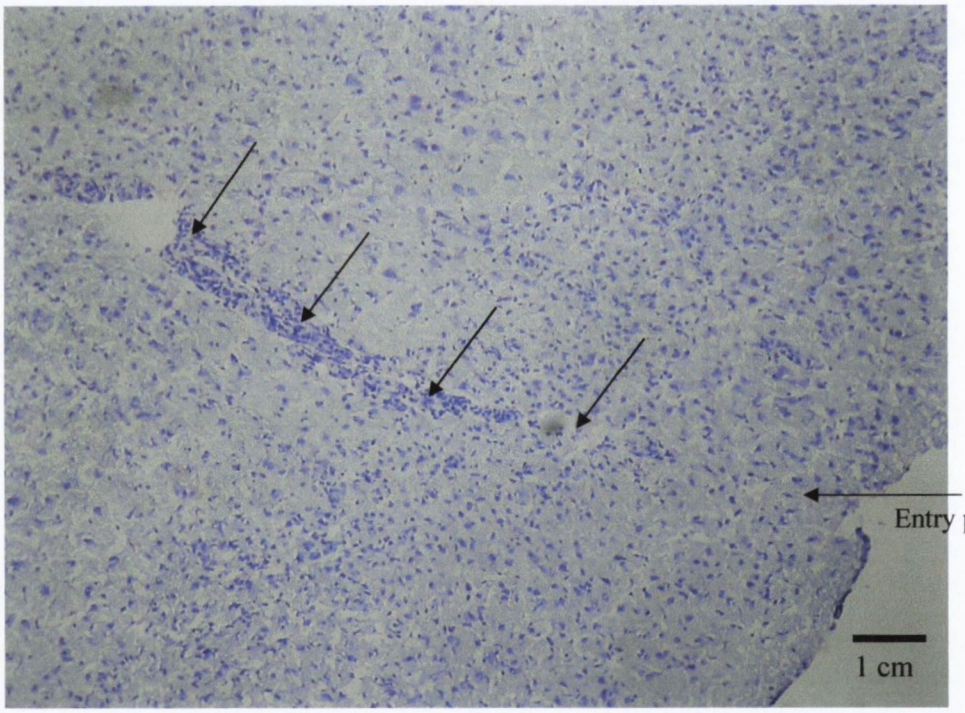

Figure 3.7 *Entry point of the needle track into the mouse brain. Magnification X 100. Cresyl violet staining. Scale bar – 1 cm.*

Arrows point to the needle track passing through the brain.

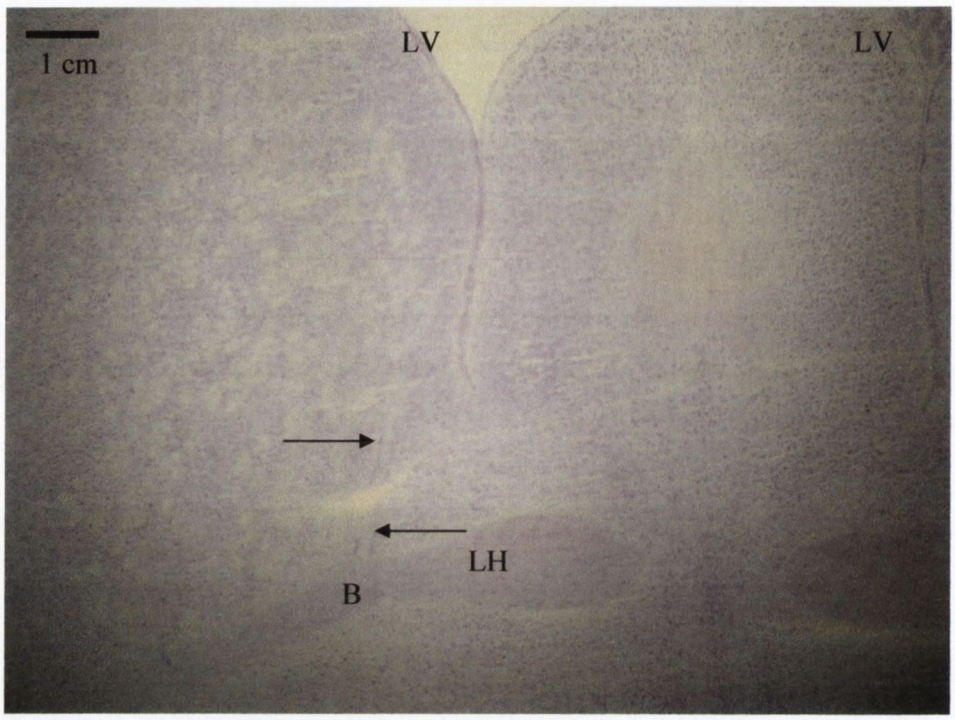

Figure 3.8 *Needle track passing lateral to the lateral ventricle and finishing at the location of the basal nucleus.*

Arrows point to the needle track. Magnification X 40. Scale bar - 1 cm. Cresyl violet staining.

LV – lateral ventricle; B – basal nucleus; LH - lateral hypothalamus.

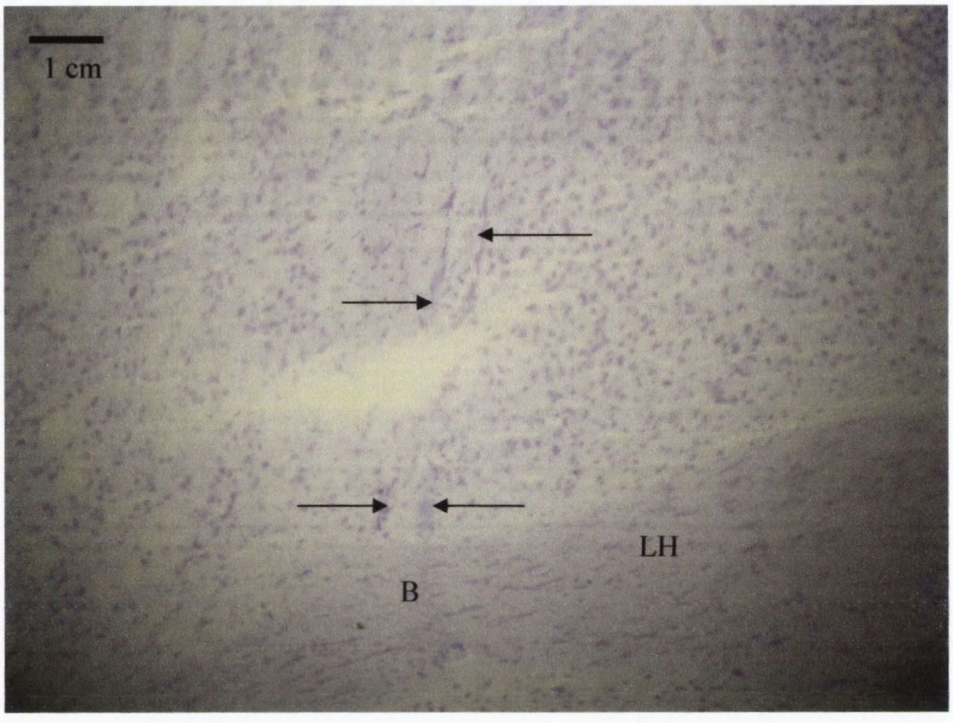

Figure 3.9 *Needle track finishing at the location of the basal nucleus. Arrows point to needle track. Cresyl violet staining. Magnification X 100. Scale bar – 1 cm.*

B – basal nucleus; LH – lateral hypothalamus

3.10.2 Results: Morris water maze

3.10.2.1 Latency to platform

While the sham lesioned animals treated with saline had the shortest latency to the platform their latency decreased by approximately 7 seconds from day 1 to day 5. The IBO lesioned drug-treated animals had a steepest learning curve and showed a 15 second decrease in their latency on comparison of day 1 and day 5. The IBO lesioned saline-treated animals had a latency of 38.45 seconds on day 1 and 34.95 seconds on day 5. The worst perfomers were the sham lesioned drug group as training did not improve their latency to the platform. A statistically significant difference was found among the groups using a two-way ANOVA for repeated measures, $F(1, 26) = 8.564$; $P < 0.001$. Tukey's HSD post-hoc tests revealed a difference between the IBO lesioned saline group and the IBO lesioned drug group ($P < 0.05$) and also between the sham lesioned saline group and the sham lesioned drug group ($P < 0.05$).

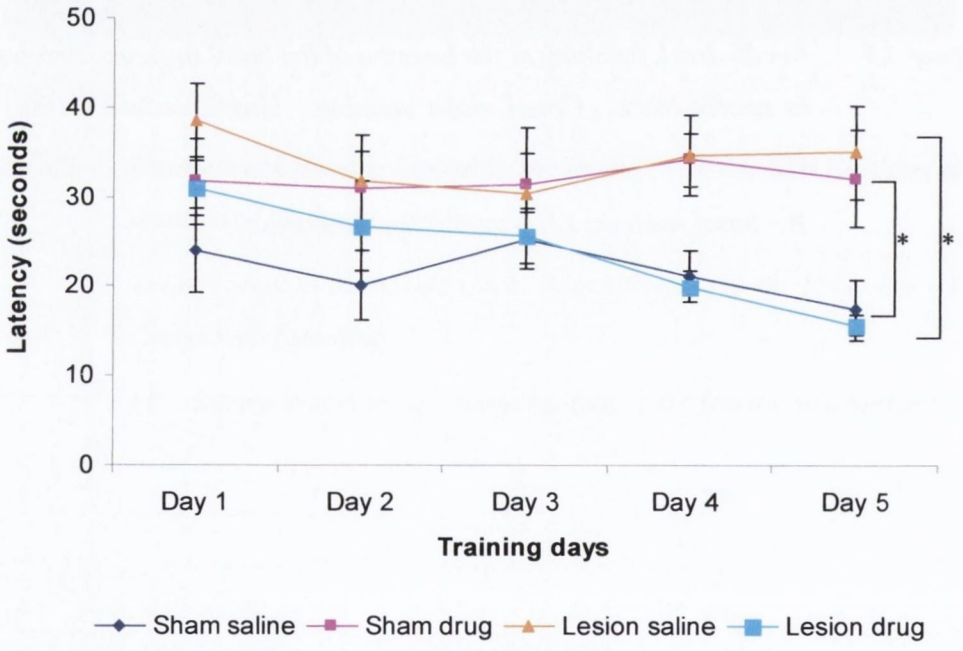

Figure 3.10 *Latency to reach the platform (s) during water maze training days 1 - 5. IBO lesioned drug-treated, IBO lesioned saline-treated, sham lesioned drug-treated and sham lesioned saline-treated 2 -3 month old male C57BL/6 mice. Mean ± SEM. n = 8 per group. * P < 0.05.*

3.10.2.2 Path length

All of the groups had a decrease of approximately 100 cm in their path lengths to the platform across the training days except the IBO lesioned saline-treated group. The lesioned animals treated with saline had an increase of approximately 70 cm over the training days. The IBO lesioned saline-treated mice had the longest path length to the platform. A two-way ANOVA revealed statistically significant differences between the groups, $F(1, 27) = 4.128$, $P < 0.001$. Post-hoc analysis showed differences between the IBO lesioned saline-treated and IBO lesioned drug-treated animals, $P < 0.05$; and the sham lesioned saline-treated and IBO lesioned saline-treated animals, $P < 0.05$.

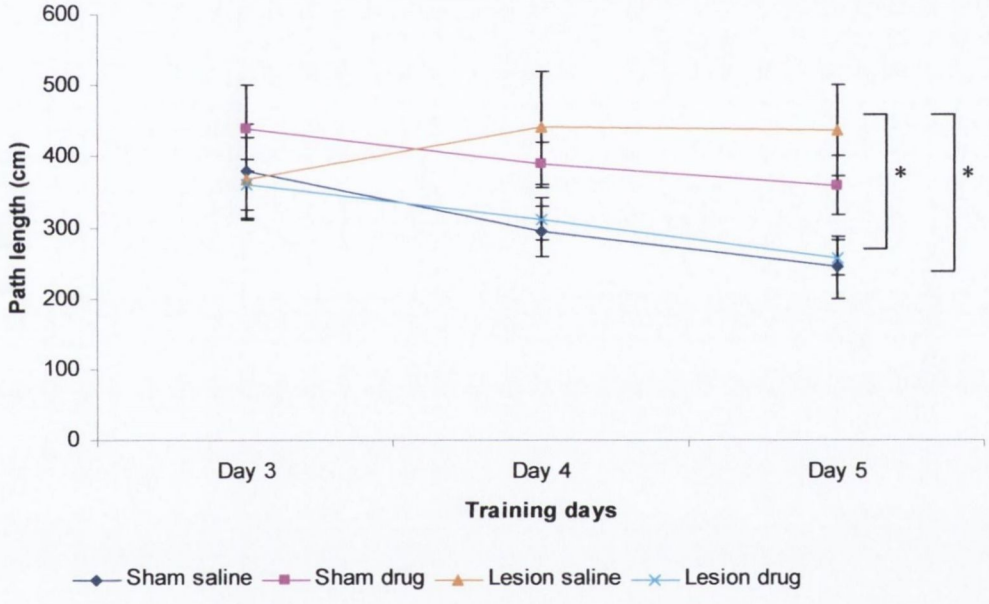

Figure 3.11 *Path length (cm) of animals to reach the platform during water maze training days 3 – 5. IBO lesioned drug-treated, IBO lesioned saline-treated, sham lesioned drug-treated and sham lesioned saline-treated 2 - 3 month old male C57BL/6 mice. Mean ± SEM. n = 8 per group. * P < 0.05.*

3.10.2.3 Swim speed

The sham lesioned mice treated with saline and the IBO lesioned drug-treated animals showed the fastest swim speed of the groups. The IBO lesioned saline-treated animals were slower swimmers; however, the sham lesioned drug-treated group had the slowest swim speed of all the groups. Statistical analysis using a two-way ANOVA for repeated measures showed a significant difference between the groups, $F(1, 27) = 8.243$, $P < 0.001$. Post-hoc analysis reveals differences between the sham lesioned saline-treated and sham lesioned drug-treated groups, $P < 0.05$; IBO lesioned saline-treated and IBO lesioned drug-treated groups, $P < 0.05$; and the sham lesioned drug and IBO lesioned drug-treated groups, $P < 0.05$.

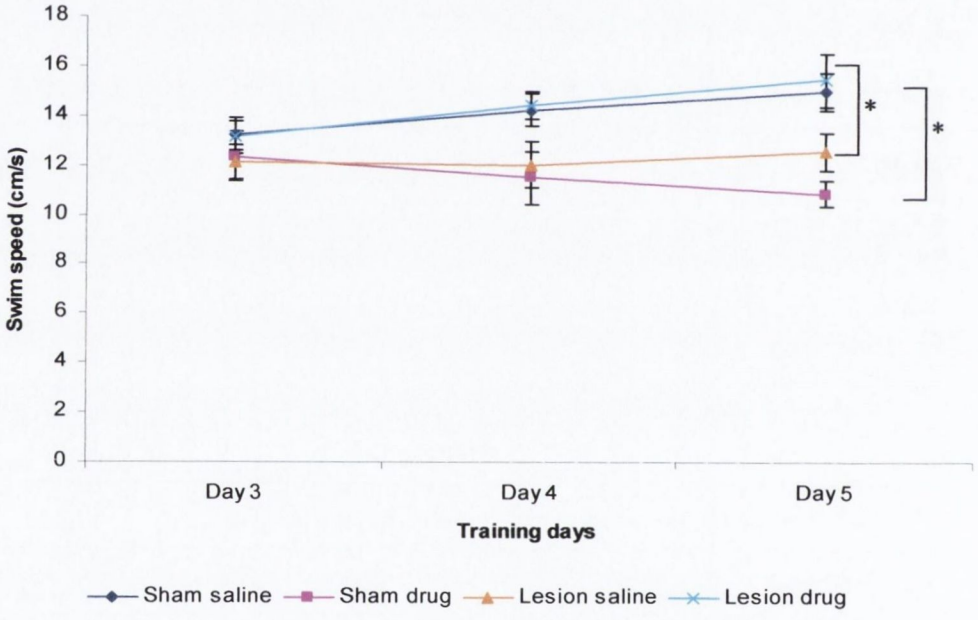

Figure 3.12 *Swim speed (cm/s) of animals during water maze training days 3 – 5. IBO lesioned drug-treated, IBO lesioned saline-treated, sham lesioned drug-treated and sham lesioned saline-treated 2 -3 month old male C57BL/6 mice. Mean ± SEM. n = 8 per group. * P < 0.05.*

3.10.2.4 Thigmotaxis

The sham lesioned drug-treated group and the IBO lesioned saline-treated group exhibited the lowest thigmotaxic behaviour during training days 3-5. From the previous results they had the longest latencies and path lengths indicating that they were not familiar with the platform's location but searched for it by non-thigmotaxic means. The sham lesioned saline-treated group and the IBO lesioned drug-treated animals spent more time in thigmotaxic behaviour. Statistically a two-way ANOVA for repeated measures showed significant differences between the groups, $F(1, 27) = 17.609$; $P < 0.001$. Post-hoc analysis revealed differences between the sham lesioned saline-treated group and the sham lesioned drug-treated group, $P < 0.05$, the IBO lesioned saline-treated animals and the IBO lesioned drug-treated group, $P < 0.05$, the sham lesioned saline-treated group and the IBO lesioned drug-treated animals, $P < 0.05$, and finally between the IBO lesioned drug-treated and sham lesioned drug-treated groups, $P < 0.05$.

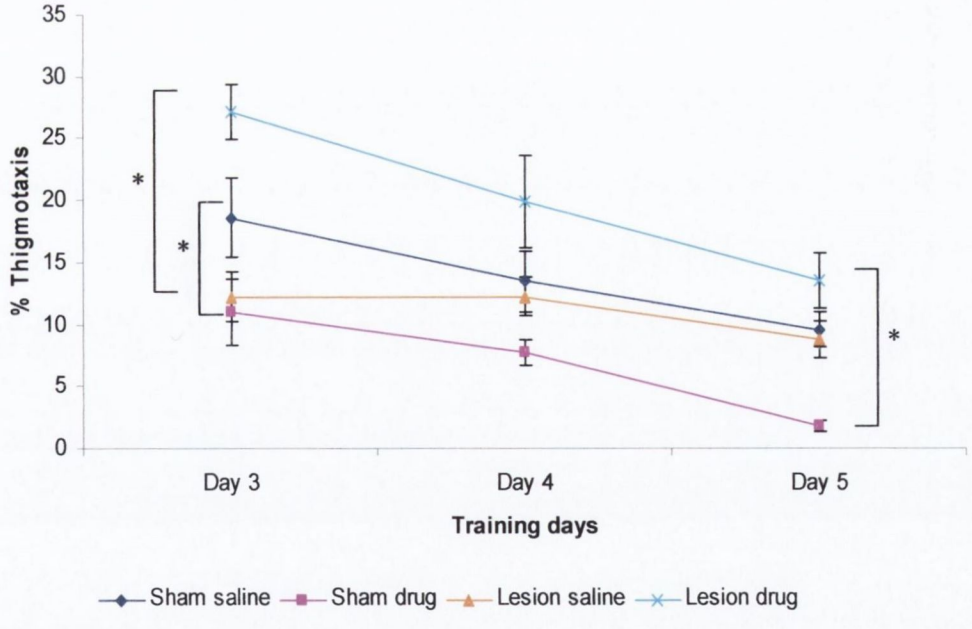

Figure 3.13 *% of total time animals spent in thigmotaxis. IBO lesioned drug-treated, IBO lesioned saline-treated, sham lesioned drug-treated and sham lesioned saline-treated 2 -3 month old male C57BL/6 mice. Mean ± SEM. n = 8 per group. * P < 0.05.*

3.10.2.5 Time spent in quadrant containing platform during training

The sham lesioned saline-treated animals and the IBO lesioned animals treated with compound 51 spent more time in the quadrant containing the platform during the final three training days. The sham lesioned animals treated with compound 51 spent less time in the southeast quadrant than the sham lesioned animals treated with saline. The IBO lesioned mice treated with saline spent the least time of all the groups in the platform-containing quadrant. A two-way ANOVA for repeated measures shows a statistically significant difference between the groups, $F(1, 27) = 3.991$, $P < 0.001$. Post-hoc analysis reveals significant differences between the IBO lesioned saline and the IBO lesioned drug treated groups, $P < 0.05$, and the sham lesioned saline and the IBO lesioned saline treated groups, $P < 0.05$.

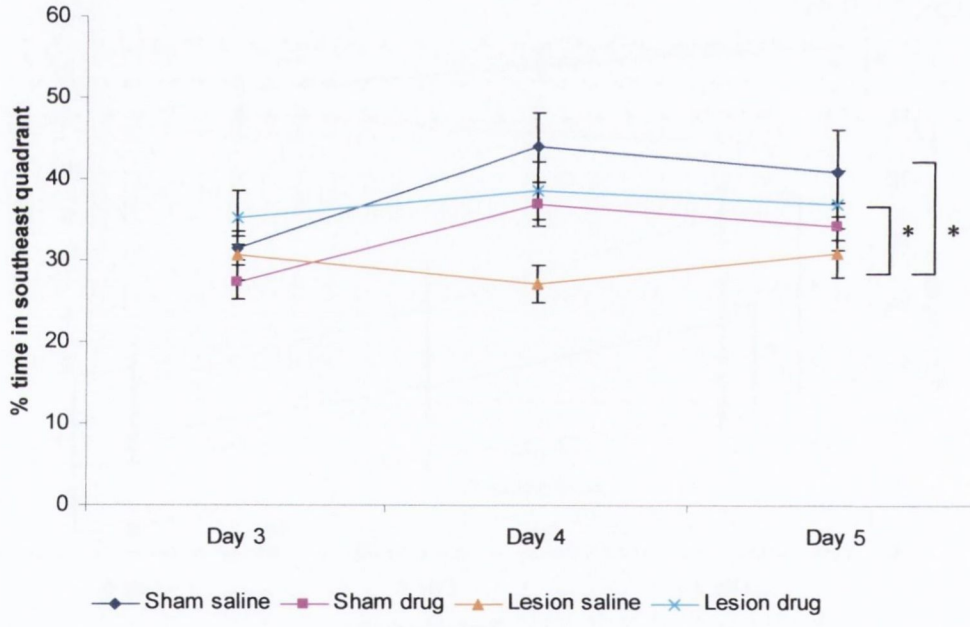

Figure 3.14 *% time animals spent swimming in the quadrant containing platform during water maze training days 3 – 5. IBO lesioned drug-treated, IBO lesioned saline-treated, sham lesioned drug-treated and sham lesioned saline-treated 2 -3 month old male C57BL/6 mice. Mean ± SEM. n = 8 per group. * P < 0.05.*

3.10.2.6 Probe trial

During the probe trial the sham lesioned saline-treated group tended to spend the most time in the southeast quadrant when compared to the sham drug-treated group; however, this was not statistically significant (two-way ANOVA, $P > 0.05$). The IBO lesioned drug-treated and IBO lesioned saline-treated groups spent a similar proportion of their time in the southeast quadrant but the SEM for the IBO lesioned drug group is larger than that for the IBO lesioned saline group. There was no statistically significant difference between the groups, $P > 0.05$ (two-way ANOVA for repeated measures).

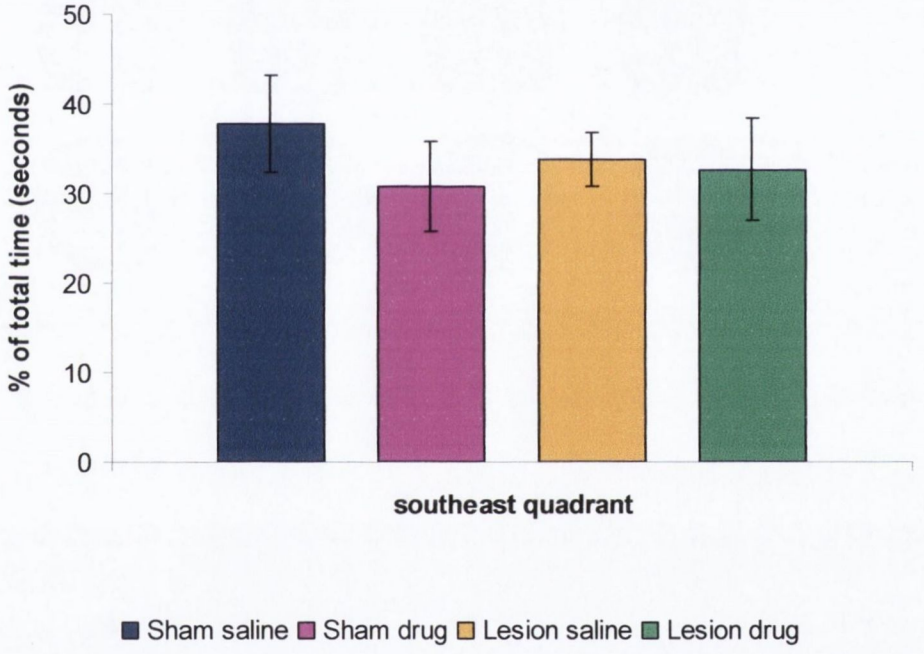

Figure 3.15 *% time spent each group spent swimming in the southeast quadrant (formerly occupied by the platform) during the probe trial for IBO lesioned drug-treated, IBO lesioned saline-treated, sham lesioned drug-treated and sham lesioned saline-treated 2 -3 month old male C57BL/6 mice. Mean ± SEM. n = 8 per group.*

3.10.2.7 Training and probe plots

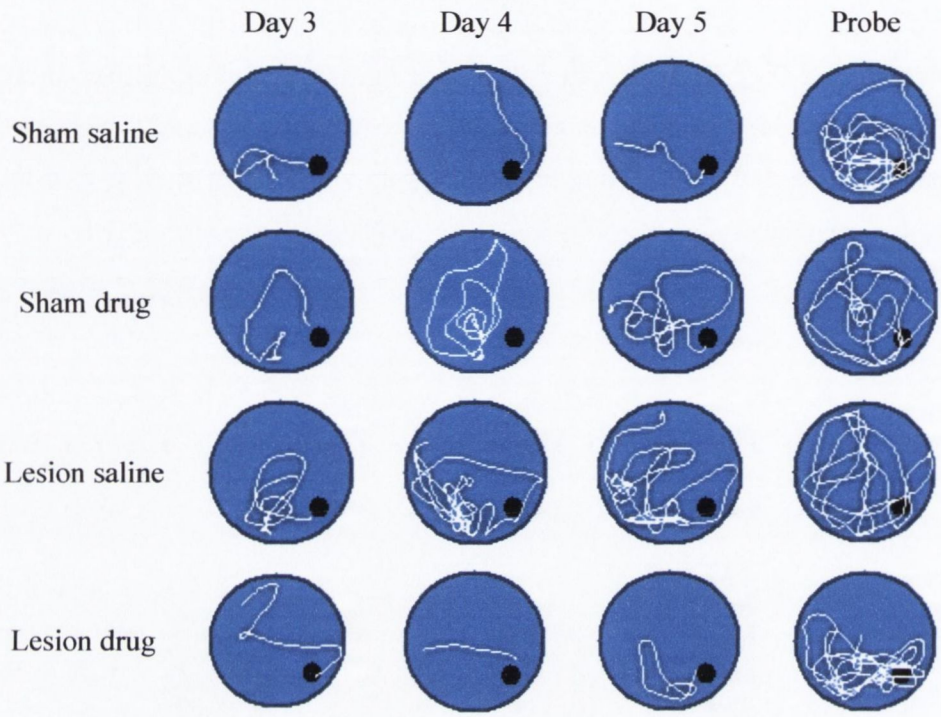

Figure 3.16 *Paths to the platform during water maze training and the probe trial of the best performing animal for each group. Sham saline-treated, sham drug-treated, IBO lesioned saline-treated and IBO lesioned drug-treated 2 – 3 month old male C57BL/6 mice.*

3.10.3 Results: object recognition task

3.10.3.1 Habituation session

The sham lesioned drug and IBO lesioned saline groups did not habituate to the objects across the sessions as they showed greater object exploration in session 2 than session 1. The sham lesioned saline and IBO lesioned drug groups habituated well to the objects with a decreased interest in exploration of the objects across the sessions. A two-way ANOVA for repeated measures showed a significant difference between the groups, $F(1, 28) = 4.084$; $P < 0.001$. Post-hoc analyses revealed a significant difference between the sham lesioned saline-treated and sham lesioned drug-treated groups, $P < 0.05$. There was no significant difference between the IBO lesioned saline and IBO lesioned drug groups, $P > 0.05$.

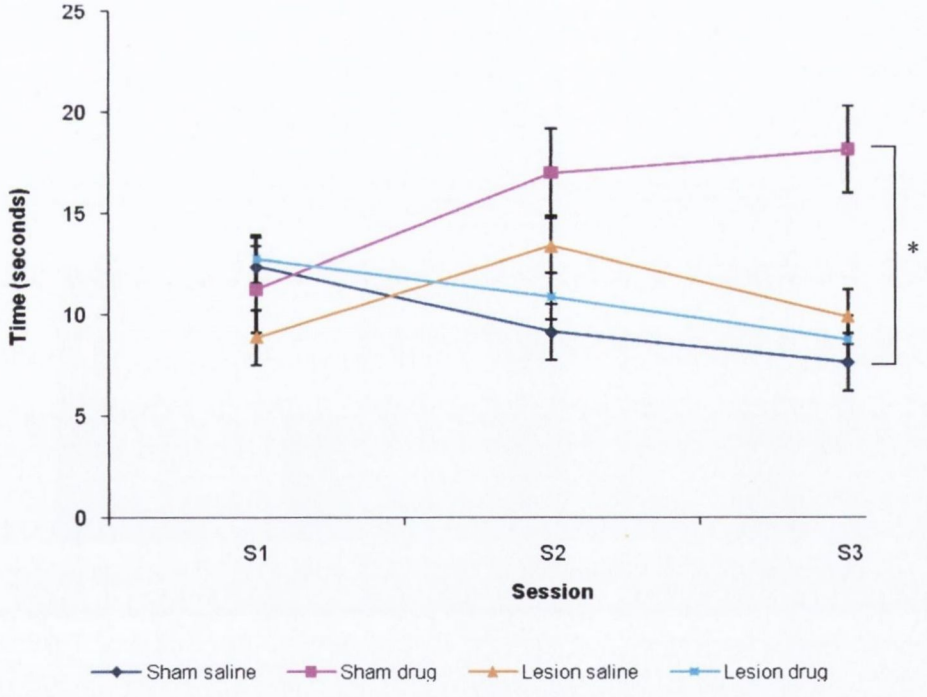

*Figure 3.17 Habituation of object exploration during sessions 1 – 3. Mean duration of contacts with the objects (± SEM) in each session in IBO lesioned drug-treated, IBO lesioned saline-treated, sham lesioned drug-treated and sham lesioned saline-treated 2 -3 month old male C57BL/6 mice. * $P < 0.05$.*

3.10.3.2 Spatial novelty

All of the groups reacted to spatial novelty with the exception of the IBO lesioned saline-treated animals. The sham lesioned saline-treated groups spent the most time interacting with the displaced objects (DOs). There was no difference between the sham lesioned saline-treated or sham lesioned drug-treated groups in their interaction with the non-displaced objects (NDOs) or DOs. However, there was a statistically significant difference between the groups in their interaction with the NDOs and DOs; $F(3, 28) = 4.068$; $P < 0.05$ (two-way ANOVA for repeated measures). The IBO lesioned drug-treated animals spent approximately twice the amount of time exploring DOs than the IBO lesioned saline-treated group; $P < 0.05$. There was a difference in the exploratory time for the DOs by the sham lesioned saline and sham lesioned drug-treated groups; however this just missed significance, $P = 0.052$. The sham lesioned saline was the group that spent most of the time interacting with the displaced objects. They also spent almost double their time in contact with the DOs than the NDOs; $P < 0.05$.

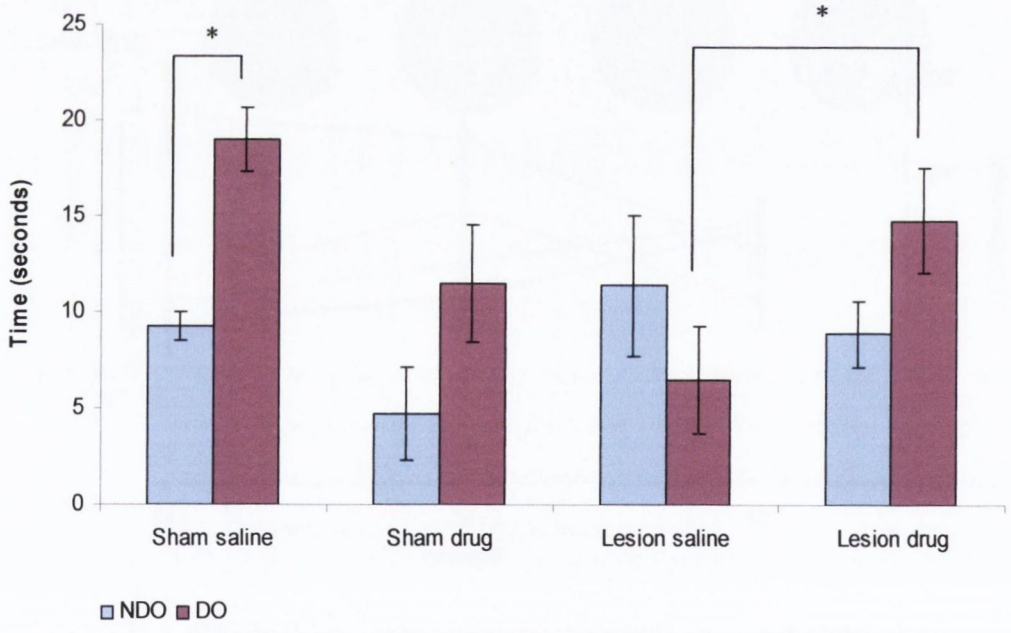

Figure 3.18 *Reactivity to spatial novelty. Mean change in duration of time (± SEM) in contact with the non-displaced (NDOs) and displaced objects (DOs) during sessions 4 – 5. IBO lesioned drug-treated, IBO lesioned saline-treated, sham lesioned drug-treated and sham lesioned saline-treated 2 -3 month old male C57BL/6 mice. n = 8 per group. * P < 0.05.*

3.10.3.3 Object novelty

All of the groups reacted to object novelty except the IBO lesioned saline-treated group. The IBO lesioned saline-treated animals spent approximately 10 seconds in contact with the non-substituted objects (NSOs) and substituted objects (SO). A two-way ANOVA for repeated measures showed a significant difference between the groups, $F(1, 28) = 3.493$; $P < 0.05$. Post-hoc analysis revealed a difference between the IBO lesioned saline-treated and IBO lesioned drug-treated animals for their interaction with the NSOs; $P < 0.05$. All groups (except the IBO lesioned saline-treated animals) spent significantly more of their time interacting with the novel object, $P < 0.05$.

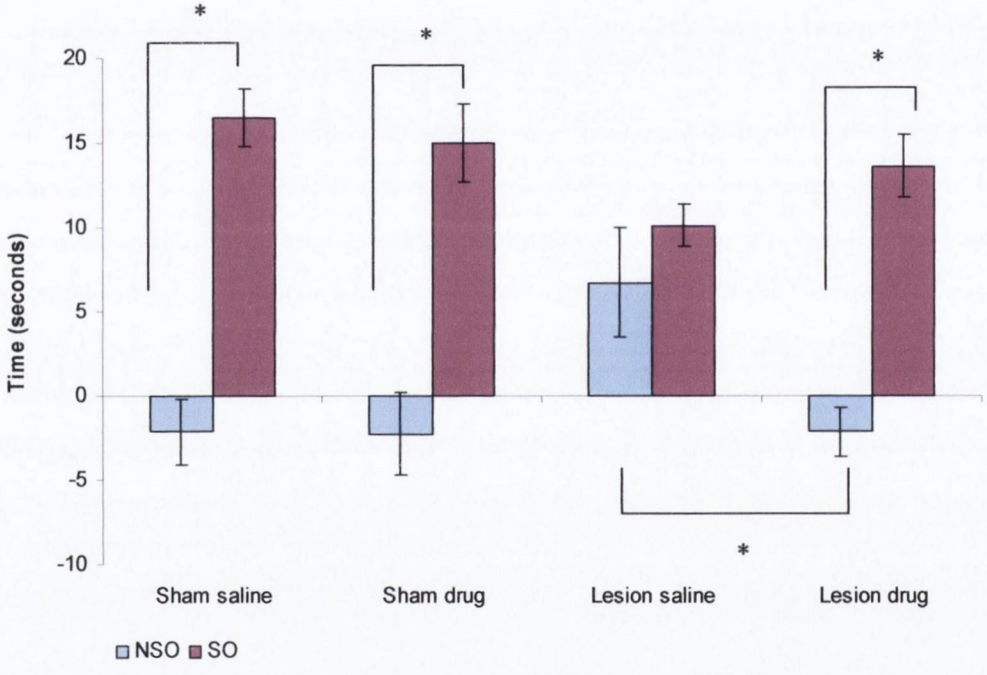

Figure 3.19 *Reactivity to object novelty. Mean change in duration of time (± SEM) in contact with the non-substituted objects (NSOs) and substituted objects (SOs) during sessions 6 – 7. IBO lesioned drug-treated, IBO lesioned saline-treated, sham lesioned drug-treated and sham lesioned saline-treated 2 -3 month old male C57BL/6 mice. n = 8 per group. * P < 0.05.*

3.11 Discussion

3.11.1 Morris water maze

This study sought to determine whether a novel isosorbide-based BuChE inhibitor could restore cognitive function following a cellular insult. Chemical damage was produced by ibotenic acid lesioning in the nBM. It was hypothesized that the novel BuChE inhibitor could restore cognitive function by inhibiting BuChE centrally and thus secondarily increasing the level of acetylcholine.

Injection of ibotenic acid into the basal nucleus in mice produced effective lesions on the basis of results of cognitive testing in the MWM. The needle tracks were identified histologically and they entered the basal nuclei bilaterally. ChAT staining was not used to determine whether the damage was specific to cholinergic neurons as it is well known that ibotenic acid is a non-specific lesioning agent: The spread of cellular damage is not exclusive to the cholinergic neurons following lesioning with ibotenic acid, but rather it produces large lesion volumes with parvocellular neuronal damage [101]. It has been shown that bilateral lesions of the basal nucleus in rodents and non-human primates with ibotenic acid impair cognitive performance and spatial memory in radial maze testing [272] and object discrimination tasks [273]. In general, lesions of the nBM are accompanied by cortical cholinergic impairment [101]. In terms of cognition, the ibotenic acid lesioned animals that were treated with saline performed poorly in spatial memory testing in this study when compared to ibotenic acid lesioned animals treated with the novel compound and sham lesioned animals treated with saline.

Acute treatment with the novel isosorbide-based BuChE inhibitor, compound 51, improved cognition in IBO lesioned animals (*Figures 3.10 and 3.11)*. The IBO lesioned animals treated with compound 51 performed better than the IBO lesioned animals treated with saline alone. Contrary to this the sham lesioned animals treated with the novel compound exhibited impaired cognition function. In fact these sham lesioned animals treated with compound 51 performed worse in the water maze than lesioned animals treated with compound 51 and sham lesioned animals treated with saline. Despite lesions of the basal nucleus with ibotenic acid the lesion drug-treated animals were able to spatially learn the location of the platform relative to the proximal visual cues. The

continued improvement in the performance of the IBO lesioned mice treated with compound 51 over the five training days suggests that these animals were capable of processing spatial information. Their ability to retrieve learned information over the training days also suggests that information from their working memory was converted to their LTM as this information was retrieved as they remembered the location of the platform on each training day. The IBO lesioned animals treated with saline did not show the same improvement suggesting that acute treatment with compound 51 in IBO lesioned mice produces cognitive benefits.

From previous studies in the literature it has been shown that cholinesterase inhibitors improve cognitive function in lesioned animals in memory-related tasks. Janas *et al.* showed that rats administered the muscarinic antagonist scopolamine showed improved cognition in the MWM when treated acutely with the AChE inhibitor, phenserine [274]. Acute treatment with the AChE inhibitor physostigmine improved cognitive performance in rats with IBO lesions of the nBM in the MWM [275]. It seems that levels of the neurotransmitter ACh are increased in the cortex following administration of AChE inhibitors, facilitating neurotransmission by the remaining undamaged cholinergic neurons. Moreover, cholinesterases, in particular BuChE, is found in the blood vessels of the brain [276] and it is thought to play a role in vasodilatation [277]. It has been suggested that cholinesterase inhibitors can increase blood flow to areas of the brain affected by lesions. Lesions of the substantia innomata with ibotenic acid in rats resulted in a decrease in blood flow to the parietal and frontal cortices. This was corrected by administration of the AChE and BuChE inhibitor tacrine into the ventricles causing up to a three-fold increase in the blood flow to these brain areas [278]. It is possible that acute treatment with compound 51 in the lesioned animals may have compensated for the lesion to the basal nucleus by increasing blood flow to the cortices thus improving cognitive performance. Thus a combination of increased ACh along with increased blood flow to lesion damaged areas of the brain may account for improved cognitive performance seen in lesion treated animals.

The cognitive impairment observed in the sham lesioned animals treated with compound 51 may be a result of excessively high levels of ACh in the brain accompanied by an increased blood flow. This increase in both ACh and blood flow may produce

detrimental effects cognitively when there is no lesion present or no compensatory mechanism is necessary.

Cognitive testing of sham lesioned animals treated with saline and lesioned drug-treated animals in the water maze has shown that these animals can learn the maze relative to proximal visual cues. However, the lesioned animals with saline treatment and sham lesioned animals treated with compound 51 appear to have difficulty in learning the task quickly.

3.11.2 Object recognition

The object recognition task was a second paradigm used to evaluate cognitive function in the sham and lesioned animals. This paradigm was chosen as another means by which to measure cognitive function in animals as it is thought to be a less stressful task than the water maze [279].

This study confirmed the findings of the MWM study with the IBO lesioned mice treated with saline performing worse than the IBO lesioned animals treated with compound 51. The sham lesioned mice treated with compound 51 also showed poorer learning ability than the sham lesioned mice treated with saline.

It transpired that during the habituation session the sham lesioned mice treated with compound 51 and IBO lesioned mice treated with saline failed to habituate to object exploration. However, the IBO lesioned animals treated with compound 51 and the sham lesioned animals treated with saline habituated to object exploration with a declining interest in investigating the objects across the sessions. Generally there should be a decrease in exploration of the objects across the sessions as the animals become familiar with the objects. Usually open arenas represent stressful environments for rodents and they tend to stay in the perimeter of the arena [280]. It was initially thought that the animals considered an open arena in a brightly lit room stressful. However, they had been placed in the open arena in the absence of the objects for 5 minutes on the previous day to reduce stress. Had the open arena and bright lights represented an aversive environment all of the groups would have reacted negatively to this habituation session.

When the location of the objects was changed in the spatial novelty task it was evident that all the groups recognised this change except the IBO lesioned animals treated with saline.

The basis of development of the object recognition task is that rodents react positively to object novelty [268]. The novel object elicits curiosity in the animal for exploring this new object as opposed to exploring the familiar objects. In this study the sham lesioned mice treated with saline, the sham lesioned animals treated with compound 51, and IBO lesioned animals treated with compound 51 reacted positively to the novel object and spent significantly more time exploring this than the non-substituted objects. It was only the IBO lesioned group treated with saline that failed to react to object novelty and spent a similar proportion of time exploring both the novel object and non-substituted objects.

As the IBO lesioned animals treated with saline failed the object recognition task it must be concluded that the lesion of the nBM with IBO caused significant impairment in cognition in these animals. These animals failed to habituate to object exploration and to recognise both spatial and object novelty. In fact Rispoli *et al.* also found that rats lesioned with AMPA (α-amino-3-hydroxy-5-methyl-4-isoxazole proprionic acid) in the basal nucleus magnocellularis could not discriminate between familiar and novel objects [281]. Moreover, the IBO lesioned mice treated acutely with compound 51 were able to successfully complete the object recognition task. This suggests that the novel BuChEI, compound 51, is capable of reversing cognition impairments produced as a result of IBO lesioning in the nBM. Previous studies have found that choline esters [281] or the mixed AChEI/BuChEI rivastigmine [282] are capable of reversing cognitive deficits.

3.12 Conclusion

In conclusion bilateral lesions of the basal nucleus with ibotenic acid produced cognitive impairments in mice in both the Morris water maze and in an object recognition trial. However, treatment of IBO lesioned animals with the novel BuChE inhibitor, compound 51, showed improvement in spatial learning and memory in both paradigms. In sham lesioned animals treatment with compound 51 resulted in cognitive decline as sham lesion animals treated with saline outperformed those treated with compound 51 in both the water maze and object recognition task. It appears that BuChE inhibition with compound 51 can improve cognitive deficits where a lesion exists but it appears to reduce the ability of animals to perform in a spatial memory task where there is no lesion or damage to the basal nucleus. Additionally the IBO lesioned animals treated with compound 51 possessed the ability to convert their STM into LTM and rehearse learned information in both cognitive tasks.

Chapter 4

Young and middle-aged mice in cognitive testing

Chapter 4 Young and middle-aged mice in cognitive studies

4.1 Introduction

4.1.1 Background

In humans cognition and memory are known to naturally decline with age [93]. The cognitive performance of animals in mazes also declines with age and these age-related deficits may also include changes in locomotion and exploration [92, 260]. Additionally, animals may show deficits in attention, the ability to process spatial information and the ability to develop efficient spatial strategies [283]. Aged animals are also less efficient at processing long-term memory than younger animals and they exhibit frontal lobe and hippocampal dysfunction in normal aging [284, 285]. The cholinergic system has long been implicated in long-term potentiation and learning, and cholinergic dysfunction results in cognitive impairments [86, 191]. Atrophy of cholinergic neurons in aging animals is characteristic of their poor learning in cognitive tasks [286]. Many studies have demonstrated that enhancement of the cholinergic system by inhibitors of both AChE and BuChE has increased ACh levels in the brain and produced improvement of cognitive abilities in maze tasks in animals [96, 287-290 291] .

C57BL male mice are known to have an average life span of approximately 25 months [292]. Many cognitive studies on aged mice use animals from 18 – 24 months old and consider young mice to be animals aged 3 – 6 months [293, 294]. In this context, mice of 12 months of age are considered to be middle-aged. Generally elderly animals show poorer spatial memory than middle-aged animals. Additionally, older animals fail to react to spatial novelty in an object recognition task when compared to middle-aged animals but they do however react to object novelty [295].

As young animals do not show any signs of cognitive impairment it was interesting to test the effect of the novel BuChE inhibitor in young mice. Aged rodents are known to display obvious signs of cognitive decline and perform poorly in the MWM. Pathophysiologically they exhibit cholinergic hypofunction resulting in an age-related

decline in spatial memory and a reduced Morris water maze (MWM) performance [296, 297].

4.1.2 Aims

The purpose of this study was to determine whether treatment of aged animals with the novel BuChE inhibitor, compound 51, could reverse age-related cognitive decline. In addition it was also interesting to study the effects of this novel compound on the cognitive performance of young animals with no age-related cognitive decline. Young and middle-aged animals were tested in two paradigms, the Morris water maze and an object recognition task. A second group of young and aged animals were tested in a modified radial arm maze.

In this present study 12-month old and 24-month old mice were tested to determine whether there are any cognitive differences between them to decide upon which group to use as an aged model for cognitive testing.

4.2 Animals

4.2.1 Comparison of one and two-year old animals

Healthy experimentally naïve 9 month old ex-breeder male C57BL/6 mice (n = 12) were obtained from Harlan, UK. The animals were aged in the Bioresources Unit in TCIN until they were 24 months of age. Five of these animals died during the aging due to unknown causes. When these animals were 21 months old a second group of healthy naïve 9 month old ex-breeder C57BL/6 males (n = 8) were obtained from Harlan, UK and aged for 3 months.

4.2.2 Comparison of young and aged animals

Healthy experimentally naïve 2 - 3 month old (20 – 25 g) and 9 month old (27 – 40 g) male C57BL/6 ex-breeder mice were also obtained from Harlan, UK. The 9-month old ex-breeders were aged for 3 months until they were 12 months old.

4.2.3 Housing of animals

All animals were housed in single cages in an SPF environment with *ad libitum* access to food and water. Cages were placed in a well-ventilated sound proof room with optimal temperature and humidity. A 12 hour light/dark cycle was in operation (lights on from 7 a.m. – 7 p.m. GMT). All experiments were performed during the light cycle. Daily handling of the animals was carried out upon arrival of the animals to their new environment to minimize stress and adjust to handling by the experimenter. All experiments were carried out in accordance with the European Communities (Amendment of Cruelty to Animals Act 1876) Regulations 2002.

4.3 Drug preparation

1 g of compound 51 was weighed and transferred to a 10 ml volumetric flask. Sterile WFI (Braun, Germany) was added to reach a final volume of 10 ml. Compound 51 did not immediately form a solution in the sterile WFI and was therefore sonicated for 20 minutes at 30°C (Branson Sonicator Model 3510, Branson Ultrasonics BV, Netherlands). Following sonication a solution of the drug was formed in the sterile WFI.

4.4 Drug treatment of young and aged animals

All young and aged animals were randomly divided into control and drug treatment groups. Animals were treated daily with 0.1 ml of 0.9% saline (Baxter, UK) per 10 g of body weight (n = 16) or 1 mg/kg of compound 51 (n = 16) (0.1 ml per 10 g body weight) p.o. using sterile gavage needles (20G x 1½") (Popper, New York), for two weeks prior to commencement of any cognitive testing, and throughout and between both testing periods. On cognitive testing days, dosing was one hour before the test.

4.5 Analysis of BuChE activity in young and aged animals

4.5.1 Procurement of tissue samples

Upon completion of both maze paradigms the young and aged saline treated animals' submandibular blood samples were taken from the mice using a sterile 18 gauge needle (Sherwood Medical, UK). The venous blood was collected in 200 µl lithium heparinized Microvette capillary tubes (Sarstedt, Germany). The animals were then sacrificed by cervical dislocation. The brains and livers were carefully removed from all animals, placed on dry ice and subsequently frozen at -80°C until tested for BuChE activity.

4.5.2 Processing of tissue samples

4.5.2.1 Blood samples

Upon procurement of the blood samples from the mice, the blood was centrifuged for 10 minutes at 4°C at 3,000 rpm using a Sorvall centrifuge RT6000B. The plasma was removed using a Pasteur pipette and transferred into labelled 1 ml Eppendorfs (Braun, Germany).

4.5.2.2 Brain and liver samples

Brain and liver samples were homogenised on ice in 10 volumes of 0.1 M PBS pH 7.4 using an Ultra-turrax T10 Basic (IKA-Werke, Germany) at 10,000 rpm. The brain samples were homogenised on ice for two 5 second bursts and liver samples were homogenised on ice for three 5 second bursts. The samples were transferred to labelled 15 ml glass test tubes, parafilmed and centrifuged for 10 minutes at 4°C at 10,000 rpm (Sorvall RT6000B, GMI, USA).

4.5.2.3 Analysis of BuChE activity

The Ellman assay was carried out as previously described in section 2.2.2.3 in chapter 2. The activity of butyrylcholinesterase was determined in each plasma sample and the

supernatant of the brain and liver tissues using butyrylthiocholine as a substrate [214]. Eight replicates were used and the average absorbances were recorded for each of the three samples. The absorbance values were converted to units of activity using the extinction coefficient for nitrothiobenzoate, 1.36×10^4. The values were plotted in Graphpad Prism v 4.0 as percentages of the control (each mouse acted as its own control).

4.6 The Morris Water Maze

Both saline and drug-treated young and aged animals were trained in the MWM to assess their cognitive ability following treatment. Animals first underwent a habituation session. Following this the animals had 10 days of training for a more extensive training period than 5 days previously used for the animals in the lesioned study. The probe trial was carried out on day 11 following the last water maze training day to determine the ability of the animals to retain and use learned information.

4.6.1 Habituation

As previously described in section 3.5.3 on page 134.

4.6.4 Training

As previously described in section 3.5.4 on page 134 with the exception that water maze training consisted of 10 training days as opposed to 5 days.

4.6.5 Probe trial

As previously described in section 3.5.5 on page 135.

4.7 Statistical analyses

4.7.1 One and two year old mice

A two-way ANOVA for repeated measures was used to determine any statistical differences between the groups using SPSS version 14.0. Latency, path length, swim speed, thigmotaxis and time spent in the quadrant containing the platform were within-subject factors and age was a between-subject factor. All parameters were analysed separately. Post-hoc pair comparisons were not calculated as there were only two groups.

4.7.2 Young and aged mice

The mean latency, path length and swim speed were assessed by a two-way ANOVA for repeated measures using SPSS version 14.0 with latency, path length, swim speed, thigmotaxis and time spent in the platform-containing quadrant as within-subject factors and age and treatment as between-subject factors. Post-hoc pair comparisons, Tukey's HSD test, were calculated where appropriate.

4.8 Object recognition task

4.8.1 Introduction

As the Morris water maze is known to be an aversive task to mice thus any benefits of the novel compounds might not be apparent in this paradigm [298]. A second paradigm, the object recognition task (described in section 3.7.1), was employed to determine the effects of the novel BuChE inhibitors on cognition in mice in a less stressful environment.

4.8.2 Training

4.8.2.1 Habituation to object exploration

As previously described in section 3.7.3.1 on page 137.

4.8.2.2 Reactivity to spatial novelty

As previously described in section 3.7.3.2 on page 138.

4.8.2.3 Reactivity to object novelty

As previously described in section 3.7.3.3 on page 139.

4.9 Statistical analyses

4.9.1 One and two year old mice

Habituation to the objects (session 1 - 3) was analysed by a two-way ANOVA for repeated measures using SPSS version 14.0 with age as the between-subject factor and sessions as the within-subjects factor. Reactivity to spatial and object novelty was evaluated using a two-way ANOVA for repeated measures with age as the between-subject factor and object category as the within-subject factor. Independent t-tests were used to compare the activity of each animal between sessions. Post-hoc pair comparisons were not calculated as there were only two groups.

4.9.2 Young and aged mice

Habituation to the objects (sessions 1 - 3) was analysed by a two-way ANOVA for repeated measures using SPSS version 14.0 with age and treatment as between-subject factors and sessions as the within-subjects factor. Reactivity to spatial and object novelty was evaluated using a two-way ANOVA with age and treatment as between-subject factors and object category as a within-subject factor. Independent t-tests were used to compare the activity of each animal between sessions. Post-hoc pair comparisons, Tukey's HSD test, were calculated where appropriate.

4.10 The modified radial arm maze

4.10.1 Introduction

The radial arm maze was first described by Olton and Samuelson in 1976. This paradigm was designed to assess working and reference memory in rats. It was an eight-arm maze which was based on motivation to find a food reward. Animals were food deprived prior to beginning the maze. One food pellet was placed in each arm and the reinforcement was not replaced once it was found by the rat. Animals had to find the food reward in each arm based on a choice strategy with a limited number of arm entries. The number of correct arm entries was scored. Olton and Samuelson found that rats performed well in this novel paradigm and suggested that rats have a great capacity for memory of spatial location [299].

In this study a modified water-version of the radial arm maze was used. This paradigm was not based on food deprivation or any food motivational reward. Rather the motivation is to escape from shallow water into the safe environment of a familiar burrow tube at the end of each arm.

4.10.2 Animals

New groups of animals were used for this paradigm. Healthy experimentally naïve 2-3 month old (22 – 27 g) and one-year old (29 – 42 g) male C57BL/6 mice were obtained from Harlan, UK. The animals were housed in single cages with isopad bedding (Harlan, UK) and *ad libitum* access to food and water. Cages were housed in a well-ventilated sound proof room with controlled temperature and humidity. A 12 hour light/dark cycle was in operation (lights on from 7 a.m. – 7 p.m. GMT). All experiments were performed during the light cycle. Daily handling of the animals was carried out upon arrival of the animals to their new environment to minimize stress and adjust to handling by the experimenter. All experiments were carried out in accordance with the Amendment of the European Communities (Amendment of Cruelty to Animals Act 1876) Regulations 2002.

4.10.3 Drug preparation

The compounds were prepared as previously described in section 4.3.

4.10.4 Drug treatment

The animals were treated with the novel compounds as previously described in section 4.4.

4.10.5 Apparatus

The novel modified radial arm maze was designed in Oxford University, UK by Dr. Colm Cunningham. The modified radial arm maze consisted of an eight arm clear pliable plastic maze 85 cm in diameter mounted on a white round wooden base. Eight holes of 40 mm were made in the plastic at 2 cm above the base of the maze and were placed equidistantly around the circumference of the maze. Eight plastic two-sided wedges were made with each arm 30 cm in length and 16 cm in height with an angle of 45°. Placement of these eight wedges inside the circular maze produced an eight arm radial arm maze with an arm width of 10 cm and a central area of 25 cm diameter. At the distal end of each arm was a hole, 4 cm in diameter, set with its lower annulus 2 cm above the floor of the maze. Seven of these holes were filled with black tubes which are stopped off by being closed with black plastic fillings, making them impassable. However, the eighth hole was filled with an unfilled plastic tube allowing escape to a burrow tube which was used to transport the animal back to its home cage. From the centre of the maze each arm appears to have a black hole at its end, but only one arm allows the mouse to freely exit.

The maze was placed at waist height in a small sound-proof room with fluorescent lighting. Eight salient proximal visual cues were placed on the surrounding walls. The maze was filled with 2 cm of water (to the base of the black tubes) at room temperature (20°C). The maze was located in the corner of the room so that a white wall was on each side at a 90° angle and two white boards (110 cm in height and 120 cm in

diameter) were placed on the opposite sides to screen the maze off from the rest of the room. Sufficient room was left between the maze and the walls so that the maze could be freely rotated between trials. Eight visual cues (30 cm x 30 cm) were attached to the walls and boards with one visual cue above each arm of the maze. The visual cues consisted of a blue circle, a green triangle, a red cross, a black and white vertically striped box, a red arrow, a green diamond (all the above mentioned visual cues were made from art paper), a navy and white rectangular object made from felt with a small narrow vertical extension from the left hand corner, and a black and white horizontally striped rectangle made from plastic.

Prior to training the black plastic burrowing tubes were introduced to each animal's home cage on two separate days so that during the maze training the burrow tubes were already familiar to the animals. The tubes were filled with food pellets (Harlan, UK) and left overnight in each animal's home cage. The following morning it was observed that each animal had removed the food pellets from the burrow tube and was sleeping in the tube.

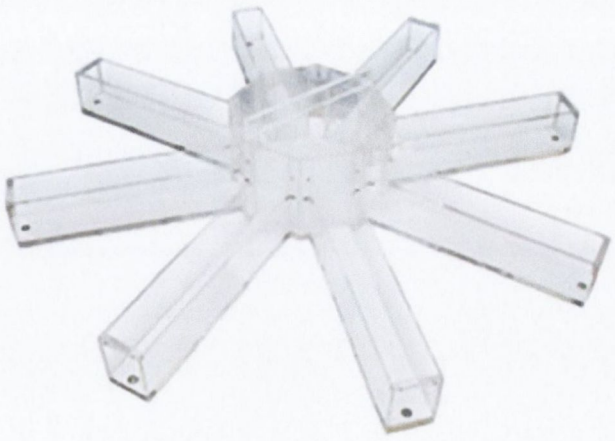

Figure 4.1 The radial arm maze.

4.10.6 Training

Each animal had seven 90 second trials per day over a period of 6 training days with an inter-trial interval of 24 minutes. Each mouse was placed at the end of a 'blind arm' facing away from the maze centre and allowed 90 seconds to find the exit. Once the exit was found and the animal entered the burrow tube it was returned to its home cage. If the animal failed to find the exit within this time it was gently guided towards the exit using a clear plastic sheet. The task was counterbalanced so that each group of 8 animals was assigned a different exit; hence each individual mouse always exits via the same arm. For example the young drug group was assigned to exit 1. The order in which the animals were placed in the maze was completely randomized. After every 3 - 4 trials the maze was rotated so that the animals would not rely on olfactory cues to solve the maze. This task was manually recorded by the experimenter. All arms were numbered and on the results sheet the latency to actually enter the escape tube and the number for each arm entered to achieve the goal were recorded. Thus "1, 3, 4, 6" represents three incorrect arms followed by the correct choice of arm 6. An arm entry was defined as full body and tail entering the arm. If the animals did not leave the start arm they were encouraged to move using the Perspex paddle. If this was persistent the animal was not scored, as failure to move did not equate to inability to solve the maze.

Once animals had successfully learnt the maze, the location of the exit was changed as a reversal task, on day 7. The change of location of the exit for any given mouse was done in a systematic way so that the location was moved 3 exits away from the original location in a clockwise or counterclockwise direction. This was chosen to minimize the likelihood of non-purposeful correct trials since going directly across the maze or into those exit arms immediately right and left of the original exit were the most common general strategies.

4.11 Results

4.11.1 Morris water maze with one and two-year old animals

4.11.1.1 Latency to platform

The one year-old mice took longer to locate the platform across the training days compared to the two year-old animals. However, both the one and two-year old animals showed that they learned a location of the platform with a decrease in their latency on each training day. A two-way ANOVA for repeated measures did not show a statistically significant difference between the groups, $F(1, 13) = 0.98$, $P > 0.05$.

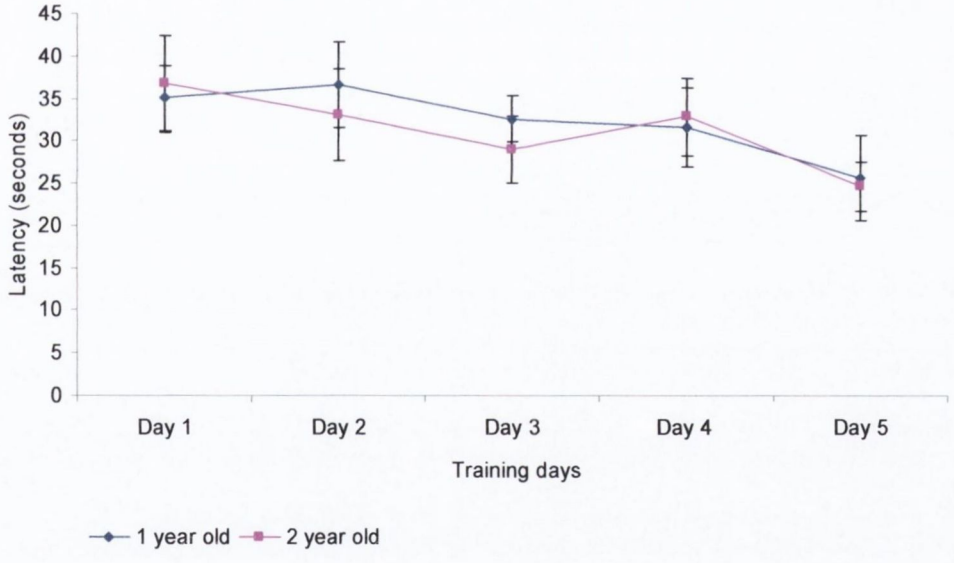

Figure 4.2 *Latency to reach the platform (s) during water maze training days 1 - 5. 12 month old (n = 8) and 24 month old (n = 7) male C57BL/6 mice. Mean ± SEM. n = 8 per group.*

4.11.1.2 Path length

The one year-old mice had an overall longer path length to the platform than the two year-old animals however, this was not statistically significant, $F(1, 13) = 0.631$, $P > 0.05$ (two-way ANOVA for repeated measures). The path length decreased for both groups over the training days as they became familiar with the task. The distance each animal swam to find the platform also decreased across the training days, $F(1, 13) = 25.865$; $P < 0.001$ (two-way ANOVA for repeated measures).

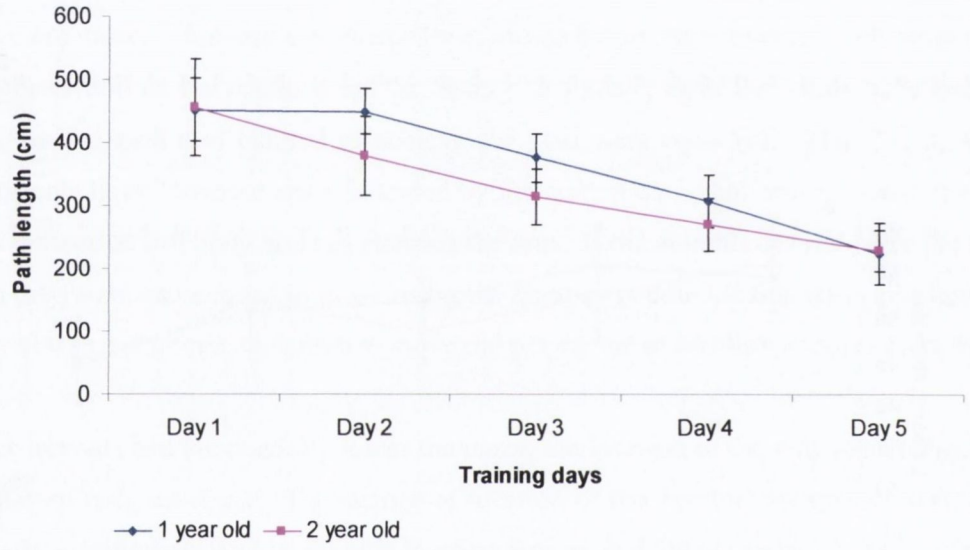

Figure 4.3 *Path length to the platform (cm) during water maze training days 1 - 5. 12 month old (n = 8) and 24 month old (n = 7) male C57BL/6 mice. Mean ± SEM. n = 8 per group.*

4.11.1.3 Swim speed

The one year-old animals swam at approximately the same speed as the two year-old mice during the training days. Statistical analysis using a two-way ANOVA for repeated measures did not show a statistically significant difference between the groups, $F(1, 13) = 1.654$, $P > 0.05$.

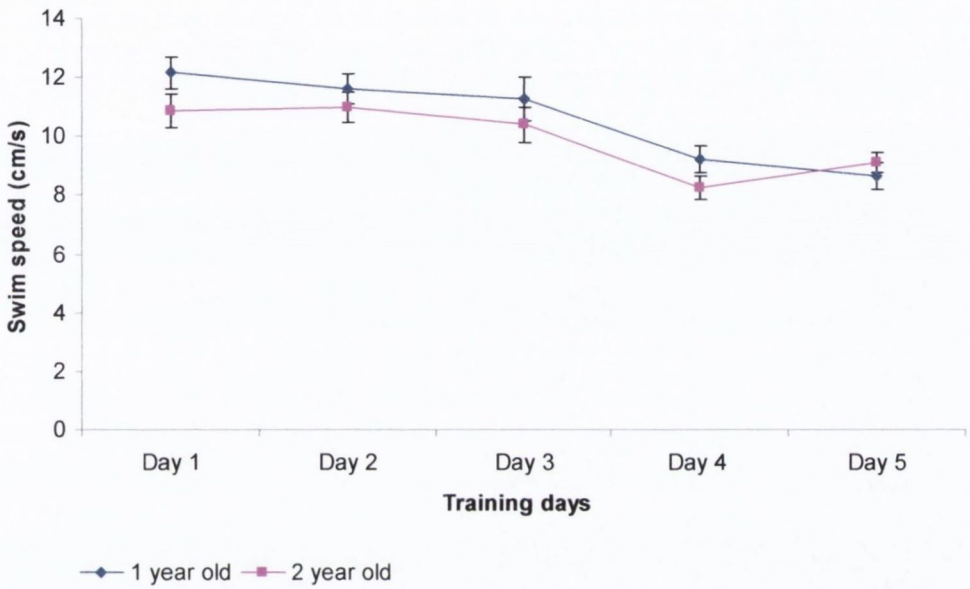

Figure 4.4 *Swim speed of the animals during water maze training days 1 - 5. 12 month old (n = 8) and 24 month old (n = 7) male C57BL/6 mice. Mean ± SEM. n = 8 per group.*

4.11.1.4 Thigmotaxis

Both groups spent a similar amout of time in thigmotaxis during the training days however, the two year-old animals exhibited greater thigmotaxic behaviour on day five compared to the one year-old group. A two-way ANOVA for repeated measures did not reveal a statistically significant difference between the groups, $F(1, 13) = 0.131$, $P > 0.05$. However, there was a statistically significant difference in the thigmotaxic behaviour between the training days, $F(4, 52) = 16.943$, $P < 0.001$. There was a significant decrease in the amount of thigmotaxic behaviour for both groups over the training days with a steep curve as the training days progressed.

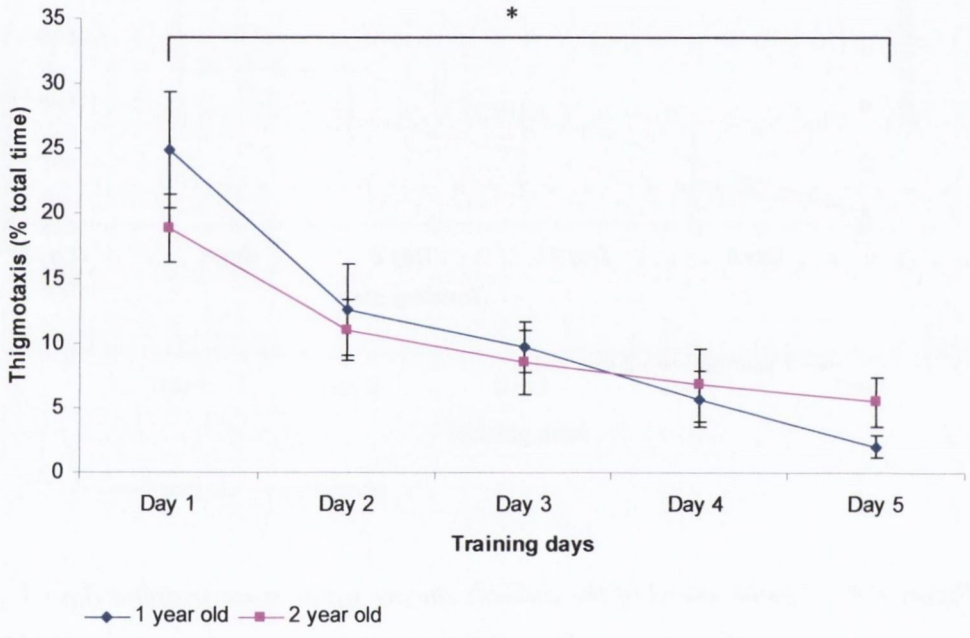

Figure 4.5 *% time spent in thigmotaxis during water maze training days 1 - 5. 12 month old (n = 8) and 24 month old (n = 7) male C57BL/6 mice. Mean ± SEM. * P < 0.001.*

4.11.1.5 Time spent in the southeast quadrant during training

The one year-old group spent more time in the southeast quadrant containing the platform during day 1 and day 4 of training than the two-year old animals. However, both groups spent the same amount of time in this quadrant on day 5. There was an overall decrease in the time spent in the southeast quadrant over the training days. A two-way ANOVA for repeated measures did not show a statistically significant difference between the groups, $F(1, 13) = 0.92$, $P > 0.05$. There was a statistically significant difference in the proportion of time spent in the southeast quadrant across the training days, $F(4, 52) = 3.407$, $P < 0.001$.

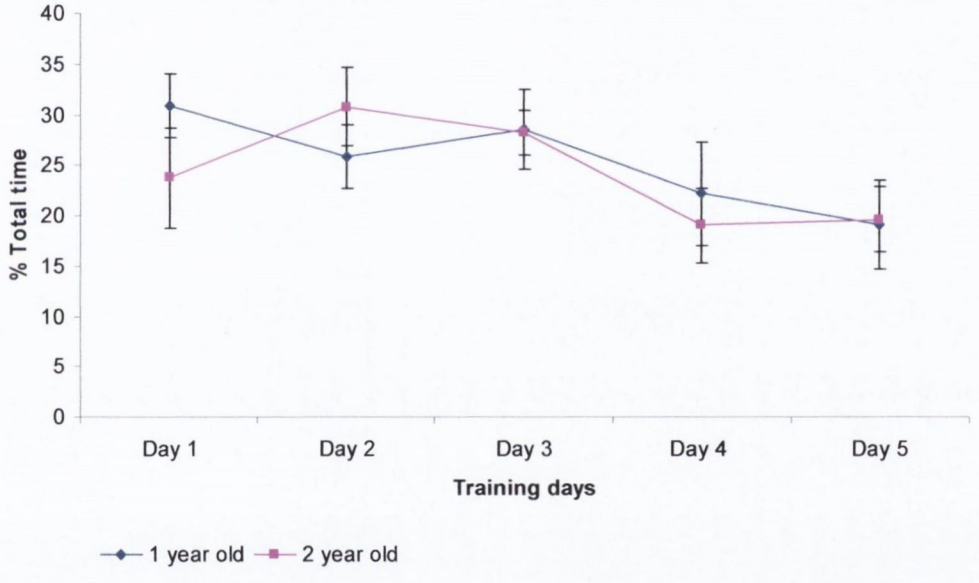

Figure 4.6 *% time spent in the southeast quadrant during water maze training days 1 - 5. 12 month old (n = 8) and 24 month old (n = 7) male C57BL/6 mice. Mean ± SEM.*

4.11.1.6 Probe trial

The probe trial was used to determine whether the animals learned the water maze. Both the one year-old and the two year-old animals spent approximately an average of 25 seconds, of the one minute trial, in the southeast quadrant that previously contained the platform. There was no difference found between the groups, $P > 0.05$ (an independent t-test).

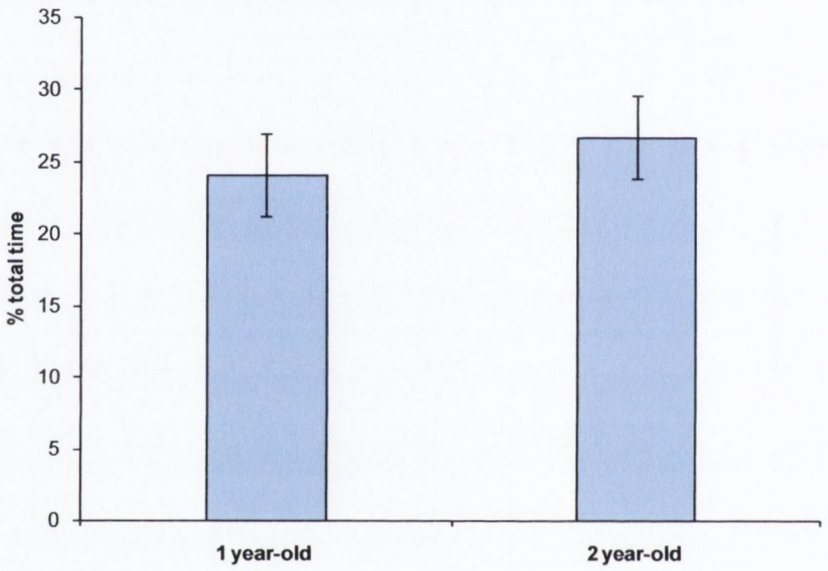

Figure 4.7 *% time spent in the southeast quadrant (previously containing the platform) during the probe trial. 12 month old (n = 8) and 24 month old (n = 7) male C57BL/6 mice. Mean ± SEM.*

4.11.2 Morris water maze with young and middle-aged animals

4.11.2.1 Latency to platform

The saline treated young animals had the lowest latency to find the platform compared to the other groups. The latencies to find the platform fluctuated after day 6 of training for all the groups, with no further improvement in learning. A statistically significant difference was found among the groups using a two-way ANOVA for repeated measures, $F(1, 28) = 2.251$; $P < 0.001$. Tukey's HSD post-hoc test revealed a difference between the young saline treated animals and the young drug group, $P < 0.05$, and also between the young saline group and the aged drug group, $P < 0.05$. There was no statistically significant difference between the aged saline and aged drug-treated groups, $P > 0.05$.

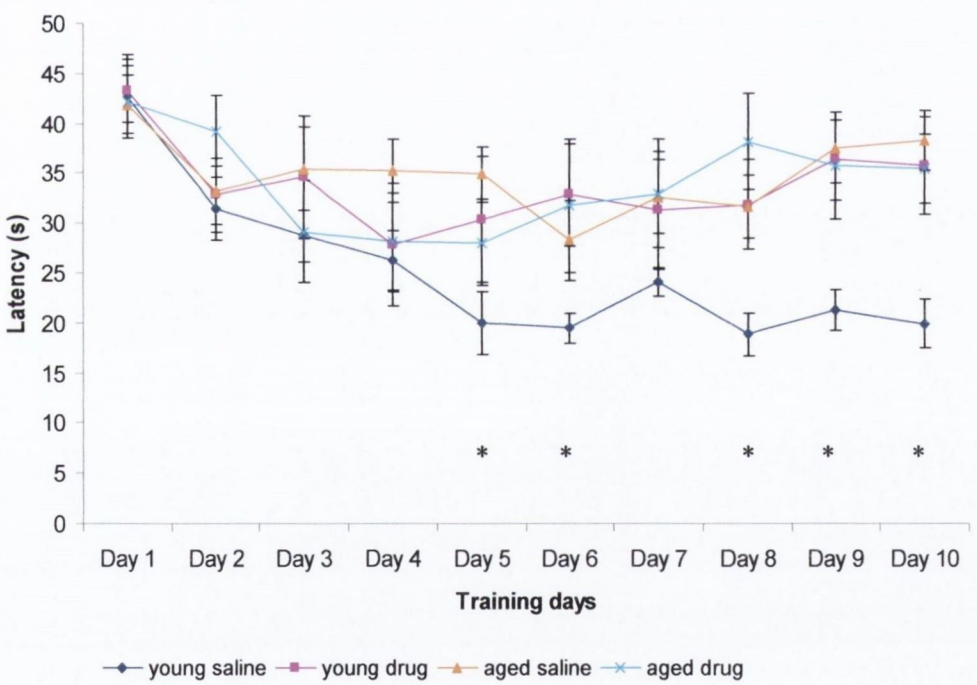

Figure 4.8 *Latency to reach the platform (s) during water maze training days 1 - 5. young saline-treated, young drug-treated, aged saline-treated and age drug-treated 2 -3 month old male C57BL/6 mice. Mean ± SEM. n = 8 per group. * P< 0.05.*

4.11.2.2 Path length

There was a decrease in the path length for each group over the first 5 days of training. However, over the remaining training days there was fluctuation in the path length among all the groups. The young saline treated animals overall had the shortest path length to the platform. Statistical analysis of the data for path length using a two-way ANOVA for repeated measures revealed a significant difference between the groups, $F(1, 28) = 2.555$; $P < 0.001$. Post-hoc analysis using Tukey's HSD showed this difference was between the young saline and young drug-treated groups, $P < 0.05$, and the young drug and aged drug treated animals, $P < 0.05$.

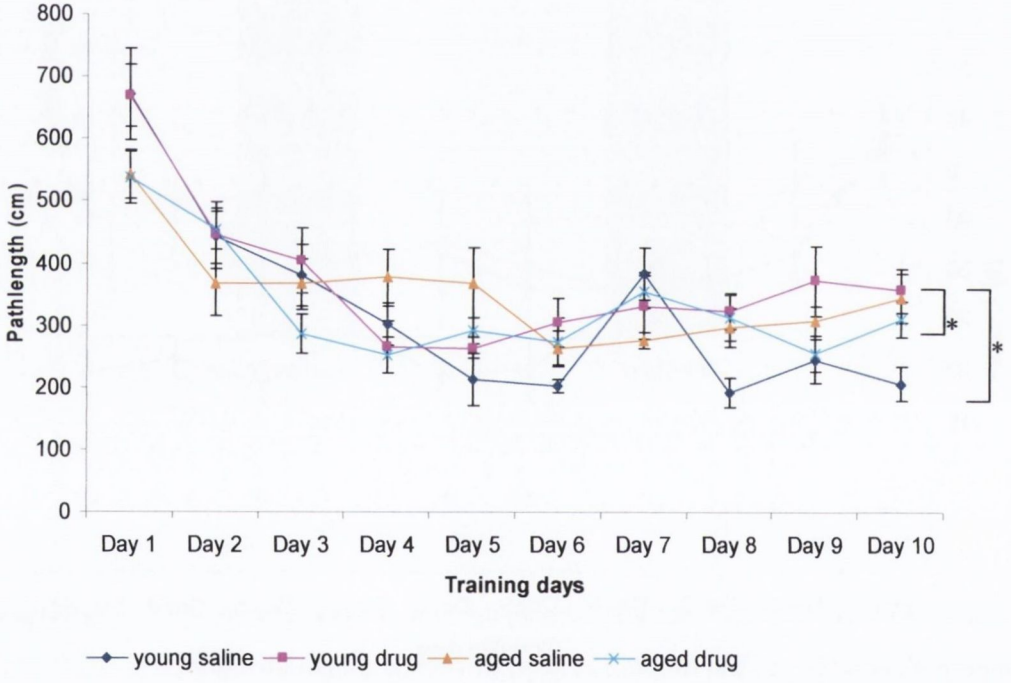

Figure 4.9 *Path length to the platform (cm) during water maze training days 1 - 5. Young saline--treated, young drug-treated, aged saline-treated and aged drug-treated 2 -3 month old C57BL/6 mice. Mean ± SEM. n = 8 per group. * P < 0.05.*

4.11.2.3 Swim speed

The young saline and young drug-treated animals had a faster swim speed across the training days compared to the aged animals. Statistical analysis of the data for mean swim speed of the animals during the ten training days using a two-way ANOVA for repeated measures revealed a significant difference between the groups, $F(1, 28) = 1.275$; $P < 0.001$. Post-hoc analyses revealed differences between the young saline and aged saline groups, $P < 0.05$; young saline and aged drug groups, $P < 0.05$, young drug and aged saline groups, $P < 0.05$, and young drug and aged saline groups, $P < 0.05$.

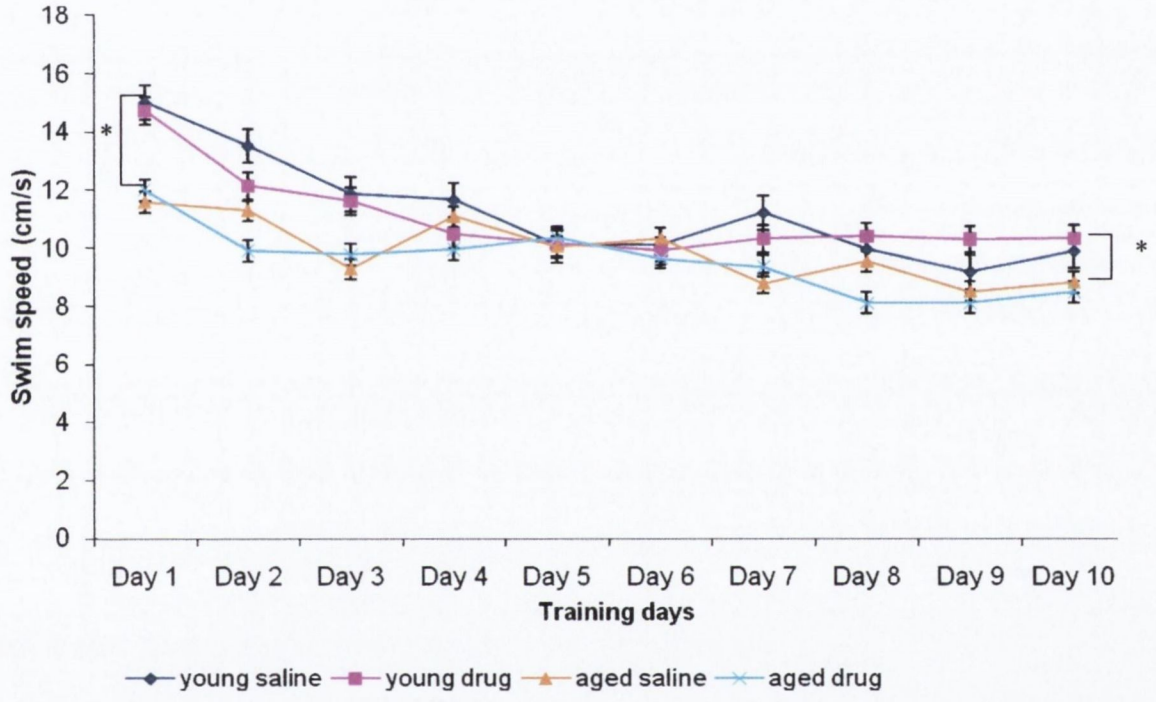

Figure 4.10 *Swim speed of animals (cm/s) during water maze training days 1 - 5. Young saline-treated, young drug-treated, aged saline-treated and aged drug-treated 2 -3 month old C57BL/6 mice. Mean ± SEM. n = 8 per group. * P < 0.05.*

4.11.2.4 Thigmotaxis

The young saline and young drug-treated animals exhibited less thigmotaxic behaviour across the training days compared to the aged saline and aged drug treated animals, $F(1, 28) = 3.198$, $P < 0.001$ (a two-way ANOVA for repeated measures). Post-hoc analysis with Tukey's HSD showed a significant difference between the young drug and aged saline treated groups, $P < 0.05$. Further post-hoc analysis with an LSD test also showed a difference between the young saline and aged saline, $P < 0.05$. There was no statistically significant difference between the young saline and young drug-treated animals ($P < 0.05$) or the aged saline and aged drug-treated animals ($P > 0.05$).

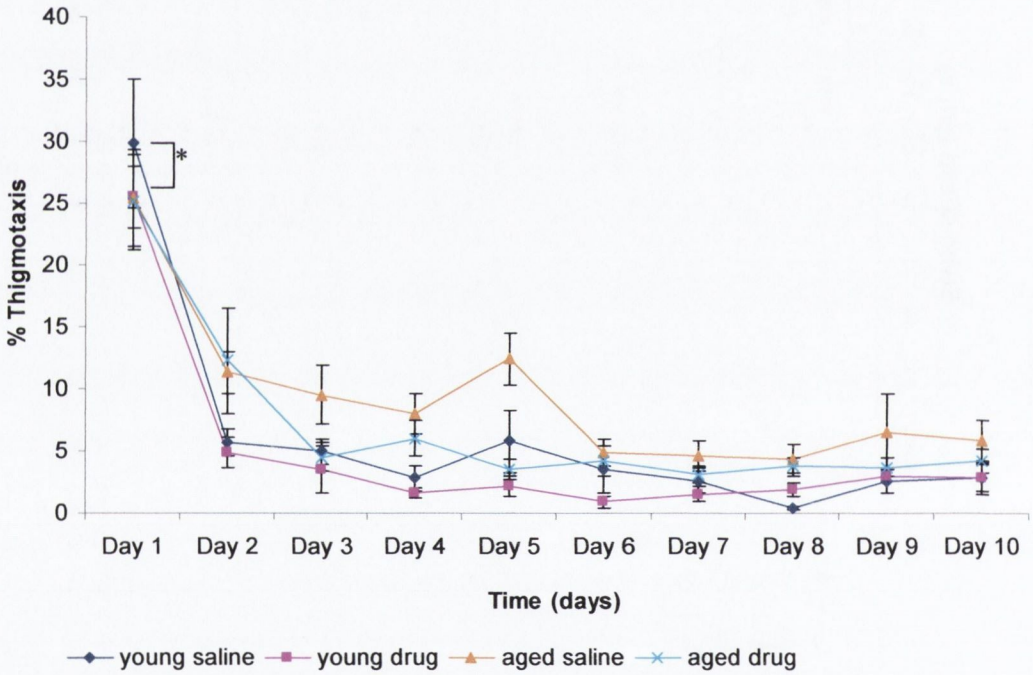

Figure 4.11 *% of total time spent animals spent in thigmotaxis during water maze training days 1 - 5. Young saline-treated, young drug-treated, aged saline-treated and aged drug-treated 2 -3 month old C57BL/6 mice. Mean ± SEM. n = 8 per group. * P < 0.05.*

4.11.2.5 Time spent in the southeast quadrant during training

The young saline-treated animals spent the greatest amount of time in the southeast quadrant, containing the platform, across the training days compared to the other groups. A two-way ANOVA for repeated measures found a statistically significant difference between the groups for the duration of time spent in the southeast quadrant during the nine training days, $F(1, 28) = 8.040$; $P < 0.001$. Tukey's HSD post-hoc analysis revealed differences between the following groups: young saline and young drug-treated groups; young saline and aged saline groups; and young saline and aged drug-treated groups, $P < 0.05$. There was no significant difference between the aged saline and aged drug groups, $P > 0.05$.

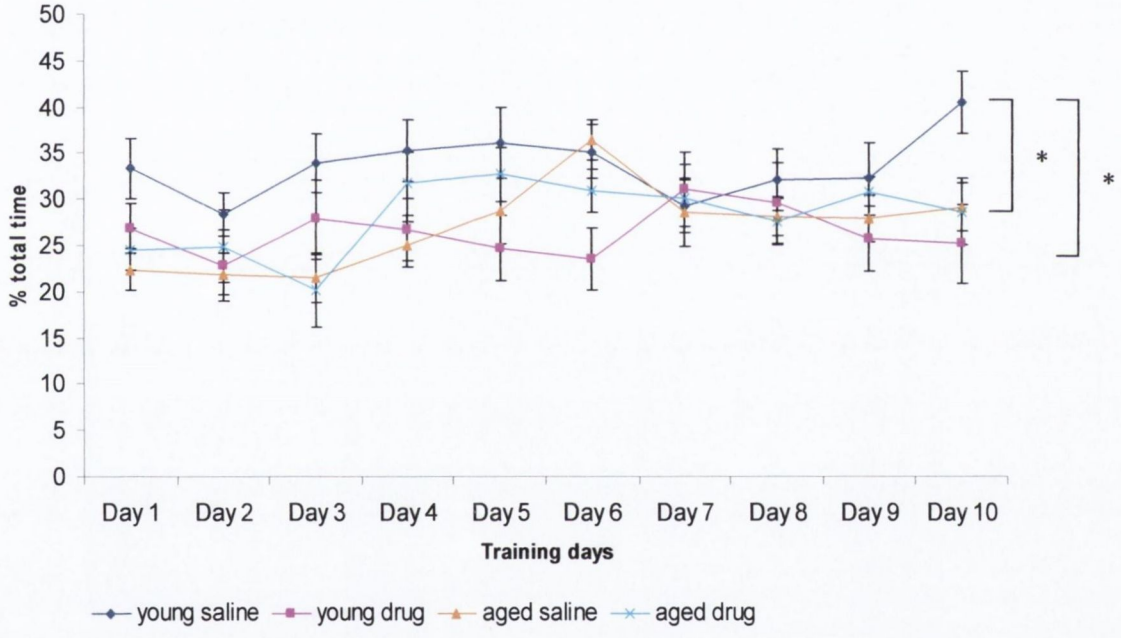

Figure 4.12 *% of total time animals spent in swimming in the quadrant containing platform during water maze training days 1 - 5. Young saline-treated, young drug-treated, aged saline-treated and aged drug-treated 2 -3 month old C57BL/6 mice. Mean ± SEM. n = 8 per group. * P < 0.05.*

4.11.2.6 Probe trial

During the probe trial the young saline treated animals spent the most time trying to locate the platform in the southeast quadrant. The young drug treated animals spent less time in this quadrant than the young saline treated animals. Although the aged drug treated group searched the southeast quadrant more than the aged saline treated controls, this difference was not statistically significant, $P > 0.05$. A two-way ANOVA found a statistically significant difference among the groups for the duration of time spent in the southeast quadrant during the probe trial, $F(3, 28) = 3.317$; $P < 0.05$. Tukey's HSD post-hoc analysis found statistically significant differences between: young saline and young drug treated groups, and young saline and aged saline treatment groups, $P < 0.05$.

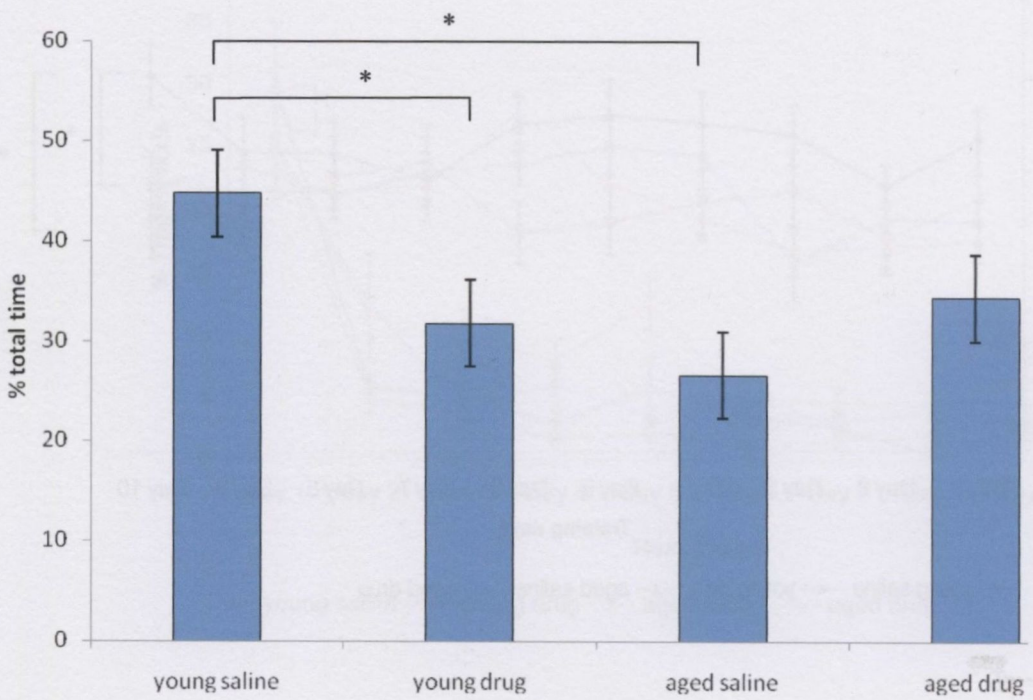

Figure 4.13 *% of total time animals spent in swimming in the quadrant containing platform during water maze training days 1 - 5. Young saline-treated, young drug-treated, aged saline-treated and aged drug-treated 2 -3 month old C57BL/6 mice. Mean ± SEM. n = 8 per group. * P < 0.05.*

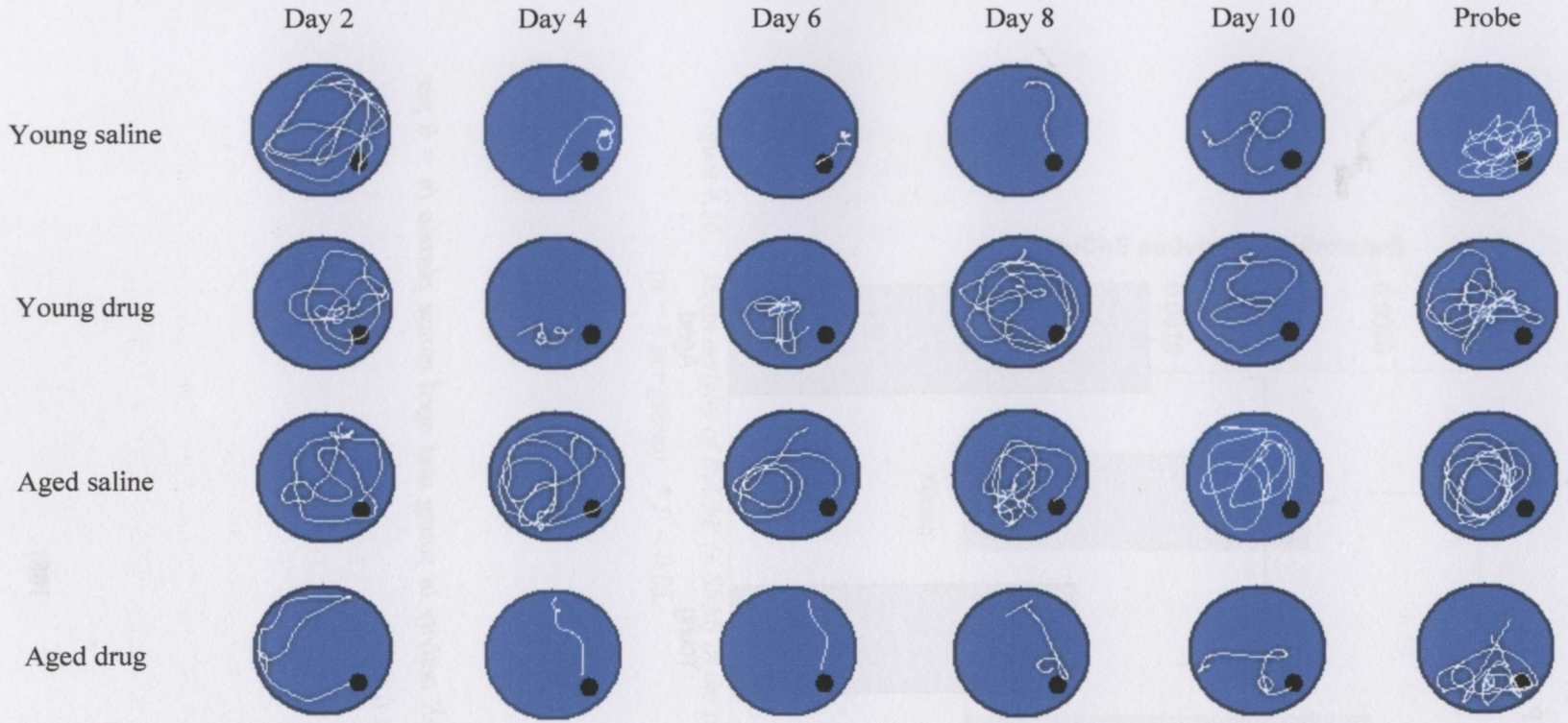

Figure 4.14 *Swim paths to the platform during training days 2, 4, 6, 8, 10 and the probe trial. The training and probe plots represent the best animal from each group. Young saline-treated, young drug –treated, aged saline-treated and aged drug-treated male C57BL/6 mice.*

4.11.2.7 BuChE activity in the mouse plasma of young and aged animals

The level of the enzyme BuChE was found to be greater in the plasma of aged animals compared to that of the young animals. An independent t-test revealed this difference was statistically significant, $P < 0.05$.

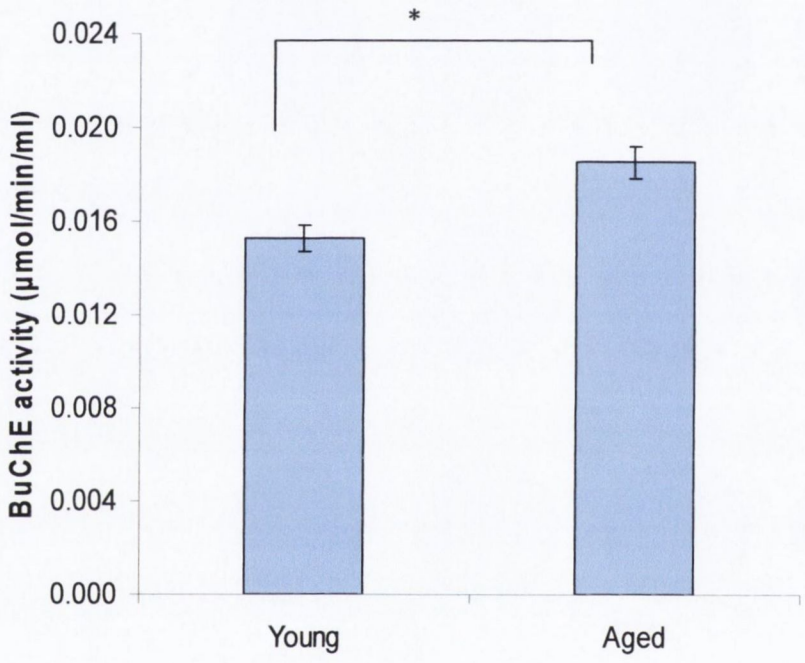

*Figure 4.15 Plasma BuChE activity in young and aged mouse plasma (n = 8 per group). * $P < 0.05$.*

4.11.2.8 BuChE activity in the brains of young and aged mice

The activity of BuChE was significantly greater in the brains of the aged animals than in the brains of the young animals ($P < 0.05$, independent t-test).

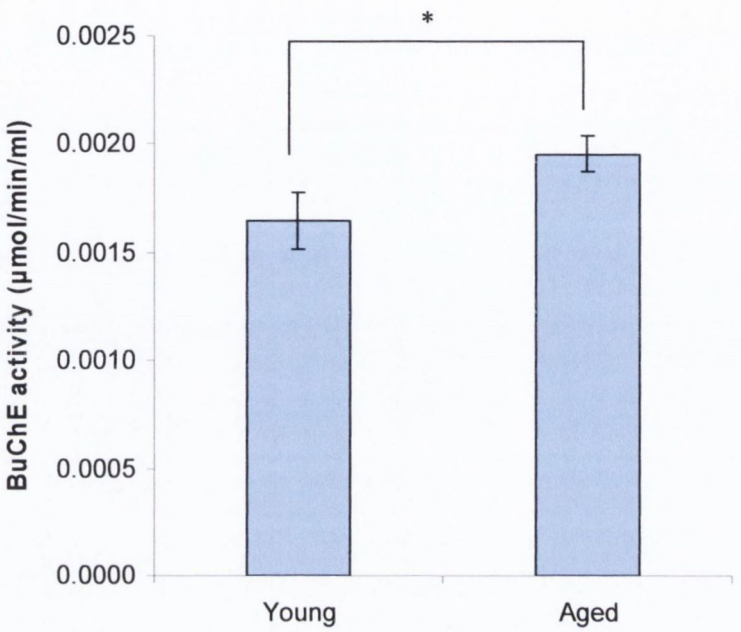

*Figure 4.16 Mean activity of BuChE (± SEM) in the plasma of young and aged mice. (n = 8 per group). * $P < 0.05$.*

4.11.2.9 BuChE activity in the liver of young and aged mice

Similar to the BuChE levels in mouse plasma and mouse brain the activity of the enzyme in the liver of aged mice was greater than that of young mice, and this difference was found to be statistically significant in an independent t-test, $P < 0.05$.

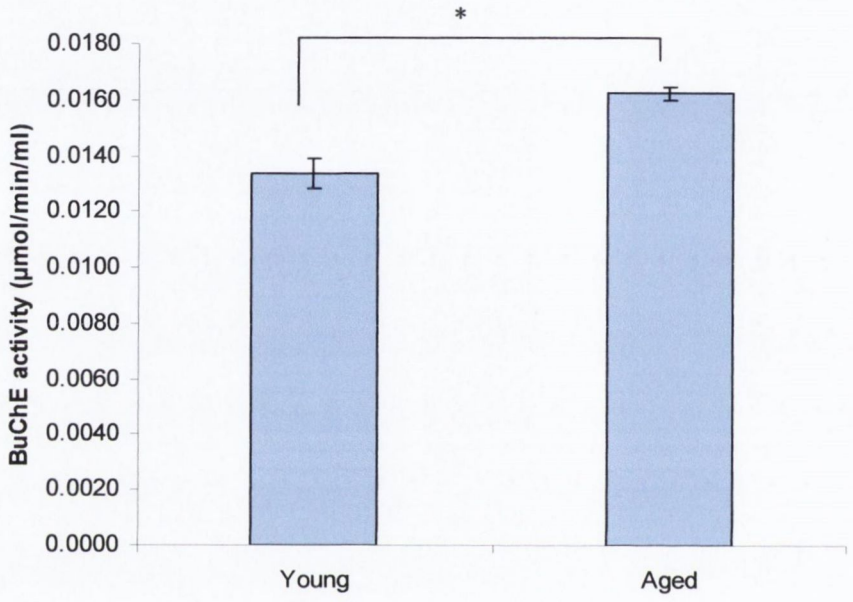

*Figure 4.17 Mean activity of BuChE (± SEM) in the liver of young and aged mouse (n = 8 per group). * P < 0.05.*

4.11.3 Object recognition task with one and two-year old mice

4.11.3.1 Habituation to object exploration

The one year-old group were more active in exploring the objects than the two year-old animals. However, the one year-old animal's failed to habituate to the task as they showed a continued increase in object exploration across the sessions. The two year-old animals spent less time exploring the objects overall but they did habituate to the task. A two-way ANOVA for repeated measures revealed a statistically significant difference between the groups, $F(1, 13) = 7.458$; $P < 0.05$. Independent t-tests revealed statistically significant differences between the one and two year-old groups during sessions 2 and 3, $P < 0.05$.

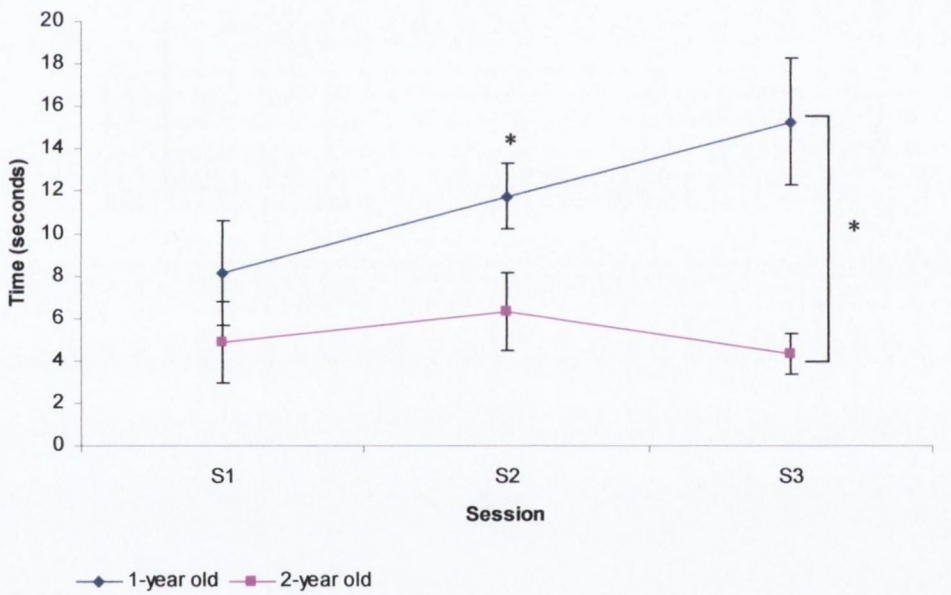

Figure 4.18 *Habituation of object exploration during sessions 1 – 3. Mean duration of contacts with the objects (± SEM) in each session in 12 month old (n = 7) and 24 month old (n = 8) male C57BL/6 mice. * $P < 0.05$.*

4.11.3.2 Spatial novelty

The two year-old animals spent a greater proportion of their time exploring both NDOs and DOs compared to the one year-old group. However, both groups failed to react to spatial novelty as they spent more time exploring the NDOs than the DOs. A two-way ANOVA did not reveal a statistically significant difference between the groups, $P > 0.05$. Additionally independent t-tests did not reveal any statistically significant difference within the groups for their interaction with the NDOs and DOs, $P > 0.05$.

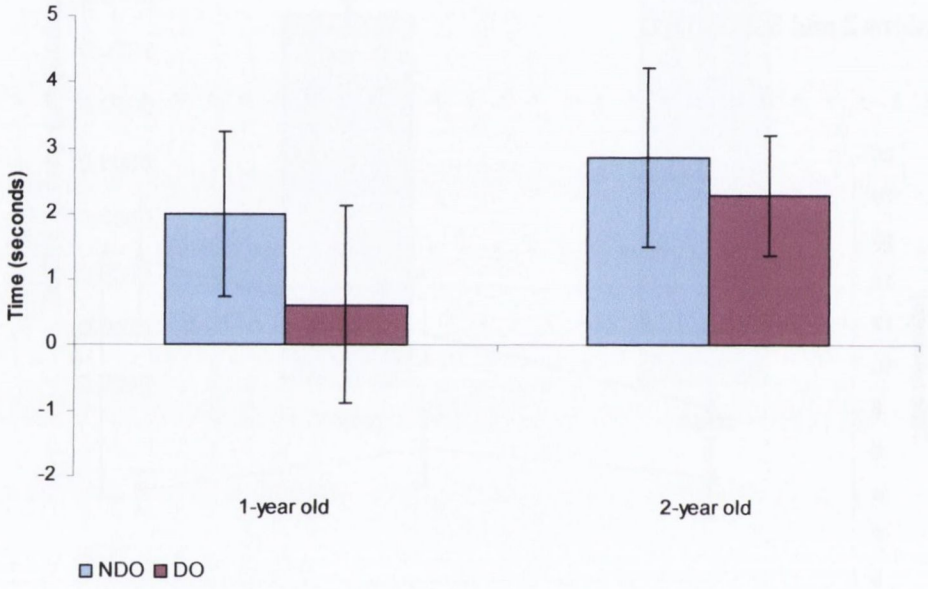

Figure 4.19 *Reactivity to spatial novelty. Mean duration of of time (s) in contact with the objects (± SEM) during sessions 4 and 5. 12 month old (n = 7) and 24 month (n = 8) old male C57BL/6 mice.*

4.11.3.3 Object novelty

Both groups reacted well to object novelty as they spent more time exploring the SO than the NSOs. The one year-old animals spent more time exploring the SO. A two-way ANOVA for repeated measures showed a statistically significant difference between the groups, $F(1, 13) = 0.705$, $P > 0.05$. However, there was a statistically significant difference within both groups for their interaction with the NSOs and SO, $F(1, 13) = 30.594$, $P < 0.001$. There was a difference in the duration of time each group spent exploring the novel object however, this was not enough to be significant, $P > 0.05$.

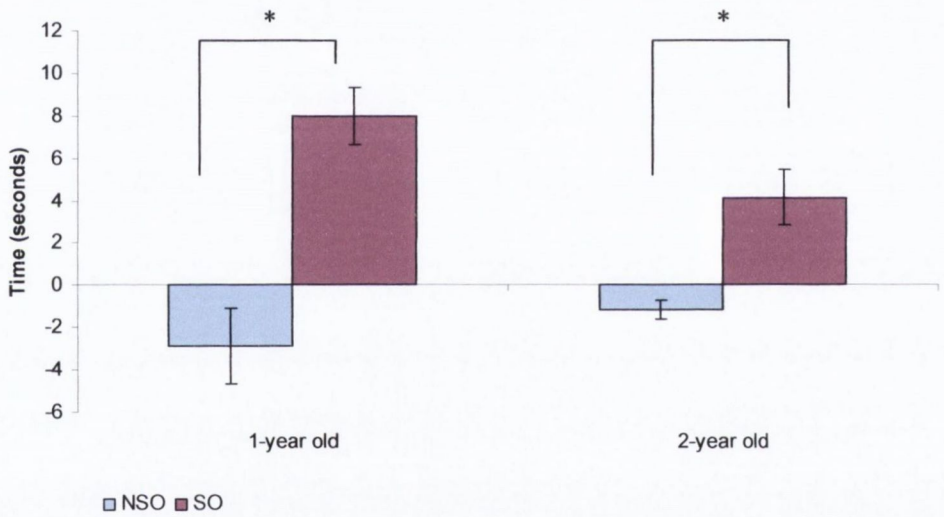

Figure 4.20 *Change in the duration of time (s) (mean ± SEM) spent by one and two-year old mice exploring non-substituted objects (NSOs) and substituted objects (SO) in sessions 6 and 7. 12 month old (n = 7) and 24 month (n = 8) old male C57BL/6 mice.* * *P < 0.001.*

4.11.4 Object recognition task with young and aged mice

4.11.4.1 Habituation to object exploration

The aged saline and aged drug treated animals spent a greater proportion of their time exploring the objects across the sessions and in addition to this they habituated to the task. The young saline and drug treated animals spent less time exploring the objects compared to the aged groups. They also did not seem to habituate. A two-way ANOVA for repeated measures revealed a significant difference between the animals exploring the objects in sessions 1 - 3; $F(1, 28) = 5.374$, $P < 0.001$. Post-hoc analyses revealed a statistically significant difference between the young saline and aged saline-treated animals during session 2 ($P < 0.05$). Both aged groups spent a similar proportion of their time exploring objects across the three sessions. The aged animals were more active in exploring the objects than the young animals across all of the sessions.

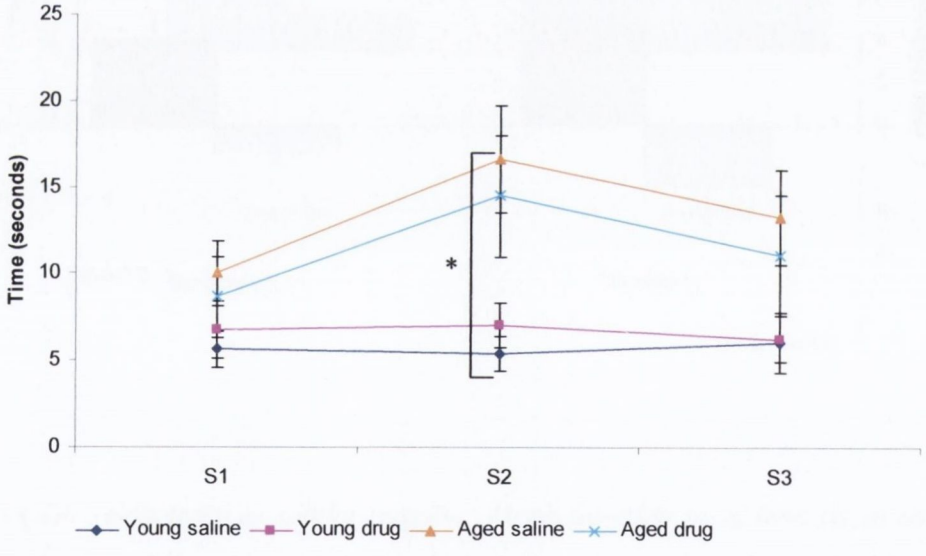

Figure 4.21 *Habituation of object exploration during sessions 1 – 3. Mean duration of contacts with the objects (± SEM) in each session in young saline-treated, young drug-treated, aged saline-treated and aged drug-treated old male C57BL/6 mice. n = 8 per group. * $P < 0.05$.*

4.11.4.2 Reactivity to spatial novelty

The aged saline and aged drug-treated groups spent more time exploring both NDOs and DOs during these sessions compared to the young saline and young drug treated groups. The aged saline treated group and the young drug-treated groups reacted to spatial novelty while the young saline treated and aged drug treated groups did not react to spatial novelty. A two-way ANOVA revealed a significant difference between the groups, $F(1, 28) = 13.170$, $P < 0.001$. Post-hoc analyses revealed differences between the young drug-treated and aged drug-treated animals during for interaction with the NDOs, $P < 0.05$; and a difference between the young saline treated and aged saline treated groups for their interaction with the DOs, $P < 0.05$. No group spent significantly more time exploring the DOs compared to the NDOs indicating failure to recognize spatial novelty.

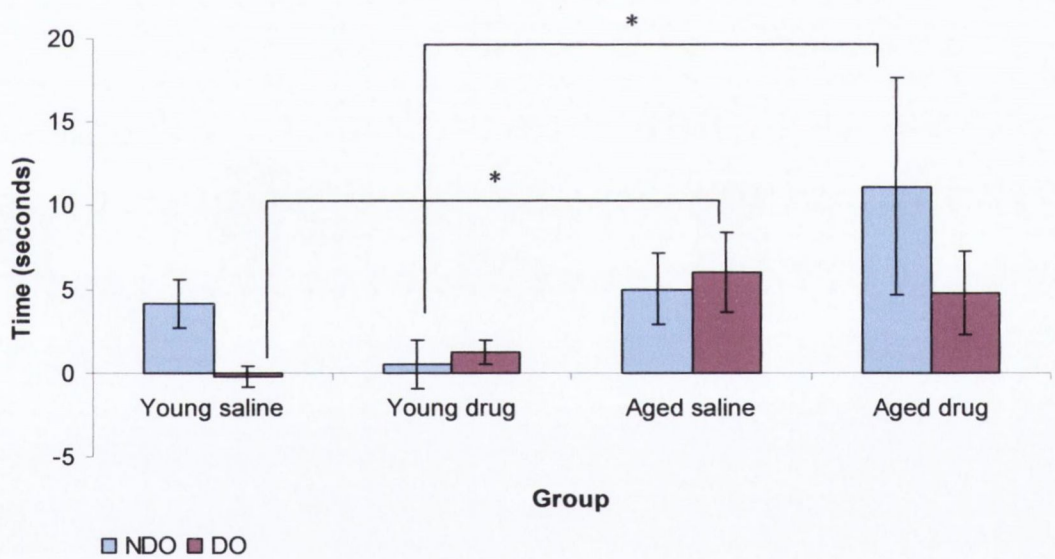

Figure 4.22 *Reactivity to spatial novelty. Mean change in duration of time (± SEM) in contact with the non-displaced objects (NDOs) and displaced objects (DOs) during sessions 4 – 5. Young saline-treated, young drug-treated, aged saline-treated and aged drug-treated old male C57BL/6 mice. n = 8 per group. * $P < 0.05$.*

4.11.4.3 Reactivity to object novelty

All groups reacted to object novelty as they spent more time with the SO than the NSOs. The aged drug-treated animals spent significantly less time exploring the NSOs than the aged saline group. Additionally, the aged drug-treated group was the only group that spent significantly more time exploring the novel object than the NSOs. A two-way ANOVA revealed a significant difference between the groups during session 6, $F(1, 28) = 4.064$; $P < 0.05$. Post-hoc analyses found differences between the aged saline-treated and aged drug-treated animals in their interaction with the NSOs, $P < 0.05$. The aged drug-treated animals spent significantly more time exploring the SO than the NSOs, $P < 0.05$. There was also a significant difference between the young drug-treated and aged saline-treated groups in their interaction with the DOs, $P < 0.05$. The young saline group also spent a significant duration of time exploring the SO compared to NSO, $P < 0.05$.

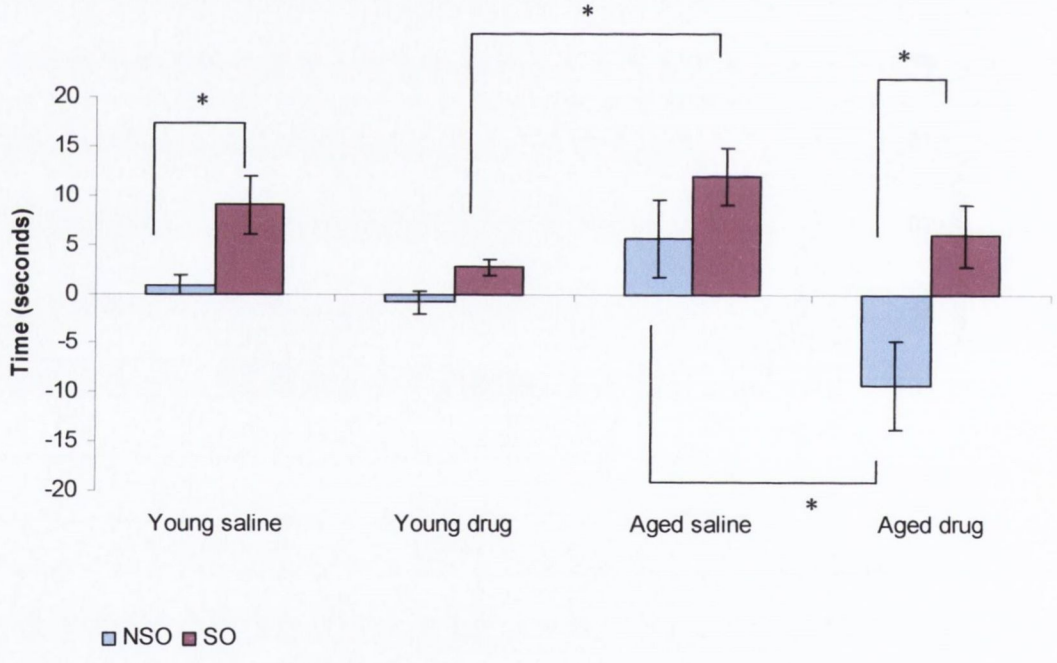

Figure 4.23 *Reactivity to object novelty. Mean change in duration of time (± SEM) in contact with the non-substituted objects (NSOs) and substituted objects (SOs) during sessions 6 – 7. Young saline-treated, young drug-treated, aged saline-treated and aged drug-treated old male C57BL/6 mice. n = 8 per group. * P < 0.05.*

4.11.5 Modified radial arm maze

4.11.5.1 Number of trials completed per training day

The results of the modified radial arm maze were inconsistent with some animals failing to find the exit or simply unmotivated to complete the task. A lot of the animals simply sat in the start arm maze and did not move to complete the trial. Therefore the number of trials completed per group per training day was recorded. After the first three days of training the animals began to become slightly more motivated to complete the trials on the subsequent training days. There was a statistically significant difference between the groups, $F(1, 28) = 0.940$; $P < 0.001$. Post-hoc analysis showed a difference between the young drug-treated animals and the aged saline treated animals, $P < 0.05$, and also between the young drug-treated animals and the aged drug-treated animals, $P < 0.05$.

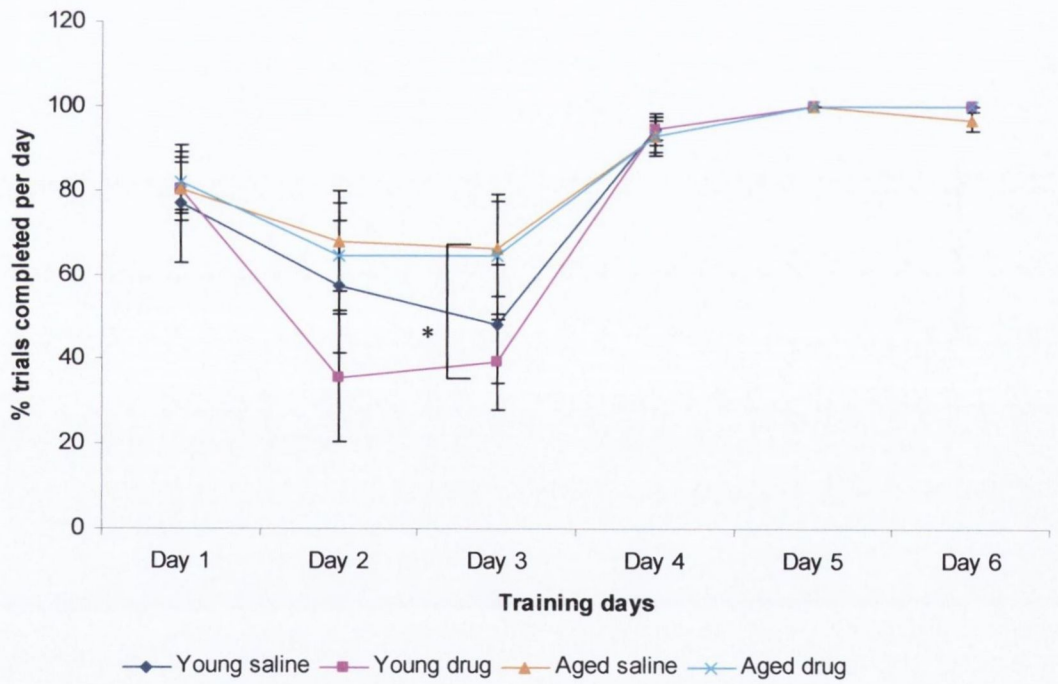

*Figure 4.24 Mean number of completed trials (± SEM) over training days 1 – 6. Young saline-treated, young drug-treated, aged saline-treated and aged drug-treated old male C57BL/6 mice. n = 8 per group. * P < 0.05.*

4.11.5.2 Number of correctly completed trials per training day

The number of trials successfully completed per group was then recorded. The number of trials completed over the first three days of training was found to be too inconsistent between the groups to report. As the animals learned to complete the trials during training days 4 – 6 these trials were analysed for the number that were completed correctly *i.e.* the number of trials during which the animal found the exit. A two-way ANOVA for repeated measures found a statistically significant difference between the groups, $F(1, 28) = 0.796$; $P < 0.001$. However, post-hoc analyses did not show any significant difference between any of the groups. .

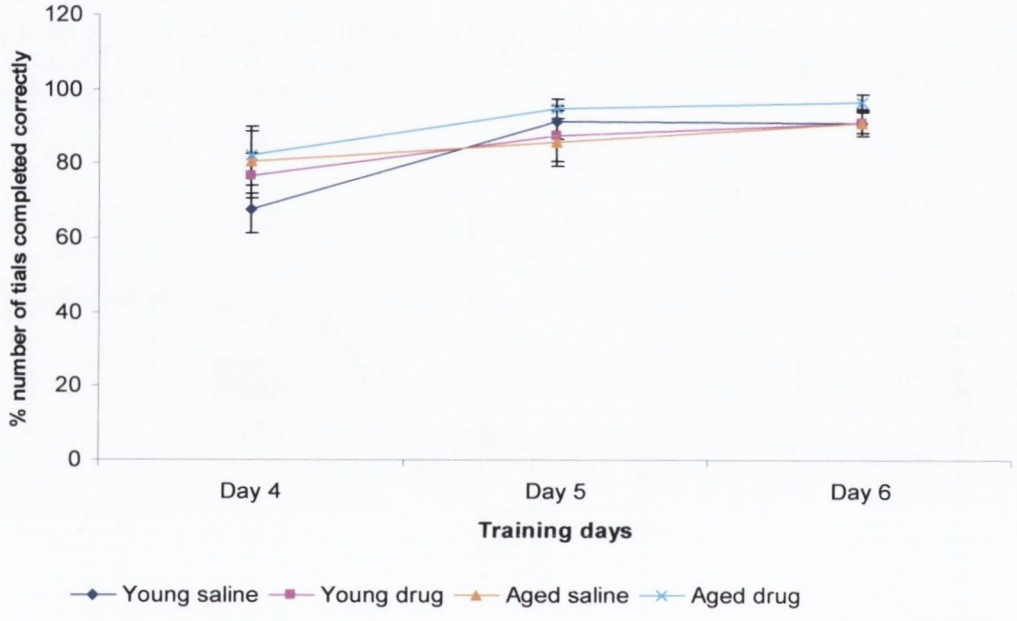

Figure 4.25 *Mean number of trials successfully completed (± SEM) during training days 4 – 6. Young saline-treated, young drug-treated, aged saline-treated and aged drug-treated 2 – 3 month old male C57BL/6 mice. n = 8 per group.*

4.11.5.3 Incorrect arm entries

The number of incorrect arm entries was recorded during the successfully completed trials. As the animal learns the maze the number of incorrect arm choices should decrease. There was a decrease in the number of incorrect arm entries for the young drug-treated and the aged saline-treated groups. However, the young saline and aged saline-treated animals showed an increase in the number of incorrect arm entries on day 6. A statistically significant difference was found between the groups, $F(1, 28) = 0.596$, $P < 0.001$. Post-hoc analysis revealed a difference between the young saline and young drug-treated animals, $P < 0.05$.

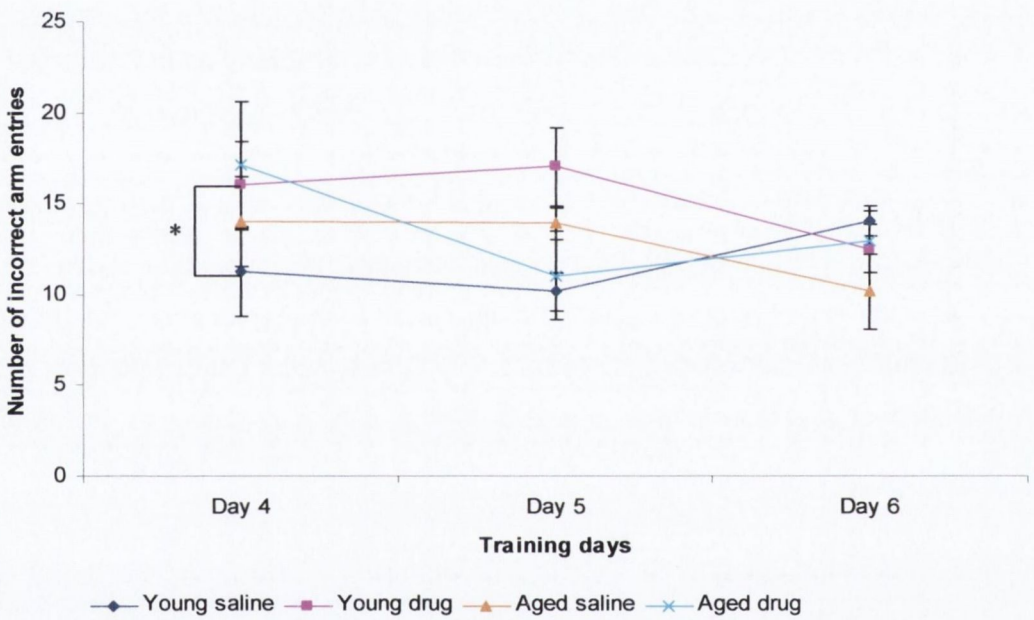

Figure 4.26 *Mean number of incorrect arm entries (± SEM) during training days 4 – 6. Young saline-treated, young drug-treated, aged saline-treated and aged drug-treated 2 – 3 month old male C57BL/6 mice. n = 8 per group. * P < 0.05.*

4.12 Discussion

4.12.1 One and two-year old mice

4.12.1.1 Morris water maze performance

This study sought to determine any differences in spatial memory performance between one and two year-old male mice. No evidence was found of a more pronounced cognitive deficit in the two year-old mice when compared to the one-year old animals. This is in contrast to a study by Benice *et al.* who found that the spatial memory was impaired in 18 – 20 month old mice when compared with 10 – 12 month old mice in the MWM [295]. Frick *et al.* have shown that middle-aged mice (17 months of age) have demonstrable moderate spatial memory impairment when compared to young mice of 5 months old; their performance lay between that of young (5 month old) and aged mice [300].

Although the cognitive performance of animals decreases with age the results of this experiment show that middle-aged and aged animals still possess the ability to retain information in their short-term memory and to convert it into long-term information as the animals showed improvement in the MWM task as the training days progressed. Nevertheless it is known that age-related decline in memory tasks exist in rodents [301, 302].

It is known that visual acuity is reduced with age [303]. However, the ability of the animals to utilize proximal visual cues to locate the platform indicates that the visual acuity in one and two year old mice is sufficient for the purpose of this experiment.

4.12.1.2 Object recognition task

The object recognition task was used as a less stressful paradigm [279] in which to test the working memory of middle aged and aged mice. The findings of this study showed that the one year-old mice exhibited greater activity in the maze and spent more time exploring the objects than the two year-old animals, which spent a lot of their time sitting in the periphery of the maze.

Failure of animals to habituate in the object recognition task may indicate decreased functioning of the hippocampus. It has been suggested that the hippocampus is involved in habitation and spatial novelty [304, 305].

The one year-old animals failed to habituate to object exploration while both the middle-aged and aged animals failed to react to spatial novelty. This may suggest that the hippocampus is in fact impaired with aging and this deterioration manifests itself in middle-age. In fact rodents with lesions of the hippocampus have been shown to perform poorly on spatial localization tasks [306, 307].
The middle-aged and aged mice both reacted well to object novelty. Reaction to object novelty is thought to be mainly dependent on the corticolimbic system [308]. Perhaps this may suggest that the cortical structures are less affected by aging than the hippocampus. In normal healthy aging, neuronal loss occurs in some brain structures such as the prefrontal cortex. It appears that there is some regression in the neuronal layers in the frontal cortex and there is some neuronal loss in the hippocampal structures with normal aging [309, 310].

Differences in the performance of one and two-year old mice in this study were not significant and from this study it can be seen that middle-aged animals also exhibit cognitive deterioration. Furthermore, pre-aged animals were not available and aging young mice until they reached two years old would result in a higher mortality rate than aging them until 12 months of age, the cost of housing and maintaining animals to two years of age would also prove more expensive and there would be a longer period of social isolation. (When housed together, aggressive behaviour led to fatalities.) For these reasons the middle-aged animals were chosen as the model of aging with which to continue cognitive testing as a comparator for young animals.

4.12.2 Young and middle-aged mice

4.12.2.1 Morris water maze performance

This experiment was designed to examine the role of BuChE in memory in young and aged mice in the MWM. We proposed that inhibition of BuChE by a novel BuChE inhibitor would be beneficial cognitively. Greig *et al.* previously found that aged rats treated with novel BuChE inhibitors, cymserine analogs, improved in cognitive tasks compared to control animals [288].

In this study young control mice were more adept at learning the maze than the control middle-aged animals. It has been previously shown in many studies that young animals outperform aged animals in memory tasks [300, 302]. The young saline-treated animals performed better than the young mice treated with compound 51. Also the young animals treated with the novel compound exhibited a performance similar to that of the middle-aged animals. Additionally, the middle-aged drug-treated group performed as well as the young saline-treated animals.

Overall treatment of young animals with the novel BuChE inhibitor, compound 51, did not confer any significant benefit in terms of enhancement in cognitive performance in the Morris water maze paradigm. However, the middle-aged drug treated animals performed slightly better than the middle-aged saline treated animals in this water maze. Middle-aged animals have higher levels of BuChE activity in the plasma, liver and brain than younger (*Figures 4.17 - 4.19).* Inhibition of BuChE by compound 51 in the brain of middle-aged animals may have increased the levels of the neurotransmitter ACh thus improving learning in aged animals. Cerbai et al. showed that a selective BuChE inhibitor, B^1 phenethyl-norcimerine, increased ACh release and activity in the cerebral cortex of rats [287].

Drug treatment in the young animals impaired their ability to learn the maze. Administration of the drug in young mice caused them to perform poorly in the MWM while aged animals improved somewhat in their ability to solve the task. There were no obvious signs of toxicity following a dose of 1 mg/kg of compound 51 thus outruling this as a cause of cognitive differences between the young and middle-aged drug-treated groups. The daily dosing regimen was chosen in accordance with previous

pharmacodynamic studies (chapter 2). The novel drug was administered one hour prior to starting the maze as this was the time when peripheral BuChE activity was inhibited maximally following a single oral dose of the drug. At a dose of 1 mg/kg the central effects of compound 51 were one third of that seen peripherally. The dose was not increased in aged animals as this may have resulted in toxic side-effects peripherally.

Previous studies have shown that rodents improve in cognitive tasks when treated with cholinergic inhibitors. Sweeney *et al.* found that 6 - 8 weeks old wild-type mice treated with galantamine had profound deficits in 24-hour retention of a passive avoidance response [290]. Additionally, wild-type mice treated with rivastigmine also exhibited cognitive deficits in the Morris water maze [266]. Galantamine is a well-known inhibitor of AChE, while rivastigmine is a dual inhibitor of both AChE and BuChE. Both of these enzymes are found in the brain although AChE is found at a higher concentration than BuChE [78]. From literature it seems that in diseased states human AChE and BuChE are co-dependent on each other. As the concentration of AChE decreases in AD BuChE concentration increases. BuChE hydrolyzes ACh optimally only under high substrate concentrations. Unlike galantamine and rivastigmine, compound 51 targets BuChE only. The findings of this study show that young animals treated with the BuChE inhibitor, compound 51, are cognitively impaired in the MWM. This may be due to a disruption in the normal balance of the enzymes, AChE and BuChE.

Treatment of the one-year old mice with the novel compound did not impair learning rather there was a slight albeit insignificant improvement in their cognitive ability to learn the maze compared to the saline treated one-year old mice. Yavich *et al.* found that tacrine improved memory performance in aged rats in the MWM [311]. Minkeviciene *et al.* found that treatment of 8-month old mice with memantine, an NMDA antagonist, improved cognitive performance in the MWM [312].

4.12.2.2 Object recognition task

The object recognition task represented a less stressful environment for the animals. This paradigm tested the ability of animals to recognize changes in the spatial arrangement of objects and object novelty. In comparison with older animals behavioural analysis showed that young mice did not actively explore the novel environment and objects. Cognitive decline is known to decrease progressively with age with a decreased ability to consolidate and store memory [284, 313]. Nevertheless middle-aged mice were more active than the younger mice in their exploration of the object across all sessions and in fact middle-aged animals retained information learned about the objects across all the sessions. This has also been suggested by Benice *et al.* who found that middle-aged mice were more active in the open field as compared to young mice [295]. However, Middei *et al.* found that 14-month old mice were less active in an object recognition task than young animals [271]. It was noted that the young mice spent the majority of their non-exploratory time in self-grooming. The young animals failed to habituate to the objects while the middle-aged animals habituated to object exploration as the objects became familiar to them.

All the groups failed to recognize the new spatial arrangement of the objects. The study design of Middei *et al.* [271] was followed for this paradigm. However, the housing conditions of the animals differed between this study and that of Middei *et al.* Individual housing may have had a negative effect on the performance of the animals in this study however group housing of the animals previously resulted in fatalities. It has previously been shown that young C57BL/6 mice (3 months old) react well to spatial novelty [314]. Failure of aging mice to recognize novel location has been previously reported and this is thought to be linked to the hippocampus [295]. The hippocampus is involved in the recognition of novel location of familiar objects [315]. Hippocampal-related memory is known to decline with age [316] and this may be the reason why the middle-aged animals treated with saline failed to recognize spatial novelty.

Object novelty may be a better test of attention and memory than object displacement as most object recognition tasks are based on exploration of familiar versus novel objects [133, 269, 270, 295, 317-319]. In this study both young and middle-aged animals reacted to object novelty and previous studies have shown that both young and middle-aged

mice respond to the presence of a novel object [295, 314]. Object novelty stimulated the animals as all groups spent a greater proportion of their time exploring the novel object than the four familiar objects. The most apparent difference was in the drug-treated middle-aged animals. They were the only group that spent more time exploring the novel object than the familiar objects. Perhaps the novel BuChE inhibitor increased ACh activity in the neocortex thus improving reaction to object novelty, as object novelty is known to be dependent upon the corticolimbic system [305].

4.12.2.3 Modified radial arm maze

The modified radial arm maze was chosen as a paradigm in which to test the spatial learning ability of young and middle-aged mice as it represented a less stressful task than the water maze and it was thought to be a more motivating than the object recognition task.

In this study both young and middle-aged mice did not show any motivation to learn this paradigm. The animals were unmotivated by this task and this lack of motivation was more evident in the young mice than in the middle-aged animals as they simply sat in each start arm during most trials. Gentle prodding to encourage movement or motivation only succeeded in the animal moving to the adjacent arm and resting there. During the final three training days both the young and middle-aged animals did appear to learn the location of the exit but on numerous occasions there was no motivation to do so. The final three training days showed that the middle-aged saline treated animals and the young drug-treated animals had a reduced number of incorrect arm entries.

However, these results cannot be taken explicitly as the animal's cognitive ability to learn the maze as the majority of animals were unmotivated during the training days. A previous study by Berstein *et al.* has shown that both young and aged male mice were capable of learning the radial arm maze with no apparent cognitive impairments in the aged animals [294]. Mizumori *et al.* showed that young CD-1 male mice were unable to solve the radial arm maze [320]. This may be due to the fact that CD-1 mice are albino with low visual acuity and were unable to solve the maze using extra-maze cues. Another water version of the radial-arm maze by Hyde *et al.* found that singly housed

young 8 – 10 week old male C57BL/6 mice were capable of learning the maze [321]. However, the maze used by Hyde *et al.* used water to a depth of 6 cm whereas the modified water version of the radial arm maze in this study had water to a depth of approximately 2 cm. The mice had to swim in the maze by Hyde *et al.* but in this study the mice could walk in the water as level only reached 2 cm. The version of the modified radial arm maze used in this study may not have been adverse enough to motivate the male mice to complete the task.

The mice used in this study were housed separately due to high mortality rates when housed together. This was thought to be a factor in their lack of motivation in this paradigm as they had been socially isolated. However, mice were also individually housed in the study by Berstein *et al.* and this did not produce any motivational problems in the radial arm maze. Although their paradigm was based on a motivational reward as animals had been deprived of water [294]. In addition to single housing the home cages of the mice in this experiment were not environmentally enriched. Environmental enrichment has been found to improve learning and memory in C57BL/6 of different ages [322]. However, the animals' home cages were changed on a weekly basis so that new isopad bedding was introduced. Once the animals were placed in the clean cage they immediately began to tear the bedding and make a sleeping area at the end of the cage furthest from the light in the room. This does indicate motivation in the home cage with respect to husbandry. It may be possible that the modified radial arm maze was not an altogether unpleasant experience for the animals and thus the motivation to escape was not the primary objective. The task may have been unstimulating to the animals as well as the lack of any motivational reward.

Previous experiments using male C57BL/6 mice of the same ages performed well in the Morris water maze and an object recognition trial. However, the young mice were also less responsive in the object recognition trial compared to the aged mice. Perhaps the reason for the good performance seen with young mice in the water maze was the fact that this is a stressful environment and the motivation to escape from the water onto the platform is high. It may be that 2 – 3 month old male C57BL/6 mice show little motivation when placed in tasks that do not have any motivational reward or do not promote forced learning. Furthermore the middle-aged animals were in fact housed

singly for a longer period of time than the young animals thus lack of environmental enrichment could not account for any differences in their motivation statuses.

4.13 Conclusion

The results of both the MWM and the object recognition paradigms correlate in that there is slight cognitive improvement in drug-treated middle-aged animals but a cognitive deficit is found in drug-treated young animals. The novel compound appears to enhance cognition in middle-aged animals where BuChE levels are high. However, inhibition of BuChE in young mice may in fact be detrimental where cholinergic function is not compromised.

Chapter 5

Chronic drug treatment study

Chapter 5 Chronic drug treatment study

5.1 Introduction

As acute treatment with compound 51 caused a moderate reversal of existing cognitive deficiency in aged mice, it was decided to determine whether chronic treatment with compound 51 as the animals aged would be able to prevent such a deficiency from developing. The aim of this study was two-fold: firstly, to determine the cognitive effects of the novel BuChE inhibitor isosorbide-2-benzylcarbamate-5-benzoate (compound 51) following a chronic treatment for a period of one year. Secondly, to determine any adverse effects of the novel drug with chronic drug treatment. It is well known that cognition and memory decrease progressively with age in both humans and animals [93, 323]. During normal aging the levels of cholinesterases in the brain change as BuChE increases while AChE decreases. However, this reversal is most apparent in AD [81, 324]. During the aging process, as cognition declines a drug may be given to intervene in the process in the hope that it will decelerate the rate of memory decline or restore cognitive functionality. This study was designed with the ideation that perhaps BuChE inhibitors, when given during the aging process, could play a prophylactic role in the deterioration of cognitive function by increasing the levels of the neurotransmitter ACh in the brain.

5.2 Animals

Healthy experimentally naïve 2-3 month old male C57BL/6 mice were obtained from Harlan, UK. All animals were housed in single cages with isopad bedding (Harlan, UK) and a paper cylindrical tube was placed in their cages for environmental enrichment. The cages were housed in an SPF environment with controlled temperature and humidity. All animals had ad libitum access to food and water under a 12 hour light/dark cycle (7.00 a.m. - 7.00 p.m. G.M.T.). All experiments were carried out during the light cycle. Animals were treated in accordance to the guidelines of the European Communities (Amendment of Cruelty to Animals Act 1876) Regulations 2002.

5.3 Drug Treatment

The animals were given a period of one week to adjust to their new environment upon arrival at the Bioresources Unit in TCIN. During this time the animals were also handled daily by the experimenter to minimize stress. The following week all mice were randomly assigned into groups using a random sequence generator programme [267]. The groups were saline treatment group or drug treatment group. All animals were weighed and given either of 0.9% saline (n = 12 per group) or 1 mg/kg of compound 51 (n = 12 per group) (per 10 g of body weight) per os using sterile gavage needles (Popper, NY) twice weekly for twelve months. Saline and the drug were routinely administered at the same time (each morning) twice weekly. At the end-point of the study there were 7 animals in the drug treatment group and 6 animals in the control group.

5.4 Health monitoring

All animals appeared healthy throughout this study. There were no signs of any cholinergic abnormalities, their coats were normal and there were no behavioural changes in the animals. As handling of the animals persisted they became more familiar with the experimenter and no aggressive behaviour was ever noted. Chronic administration of the compound did not produce any weight loss in any of the animals. The health of the animals was continually monitored during the course of the drug treatment by both the experimenter and the named veterinary surgeon. The body weights of the mice were recorded twice weekly also. During the course of the drug treatment many animals died, initially this was due to a lack of experience with the gavage procedure.

5.4 The Morris Water Maze

The MWM was used to compare cognition in chronic drug-treated animals compared to control animals.

5.4.1 Habituation

As previously described in section 3.5.3 on page 134.

5.4.2 Training

As previously described in section 3.5.4 on page 134.

5.4.4 Probe trial

As previously described in section 3.5.5. on page 135.

5.5 Object Recognition

The object recognition task was used to test the cognitive ability of animals treated chronically with compound 51. This paradigm is less stressful than the MWM and therefore cognition can be assessed in the absence of stress motivation.

5.5.1 Apparatus

As previously described in section 3.7.3.0 on page 136.

5.5.3 Training

5.5.3.1 Habituation to object exploration

As previously described in section 3.7.3.1 on page 137.

5.5.3.2 Reactivity to spatial novelty

As previously described in section 3.7.3.2 on page 138.

5.5.3.3 Reactivity to object novelty

As previously describe in section 3.7.3.3 on page 139.

5.6 Statistical analyses

5.6.1 Morris water maze

Differences in latency, path length and swim speed were assessed by a two-way ANOVA for repeated measures using SPSS version 14.0 with latency, path length, swim speed, thigmotaxis and time spent in the platform-containing quadrant as within-subject factors and drug treatment as between-subject factors. Independent t-tests were carried out to

determine any difference between the groups on each of the training days for each parameter.

5.6.2 Object recognition task

Habituation to the objects (sessions 1-3) were analysed by a two-way ANOVA repeated measures using SPSS version 14.0 with age and treatment as between-subject factors and sessions as within-subjects factor. Reactivity to spatial and object novelty was evaluated using a two-way ANOVA for repeated measures with age and treatment as between-subject factors and object category as within-subject factor. Post-hoc pair comparisons, Tukey's test, were calculated where appropriate. Independent t-tests were used to compare the activity of each animal between sessions.

5.7 Results

5.7.1 Morris water maze

5.7.1.1 Latency to Platform

The saline-treated animals and drug-treated animals took approximately the same amount of time to locate the platform over the training days, $F(1, 11) = 0.529$, $P > 0.05$ (two-way ANOVA for repeated measures). Initially on the first training day both groups took approximately 42 seconds to find the platform however, their latencies significantly decreased over the training days, $F(1, 11) = 11.515$, $P < 0.05$ (two-way ANOVA for repeated measures).

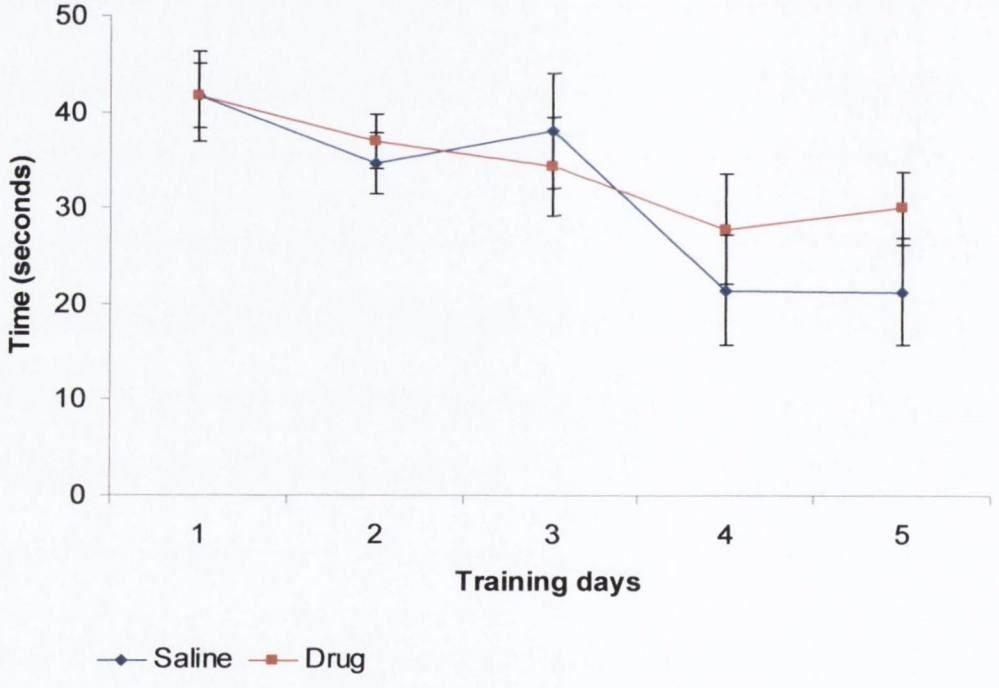

Figure 5.1 *Latency to reach the platform (s) during water maze training days 1 - 5. 14 month old chronic saline-treated (n = 6) and 14 month old chronic drug-treated (n = 7) male C57BL/6 mice. Mean ± SEM.*

5.7.1.2 Path length

The saline-treated animals had the shortest path length to the platform over the training days. This observation was consistent with the findings of the latency to the platform. The saline-treated animals consistently outperformed the drug-treated animals. On training days 4 and 5 the drug-treated animals swam approximately 100 cm more than the saline-treated animals before finding the platform, $F(1, 11) = 3.725$, $P < 0.001$ (two-way ANOVA for repeated measures).

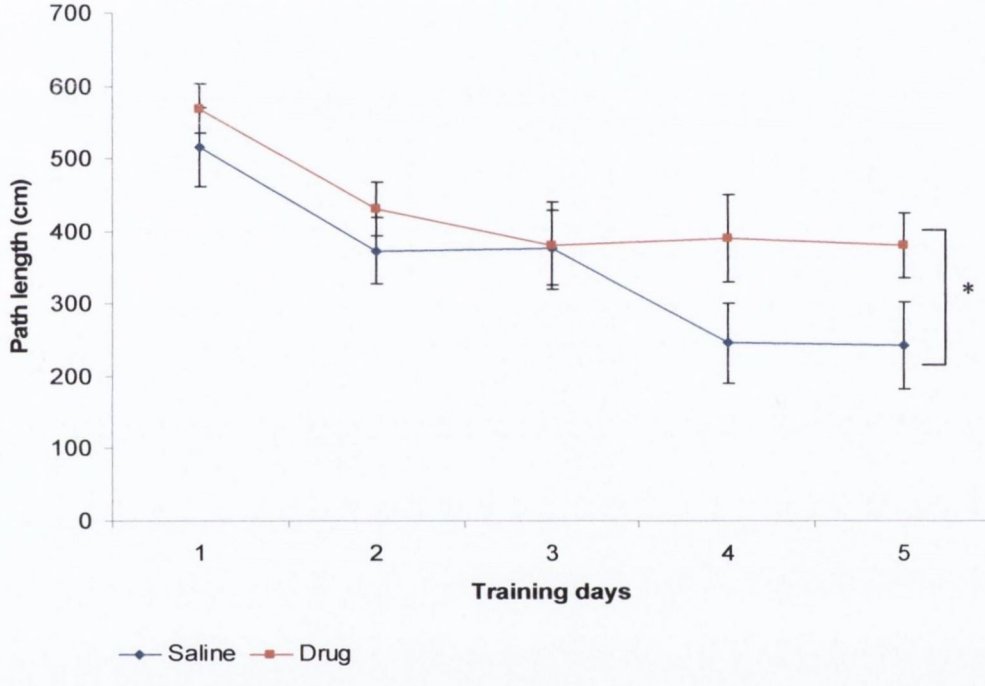

Figure 5.2 *Path length to the platform (cm/s) during water maze training days 1 - 5. 14 month old chronic saline-treated (n = 6) and 14 month old chronic drug-treated (n = 7) male C57BL/6 mice. Mean ± SEM. *P < 0.001.*

5.7.1.3 Swim speed

The saline and drug-treated animals had similar swim speeds across the training days. Statistical analysis of the data for swim speed of the animals did not reveal a statistically significant difference between the groups, $F(1, 11) = 0.642$, $P > 0.05$ (two-way ANOVA for repeated measures).

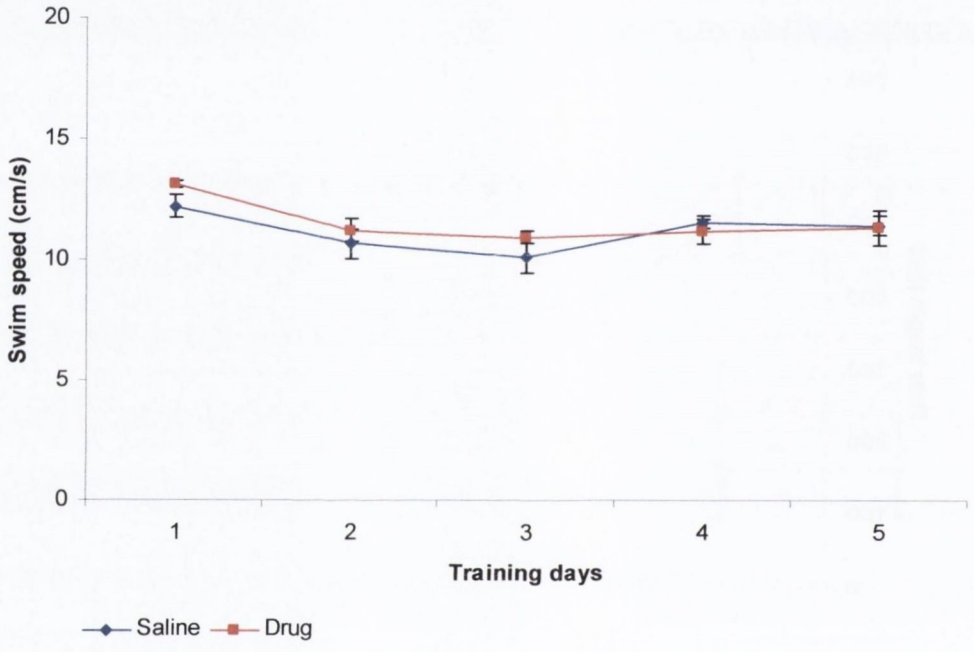

Figure 5.3 *Swim speed of the animals (s) during water maze training days 1 - 5. 14 month old chronic saline-treated (n = 6) and 14 month old chronic drug-treated (n = 7) male C57BL/6 mice. Mean ± SEM.*

5.7.1.4 Thigmotaxis

The saline and drug-treated groups both spent a similar amount of time swimming close to the wall of the pool (thigmotaxis). A two-way ANOVA for repeated measures did not reveal any statistically significant difference in the duration of time each group spent in thigmotaxis, $P > 0.05$. However, there was a statistically significant difference between the animals' performance across the training days, $F(4, 44) = 12.964$; $P < 0.001$ with far more time being spent in thigmotaxis on the first day of training than on days 2 - 5.

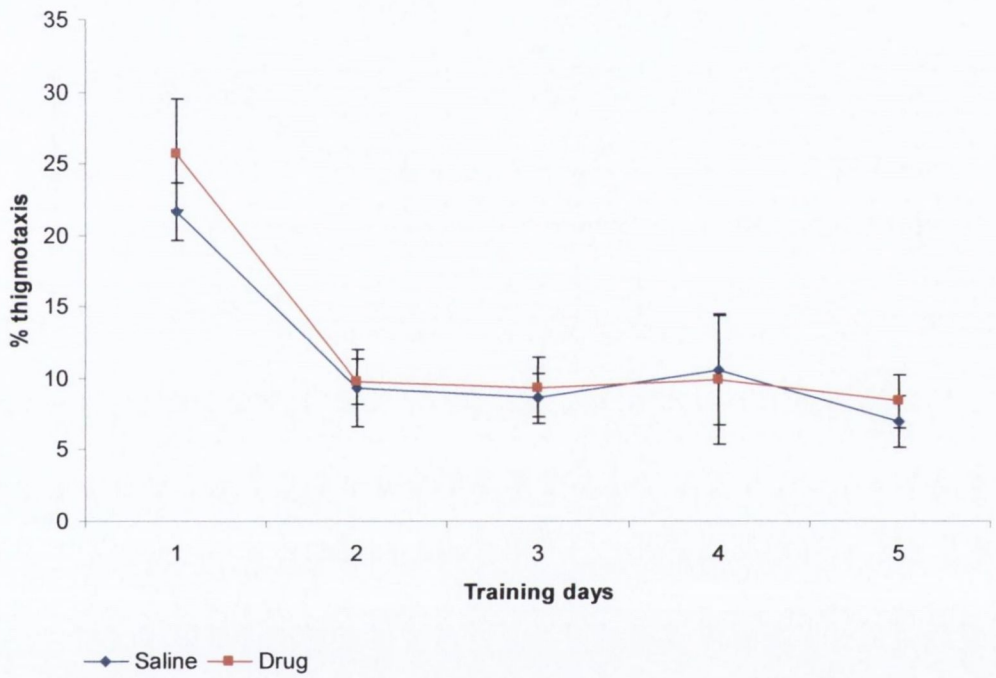

Figure 5.4 *% thigmotaxic time during water maze training days 1 - 5. 14 month old chronic saline-treated (n = 6) and 14 month old chronic drug-treated (n = 7) male C57BL/6 mice. Mean ± SEM. *P < 0.001.*

5.7.1.5 Time spent in the southeast quadrant during training

The saline-treated animals spent slightly more time in the southeast quadrant (containing the platform) during the water maze training days. However, on training days 2 and 3 the drug-treated animals spent more time in the southeast quadrant than the saline-treated controls. A two-way ANOVA for repeated measures revealed a statistically significant difference between the groups, $F(1, 11) = 0.001$, $P > 0.05$. Moreover, there was a significant difference for the time each group spent in the platform containing quadrant across the training days, $F(1, 11) = 7.280$, $P < 0.05$.

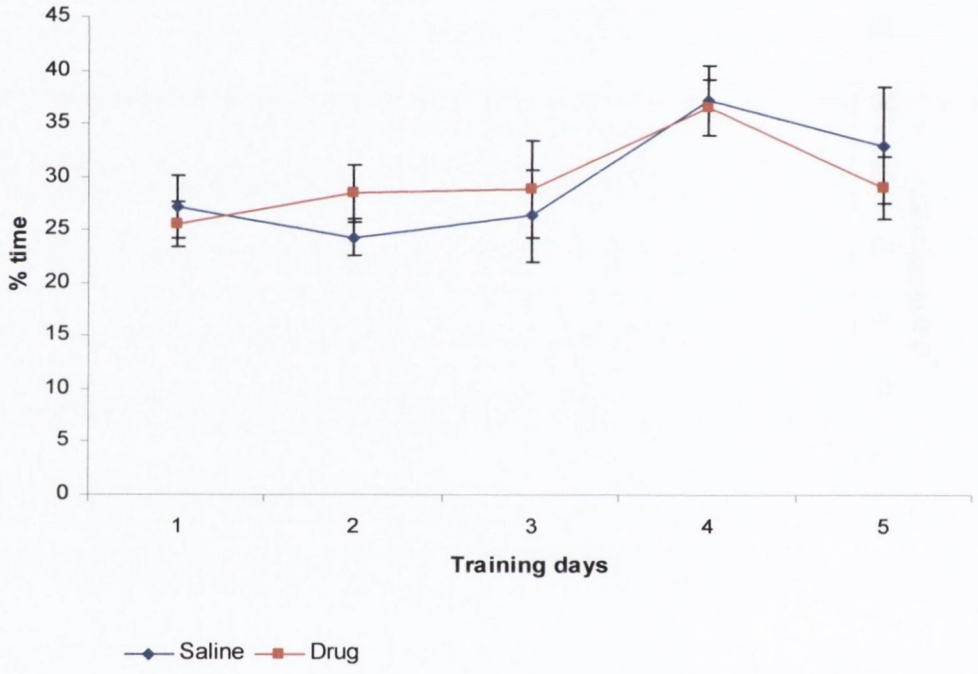

Figure 5.5 *% time in the southeast quadrant (containing the platform) during water maze training days 1 - 5. 14 month old chronic saline-treated (n = 6) and 14 month old chronic drug-treated (n = 7) male C57BL/6 mice. Mean ± SEM.*

5.7.1.6 Probe trial

Both the saline and drug-treated animals spent an equal amount of time in the platform-containing quadrant (southeast quadrant) during the probe trial. An independent t-test did not reveal any statistically significant difference between the groups for the duration of time they spent in the southeast quadrant during the probe trial, $P > 0.05$.

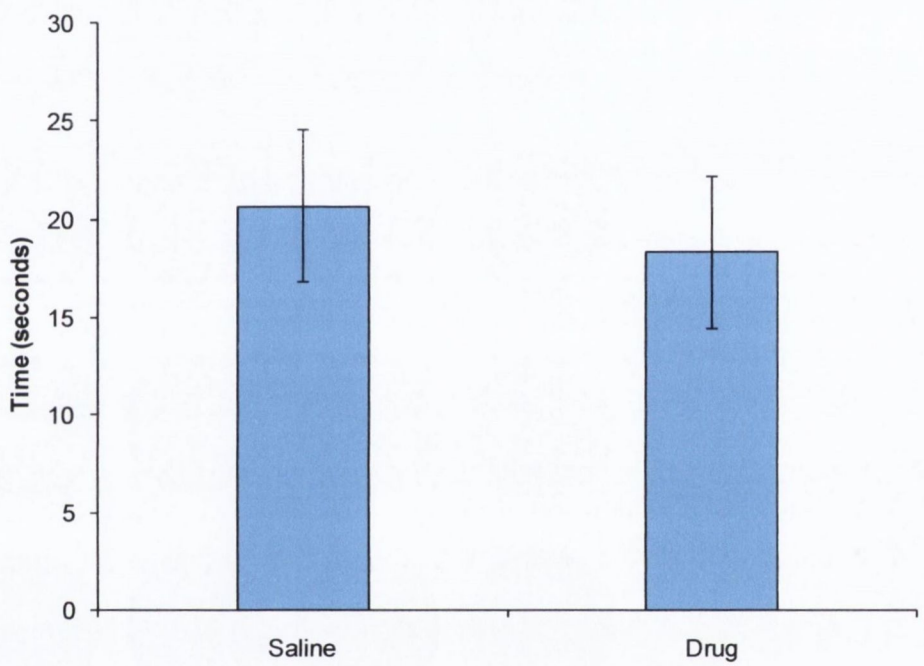

Figure 5.6 *% time in spent in the southeast quadrant (previously containing the platform) during the probe trial. 14 month old chronic saline-treated (n = 6) and 14 month old chronic drug-treated (n = 7) male C57BL/6 mice. Mean ± SEM.*

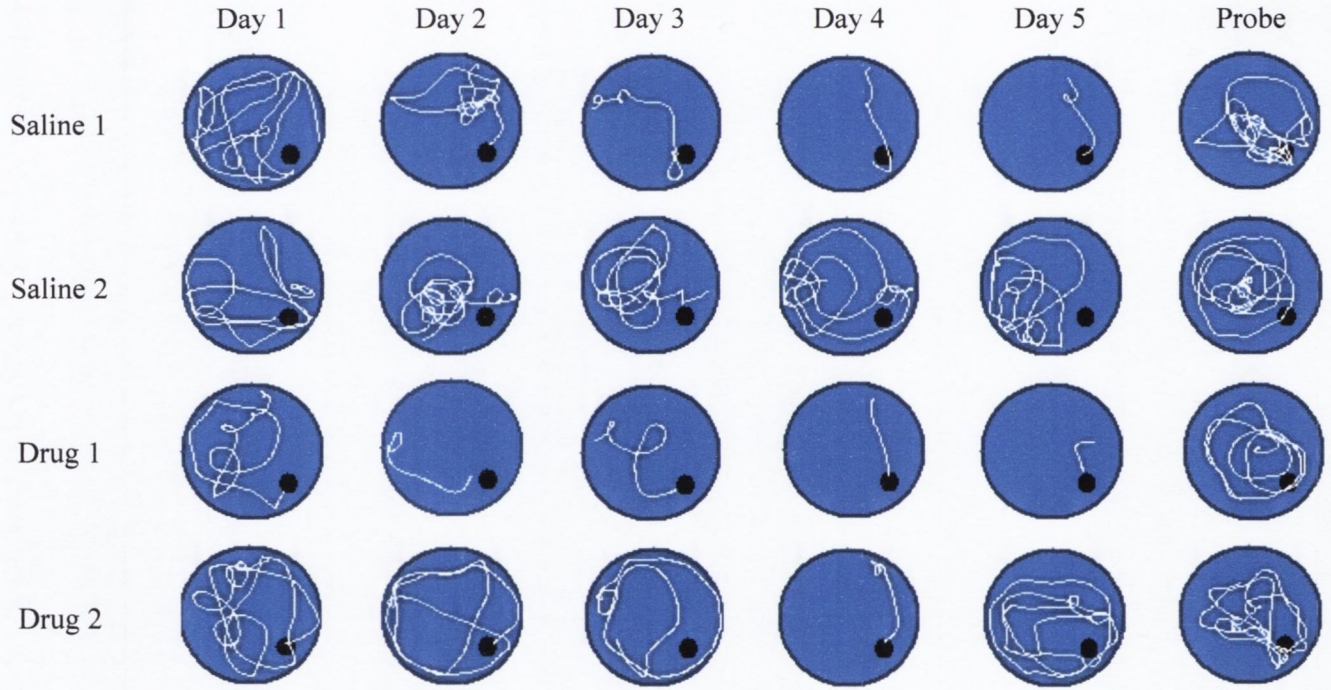

Figure 5.7 *Swim paths to the platform during training days 1 – 5 and the probe trial. The training and probe plots represent the best and worst performing animals in each group. Saline-treated and drug-treated 14 month old male C57BL/6 mice.*

5.7.1.7 Body weight

There was no difference in the body weights of the saline-treated and drug-treated animals during the course of the one-year drug treatment with compound 51, $F(1, 11) = 0.39$; $P > 0.05$, (two-way ANOVA for repeated measures). Chronic treatment with compound 51 neither resulted in weight loss nor weight gain. However, both the saline-treated and drug-treated animals gained a similar amount of weight over the course of the one year treatement, $F(12, 132) = 66.313$, $P < 0.05$.

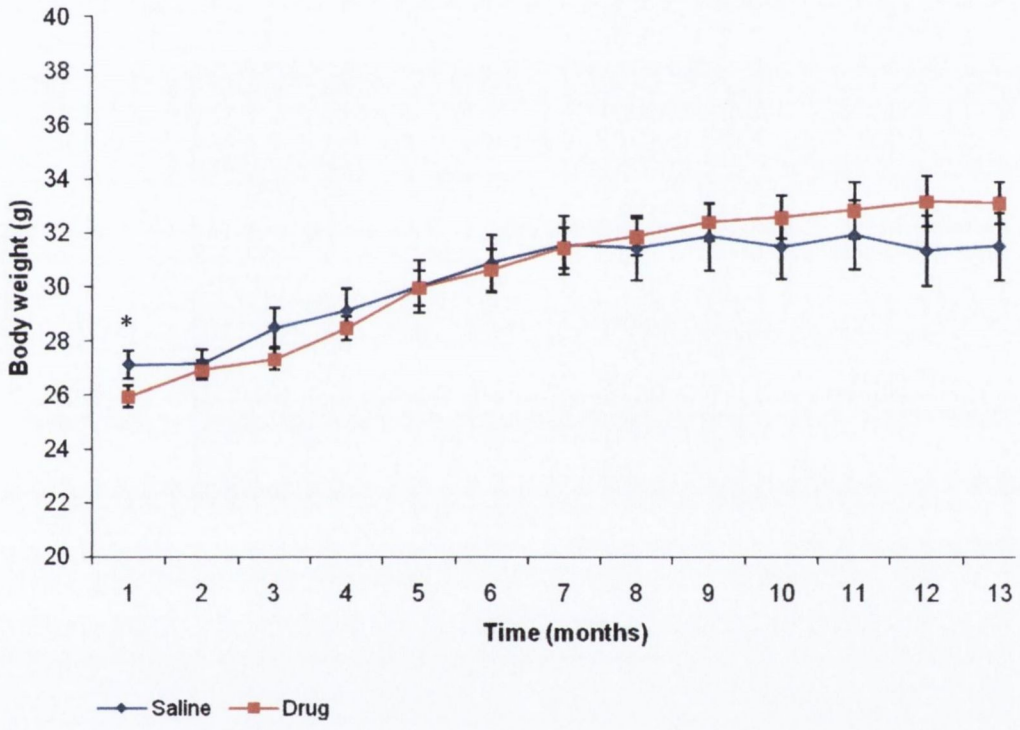

Figure 5.8 *Mean body weight (g) (± SEM) for animals over a 13 month period. 14 month old chronic saline-treated (n = 6) and 14 month old chronic drug-treated (n = 7) male C57BL/6 mice. Mean ± SEM.*

5.7.1.8 Brain BuChE levels

The level of BuChE in the brains of drug-treated animals did not differ from that of the saline-treated animals. The mean BuChE activity in the drug-treated animals was slightly lower than that for the saline group but this was insignificant, $P < 0.05$ (independent t-test).

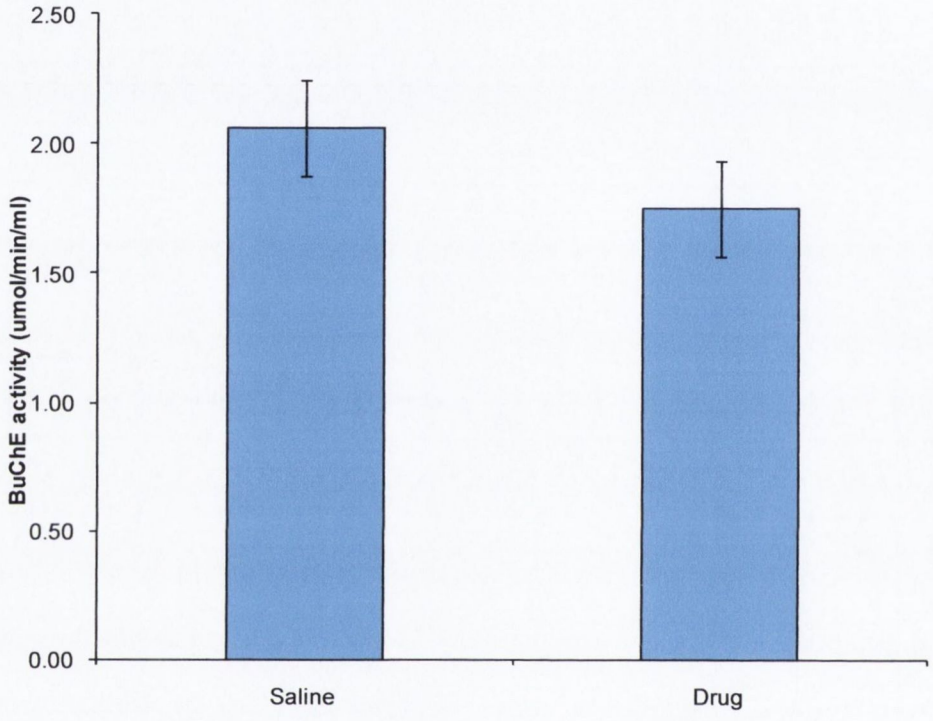

Figure 5.9 *Mean BuChE activity in mouse brain (± SEM). Saline-treated (n = 6) and drug-treated (n = 7) 14 month old male C57BL/6 mice. Chronic treatment with saline (0.1 ml /10 g body weight) or compound 51 (1 mg/kg) for one year.*

5.7.2 Object recognition task

5.7.2.1 Habituation of object exploration

The saline and drug-treated animals habituated to the objects across sessions 1 – 3 with a decline in exploring the objects across the sessions. There was no significant difference in the amount of time each group spent exploring the objects during each session, $F(1, 11) = 2.002$, $P > 0.05$ (two-way ANOVA for repeated measures).

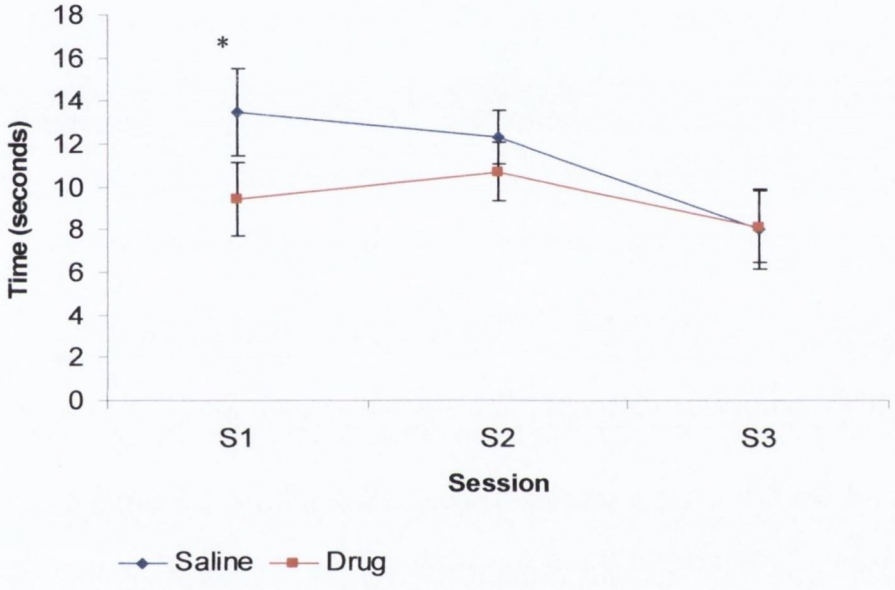

Figure 5.10 *Habituation of object exploration during sessions 1 – 3. Mean duration of contacts with the objects (± SEM) during sessions 1 – 3. Saline-treated (n = 6) and drug-treated (n = 7) 14 month old male C57BL/6 mice.*

5.7.2.2 Reactivity to spatial novelty

The saline and drug-treated animals both reacted to spatial novelty by spending more time exploring the displaced objects (DOs) than the non-displaced objects (NDOs). However, there was no difference between the groups, $F(1, 11) = 0.541$; $P > 0.05$ (two-way ANOVA). There was a difference within the saline-treated group; they spent more time exploring the DO than the NDOs, $P < 0.05$. Overall the saline-treated controls spent more time exploring the objects than the drug-treated animals.

Figure 5.11 *Reactivity to spatial novelty. Mean change in duration of of time (s) in contact with the non-displaced objects (NDOs) and displaced (DOs) (± SEM) during sessions 4 and 5. Saline-treated (n = 6) and drug-treated (n = 7) 14 month old male C57BL/6 mice. * P < 0.05.*

5.7.2.3 Reactivity to object novelty

The saline-treated controls reacted to object novelty but the drug-treated animals failed to react to object novelty. The saline-treated animals also spent a greater proportion of their time interacting with the objects overall compared to the drug-treated animals. A two-way ANOVA found a statistically significant difference between the groups for the time the groups explored the novel object, $F\ (1, 11) = 7.313$, $P < 0.05$. There was also a statistically significant difference within the saline-treated group for their exploration of the NSOs and SO; $P < 0.05$.

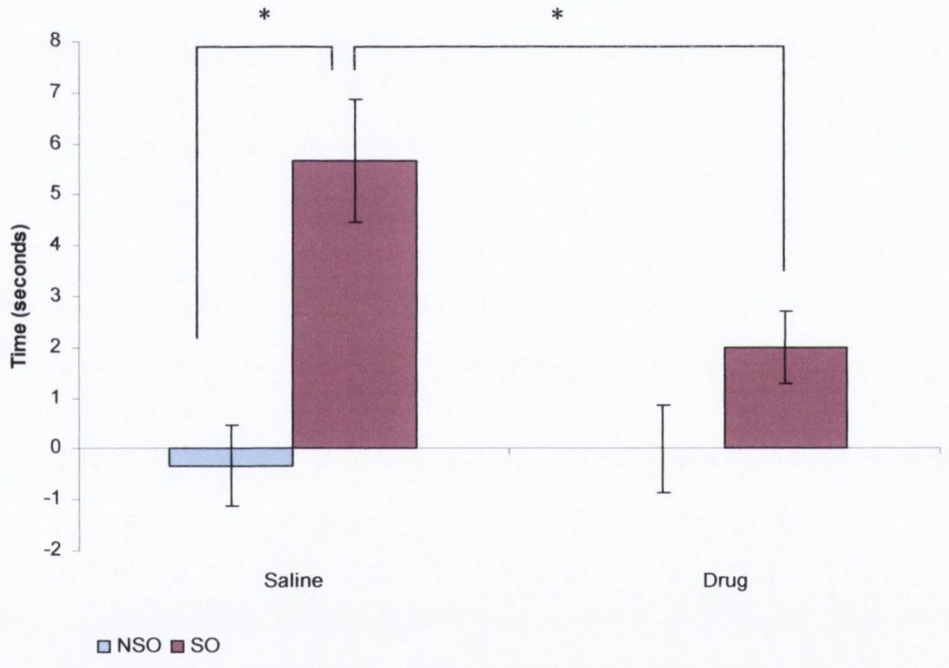

Figure 5.12 *Reactivity to object novelty. Mean change in duration of of time (s) in contact with the non-substituted objects (NSOs) and substituted objects (SOs) (± SEM) during sessions 6 and 7. Saline-treated (n = 6) and drug-treated (n = 7) 14 month old male C57BL/6 mice. * P < 0.05.*

5.8 Discussion

5.8.1 Morris water maze

The purpose of this study was to determine whether chronic treatment with the novel BuChE inhibitor, compound 51, would act as a preventative strategy in cognitive decline. This paradigm revealed that chronic treatment over a period of one year with the novel BuChE inhibitor did not produce any positive prophylactic effects on cognition in male C57BL/6 mice.

The results of this paradigm show that the saline-treated controls learned the maze faster than the drug-treated animals during the training days with respect to their latencies and path lengths. It is evident that within each group some animals were proficient at learning the maze while others were not (Figure 5.10). As there was no apparent differences in probe trials for both groups it may be surmised that the novel BuChE inhibitor did not improve cognition in drug-treated animals compared to the control groups. Although some animals failed to completely learn the maze within the training period, it was previously shown that five days of training is sufficient for middle-aged animals to learn the maze in chapter 4. A previous study found that all animals showed habituation or even disinterest in the maze following five days of training as they exhibited longer latencies and path lengths.

It has been suggested that C57BL/6 mice possess a genetically determined deficiency in cholinergic neurons in the forebrain as compared to other strains of mice [325]. Should this be the case then perhaps it is difficult for these mice to retain learned information with aging in particular with a 24-hour retention time between training days, however this was not found to be the case with middle-aged animals in chapter 4. As animals age, visual acuity declines and this may be a reason why some of the animals were inept at learning this cognitive task. In general the processing of visual stimuli is slower in aged than young rats [326]. The use of distal visual cues instead of proximal visual cues in this paradigm may have been more beneficial as aged C57BL/6 mice have been shown to prefer distal visual cues in the MWM [327].

In this study the level of BuChE activity in the brains of the drug-treated animals was slightly lower but not significantly different from that of the saline-treated animals. There was no cognitive benefit associated with this decrease. However, the observed decrease in brain BuChE activity suggests that the novel BuChE inhibitor is capable of causing a reduction in the levels of BuChE in the brain following chronic administration but this decrease may not have been sufficient to improve cognition. It was shown previously in chapter 4 that treatment of young control animals with the novel BuChE inhibitor produced unfavourable results and negative effects on cognition while middle-aged animals treated for two weeks with the novel compound showed a slight improvement in cognition. It is known that BuChE activity increases in the aging brain while AChE decreases [81]. BuChE may take over the role of ACh degradation in the aging brain as high levels of ACh in the hippocampus have been found to be controlled by BuChE in $AChE^{-/-}$ mice[118]. Butyrylcholinesterase has unique enzymatic properties and is widely distributed in the nervous system advocating a role for BuChE in neural function [328]. Spatial learning is known to be hippocampal dependent and ACh activity has been found to increase greater than 200-fold in the hippocampus during spatial learning tasks [329]. Darvesh et al. demonstrated that BuChE is located in neurons within the hippocampus and suggested that BuChE may have a specific function of co-regulating cholinergic and non-cholinergic neurotransmission [134]. As young animals possess normal levels of BuChE and any increase in this enzyme in the brain does not occur until later life it may be possible that chronic inhibition of BuChE in a young animal may in fact be detrimental to cognitive function in pertaining to the hippocampus suggesting that BuChE may have its own unique role in cognition independent of acting as a back-up to AChE.

Assessment of the level of BuChE peripherally in the blood was not analysed as they are optimally collected at the end-point of the study only [330], thus the level of peripheral BuChE inhibition could not be determined throughout chronic drug treatment.

5.8.2 Object recognition task

Reactivity to novel objects compared to interaction with familiar objects is considered as a test of memory retention in animals [268]. This paradigm offered another means of assessing the cognitive ability of animals following chronic treatment with a novel BuChE inhibitor albeit in a less stressful environment. In this study mice treated chronically with compound 51 did not appear to benefit cognitively in this paradigm when compared to control animals.

The drug-treated animals failed to habituate to the objects during the habituation session and spent less time interacting with the objects overall when compared to the aged saline group. The saline-treated animals habituated to the objects with a decrease in the time spent interacting with the objects across the sessions. There was a positive response from both groups in recognising spatial novelty and this was more apparent in the reaction of the saline-treated mice to the new spatial arrangement of the objects. During the object novelty task the saline-treated animals spent significantly more time interacting with the novel object than the drug-treated mice however both groups did react to object novelty.

Habituation and awareness of spatial novelty are thought to be hippocampal dependent as lesions of the septo-hippocampus in rats showed failure to habituate and react to displaced or non-displaced objects [331]. Reaction to object novelty is largely dependent on the corticolimbic system [308]. Cholinergic neurons are common in the corticolimbic brain regions while the hippocampus contains small ChAT immunoreactive cells but it mainly receives the septo-hippocampal cholinergic projection from the medial septum [332 333 334]. However, the hippocampus contains BuChE positive neurons [134] whereas the BuChE positive neurons found in the frontal cortex arise from projections from thalamic nuclei [335]. The BuChE neurons in the frontal cortex are thought to have roles in attention, memory and behaviour. Additional non-cholinergic functions of BuChE include modulation of proteins and regulation of cerebral blood flow [336]. Perhaps inhibition of BuChE in the brain over a chronic time period from youth to middle-age resulted in down-regulation of BuChE in the BuChE-positive neurons thus secondarily affecting neurons in other areas of the brain to which they project or disrupted cerebral blood flow. As the drug-treated animals failed to habituate to the objects and also failed to respond to spatial novelty this may suggest that the BuChE neurons in the hippocampus of young

mice were adversely affected by chronic treatment with the BuChE inhibitor. The use of cholinergic inhibitors as a prophylactic treatment prior to the onset of any diseased state is of no cognitive benefit and this is also seen in the young mice treated with compound 51 in chapter 4. The ability of the drug-treated animals to react to object novelty may indicate that the corticolimbic system is not as adversely affected by BuChE inhibition as the hippocampus. Prolonged isolation of the animals for a one-year period did not appear to have a negative impact on the animals' mood or behaviour. The animals always responded positively to handling by the experimenter and were found to be alert and reacted unfavourably to handling by a new experimenter. Should the animals have been in a depressed state following isolation they would fail to react to social contact.

5.9 Conclusion

The results of this study consistently show that chronic administration of the novel BuChE inhibitor, compound 51, did not confer any cognitive advantage in mice when compared to saline-treated animals. From this study it can be deduced that the use of a novel BuChE inhibitor as a chronic prophylactic treatment is not favourable in preventing cognitive decline. In fact, the commencement of chronic BuChE inhibition therapy in young healthy animals and its continuation in middle-age does not appear to produce any cognitive benefits in later life.

Chapter 6

Histology and toxicology

Chapter 6 Toxicology and histology

6.1 Introduction

As the liver functions in clearance, biotransformation and excretion of drugs it is not surprising that they commonly cause hepatic injury. The purpose of this study was to determine any toxicological effects of the novel BuChEIs on mouse liver 24 hours following drug administration. Assessment of any toxicological effects produced by the novel drugs, compound 51 and compound 30, were determined *in vivo* in mice. Hepatic function was also assessed one year following chronic treatment with the novel inhibitors in mice to determine the effect of long-term drug usage on the liver.

Clinical chemistry was performed on the plasma and liver to determine if the drugs produced any adverse effects on the liver. Some enzymes in the liver act as biomarkers for hepatotoxicity; that is, any hepatic damage will result in changes in these enzymes. Such biomarkers include: alanine transferase (ALT), gamma glutamyl transpeptidase (GGT), total bilirubin, alkaline phosphatase (ALP), aspartate transaminase (AST), glutamate dehydrogenase (GLDH) and albumin. ALT is generally considered the gold standard maker in clinical chemistry and increases in this enzyme usually indicate liver injury. GGT, total bilirubin and ALP are additional biomarkers of liver function and are used to supplement ALT activity studies. AST is considered a less specific biomarker of liver injury but increases in this enzyme indicate necrosis. GLDH is found on the mitochondrial matrix and a rise in the level of this enzyme indicates hepatocellular damage [337].

In addition to analysis of hepatic function following administration of the novel compounds, liver samples were examined histologically for any signs of toxic damage within the parenchyma following administration of compounds 30 and 51.

6.2 Animals

Healthy experimentally naïve 2 – 3 month old male C57BL/6 mice (20 - 33 g) from Harlan, UK were housed in single cages with isopad bedding (Harlan, UK) in an SPF environment with controlled temperature and humidity. All animals had *ad libitum* access to food and water. A twelve hour light/dark system was in operation in the animal house in the Institute of Neuroscience in Trinity College (lights on at 7 a.m. – 7 p.m. G.M.T). All experiments were carried out under the light phase of the cycle. Animals were treated in accordance with the European Communities (Amendment of Cruelty to Animals Act 1876) Regulations 2002.

6.3 Drug preparation

6.3.1 One-day toxicology study

1 mg of compounds 30 and 51 were weighed and transferred to volumetric flasks. Sterile WFI was added to reach a final volume of 10 ml producing a concentration suitable for delivery of 1 mg/kg. The drugs were sonicated at 30°C for 20 minutes after which they formed solutions.

6.3.2 One-year toxicology study

1 mg of compound 51 was weighed and transferred to a 10 ml volumetric flask. Sterile WFI was added to make a final volume of 10 ml producing a concentration suitable for delivery of 1 mg/kg. The drug was sonicated at 30°C for 20 minutes after which the drug formed a solution.

6.3.3 Histology study

1 mg of compound 30 was weighed and transferred to a 5 ml volumetric flask. Sterile water for injection was added to reach a final volume of 5 ml producing a concentration suitable for delivery of 2 mg/kg. 1 mg of compound 51 was weighed and transferred to a 1 ml volumetric flask. Sterile water for injection was added to reach a final volume

of 1 ml producing a concentration suitable for delivery of 10 mg/kg. The drug was sonicated at 30°C for 20 minutes after which the drug formed a solution.

6.4 Drug treatment

The mice were handled for 5 minutes each per day by the experimenter for three days prior to drug treatment to reduce any stress during drug administration. Three separate studies were conducted on the novel compounds.

6.4.1 One-day toxicology study

Animals were given a single oral dose of 0.9% saline (n = 3), 1 mg/kg of compound 51 (n = 3) or 1 mg/kg of compound 30 (n = 3) in a volume of 0.1 ml/10 g 24 hours prior to analysis of the clinical chemistry of plasma and liver tissue. Animals were sacrificed 24 hours following drug administration.

6.4.2 One-year toxicology study

Animals were treated with 0.9% saline (n = 12) or 1 mg/kg of compound 51 (n = 12) in a volume of 0.1 ml/10 g twice weekly for one year and during the MWM and object recognition task. The total duration of drug administration was thirteen months.

6.4.3 Histology study

Animals were administered a single oral dose 2 mg/kg compound 30 and compound 51 at 10 mg/kg (n = 3 per group) in a volume of 0.1 ml/10 g prior to histological analysis of the liver tissue only. Animals were sacrificed 24 hours following administration of the novel compounds. All samples were processed and reported by Professor Brian Sheahan in the School of Veterinary Medicine, University College Dublin.

6.5 Isolation and preparation of tissue samples

6.5.1 Toxicology studies

6.5.1.1 Isolation of tissue samples for toxicology

Blood samples were taken via the submandibular technique. An 18-gauge needle (Sherwood Medical, UK) was used to puncture the venous blood plexus at the back of the cheek pouch which drains into the jugular vein. 200 µl blood samples were collected in 200 µl lithium heparinized Microvette capillary tubes (Sarstedt, Germany) and placed on ice until tested. Following blood sampling the animals were sacrificed by cervical dislocation and the liver was carefully removed. The right lobe of the liver *(Figure 6.1)* was isolated and placed in a labelled tube on dry ice until tested.

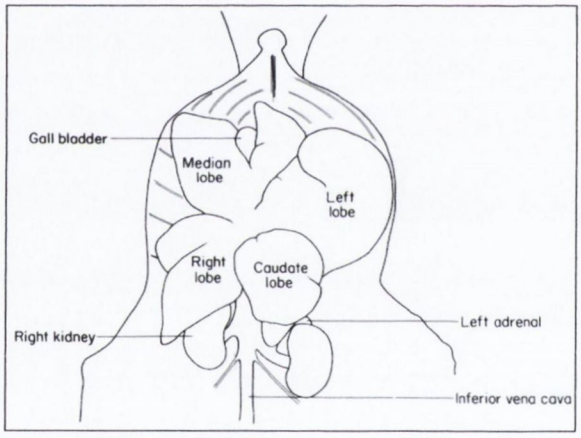

Figure 6.1 The lobes of the mouse liver [338].

6.5.1.2 Preparation of tissue samples for toxicology

Preparation of plasma samples

Plasma samples were prepared by centrifugation (Jouan centrifuge CR3i, Biosciences, Dublin) of heparinized venous blood at 3,000 rpm for 10 minutes at 4°C. Plasma was removed and transferred to labeled 1.5 ml Eppendorfs (Brand, Germany).

Preparation of liver samples

For determination of hepatic activities of the enzyme approximately 500 mg of mouse liver was homogenised on ice in ice-cold 5 ml (10 volumes) of phosphate buffered saline (PBS) pH 7.4 (100 mg/ml) in three 5 second bursts using an Ultra-turrax T-10 model (IKA-Werke, Germany) at 10,000 rpm. The homogenate was centrifuged (Jouan centrifuge CR3i, Biosciences, Dublin) at 10,000 rpm for 10 minutes at 4°C. 1:100 and 1:1000 dilutions were made of the liver homogenate in 0.1 M PBS pH 7.4.

6.5.2 Histology study

All animals in this group were sacrificed by cervical dislocation. An incision was made from the mid-abdomen up to the ribcage and the liver was then removed. The entire liver was isolated and placed in 10% formaldehyde (in 0.9% saline) for 24 hours.

6.5.2.1 Preparation of tissue samples for histology

Livers were graded through a series of alcohols to dehydrate the tissue and finally immersed in paraffin wax. Once the tissue was fixed in the paraffin wax, 20 μm sections were taken using a cryostat (Leica, Laboratory instruments, Ashbourne, Co. Meath) and placed on subbed microscope slides. The slides were stained with haematoxylin and eosin (H & E). All slides were viewed under a Nikon Eclipse E200 (Nikon, Japan) microscope at 100X. Images for photomicroscopy were taken using a Nikon coolpix 4500 4.0 megapixel (Nikon, Japan) camera attached to the microscope. Sectioning and histological analysis of the liver samples were carried out by Professor Brian Sheahan in the University Veterinary Hospital in University College Dublin.

6.5.2.2 Toxicological testing

200 µl of plasma were placed in labelled 0.5 ml paediatric microtubes (Sarstedt, Wexford). Dilutions of the liver homogenate were transferred to labelled 1.5 ml Microtubes (Sarstedt, Germany). The plasma samples were tested for activity of the enzymes ALT, AST and alk phos as well as albumin concentration. The 1:100 dilution of the liver homogenate was tested for alk phos, AST, GLDH, GGT, albumin and total bilirubin. The 1:1000 dilution of the liver homogenate was tested for ALT only. Clinical chemistry of the plasma and liver samples were analysed by a Randox Imola™ (UK) clinical analyser controlled by a Randox International Quality Assessement Scheme External Quality Assessment programme (Randox, UK).

6.7 Results

6.7.1 One-day toxicology study

6.7.1.1 Plasma biomarkers

There did not appear to be any changes in the concentrations of the hepatic biomarkers in the plasma of the animals that received 1 mg/kg of compound 30 p.o. and 1 mg/kg of compound 51 p.o. compared to saline control animals. In fact there was no statistically significant difference in the hepatic biomarkers of hepatotoxicity in the plasma of any of the animals when compared using independent t-tests, $P > 0.05$. However, there was a large variance in the data for aspartate transaminase for the control group and those animals treated with 1 mg/kg of compound 30.

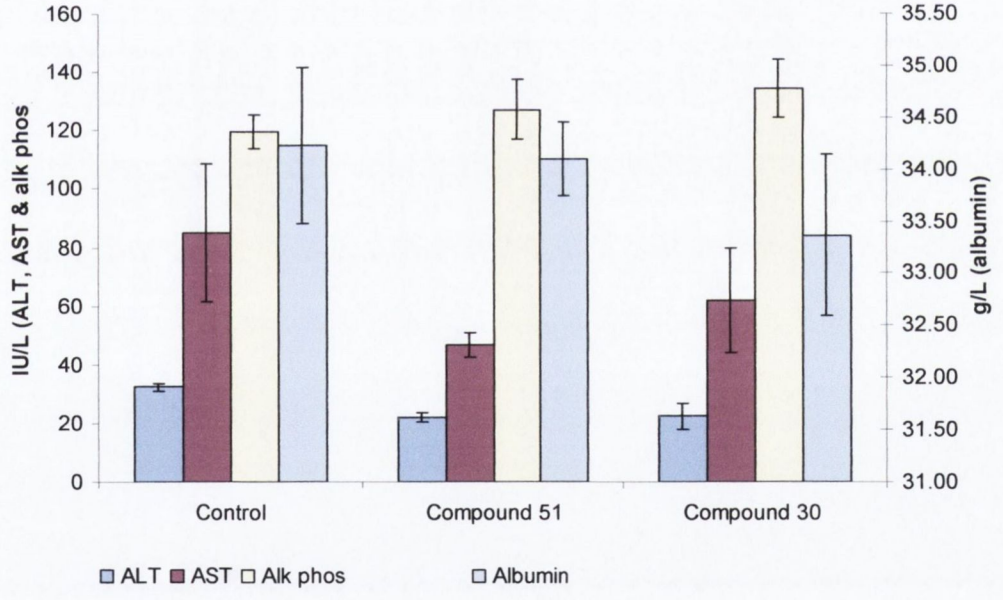

Figure 6.2 *Mean levels of alanine transferase, aspartate transaminase, alkaline phosphatase and albumin (± SEM) in mouse plasma 24 hours oral post administration of 1 mg/kg of compound 51 (n = 3) or 1 mg/kg of compound 30 (n = 3). 2 - 3 month old male C57BL/6 mice.*

6.7.1.2 Liver biomarkers

Independent t-tests did not reveal any statistically significant difference between the groups, $P > 0.05$. Large variances in the data of alkaline phosphatase in the control group meant that it was difficult to detect any potential changes alkaline phosphatase or albumin following drug treatment. However, it must be noted that the variances for the animals treated with 1 mg/kg of compound 30 p.o. were small when compared to the control values and the values of the animals treated orally with 1 mg/kg of compound 51.

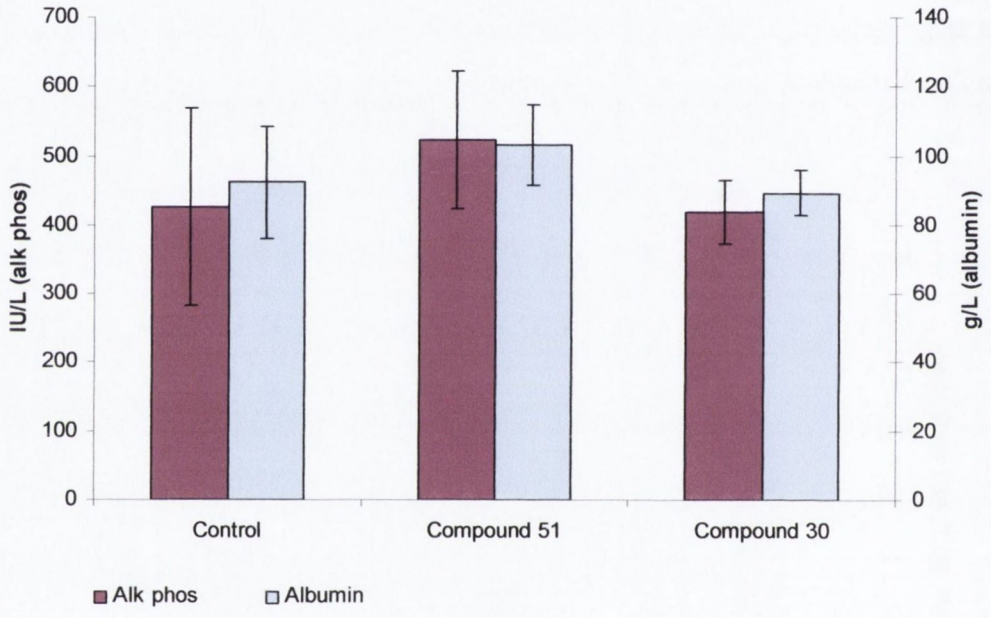

Figure 6.3 *Mean levels of alkaline phosphatase and albumin (± SEM) in mouse liver 24 hours post oral administration of 1 mg/kg of compound 51 (n = 3) or 1 mg/kg of compound 30 (n = 3). 2 - 3 month old male C57BL/6 mice.*

The levels of alanine transaminase and glutatmate dehydrogenase in mouse livers 24 hours following administration of 1 mg/kg of compounds 30 and 51 were not statistically different from the control values, $P > 0.05$ (independent t-test). In fact the control value had a larger variance for glutamate dehydrogenase than compound 51 and compound 30.

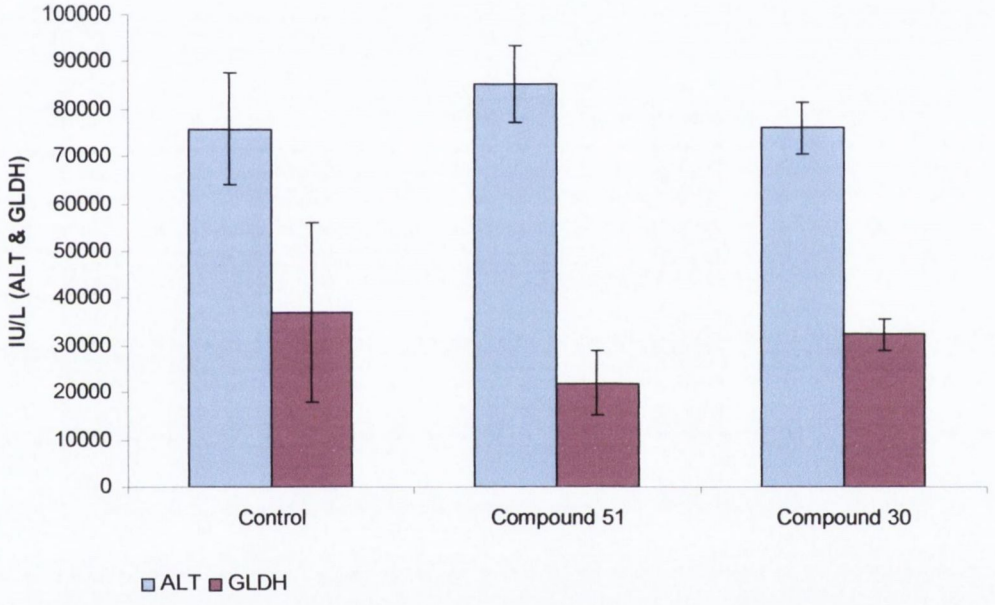

Figure 6.4 *Mean levels of alanine transferase and glutamate dehydrogenase (± SEM) in mouse liver 24 hours post oral administration of 1 mg/kg of compound 51 (n = 3) or 1 mg/kg of compound 30 (n = 3). 2 – 3 month old male C57BL/6 mice.*

6.7.2 One-year toxicology study

6.7.2.1 Plasma biomarkers

There were no apparent differences in the levels of the plasma biomarkers in the plasma of control or drug-treated mice following one year of treatment. Analysis of data using independent t-tests did not reveal any differences in the enzyme levels or albumin in the mouse plasma and livers between the groups, $P > 0.05$.

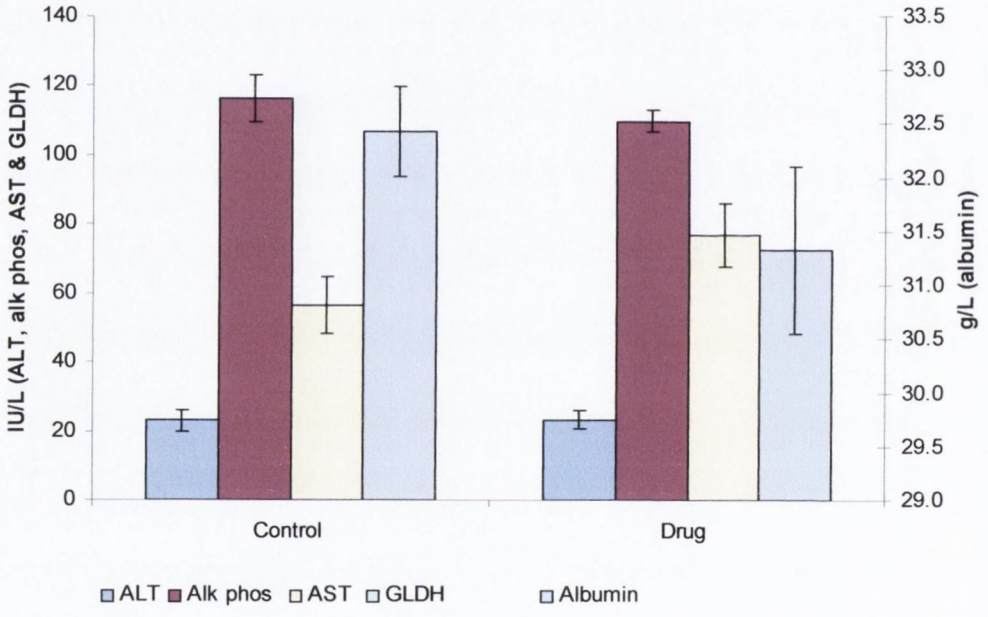

Figure 6.5 *Mean levels of alanine transferase, alkaline phosphatase, aspartate transaminase, glutamate dehydrogenase and albumin (± SEM) in mouse plasma. One year treatment with 1 mg/kg of compound 51 (n = 7) or saline 0.1 ml/10 g body weight (n = 6). 14 month old male C57BL/6 mice.*

6.7.2.2 Liver biomarkers

The biomarkers in the mouse livers of the animals treated chronically with compound 51 did not differ from those of the saline-treated controls. However, there were large variances in the values for glutamate dehydrogenase and albumin in the animals treated with compound 51. There were no statistically significant differences between the groups, $P > 0.05$ (independent t-tests).

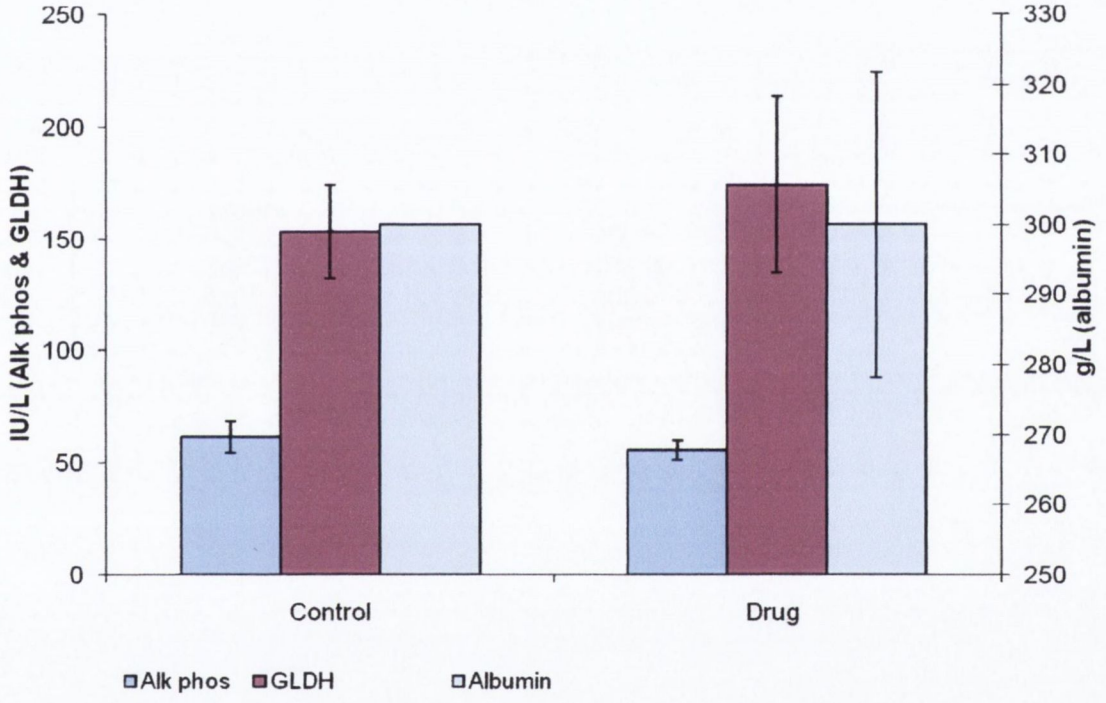

Figure 6.6 *Mean levels of alkaline phosphatase, glutamate dehydrogenase and albumin (± SEM) in mouse liver. One year treatment with 1 mg/kg of compound 51 (n = 7) or 0.1 ml/10 g body weight of saline (n = 6). 14 month old male C57BL/6 mice.*

The levels of the bilirubin and the enzymes alanine transferase, aspartate transaminase and gamma glutamyl transpeptidase did not differ among the groups, $P > 0.05$ (independent t-test). However, there was a large variation in the level of aspartate transaminase for the drug treated animals.

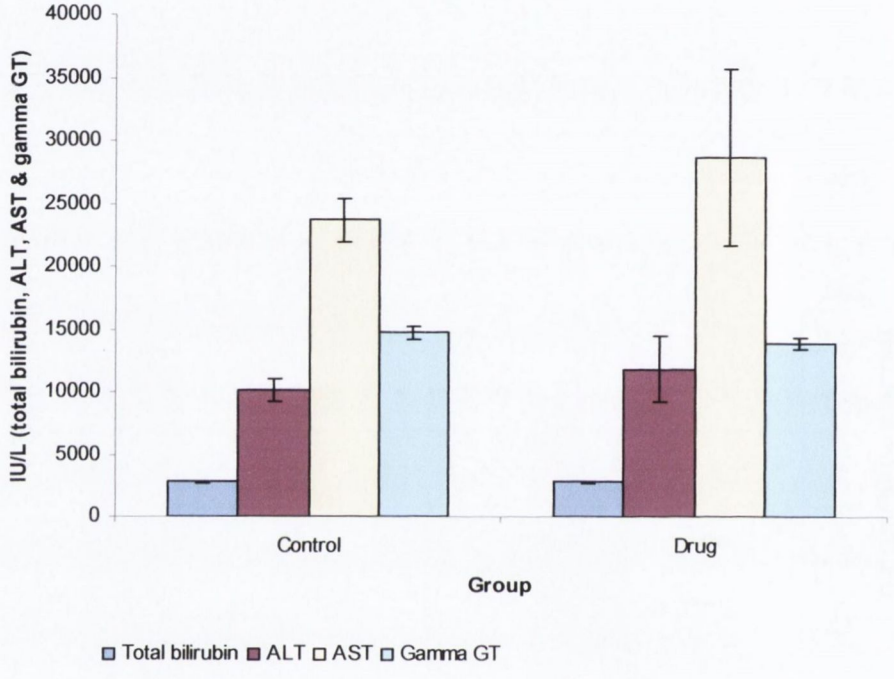

Figure 6.7 *Mean levels of total bilirubin, alanine transferase, aspartate transaminase and gamma glutamyl transpeptidase (± SEM) in mouse liver. One year treatment with 1 mg/kg of compound 51 (n = 7) or 0.1 ml/10 g body weight of saline (n = 6). 14 month old male C57BL/6 mice.*

6.7.3 Histology

The purpose of this study was to determine whether the novel compounds had any effect on mouse liver. Histological analysis of the liver following a single dose of 2 mg/kg of compound 30 and 10 mg/kg of compound 51, revealed liver necrosis. The histology report was as follows:

> Histological examination of the sections of liver showed occasional, well-defined foci of fibrosis and coagulation necrosis located in subcapsular areas and perivascular spaces. The necrotic lesions were circumscribed by low-grade pleocellular leucocytic infiltrates. Fibrin and leucocytic thrombi were present in association with the fibrotic lesions.
>
> The appearance of the lesions was of avascular necrosis and scarring secondary to thrombosis. The aetiology of the thrombotic lesions was not determined. No evidence of mycotic infection was detected.
>
> Diagnosis: Focal hepatic necrosis and scarring.

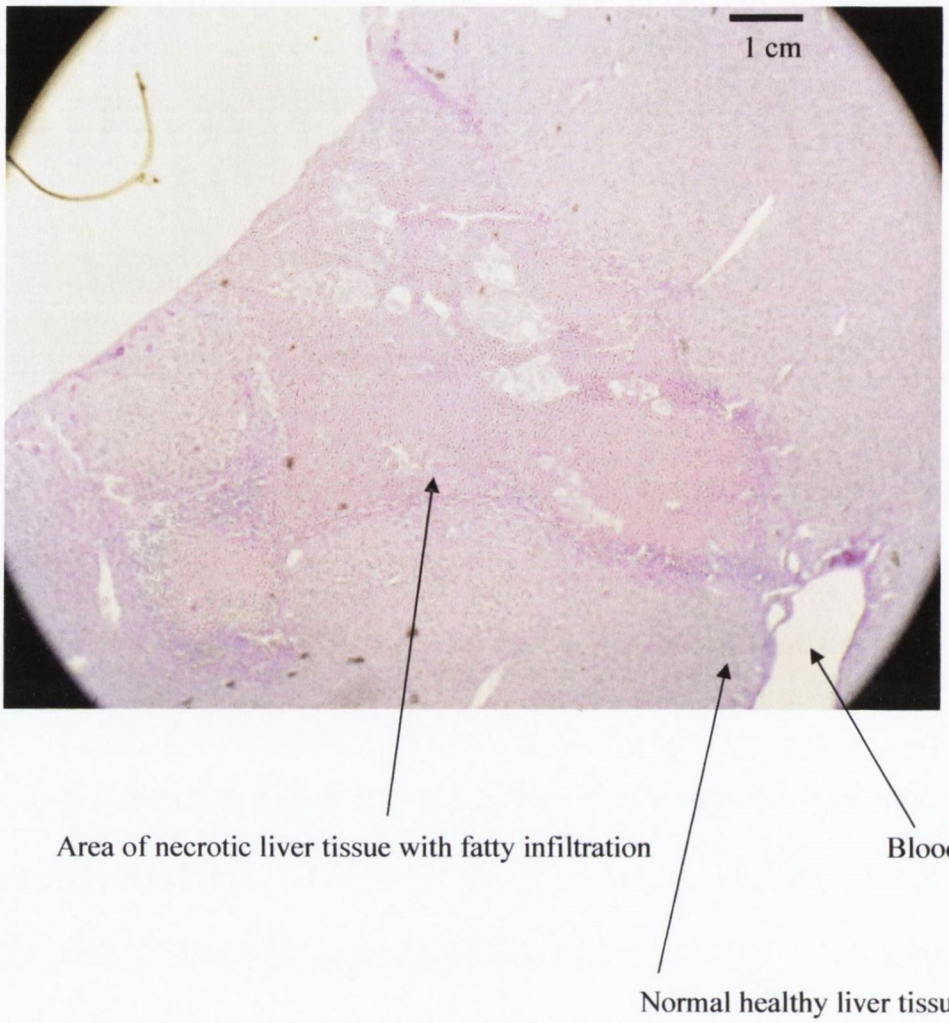

Figure 6.8 *Area of necrosis in mouse liver tissue 24 hours post administration of a single oral dose of 10 mg/kg of compound 51. Haematoxylin and eosin staining. LM x 100. Scale bar – 1 cm.*

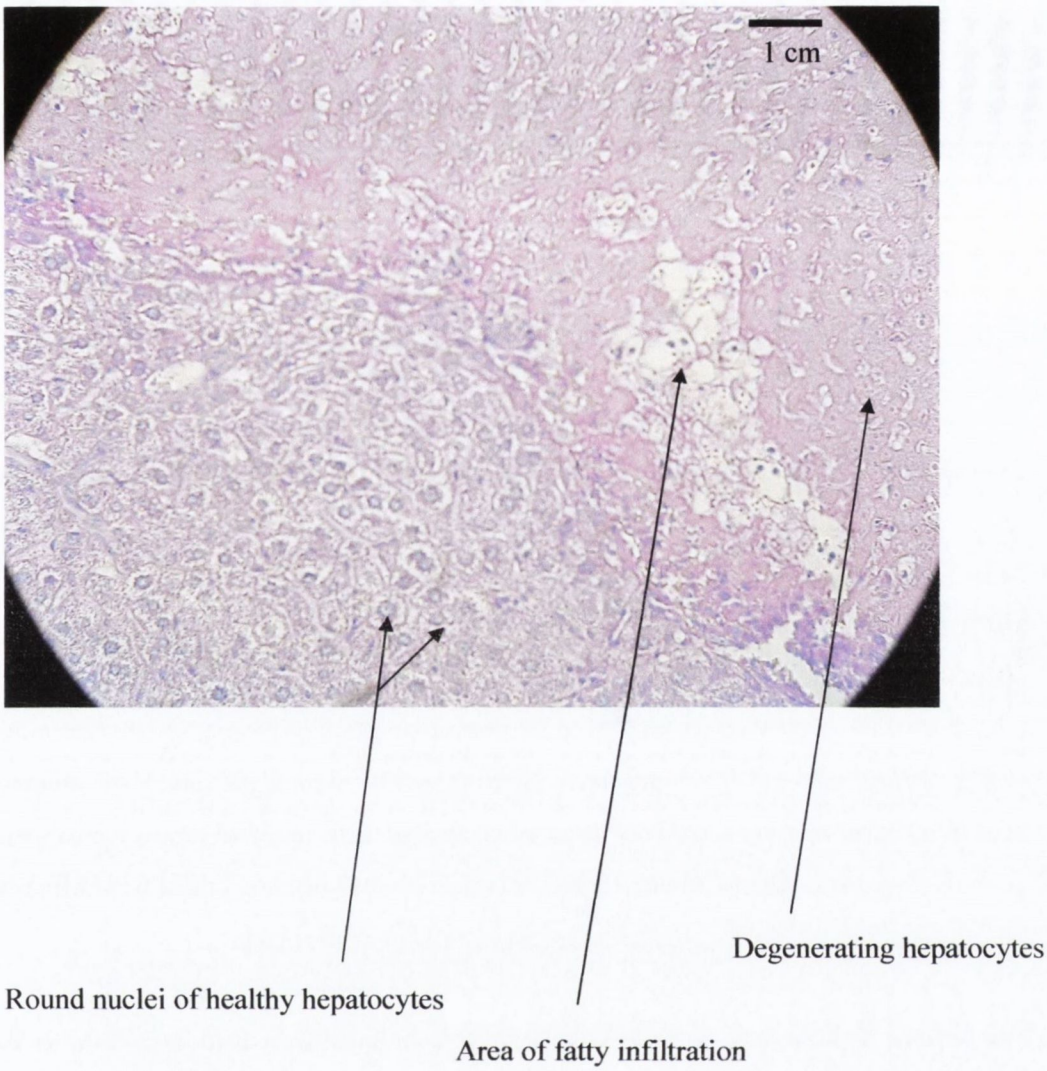

Figure 6.9 *Area of necrosis in mouse liver tissue 24 hours post administration of a single oral dose of 10 mg/kg of compound 51. Haematoxylin and eosin staining. LM x 400. Scale bar – 1 cm.*

6.8 Discussion

These studies sought to evaluate the hepatotoxicity of the novel BuChE inhibitors, compounds 30 and 51, both *in vitro* and *in vivo.* Clinical chemistry was assessed by analysis of the levels of enzymes in the plasma and liver. The aminotransferases, ALT and AST, and glutamate dehydrogenase are generally measured as markers of hepatocellular function, while hepatobiliary function is evaluated by alkaline phosphatase, GGT and total bilirubin [330].

The results indicate that neither compound 30 nor compound 51 were toxic to mouse liver 24 hours following administration of an oral dose of 1 mg/kg. Hepatocellular and hepatobiliary functions in the drug-treated groups were similar to those of the control group. However, there were large variances in the data, in particular in the levels of alkaline phosphatase and glutamate dehydrogenase in the liver samples (*Figure 6.3).* Glutamate dehydrogenase is known to be the most effective biomarker in determining hepatocelluar injury [339]. However, since the variance in the level of glutamate dehydrogenase was also large in the control group then any difference seen in those animals that received compound 30 was found to be insignificant and it was difficult to detect clinically whether any changes were as a result of the drugs.

The chronic dosing study did not show any significant differences in the plasma or liver biomarkers between the control and drug-treated animals. However, large variances in the data for the liver biomarkers GLDH, AST and albumin may suggest some slight toxicological effects produced by the novel compounds. In general, an increase in GLDH indicates hepatocellular damage and while AST is considered a less specific biomarker variation in the data for this enzyme may be a sign of necrosis. The deviation in the data albumin may be indicative of liver toxicity.

Secondly the histology study was carried out to determine any changes in the histology of the liver tissue following dosing with the novel compounds. Administration of 2 mg/kg of compound 30 and 10 mg/kg of compound 51 were found to cause hepatotoxicity in mice. Histological findings were consistent in both liver samples and a diagnosis of focal hepatic necrosis and scarring was made. This suggests that the dose of these compounds caused an inflammatory reaction in the liver tissue. It may be

possible that the carbamate moiety of the drugs caused this reaction as carbamates have been known to pose a hepatotoxic risk. A carbamate drug, N-methyldithiocarbamate, has previously been found to be hepatotoxic following oral dosing in rats [340]. On the other hand, rivastigmine also possesses a carbamate moiety and is sufficiently non-toxic to be marketable.

As the animals were dosed orally with the novel compounds in this study there is a possibility that the drugs were absorbed through the portal venous system directly into the liver to cause this reaction. Alternatively the drugs may have been absorbed into the venous system and then circulated in the systemic circulation to reach the hepatic arterial system causing an inflammatory reaction resulting in thrombosis and necrosis. The fact that the saline-control animal did not exhibit any gross changes in the liver tissue supports the contention that the drugs were responsible for the hepatic lesions seen. Another possible explanation for the hepatocellular damage is that the drugs were deposited in the microvasculature of the liver occluding the blood supply to areas of the liver tissue causing areas of focal necrosis. This may be the most likely explanation for this finding as isosorbides in general are not found to be hepatotoxic. However, carbamate derivatives are known to have the potential for hepatotoxicity as was found in a study using vinyl carbamate [341]. It is difficult to determine whether the combination of the isosorbide and the carbamate moieties actually caused the focal necrosis as such drugs have never been synthesized to date. Nevertheless, as the necrosis occured secondary to thrombosis it is most likely that particles of the drug caused occlusion of the liver microvasculature rather than the nature of the drug being culpable.

Chapter 7

Stability of novel BuChE inhibitors *in vitro*

Chapter 7 Stability of Novel Compounds *in vitro*

7.1 Aims

From the preceding animals studies it has been identified that the novel compounds were active *in vivo* and they may produce positive effects on cognition. The purpose of this study was to determine the stability of the novel compounds *in vitro.* Additionally it was necessary to reconcile the differences in the potencies of the novel compounds *in vitro* and *in vivo*. It was also interesting to determine whether any other plasma or liver esterases contribute to the hydrolysis of the novel compounds. The stability of the novel BuChE inhibitor, compound 51 (isosorbide 2-benzylcarbamate 5-benzoate) was assessed *in vitro* in mouse plasma, mouse liver, human plasma, and human liver and intestinal microsomes. The stability of compound 30 (2-benzylcarbamate 5-salicylate) was determined in mouse plasma, mouse liver and human plasma. The rate of hydrolysis of compound 21 (2-benzylcarbamate 5-nicotinate) and rivastigmine were assessed in mouse liver and human plasma. A HPLC method was employed to analyse the rates of hydrolysis of the novel inhibitors *in vitro*.

7.2 Procurement of blood

7.2.1 Mouse blood

Mouse blood was procured from healthy experimentally naïve male CD-1 mice (n = 3) via cardiac puncture. The animals were anaesthetized using halothane gas. Once there was no response to toe pinch blood was procured. A sterile 25 gauge needle (25G x 1½") containing a small amount of lithium heparin (25,000 Units/ml) (Leo Laboratories, Dublin) in its base was attached to a 1 ml syringe (Brand, UK). The needle was inserted beneath the xiphisternum and passed superolaterally to the pericardium into the ventricles of the heart. The cardiac blood was slowly procured and transferred into a 10 ml clean glass vial

7.2.2 Human blood

Healthy human male volunteers (n = 3) were chosen, given a volunteer information leaflet (Appendix I) and signed a consent form (Appendix I). Human venous blood was procured from the cubital vein in the cubital fossa of the forearm using a sterile 21 gauge needle (21G x 1½") (Greiner Bio-one, UK) and collected into 4 ml lithium heparinized vacutte vials (Greiner Bio-one, UK).

7.3 Sample preparation

7.3.1 Phosphate buffered saline

0.1 M phosphate buffered saline (PBS) was prepared from disodium hydrogen phosphate (Fluka Biochemika, Germany) and sodium dihydrogen phosphate (Fluka Biochemika, Germany) in distilled water. The buffer was brought to pH 7.4 using ortho-phosphoric acid (Riedel-de-Haen, Germany).

7.3.2 Zinc sulphate

A 2% zinc sulphate solution was prepared by weighing 2 g of zinc sulphate (heptahydrate) (Sigma-Aldrich, Dublin). 50 ml of distilled water and 50 ml of CH_3CN (acetonitrile) (Sigma-Aldrich, Dublin) were added.

7.3.3 Drug standards

3 mg of compounds 21, 30, 51 and rivastigmine were dissolved in 1 ml of CH_3CN in a 1 ml volumetric flask producing stock solutions of approximately 7mM.

3 mg of benzoic acid and benzyl carbamate were each dissolved in 5 ml of CH_3CN producing 5 mM and 4 mM stock solutions respectively.

3.6 mg of bis(p-nitrophenyl) phosphate (BNPP) (Sigma-Aldrich, Dublin) was dissolved in 5 ml CH_3CN producing a 2 mM stock solution.

7.3.4 Plasma samples

Plasma samples were prepared by centrifugation (Sorvall RT6000B, GMI, USA) of lithium heparinized mouse cardiac blood or human venous blood at 3,000 rpm for 10 minutes at 4°C. 2 ml of the plasma were added to 4 ml of 0.1 M phosphate buffered saline (PBS) pH 7.4 (33% solution) incubated at 37°C for 5 minutes. For the 50% human plasma solution 2 ml of plasma was added to 2 ml of 0.1 M PBS pH 7.4. 250 µl of the plasma/PBS solution was transferred to an Eppendorf (Brand, Germany) containing 250 µl CH_3CN and 250 µl of 2% zinc sulphate solution (Sigma-Aldrich, Dublin) solution (1:1 solution).

7.3.5 Mouse liver samples

Mouse livers were separately homogenised on ice in 10 volumes of 0.1 M PBS pH 7.4 (100 µg/ml) in three 5 second bursts using an Ultra-turrax (T-10 model, IKA-Werke, Germany) at 10,000 rpm. The homogenates were then centrifuged for 10 minutes at 10,000 rpm at 4°C. 20 µl of the supernatants were removed and added to 4 mls of PBS pH 7.4 (0.5% solution). 250 µl of the liver/PBS solution was removed and added to an Eppendorf containing 1:1 solution of CH_3CN (250 µl) and 2% zinc sulphate solution (250 µl).

7.3.6 Human liver microsomes

5 ml of 0.1 M PBS pH 7.4 was added to a 10 mg of pooled human liver microsomes (BD Biosciences, UK) producing a stock solution of 2 mg/ml. 1 ml aliquots of the microsomes were stored -80°C. The pooled human liver microsomes contained the following cytochrome P450 enzymes: CYP1A2, CYP2D6, CYP2E1, CYP2A6, CYP2B6, CYP2C19, CYP3A4, CYP2C8 and CYP4A.

7.3.7 Human intestinal microsomes

5 ml of 0.1 M PBS pH 7.4 were added to pooled human intestinal microsomes (BD Biosciences, UK), containing 2 mg/ml of protein, producing a stock solution of 80

µg/ml protein. 1 ml aliquots of the microsomes were stored at -80°C. The pooled human intestinal microsomes contained the following enzymes: cytochrome C reductase, CYP2D6, CYP3A4, CYP2J2/4F12, UGT1A1 (oestradiol 3-glucoronidation) and CE1/2.

7.3.8 BuChE activity

The activity of the enzyme BuChE in human plasma, mouse plasma and mouse liver was calculated.

Human plasma contains approximately 5mg of BuChE per litre of plasma [225]. Using the specific activity of 720 units/mg for butyrylthiocholine. There are 3600 units/L plasma or 3.6 µmol/min/ml plasma. In a 33% and 50% human plasma solution the activity of BuChE is approximately 1.2 µmol/min/ml and 1.8 µmol/min/ml respectively.

Mouse plasma contains 2.6 mg of BuChE per litre of plasma [225]. The activity of BuChE in mouse plasma is therefore 1.872 µmol/min/ml. A 33% plasma solution of mouse plasma contains approximately 0.624 µmol/ml/min.

Mouse liver contains 67 units of BuChE activity per ml of tissue [342]. A 20 µl sample therefore contains an estimated activity of 1.34 µmol/min/ml.

7.4 Hydrolysis of compounds

7.4.1 Plasma/liver and novel compound

80 µl of 7 mM of the novel compound was added to the plasma/PBS solution for the 33% solution (60 µl of 7 mM novel compound was used for the 50% human plasma solution). 55 µl of 7 mM of the novel compound was added to the liver/PBS solution and the stopwatch was then started. 250 µl aliquots of the plasma/PBS/drug or liver/PBS/drug solutions were removed and added to labelled Eppendorfs containing a

1:1 solution of CH_3CN and 2% zinc sulphate (to quench the reaction). The time points used were: 5, 10, 15, 20, 30, 40, 50 and 60 minutes. The Eppendorfs containing the solutions were then centrifuged at 10,000 rpm for 7 minutes (Micromax centrifuge, IEC, USA). The supernatant was removed and pipetted into 1 ml HPLC vials (ABG Scientific Ltd, Dublin). 20 µl aliquots of the supernatant were analysed by high-performance liquid chromatography (HPLC) (Waters, Dublin).

7.4.2 Plasma/ liver /BNPP & novel compound

100 µl of 2 mM BNPP (carboxylesterase inhibitor) was incubated with 2 ml of mouse or human plasma for 10 minutes at 37°C in an incubator (Memmert Model 400, Schwabach, Germany). The plasma/BNPP solution was added to 4 ml of 0.1 M PBS pH 7.4 and a 250 µl sample was taken as t = 0 and transferred to an Eppendorf containing 1:1 acetonitrile and 2% zinc sulphate. 100 µl of 7 mM drug (100 µM) was added to the plasma/BNPP/PBS solution and the stopwatch was started. 250 µl samples were removed at appointed time intervals 5, 10, 15, 20, 30, 40, 50 and 60 minutes. The samples were centrifuged for 7 minutes at 10,000 rpm (Micromax centrifuge, IEC, USA).

1 µl of 2 mM BNPP was incubated with 20 µl of a mouse liver homogenate for 10 minutes at 37°C. The liver/BNPP solution was added to 4 mls of 0.1 M PBS pH 7.4 and a 100 µl sample was taken and transferred to an Eppendorf containing 1:1 acetonitrile and 2% zinc sulphate. 55 µl of 7 mM drug (100 µM) was added to the liver/BNPP/PBS solution and the stopwatch was started. 100 µl samples were removed at appointed time intervals 5, 10, 15, 20, 30, 40, 50 and 60 minutes. The samples were centrifuged for 7 minutes at 10,000 rpm (Micromax centrifuge, IEC, USA).

7.4.3 Human liver microsomes

100 µl of the microsome/buffer solution was transferred to an Eppendorf containing a 1:1 solution of CH_3CN (100 µl) and 2% zinc sulphate (100 µl). 14 µl of a 7 mM stock of compound 51 (100 µM) was then added to the microsome/buffer solution and the stop watch was started. 100 µl of the microsome/buffer/drug solution were removed

and transferred to a labelled Eppendorf containing a 1:1 solution of CH_3CN (100 µl) and 2% zinc sulphate (100 µl) at the following time points: 1, 5, 10, 15, 20, 30, 40, 50, 60 minutes. The samples were centrifuged for 7 minutes at 10,000 rpm (Micromax centrifuge, IEC, USA).

7.4.4 Human intestinal microsomes

100 µl were removed from 1000 µl of an 80 µg/ml stock of human intestinal microsomes and transferred to 1:1 solution of CH_3CN (100 µl) and 2% zinc sulphate (100 µl). 14 µl of a 7 mM stock solution of compound 51 (100 µM) was added to the remaining 900 µl of human intestinal microsomes and the stop watch was started. 100 µl samples were removed at appropriate time intervals to determine the rate of hydrolysis of compound 51 by the microsomes. Samples were taken at 1, 5, 10, 15, 20, 30, 40, 50 and 60 minutes. Each sample was transferred to a labelled Eppendorf containing a 1:1 solution of acetonitrile (100 µl) and 2% zinc sulphate (100 µl). The samples were centrifuged for 7 minutes at 10,000 rpm (Micromax centrifuge, IEC, USA).

7.5 High-Performance Liquid Chromatography

7.5.1 Mobile phase

7.5.1.1 Sodium phosphate buffer

A 16 mM sodium phosphate buffer was prepared from disodium hydrogen phosphate salts (Fluka Biochemika, Germany). The salt was dissolved in 1 L of Millipore water and the pH was determined using a pH meter (IKA, Labortechnik, Germany). The phosphate buffer was brought to pH 2.5 using ortho-phosphoric acid (Riedal-de-Haen, Germany). The sodium phosphate buffer was filtered using a 0.22 µm Steritop vacuum driven disposable filter (Millipore, Ireland). The buffer was passed through line B; separate from the acetonitrile.

7.5.1.2 Acetonitrile

1 L of gradient grade acetonitrile (Sigma-Aldrich, Dublin) was used and passed through line A; separate from the phosphate buffer

7.5.2 HPLC Method

HPLC was performed using a system consisting of a Waters 600 pump and controller, Waters autosampler 717 plus, and a Waters 2996 photodiode-array (PDA) detector controlled by Empower software (Waters, Dublin). A Hichrom Nucleosil C18 column 4.0 x 250 mm was used for both the plasma and liver samples. A gradient method was employed using a mobile phase of 16 mM phosphate buffer (pH 2.5) – acetonitrile 80:20 for the first 10 minutes grading to 20:80 to 15 minutes, grading to 60:40 to 17 minutes and finally returning to 80:20 until the end of the 20 minute run (*Table 7.1*). The flow rate was 1 ml per minute. The mobile phase was sparged with Helium gas at a rate of 20 ml per minute. The eluent was monitored at 210.5 nm and 230 nm. Quantitation was measured by comparison of the drug peaks to external standards run under the same conditions. The R.S.D. (relative standard deviation) on six injections was < 1%. The method was validated for precision, linearity, sensitivity and specificity.

Table 7.1 *Gradient HPLC method for hydrolysis studies on novel BuChE compounds.*

Time (mins)	**% Phosphate buffer (16mM pH 2.5)**	**% Acetonitrile**
0	80	20
10	20	80
15	60	40
17	80	20
20	80	20

7.6 Data analysis

The chromatograms were read at 210.5nm and 230 nm using Empower software (Waters). The PDA was used to confirm the wavelengths of the compounds and metabolites in the samples tested with the external standards. Known concentrations of the external standards were run and these were used to calculate the concentrations of the compounds and metabolites in the samples. The data was processed using peak summary to calculate the area under the curve for the standards and the samples.

7.7 Hydrolysis pathway for compound 51

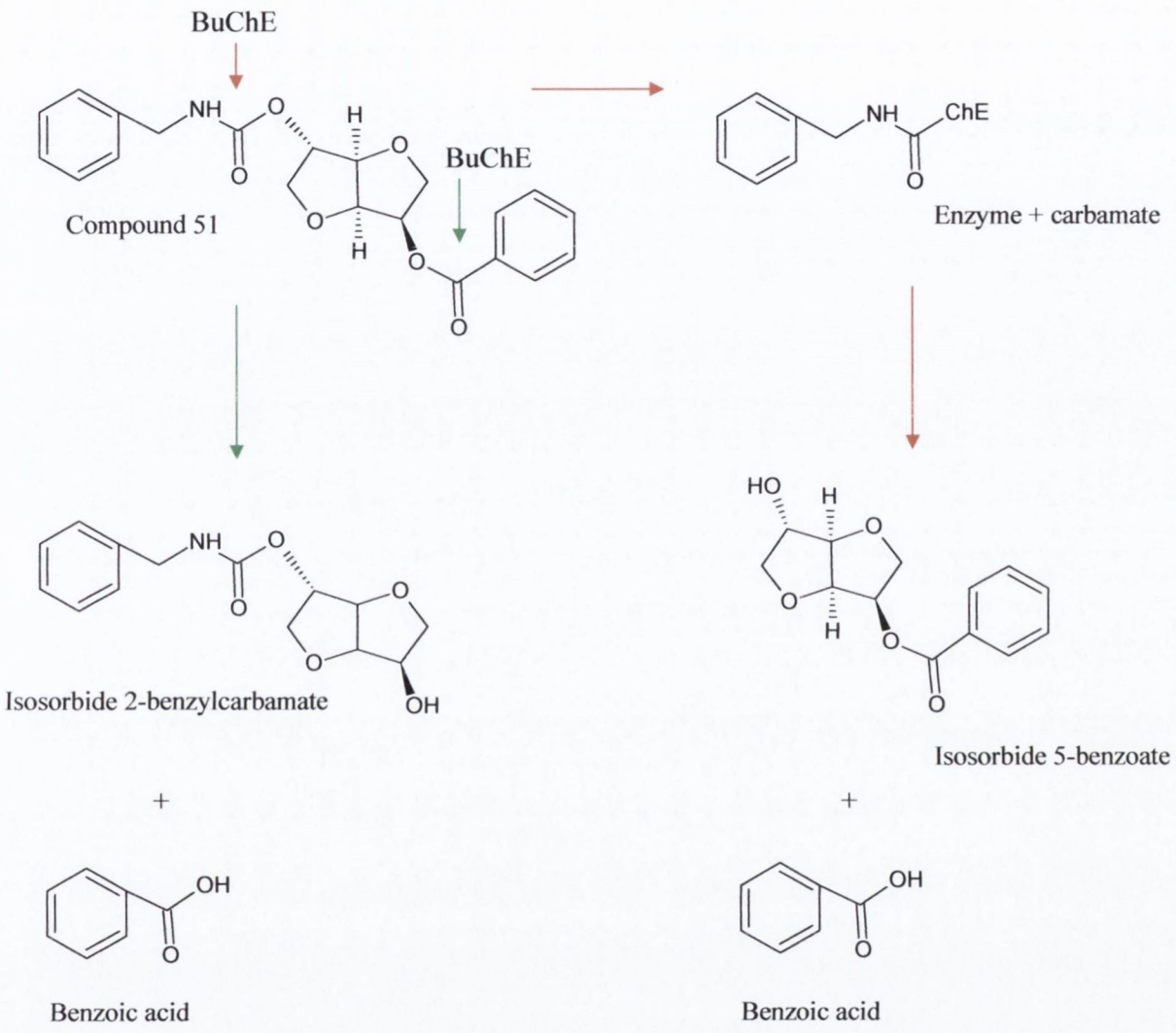

Figure 7.1 *Pathway of hydrolysis for compound 51 (isosorbide 2-benzylcarbamate 5-benzoate) by butyrylcholinesterase. Normal ester hydrolysis at the 2' position producing metabolites isosorbide 5-benzoate and benzoic acid (red arrow). Rapid ester hydrolysis at 5' position producing metabolites isosorbide 2-benzylcarbamate and benzoic acid (green arrow).*

7.7 Results

7.7.1 Compound 51

7.7.1.1 Compound 51 in mouse plasma

Compound 51 appears to be completely hydrolyzed in a 33% mouse plasma solution within 20 minutes. The disappearance of the compound correlates with the appearance of the metabolites benzoic acid and benzyl carbamate.

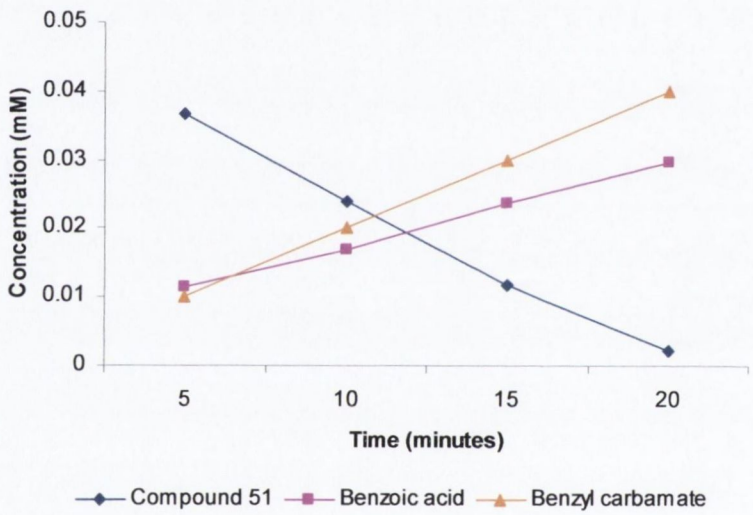

Figure 7.2 Hydrolysis of compound 51 in a 33% mouse plasma solution. Metabolites benzyl carbamate and benzoic acid. n = 3.

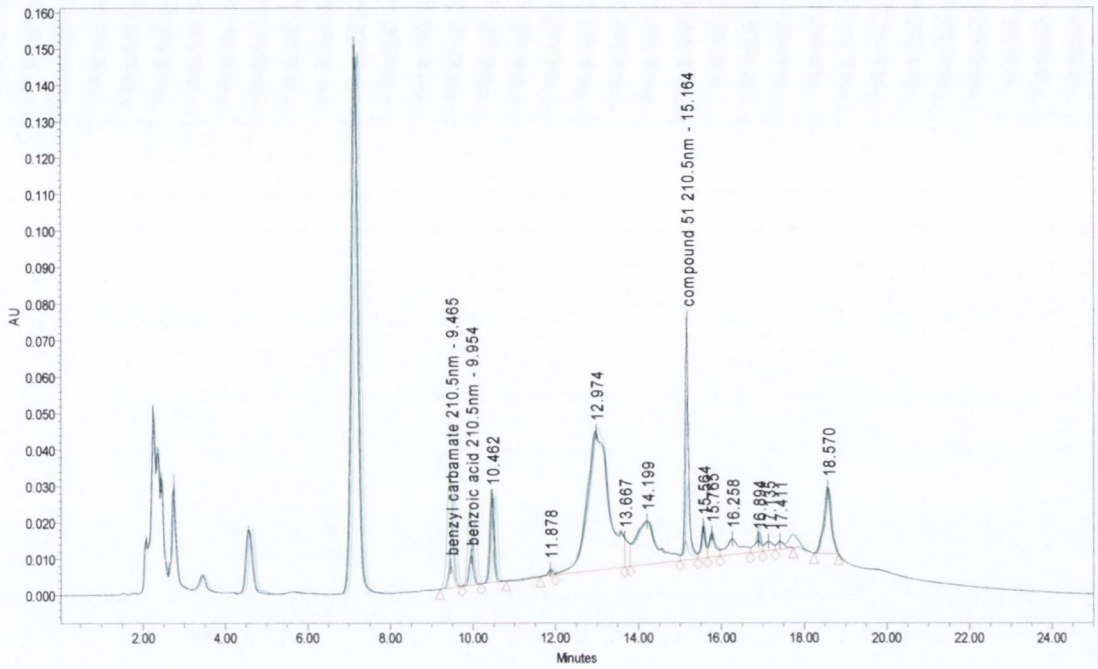

Figure 7.3 *Overlay of chromatograms from hydrolysis of compound 51 in mouse plasma. Retention times: benzyl carbamate 9.465 minutes; benzoic acid 9.954 minutes and compound 51 15.164 minutes. (Colours represent sample times).*

7.7.1.2 Compound 51 in mouse plasma with BNPP

Inhibition of mouse plasma carboxylesterase by BNPP resulted in a decrease in the rate of hydrolysis of compound 51. The metabolite benzoic acid was only formed. After 20 minutes 60% of the compound remained (*Figure 7.4*) whereas in mouse plasma in the absence of BNPP only 6% of the compound remains (*Figure 7.2*).

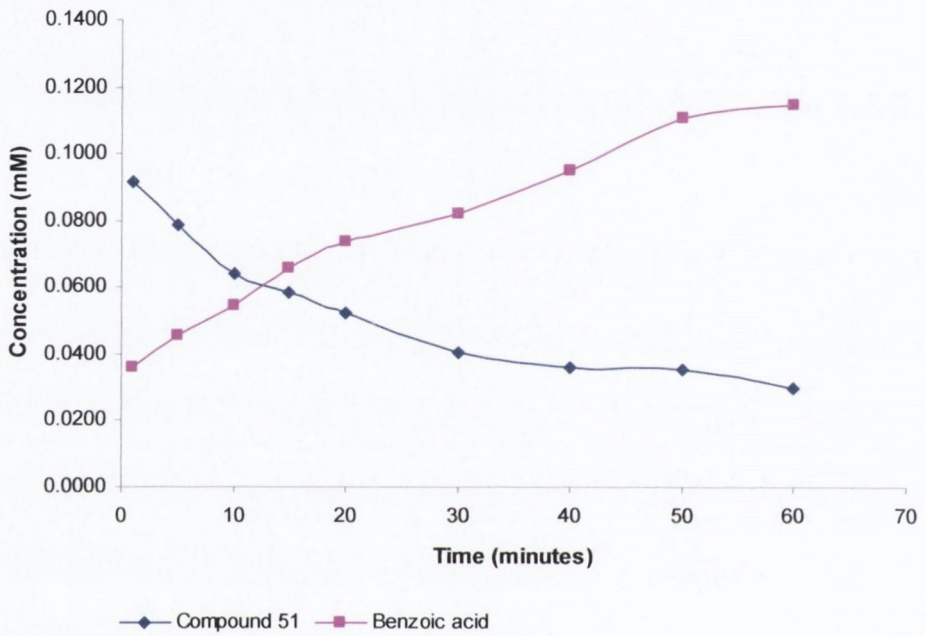

Figure 7.4 *Hydrolysis of compound 51 in a 33% mouse plasma solution in the presence of 100 μM BNPP. Metabolite benzoic acid. n = 3.*

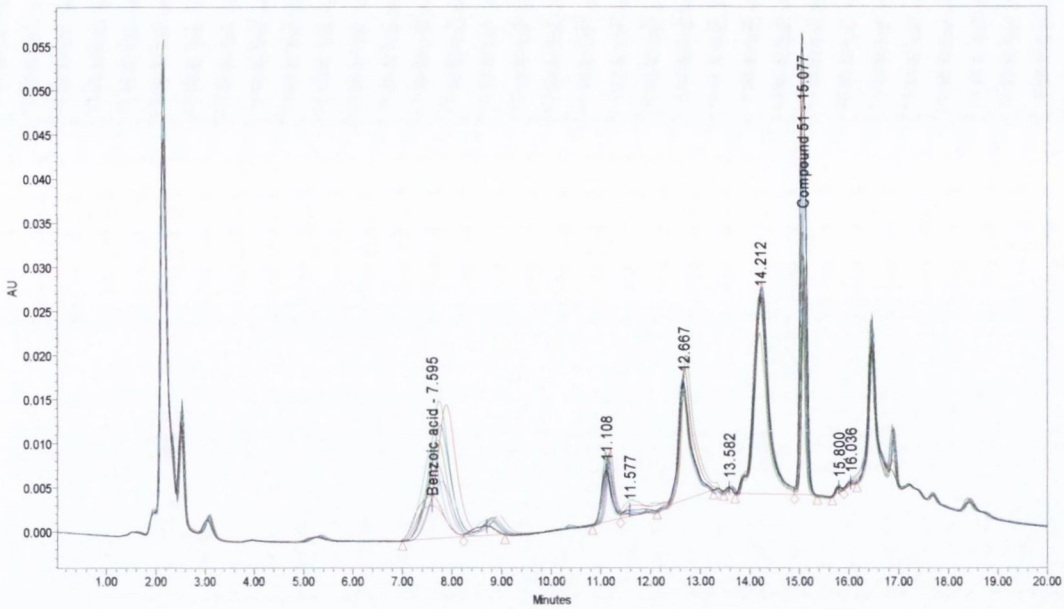

Figure 7.5 *Overlay of chromatograms for compound 51 in a 33% mouse plasma solution with BNPP. Retention times: benzoic acid 7.595 minutes and compound 51 15.077 minutes. (Colours represent sample times).*

7.7.1.3 Compound 51 in mouse liver

Compound 51 was hydrolyzed in mouse liver homogenate. The metabolites benzoic acid and benzyl carbamate were formed as the drug was hydrolyzed. However, the rate of hydrolysis of compound 51 in mouse liver was at a slower rate than the rate of hydrolysis seen in mouse plasma (*Figure 7.2)*.

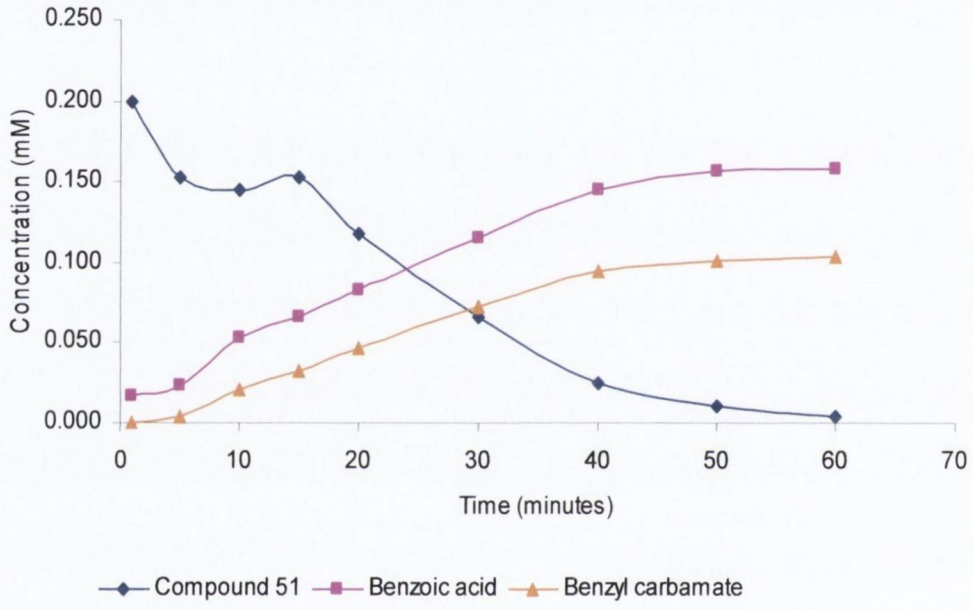

Figure 7.6 *Hydrolysis of compound 51 in a 0.5% mouse liver solution. Metabolites benzoic acid and benzyl carbamate. n = 3.*

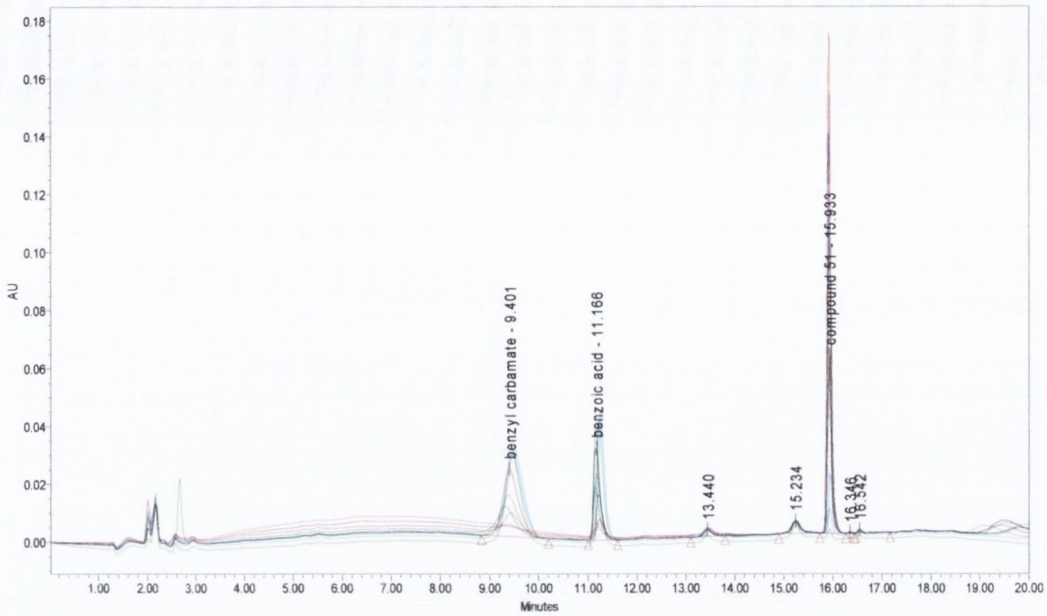

Figure 7.7 *Overlay of chromatograms of hydrolysis of compound 51 in mouse liver. Retention times: benzyl carbamate 9.401 minutes; benzoic acid 11.166 minutes and compound 51 15.933 minutes. (Colours represent sample times).*

7.7.1.4 Compound 51 in mouse liver with BNPP

In the presence of the carboxylesterase inhibitor, BNPP, the rate of hydrolysis of compound 51 was decreased. After 20 minutes 70% of the drug remained however in the absence of BNPP 60% of the compound remains at 20 minutes (*Figure 7.6*).

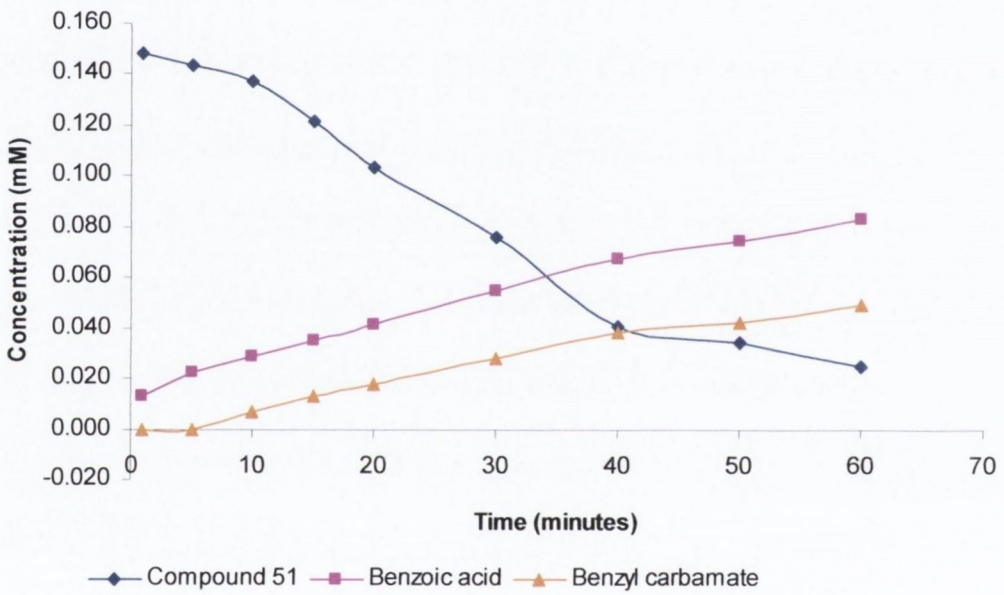

Figure 7.8 *Hydrolysis of compound 51 in a 0.5% mouse liver solution in the presence of 100 μM BNPP. Metabolites benzyl carbamate and benzoic acid. n = 3.*

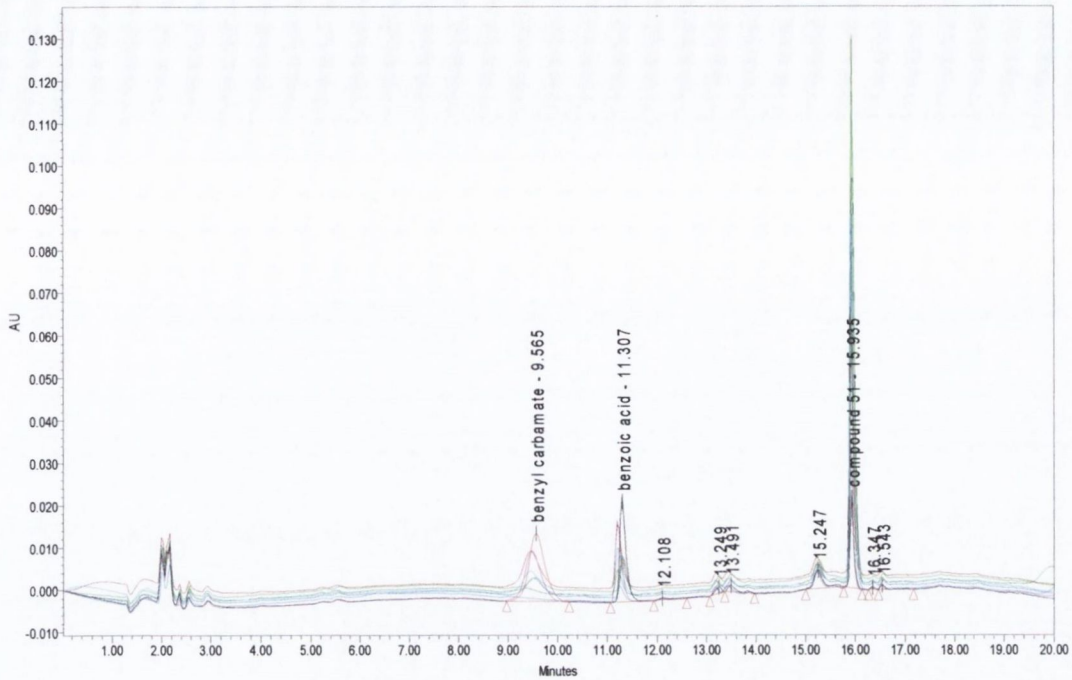

Figure 7.9 *Overlay of chromatograms from hydrolysis of compound 51 in mouse liver in the presence of BNPP. Retention times: benzyl carbamate 9.565 minutes; benzoic acid 11.307 minutes and compound 51 15.935 minutes. (Colours represent sample times).*

7.7.1.5 Compound 51 in mouse liver with BNPP and rivastigmine

The concentration of compound 51 in the mouse liver solution is not hugely decreased in the presence of both BNPP and rivastigmine. After 60 minutes 75% of the drug remains. Only the metabolite benzoic acid was found.

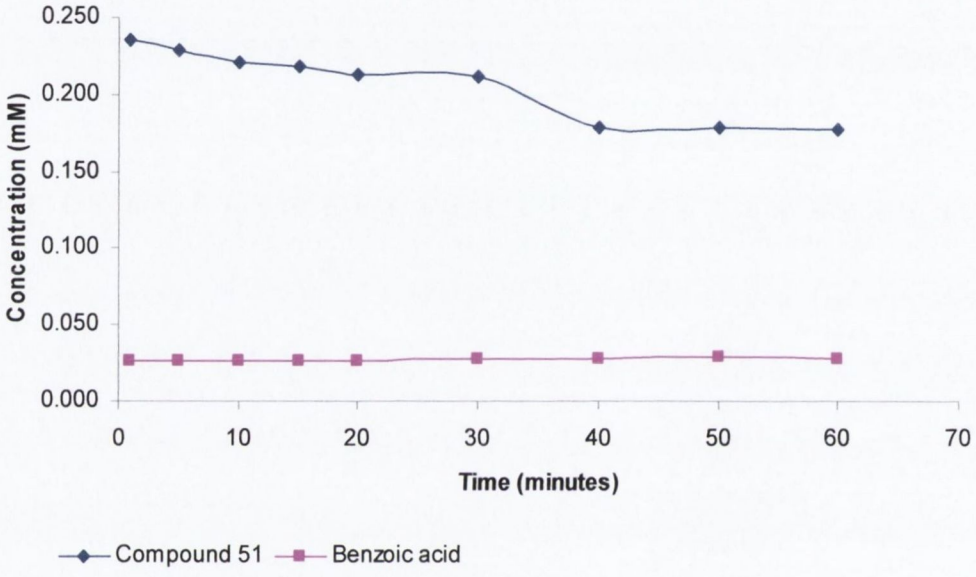

Figure 7.10 Hydrolysis of compound 51 in a 0.5% mouse liver solution in the presence of 100 μM BNPP and 100 μM rivastigmine. Metabolite benzoic acid. n = 3.

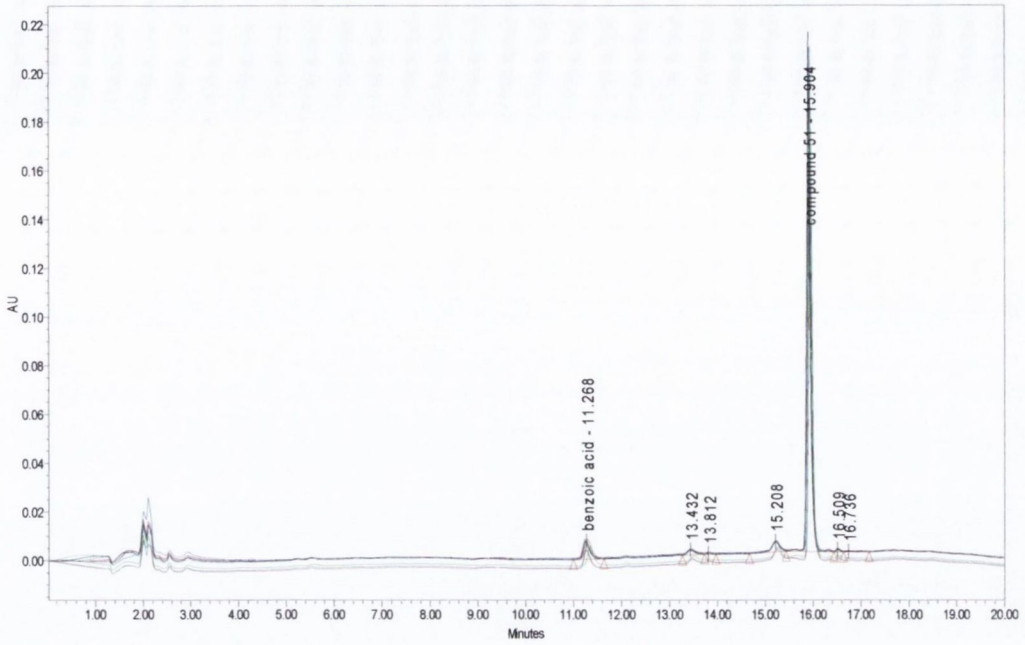

Figure 7.11 *Overlay of chromatograms from hydrolysis study of compound 51 in the presence of BNPP and rivastigmine. Retention times: benzoic acid 11.268 minutes and compound 51 15.904 minutes. (Colours represent sample times).*

7.7.1.6 Compound 51 in human plasma

Compound 51 appears to remain stable in human plasma with no hydrolysis occurring after 60 minutes.

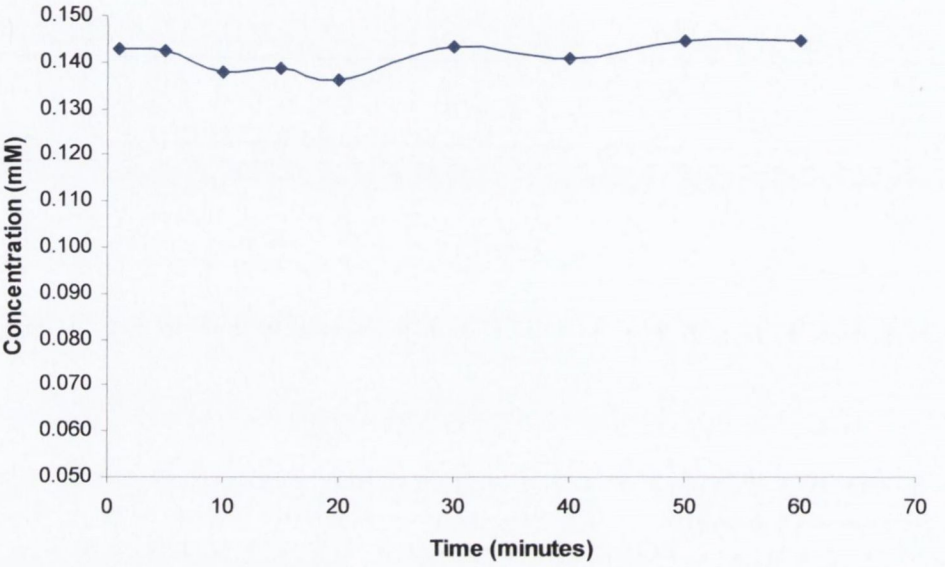

Figure 7.12 Stability of compound 51 in a 33% human plasma solution.

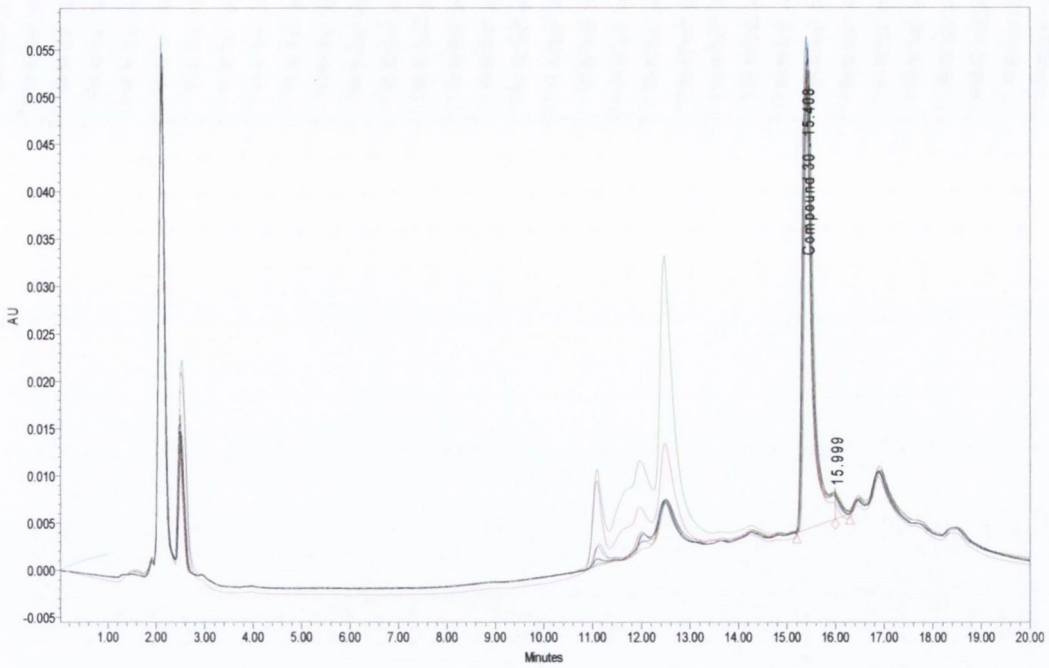

Figure 7.13 Overlay of chromatograms from stability of compound 51 in human plasma. Retention time: compound 51

7.7.1.7 Compound 51 in human intestinal microsomes

Compound 51 is readily hydrolyzed by human intestinal microsomes. 40% of the compound remains after 60 minutes. This suggests that the cytochrome enzymes and carboxylesterases 1 & 2 are capable of hydrolyzing compound 51.

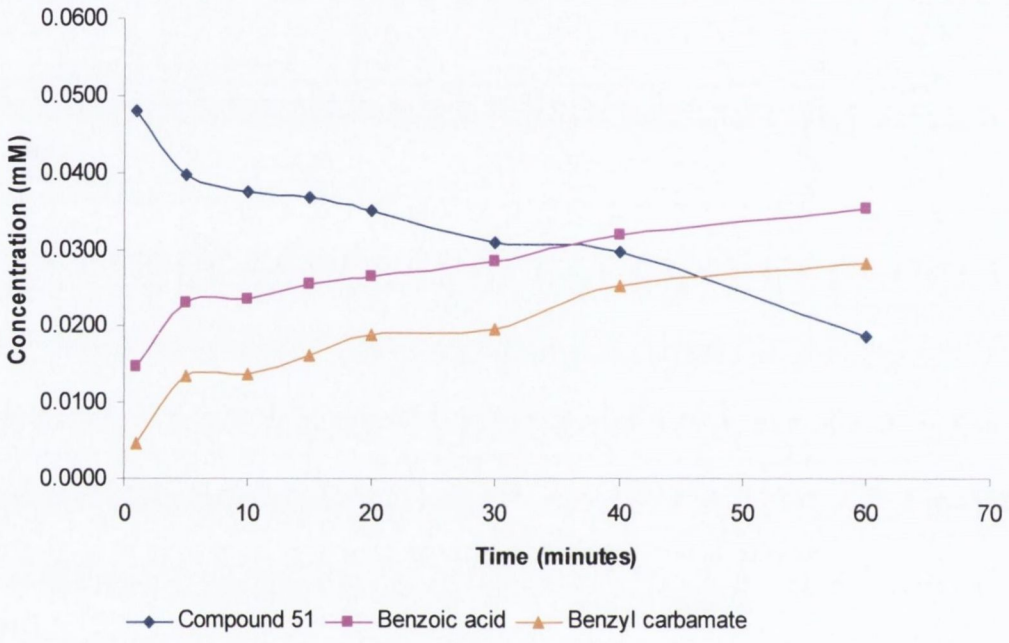

Figure 7.14 Hydrolysis of compound 51 in human intestinal microsomes.

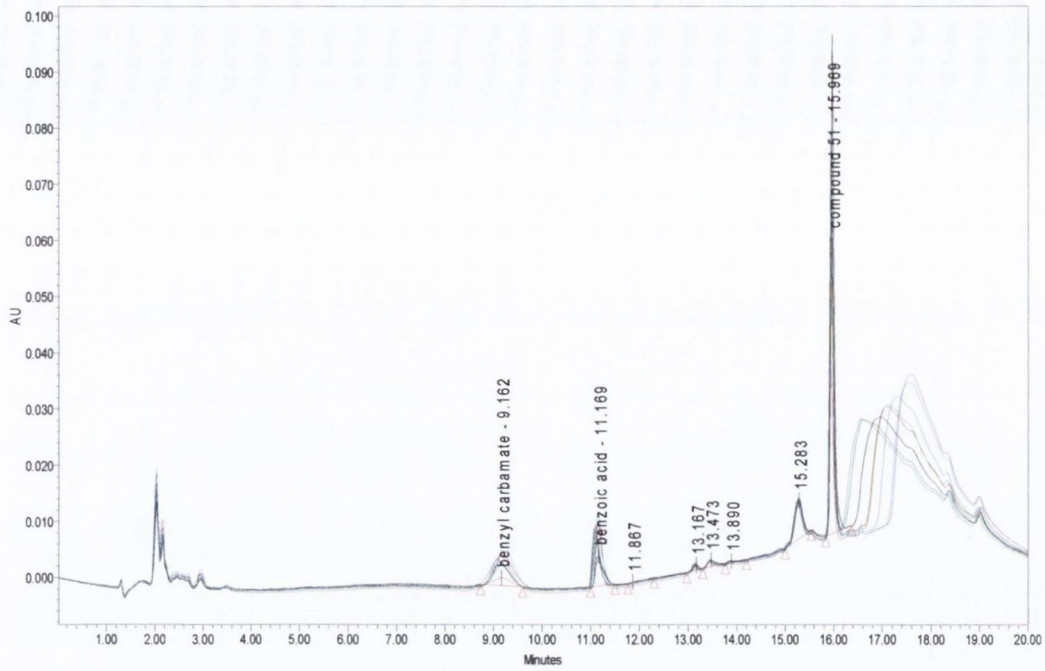

Figure 7.15 *Overlay of chromatograms for the hydrolysis of compound 51 in human intestinal microsomes. Retention times: benzyl carbamate 9.162 minutes; benzoic acid 11.159 minutes and compound 51 15.959 minutes. (Colours represent sample times).*

7.7.1.8 Compound 51 in human liver microsomes

In human liver microsomes compound 51 is readily hydrolyzed. 27% of the compound remains after 60 minutes. As only cytochrome enzymes are present in this liver microsomal preparation it is apparent that compound 51 is exclusively hydrolysed by them.

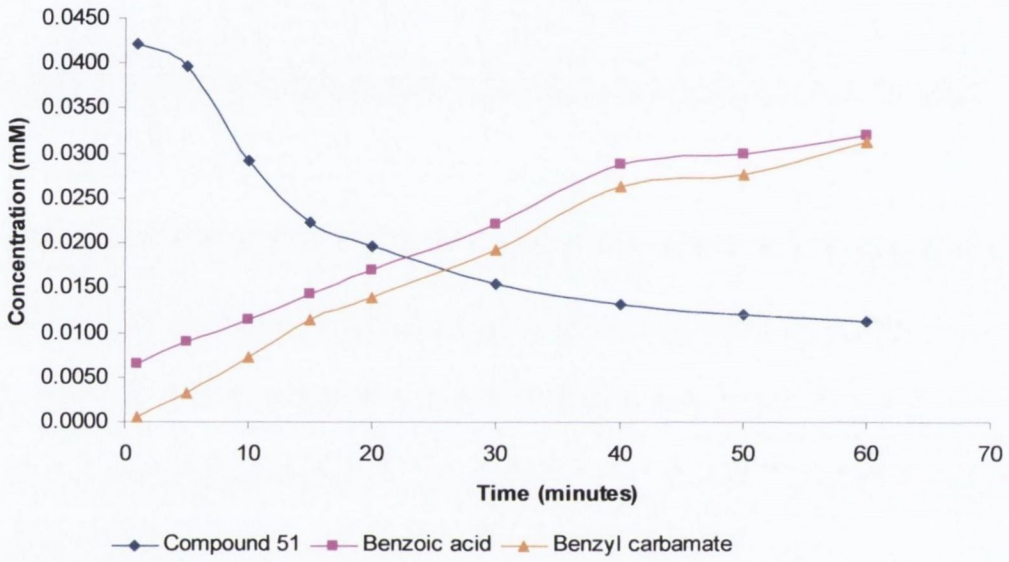

Figure 7.16 Hydrolysis of compound 51 in human liver microsomes. Metabolites benzyl carbamate and benzoic acid.

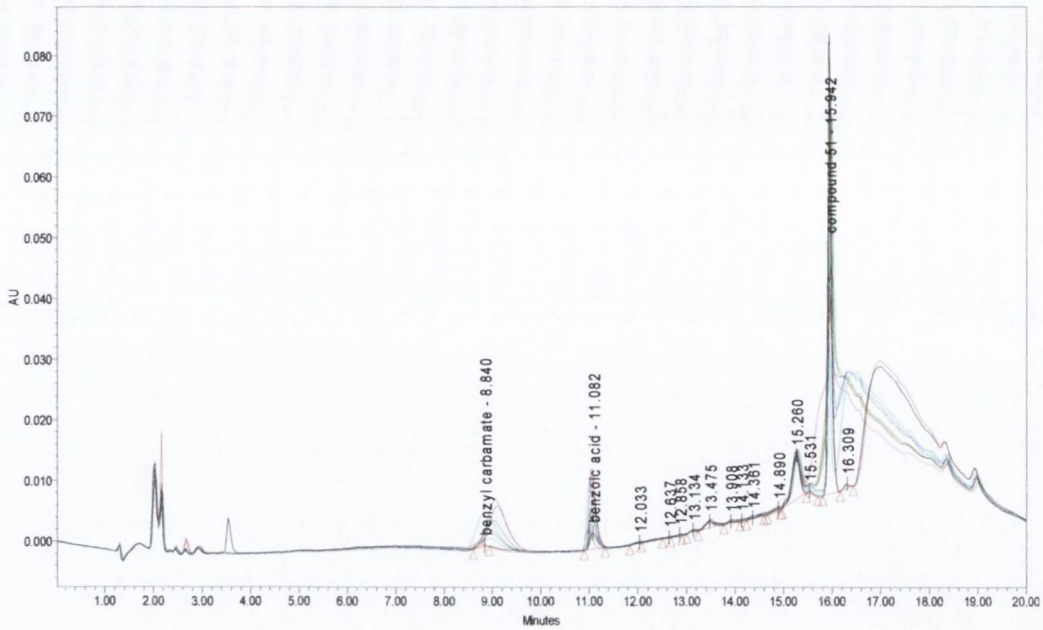

1 minute
5 minutes
10 minutes
15 minutes
20 minutes
30 minutes
40 minutes
50 minutes
60 minutes

Figure 7.17 *Overlay of chromatograms from hydrolysis of compound 51 in human liver microsomes. Retention times: benzyl carbamate 8.840 minutes; benzoic acid 11.082 minutes and compound 51 15.942 minutes. (Colours represent sample times).*

7.7.2 Compound 30

7.7.2.1 Compound 30 in mouse plasma

Compound 30 is completely stable in mouse plasma even after 60 minutes. This suggests that it is not hydrolyzed rapidly by BuChE or CE in mouse plasma.

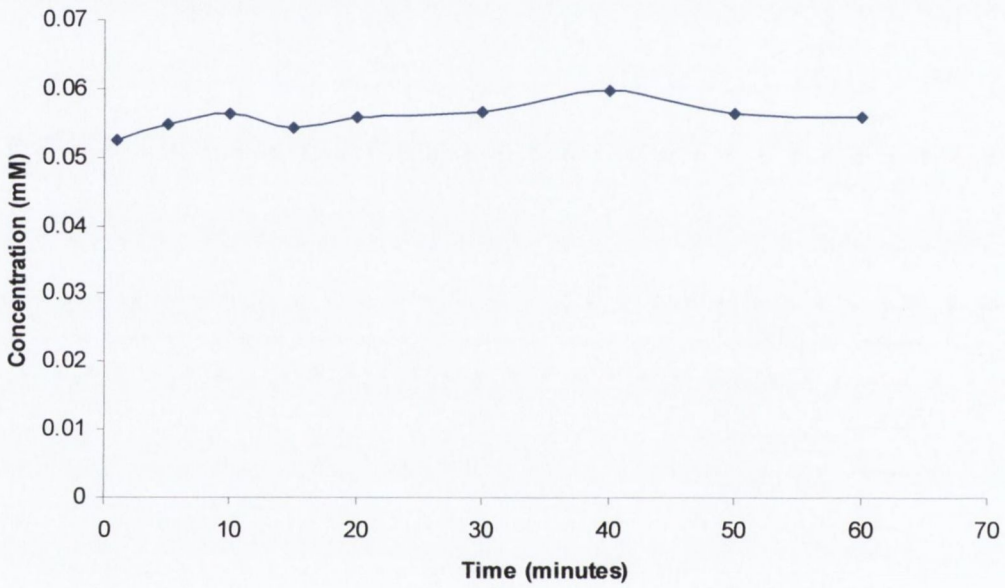

Figure 7.18 Stability of compound 30 in a 33% mouse plasma solution. n = 3.

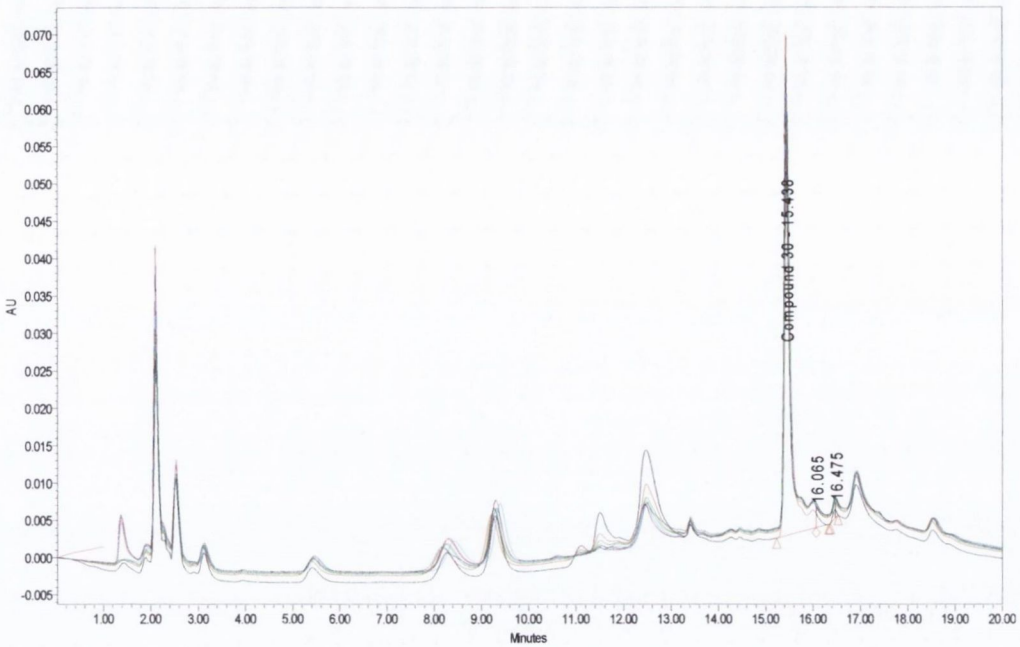

Figure 7.19 Overlay of chromatograms for compound 30 in mouse plasma. Retention time: compound 30 15.498 minutes.

7.7.2.2 Compound 30 in mouse liver

Compound 30 is stable in a solution of mouse liver and shows no sign of hydrolysis after 60 minutes.

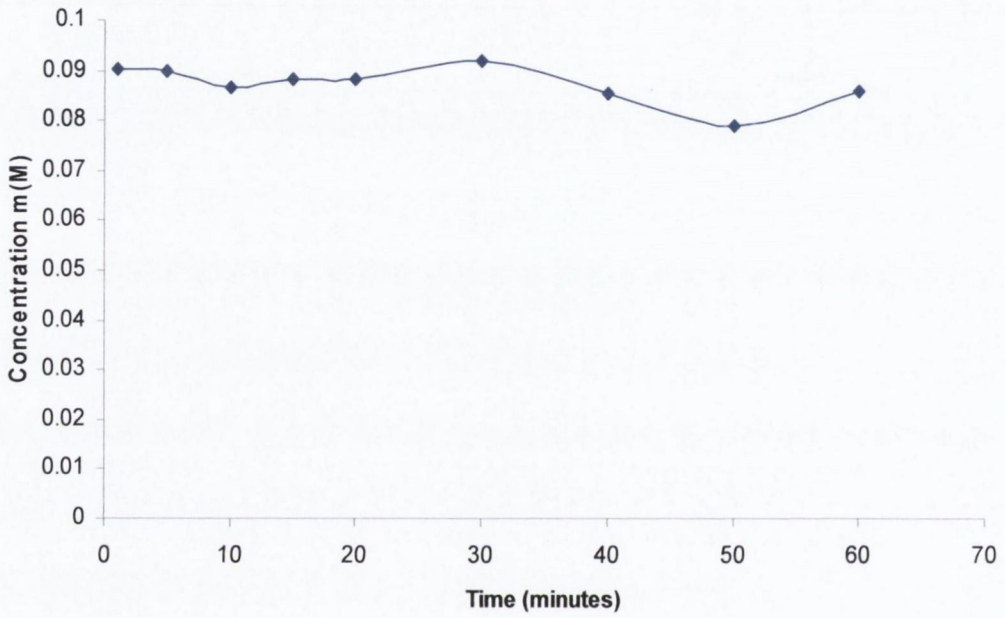

Figure 7.20 Stability of compound 30 in a 0.5% mouse liver solution. n = 3.

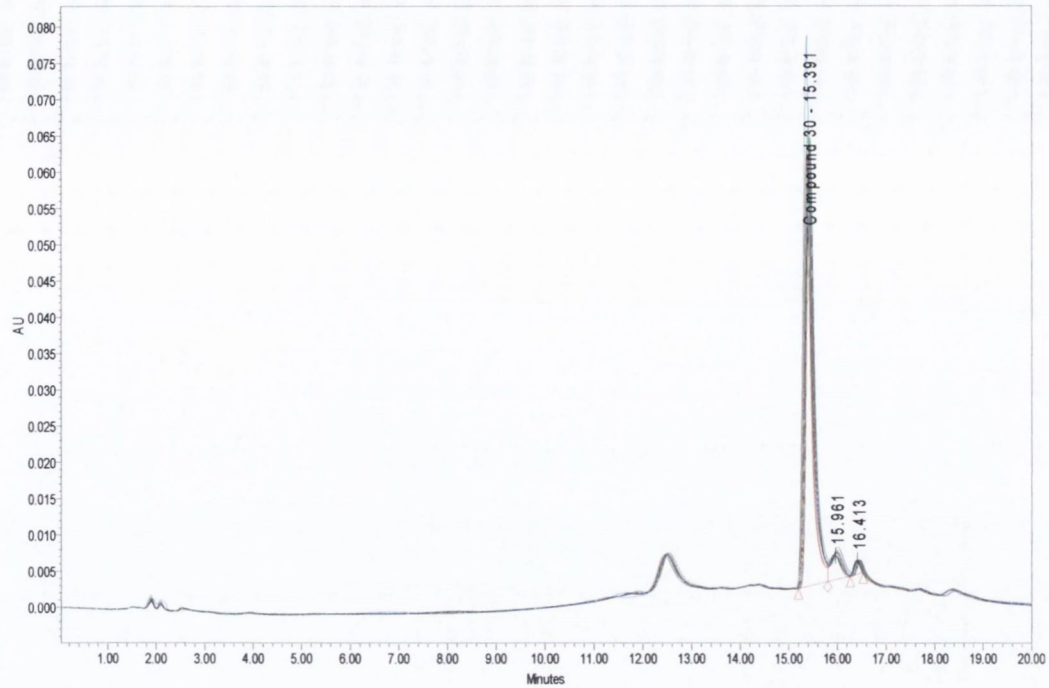

Figure 7.21 Overlay of chromatograms for compound 30 in mouse liver. Retention time: compound 30 15.391 minutes.

7.7.2.3 Compound 30 in a 33% human plasma

In a 33% human plasma solution compound 30 appears to remain stable. 100% of the compound remains after 60 minutes. The compound is not rapidly hydrolyzed by human BuChE *in vitro*.

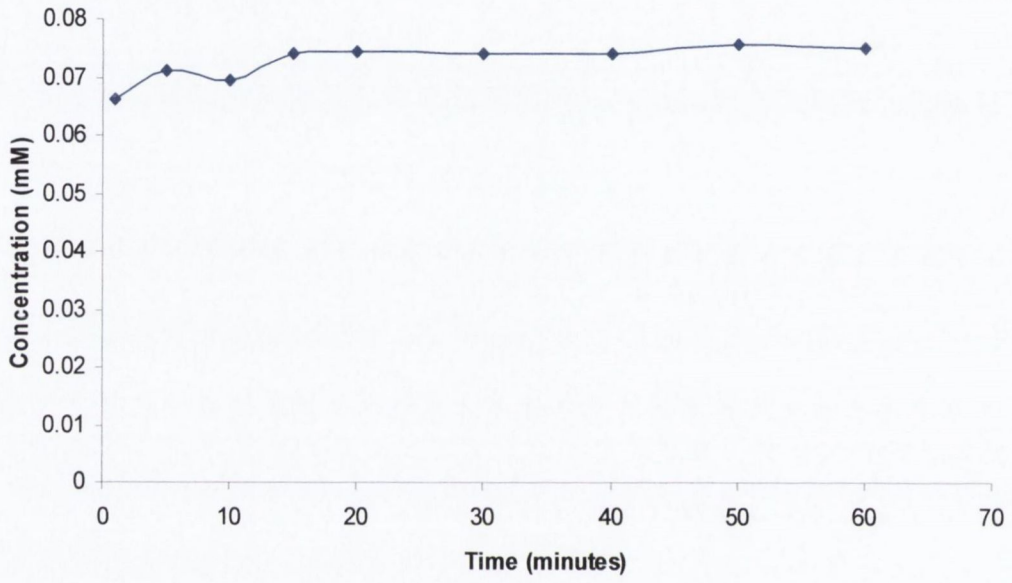

Figure 7.22 Stability of compound 30 in a 33% human plasma solution. n = 3.

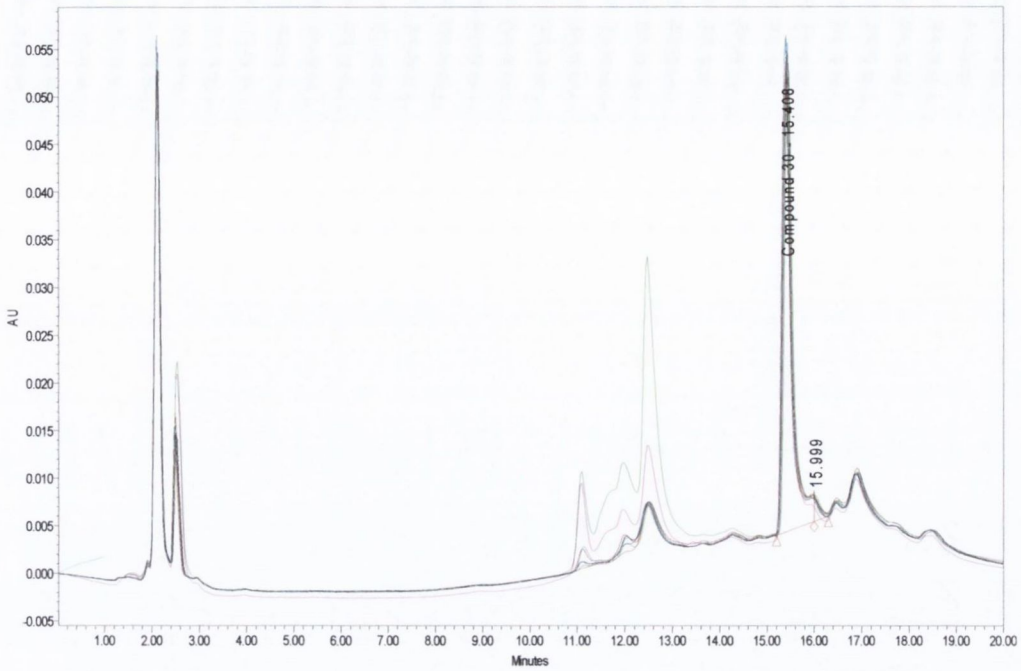

Figure 7.23 Overlay of chromatograms at various time points for compound 30 in human plasma. Retention time: compound 30 15.408 minutes.

7.7.2.4 Compound 30 in a 50% human plasma

In a 50% human plasma solution compound 30 was also stable and there was no hydrolysis after 60 minutes of incubation.

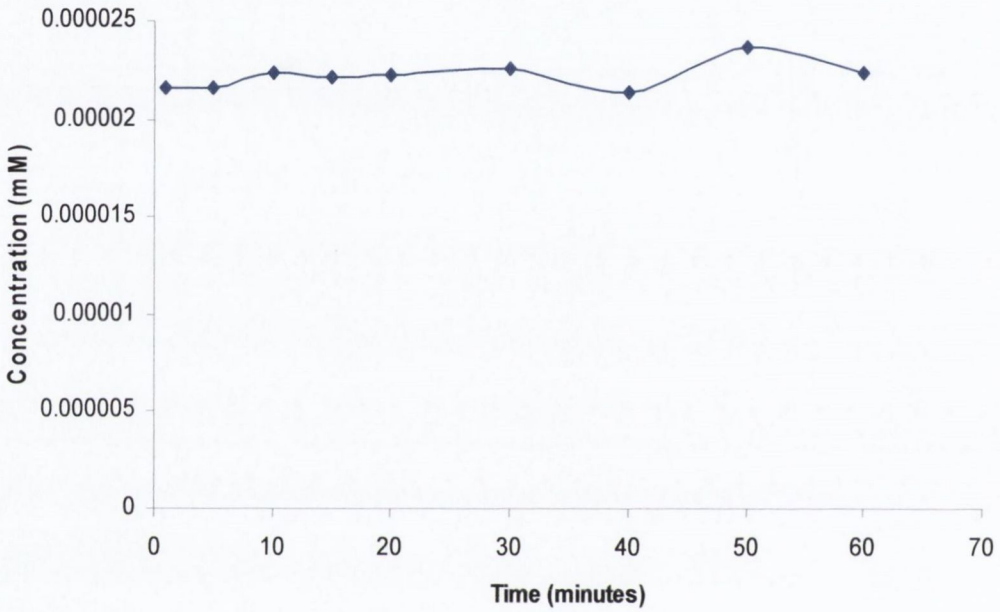

Figure 7.24 Stability of compound 30 in a 50% human plasma solution. n = 3.

7.7.3 Compound 21

7.7.3.1 Compound 21 in mouse liver

This compound was stable in mouse liver over a period of one hour. The enzymes BuChE or CE did not appear to rapidly hydrolyze the compound.

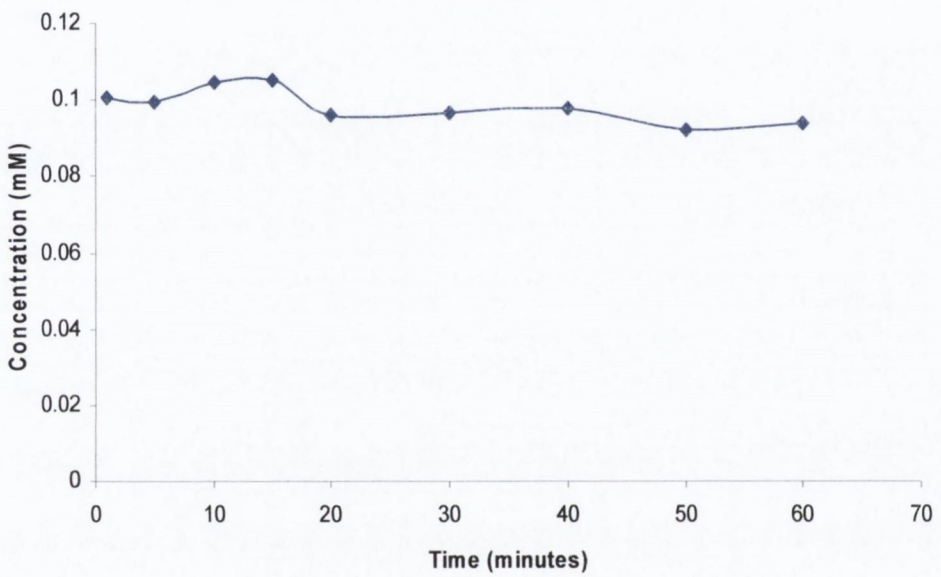

Figure 7.25 Stability of compound 21 in a 0.5% mouse liver solution. n = 3.

7.7.3.2 Compound 21 in human plasma

In a 33% human plasma solution compound 21 was found to be completely stable. There was no decrease in the concentration of the drug after 40 minutes nor were any metabolites formed.

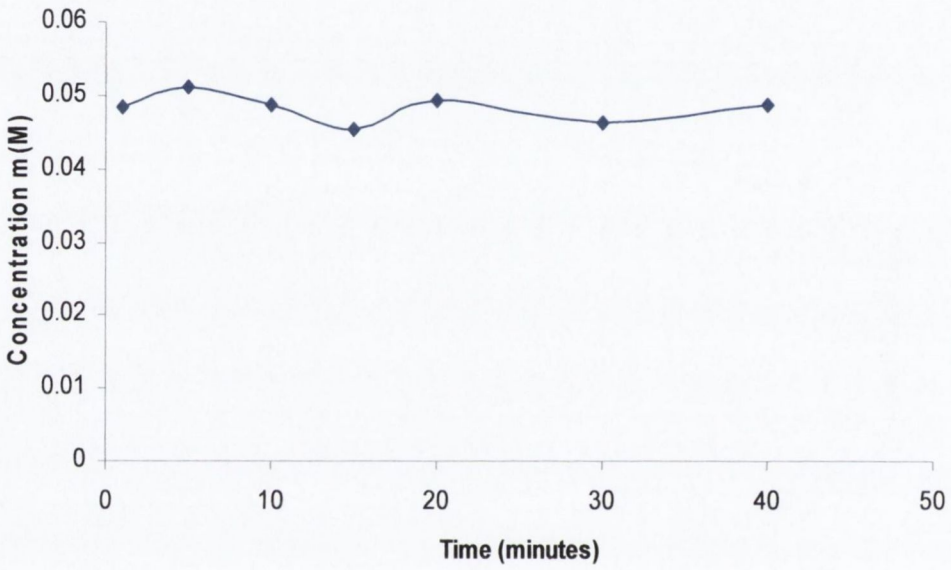

Figure 7.26 Stability of compound 21 in a 33% human plasma solution.

7.7.4 Rivastigmine

7.7.4.1 Rivastigmine in mouse plasma

Rivastigmine, the non-competitive reversible inhibitor of AChE and BuChE, was found to be stable in mouse plasma even after one hour.

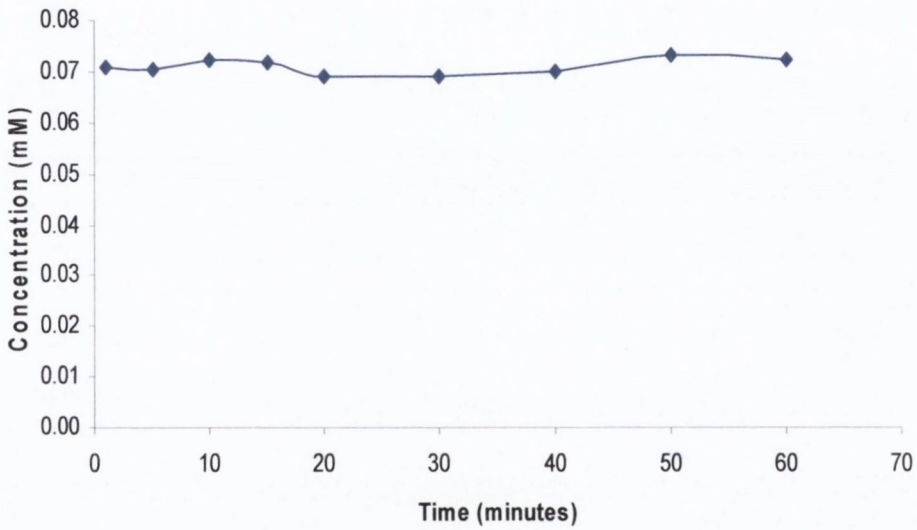

Figure 7.27 Stability of rivastigmine in a 33% mouse plasma solution

7.7.4.2 Rivastigmine in human plasma

Rivastigmine was also stable in human plasma after one hour with neither a decrease in the concentration of the drug nor any metabolite formation.

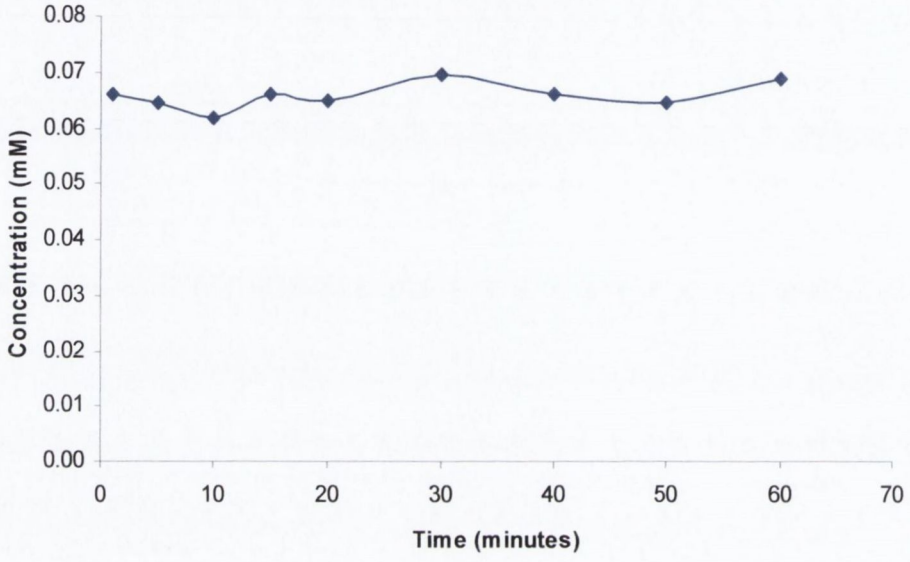

Figure 7.28 Stability of rivastigmine in a 33% human plasma solution

7.8 Discussion

This study sought to evaluate the stability of the novel compounds and rivastigmine *in vitro*. However, the primary objective for this study was to somehow reconcile the short half-life of compound 51 *in vivo*.

This *in vitro* study found that compound 51 was rapidly hydrolyzed in mouse plasma. Compound 51 is normally undergoes ester hydrolysis at the 2' position to yield the metabolites isosorbide 5-benzoate and benzoic acid. However, this study revealed that compound 51 was being rapidly hydrolysed at the 5' position in mouse plasma and liver producing the metabolites isosorbide 2-benzylcarbamate and benzoic acid. This somehow accounts for the short half-life of the compound *in vivo*. Moreover, the stability of compound 51 in human plasma *in vitro* suggests that either the binding site of BuChE in humans and mice differs or that other esterases contribute to the hydrolysis of compound 51. Since human and mouse BuChE have low sequence homology it is possible that this may be a factor in the different rates of metabolism. Howerver, it was also surmised that perhaps another esterase was partaking in the hydrolysis of this compound 51 it was stable in human plasma despite the fact that human plasma has double the BuChE concentration of mouse plasma. Inhibition of the enzyme carboxylesterase in mouse plasma profoundly slowed down the rate of hydrolysis of compound 51 thus confirming that CE was also hydrolyzing this novel drug. Interestingly compound 51 was hydrolyzed at a slower rate in mouse liver than in mouse plasma even though CE is also present in mouse liver. Moreover, the addition of the CE inhibitor, BNPP, to the liver solution did not substantially reduce the rate of hydrolysis of compound 51 as was previously observed with mouse plasma. The differences in the rates of hydrolysis for compound 51 found in mouse plasma and mouse liver might be explained by the existence of different CEs in mouse plasma and liver [141]. The carboxylesterase A1 subfamily includes all the major isoforms of mouse CE [343]. However, mouse liver possesses a different type of CE that has no homology to other CEs. This esterase, ES 46.5kDa, has been classified under the CES 5 family. It exhibits esterase activity higher than that of other mouse liver microsomes [344]. CEs are known as phase-I drug-metabolizing enzymes and can hydrolyze a range of drugs and prodrugs [343]. From this study it is evident that compound 51 acts as a substrate for both mouse BuChE and CE.

In human plasma it was found that compound 51 was stable and was not hydrolyzed by human BuChE after one hour. A previous study has shown that an aspirin isosorbide-based prodrug was rapidly hydrolyzed by human BuChE [204]. However, this was not the case for this novel isosorbide-based inhibitor. Perhaps a longer incubation time of compound 51 in human plasma would have shown hydrolysis. The stability of compound 51 in human plasma suggests that CE plays a greater role in its hydrolysis as it is rapidly hydrolyzed in mouse plasma which has abundant CE. Mouse plasma contains 32-fold more CE than BuChE while CE is absent in human plasma [225]. Howerver, as previously mentioned there may be differences in the BuChE enzyme between both mouse and human. The sequence homology in exon 2 (which contains the active site) of BuChE is low [169]. The differences in the active site could explain the fact that compound 51 is stable in human plasma yet it is hydrolysed in mouse plasma even when CE is inhibited.

In human intestinal microsomes and human liver microsomes compound 51 undergoes hydrolysis albeit at a slower rate than in mouse plasma. This suggests that CE1, CE2 and the cytochrome P450 enzymes are responsible for the hydrolysis of the compound. It was expected that the cytochrome enzymes would hydrolyze compound 51 as they are the most versatile biological catalysts and the major enzyme system present in the liver [345].

Compound 30 was completely stable in mouse plasma, liver and also in human plasma. The stability of compound 30 implies that neither BuChE nor CE hydrolyze this compound *in vitro* at a rapid rate. Perhaps the presence of the salicylate at the 5′ position confers greater stability over compound 51 which possesses a benzoate at its 5′ position and results in compound 30 being hydrolyzed at a much slower rate.

In mouse liver and human plasma compound 21 was also found to be stable. This compound is different from compound 51 in that there is a benzoate at its 5′ position. The presence of the benzoate may produce a conformational change in the drug that results in it being less likely to be rapidly hydrolyzed in the active sites of mouse or human BuChE or mouse CE.

Similarly rivastigmine, which possesses a methylcarbamate, was found to be completely stable in human plasma over a period of one hour. However, in patients with AD rivastigmine has a half-life of 1.7 hours and it is hydrolyzed by human plasma BuChE [346]. Perhaps the use of longer time points or the addition of more plasma (thus a greater enzyme concentration) in this study would have shown hydrolysis of the compounds 21 and 30 and additionally rivastigmine by human and mouse BuChE.

7.9 Conclusion

In conclusion, the novel compounds exhibit different patterns of stability in mouse plasma and liver and also in human plasma. Compound 51 appears to be hydrolyzed by both mouse BuChE and CE indicating that it is a substrate for both enzymes and this may account for the short half-life previously seen *in vivo*. Compound 21, compound 30 and rivastigmine are stable in human plasma and mouse liver suggesting that they are not rapidly hydrolyzed by BuChE or CE. Additionally compound 30 was not hydrolyzed in mouse plasma.

Chapter 8

Conclusion and Future work

Chapter 8 Conclusion and Future work

8.1 Conclusion

These studies were designed to determine the pharmacological effects of a novel class of isosorbide-based butyrycholinesterase inhibitors. These novel compounds were previously found to be highly specific and selective for BuChE in human plasma *in vitro*, with 1000-fold greater selectively for BuChE over AChE than the prototypical butyrylcholinesterase inhibitor iso-OMPA.

The potencies of the novel compounds were assessed *in vitro* in human and mouse plasma. The most potent of the novel compounds were selected for *in vivo* testing. The mouse model was chosen as the animal model on which to test the novel compounds based upon *in vitro* analysis of plasma BuChE activity: Plasma BuChE activity in the mouse was higher than in the rat and it was more comparable to that of humans.

In vitro data showed that the IC_{50} values of the compounds in plasma differed between human and rodents. It transpired that the values were lower in human plasma than in mouse or rat plasma. The levels of enzyme were standardized among the species to ensure approximately equal concentrations of the enzyme were present in each well during the Ellman assay for analysis of the IC_{50} study. The discrepancies between IC_{50} values for different species may stem from interspecies differences in the active binding site as the sequence homology of BuChE differs between species. Furthermore, there are interspecies differences in esterases in rodent and human plasma, with rodents possessing carboxylesterase in their plasma unlike humans. Hydrolysis studies using HPLC were employed to determine the rates of hydrolysis of the compounds *in vitro* in human and mouse plasma, and this study also explored whether carboxylesterase was acting as an additional substrate for the novel compounds. It emerged that compounds 21, 30 and 51 were stable in human plasma. However, compound 51 was hydrolysed in human liver and intestinal microsomes. This was thought to be due to the presence of carboxylesterase in the liver and intestine of humans. Compound 21 and 30 were also stable in mouse plasma with no evidence of hydrolysis after one hour. Overall, it was

concluded that the compounds were indeed potent, and were highly selective for the enzyme BuChE over AChE. However, these studies revealed that compound 51 also acts as a substrate for carboxylesterase which was not previously known

.

Behavioural monitoring following administration of varying doses of the most potent novel compounds was based upon modification of the SHIRPA profile. Administration of compounds 30 and 51 did not reveal any abnormal behaviour in the mice. However, 10 mg/kg of compound 51 did appear to cause slight hypothermia in mice perhaps as a result of CNS depression. Following on from behavioural monitoring, doses from 1-10 mg/kg of the compounds were used for pharmacodynamic profiling. Both compound 51 and compound 33 showed central BuChE inhibition at a dose of 1 mg/kg i.p. This was not observed with 1 mg/kg or 5 mg/kg of compound 33 i.p., although it was capable of peripheral BuChE inhibition.

Compound 51 was pursued for cognitive testing in two paradigms namely the Morris water maze and an object recognition task. Prior to cognitive testing a toxicological study was carried out as gross examination of the livers of animals who received 10 mg/kg of compound 51 showed the appearance of necrotic lesions on the liver. Histological examination revealed focal hepatic necrosis with scarring. This avascular necrosis was secondary to thrombosis but the exact cause of the thrombosis was undetermined. It was therefore decided to use a dose of 1 mg/kg of compound 51 for further testing.

A mouse model of Alzheimer's disease was used to determine the effect of compound 51 on cognition. Injection of the basal nucleus of mice with the lesioning agent ibotenic acid impaired the ability of mice to learn the Morris water maze and an object recognition task. When IBO lesioned animals were treated acutely with compound 51 they performed better cognitively than the IBO lesioned animals treated with saline alone, indicating this agent shows promise in reversing cognitive impairment stemming from cholinergic deficiency, by reducing the rate of ACh degradation. However, sham lesioned animals administered the drug performed worse than sham lesioned mice treated with saline. A similar pattern was seen when the potential of compound 51 to reverse age-related cognitive decline was explored. Aged mice treated with compound 51 performed better in the two paradigms, the Morris water maze and the object recognition task, than aged saline controls. However, when young mice were challenged with the novel drug their

ability to solve the mazes was significantly worse than those young animals treated with saline. Therefore, in the absence of any deficit in BuChE, the use of compound 51 could impair cognition.

Chronic treatment with 1 mg/kg compound 51 over a period of one year did not prevent age-related cognitive decline. Animals were maintained on the chronic treatment from 2-3 months of age until they were 14-15 months old. This is in keeping with the finding that BuChE inhibition does not confer cognitive benefit unless/until there is a cholinergic deficit to be addressed. Once age-related cholinergic deficiency had arisen, the low dose of 1 mg/kg compound 51 p.o. twice weekly, chosen to reduce the likelihood of fatal toxicity in the chronic study, was not sufficient to counter it, in contrast to the positive response seen with daily dosing.

In conclusion, these studies demonstrate that inhibition of BuChE in cholinergic deficiency produces positive effects on cognitive function. This provides a rationale for the use of a pure BuChE inhibitor in the treatment of dementia or Alzheimer's disease. However, administration of the compound to subjects with adequate ACh activity would in fact be detrimental to their cognitive function. Additionally, the toxicological effects could prove greater in the human population than that already seen in rodents administered with the compound. Before considering extension of the use of this novel BuChEI class into clinical trials further preclinical testing would be necessary in animals, in particular with regard to transgenic mice, to gain a full picture of the potential effectiveness of this type of therapy in the treatment of Alzheimer's disease. For now this BuChE inhibition therapy is still in its infancy although there is certainly potential for the use of this therapeutic strategy in the treatment of dementias or Alzheimer's disease.

8.2 Future work

From these studies it is indeed evident that BuChE inhition improves coginition where a cholinergic deficient exists. However, future studies could potentially reveal more information about the enzyme BuChE and its role in cognition. A more detailed pharmacodynamic profile with larger group sizes and more time points would produce a better profile and understanding of the half-life of the compounds *in vivo*. A pharmacokinetic profile using liquid chromatography mass spectrometry (LCMS) to analyse the concentration of the compounds in the animals' tissues would allow for better profiling of the drugs *in vivo*. As the compounds undergo metabolism when administered peripherally, analysis of the level of inhibition of BuChE activity in the brain via intracereboventricular injection at greater intervals would yield valuable information as to the rate of hydrolysis of the compounds in the brain.

As toxicity was an issue with these novel compounds, an *in vitro* toxicology assay using human hepatocytes could potentially determine which compounds would cause toxicity *in vivo*. Furthermore, it would reveal how changing the moieties at the 2' and 5' position would alter the toxicity of compounds and possibly determine which moieties cause toxicity. In terms of cognition, it would be interesting to determine the loss of cholinergic neurons and comparison of this to the level of cognitive performance of animals. This could be achieved by ChAT staining following lesioning of the basal nucleus.

The use of BuChE inhibition as a therapeutic strategy in dementia and Alzheimer's disease is an area with great potential and inhibition of BuChE could decipher the enigmatic role of this cholinesterase in cognition.

Bibliography

Bibliography

1. Livingstone, C. *Pocket Medical Dictionary.* 15th ed.; Churchill Livingstone: London, 2003; p 402.

2. Tulving, E. Episodic memory and common sense: how far apart? *Philos Trans R Soc Lond B Biol Sci* **2001,** 356, 1505-1515.

3. Anderson, J. R. Retrieval of long-term memory. *Science* **1983,** 220, 25-30.

4. Guyton, A. C.; Hall, J. E. *Textbook of Medical Physiology.* W.B. Saunders Company: Pennsylvania, 2000; p 663-677.

5. Tulving, E. Episodic memory: from mind to brain. *Annu Rev Psychol* **2002,** 53, 1-25.

6. Lepage, M.; Ghaffar, O.; Nyberg, L.; Tulving, E. Prefrontal cortex and episodic memory retrieval. *Proc Natl Acad Sci U S A* **1999,** 97, 506-511.

7. Tulving, E.; Kapur, S.; Craik, F. I.; Moscovitch, M.; Houle, S. Hemispheric encoding/retrieval asymmetry in episodic memory: positron emission tomography findings. *Proc Natl Acad Sci U S A* **1994,** 91, 2016-2020.

8. Ciaramelli, E.; Grady, C. L.; Moscovitch, M. Top-down and bottom-up attention to memory: A hypothesis (AtoM) on the role of the posterior parietal cortex in memory retrieval. *Neuropsychologia* **2008,** 46, 1828-1851.

9. Davidson, P. S.; Anaki, D.; Ciaramelli, E.; Cohn, M.; Kim, A. S.; Murphy, K. J.; Troyer, A. K.; Moscovitch, M.; Levine, B. Does lateral parietal cortex support episodic memory? Evidence from focal lesion patients. *Neuropsychologia* **2008,** 46, 1743-1755.

10. Tulving, E. *The Oxford Handbook of Memory.* Oxford University Press: New York, 2000; p 3-27.

11. Perner, J.; T., R. Episodic memory and autonoetic conciouness: developmental evidence and theory of childhood amnesia. *J Exper Child Psychol* **1995,** 59, 516-548.

12. Spence, K. W.; Spence, J. T. *The Psychology of Learning and Memory: Advances in Research and Theory.* Academic Press: New York, 1968; Vol. 2, p 89-195.

13. Wong, C. W. A brain model with the circuit to convert short-term memory into long-term memory. *Med Hypotheses* **1997,** 48, 221-226.

14. Kelly, A.; Laroche, S.; Davis, S. Activation of mitogen-activated protein kinase/extracellular signal-regulated kinase in hippocampal circuitry is required for

consolidation and reconsolidation of recognition memory. *J Neurosci* **2003,** 23, 5354-5360.

15. Moscovitch, M.; Winocur, G. Frontal lobes, memory, and aging. *Ann N Y Acad Sci* **1995,** 769, 119-150.

16. Cohn, M.; Emrich, S. M.; Moscovitch, M. Age-related deficits in associative memory: The influence of impaired strategic retrieval. . *Psychol Aging* **2008,** 23, 93-103.

17. Old, S. R.; Naveh-Benjamin, M. Memory for people and their actions: further evidence for an age-related associative deficit. *Psychol Aging* **2008,** 23, 467-472.

18. Forster, M. J.; Dubey, A.; Dawson, K. M.; Stutts, W. A.; Lal, H.; Sohal, R. S. Age-related losses of cognitive function and motor skills in mice are associated with oxidative protein damage in the brain. *Proc Natl Acad Sci U S A* **1996,** 93, 4765-4769.

19. van Dijk, K. R. A.; van Gerven, P. W. M.; van Boxtel, M. P. J.; van der Elst, W.; Jolles, J. No protective effects of education during normal cognitive aging: Results from the 6-year follow-up of the Maastricht Aging Study. *Psychol Aging* **2008,** 23, 119-130.

20. Fulton, A.; Bartlett, J. C. Young and old faces in young and old heads: the factor of age in face recognition. *Psychol Aging* **1991,** 6, 623-630.

21. James, L. E.; Fogler, K. A.; Tauber, S. K. Recognition memory measures yield disproportionate effects of aging on learning face-name associations. *Psychol Aging* **2008,** 23, 657-664.

22. Connelly, S. L.; Hasher, L.; Zacks, R. T. Age and reading: the impact of distraction. *Psychol Aging* **1991,** 6, 533-541.

23. Emilien, G.; Durlach, C.; Minaker, K. L.; Winblad, B.; Gauthier, S.; Maloteaux, J.-M. *Alzheimer Disease: Neuropsychology and Pharmacology.* Birhauser: Berlin, 2004; p 288.

24. The Alzheimer Society of Ireland. 2008. [cited Jul 26 2008]. Available from: http://www.alzheimer.ie

25. Alzheimer's Association. 2008. [cited Jul 26 2008]. Alzheimer's Disease Prevalence Rates Rise to More than Five Million in the United States. Available from: http://www.alz.org

26. Folstein, M. F.; Folstein, S. E.; McHugh, P. R. "Mini-mental state". A practical method for grading the cognitive state of patients for the clinician. *J Psychiatr Res* **1975,** 12, 189-198.

27. Association, A. P. *Diagnostic and Statistical Manual of Mental Disorders. 4th Edition.* 4th Edition ed.; Washington DC: American Psychiatric Association, 1994.

28. Kindersley, D. *The Visual Dictionary of the Human Body*. DK Publishing, London: London, 1991.

29. The National Institute on Aging, Consensus Recommendations for the Postmortem Diagnosis for Alzheimer's Disease. . *Neurobiol Aging* **1997,** 18, S1-S2.

30. Leonard, B. E. *Fundamentals of Psychopharmacology*. 3rd Edition ed.; Wiley: Sussex, England, 2003; p 520.

31. How Stuff Works. 1998-2008. [cited Jul 26 2008]. Available from: http://static.howstuffworks.com/gif/swearing-1.gif.

32. Lemere, C. A.; Blusztajn, J. K.; Yamaguchi, H.; Wisniewski, T.; Saido, T. C.; Selkoe, D. J. Sequence of deposition of heterogeneous amyloid beta-peptides and APO E in Down syndrome: implications for initial events in amyloid plaque formation. *Neurobiol Dis* **1996,** 3, 16-32.

33. Naslund, J.; Haroutunian, V.; Mohs, R.; Davis, K. L.; Davies, P.; Greengard, P.; Buxbaum, J. D. Correlation between elevated levels of amyloid beta-peptide in the brain and cognitive decline. *JAMA* **2000,** 283, 1571-1577.

34. Selkoe, D. J. The cell biology of beta-amyloid precursor protein and presenilin in Alzheimer's disease. *Trends Cell Biol* **1998,** 8, 447-453.

35. Genetics Home Reference. 2008. [cited Aug 12 2008]. Available from: http://ghr.nlm.nih.gov/gene=app

36. Richardson, J. A.; Burns, D. K. Mouse models of Alzheimer's disease: a quest for plaques and tangles. *Ilar J* **2002,** 43, 89-99.

37. Sisodia, S. S. Beta-amyloid precursor protein cleavage by a membrane-bound protease. *Proc Natl Acad Sci U S A* **1992,** 89, 6075-609.

38. Biocarta. 2008. [cited Aug 12 2008]. Available from: http://www.biocarta.com/pathfiles/h_appPathway.gif.

39. Cai, H.; Wang, Y.; McCarthy, D.; Wen, H.; Borchelt, D. R.; Price, D. L.; Wong, P. C. BACE1 is the major beta-secretase for generation of Abeta peptides by neurons. *Nat Neurosci* **2001,** 4, 233-234.

40. Frasca, G.; Carbonaro, V.; Merlo, S.; Copani, A.; Sortino, M. A. Integrins mediate beta-amyloid-induced cell-cycle activation and neuronal death. *J Neurosci Res* **2008,** 86, 350-355.

41. Luo, Y.; Bolon, B.; Kahn, S.; Bennett, B. D.; Babu-Khan, S.; Denis, P.; Fan, W.; Kha, H.; Zhang, J.; Gong, Y.; Martin, L.; Louis, J. C.; Yan, Q.; Richards, W. G.; Citron,

M.; Vassar, R. Mice deficient in BACE1, the Alzheimer's beta-secretase, have normal phenotype and abolished beta-amyloid generation. *Nat Neurosci* **2001,** 4, 231-232.

42. Schubert, D.; Jin, L. W.; Saitoh, T.; Cole, G. The regulation of amyloid beta protein precursor secretion and its modulatory role in cell adhesion. *Neuron* **1989,** 3, 689-694.

43. Mattson, M. P.; Barger, S. W.; Cheng, B.; Lieberburg, I.; Smith-Swintosky, V. L.; Rydel, R. E. beta-Amyloid precursor protein metabolites and loss of neuronal Ca2+ homeostasis in Alzheimer's disease. *Trends Neurosci* **1993,** 16, 409-414.

44. Zheng, H.; Jiang, M.; Trumbauer, M. E.; Sirinathsinghji, D. J.; Hopkins, R.; Smith, D. W.; Heavens, R. P.; Dawson, G. R.; Boyce, S.; Conner, M. W.; Stevens, K. A.; Slunt, H. H.; Sisoda, S. S.; Chen, H. Y.; Van der Ploeg, L. H. beta-Amyloid precursor protein-deficient mice show reactive gliosis and decreased locomotor activity. *Cell* **1995,** 81, 525-531.

45. Dawson, G. R.; Seabrook, G. R.; Zheng, H.; Smith, D. W.; Graham, S.; O'Dowd, G.; Bowery, B. J.; Boyce, S.; Trumbauer, M. E.; Chen, H. Y.; Van der Ploeg, L. H.; Sirinathsinghji, D. J. Age-related cognitive deficits, impaired long-term potentiation and reduction in synaptic marker density in mice lacking the beta-amyloid precursor protein. *Neuroscience* **1999,** 90, 1-13.

46. Ring, S.; Weyer, S. W.; Kilian, S. B.; Waldron, E.; Pietrzik, C. U.; Filippov, M. A.; Herms, J.; Buchholz, C.; Eckman, C. B.; Korte, M.; Wolfer, D. P.; Muller, U. C. The secreted beta-amyloid precursor protein ectodomain APPs alpha is sufficient to rescue the anatomical, behavioral, and electrophysiological abnormalities of APP-deficient mice. *J Neurosci* **2007,** 27, 7817-7826.

47. Sherrington, R.; Rogaev, E. I.; Liang, Y.; Rogaeva, E. A.; Levesque, G.; Ikeda, M.; Chi, H.; Lin, C.; Li, G.; Holman, K.; Tsuda, T.; Mar, L.; Foncin, J. F.; Bruni, A. C.; Montesi, M. P.; Sorbi, S.; Rainero, I.; Pinessi, L.; Nee, L.; Chumakov, I.; Pollen, D.; Brookes, A.; Sanseau, P.; Polinsky, R. J.; Wasco, W.; Da Silva, H. A. R.; Haines, J. L.; Pericak-Vance, M. A.; Tanzi, R. E.; Roses, A. D.; Fraser, P. E.; Rommens, J. M.; St George-Hyslop, P. H. Cloning of a gene bearing missense mutations in early-onset familial Alzheimer's disease. *Nature* **1995,** 375, 754-760.

48. Sherrington, R.; Rogaev, E. I.; Liang, Y.; Rogaeva, E. A.; Levesque, G.; Ikeda, M.; Chi, H.; Lin, C.; Li, G.; Holman, K.; et al. Cloning of a gene bearing missense mutations in early-onset familial Alzheimer's disease. *Nature* **1995,** 375, 754-760.

49. Levy-Lahad, E.; Wijsman, E. M.; Nemens, E.; Anderson, L.; Goddard, K. A. B.; Weber, J. L.; Bird, T. D.; Schellenberg, G. D. A familial Alzheimer's disease locus on chromosome 1. *Science* **1992,** 269, 970-973.

50. R&D Systems. 2008. [cited Jul 20 2008]. Available from: http://www.rndsystems.com/DAM_public/5217.jpg.

51. Lee, M. K.; Slunt, H. H.; Martin, L. J.; Thinakaran, G.; Kim, G.; Gandy, S. E.; Seeger, M.; Koo, E.; Price, D. L.; Sisodia, S. S. Expression of presenilin 1 and 2 (PS1 and PS2) in human and murine tissues. *J Neurosci* **1996,** 16, 7513-7525.

52. de Strooper, B.; Annaert, W.; Cupers, P.; Saftig, P.; Craessaerts, K.; Mumm, J. S.; Schroeter, E. H.; Schrijvers, V.; Wolfe, M. S.; Ray, W. J.; Goate, A.; Kopan, R. A presenilin-1 dependent gamma-secretase-like protease mediates release of Notch intracellular domain. *Nature* **1999,** 398, 518-522.

53. Marambaud, P.; Shioi, J.; Serban, G.; Georgakopoulos, A.; Sarner, S.; Nagy, V.; Baki, L.; Wen, P.; Efthimiopoulos, S.; Shao, Z.; Wisniewski, T.; Robakis, N. K. A presenilin-1/gamma-secretase cleavage releases the E-cadherin intracellular domain and regulates disassembly of adherens junctions. *Embo J* **2002,** 21, 1948-1956.

54. Marambaud, P.; Wen, P. H.; Dutt, A.; Shioi, J.; Takashima, A.; Siman, R.; Robakis, N. K. A CBP binding transcriptional repressor produced by the PS1/epsilon-cleavage of N-cadherin is inhibited by PS1 FAD mutations. *Cell* **2003,** 114, 635-645.

55. Zhang, Y. W.; Wang, R.; Liu, Q.; Zhang, H.; Liao, F. F.; Xu, H. Presenilin/gamma-secretase-dependent processing of beta-amyloid precursor protein regulates EGF receptor expression. *Proc Natl Acad Sci U S A* **2007,** 104, 10613-10618.

56. De Strooper, B.; Saftlg, P.; Craessaerts, K.; Vanderstichele, H.; Guhde, G.; Annaert, W.; Von Figura, K.; Van Leuvan, F. Deficiency of presenilin-1 inhibits the normal cleavage of amyloid precursor protein. *Nature* **1998,** 391, 387-390.

57. Vetrivel, K. S.; Zhang, Y. W.; Xu, H.; Thinakaran, G. Pathological and physiological functions of presenilins. *Mol Neurodegener* **2006,** 1, 4.

58. Schroeter, E. H.; Ilagan, M. X.; Brunkan, A. L.; Hecimovic, S.; Li, Y. M.; Xu, M.; Lewis, H. D.; Saxena, M. T.; De Strooper, B.; Coonrod, A.; Tomita, T.; Iwatsubo, T.; Moore, C. L.; Goate, A.; Wolfe, M. S.; Shearman, M.; Kopan, R. A presenilin dimer at the core of the gamma-secretase enzyme: insights from parallel analysis of Notch 1 and APP proteolysis. *Proc Natl Acad Sci U S A* **2003,** 100, 13075-13080.

59. Handler, M.; Yang, X.; Shen, J. Presenilin-1 regulates neuronal differentiation during neurogenesis. *Development* **2000,** 127, 2593-2606.

60. Shen, J.; Bronson, R. T.; Chen, D. F.; Xia, W.; Selkoe, D. J.; Tonegawa, S. Skeletal and CNS defects in presenilin-1-deficient mice. *Cell* **1997,** 89, 629-639.

61. Kaplan, M. S. Neurogenesis in the 3-month-old rat visual cortex. *J Comp Neurol* **1981,** 195, 323-328.

62. Bernier, P. J.; Bedard, A.; Vinet, J.; Levesque, M.; Parent, M. Newly generated neurons in the amygdala and adjoining cortex of adult primates. *Proc Natl Acad Sci U S A* **2002,** 99, 11464-11469.

63. Kosik, K. S.; McConlogue, L. Microtubule-associated protein function: lessons from expression in Spodoptera frugiperda cells. *Cell Motil Cytoskeleton* **1994,** 28, 195-198.

64. Trinczek, B.; Biernat, J.; Baumann, K.; Mandelkow, E. M.; Mandelkow, E. Domains of tau protein, differential phosphorylation, and dynamic instability of microtubules. *Mol Biol Cell* **1995,** 6, 1887-1902.

65. Max-Planck Arbeitsgruppen fur strukturelle Molekularbiologie Hamburg. 2008. [cited Jun 5 2008]. Available from: http://www.mpasmb-hamburg.mpg.de/mandelkow2/taubuilder.htm.

66. Larson, C. Attacking Alzheimer's. The latest news on treatment and diagnosis. In *U.S. News and World Report* 2008.

67. Alzheimer's Society of Canada. 1997-2008. [cited Jul 21 2008]. Available from: http://www.alzheimer.ca/english/alzheimer_brain_mini_site/13.htm.

68. Alzheimer's association. 2008. [cited Jul 21 200]. Available from: http://www.alz.org/brain.

69. Singh, V.; Chertkow, H.; Lerch, J. P.; Evans, A. C.; Dorr, A. E.; Kabani, N. J. Spatial patterns of cortical thinning in mild cognitive impairment and Alzheimer's disease. *Brain* **2006,** 129, 2885-2893.

70. Im, K.; Lee, J. M.; Seo, S. W.; Yoon, U.; Kim, S. T.; Kim, Y. H.; Kim, S. I.; Na, D. L. Variations in cortical thickness with dementia severity in Alzheimer's disease. *Neurosci Lett* **2008,** 436, 227-231.

71. Karas, G.; Scheltens, P.; Rombouts, S.; van Schijndel, R.; Klein, M.; Jones, B.; van der Flier, W.; Vrenken, H.; Barkhof, F. Precuneus atrophy in early-onset Alzheimer's disease: a morphometric structural MRI study. *Neuroradiology* **2007,** 49, 967-976.

72. Cavanna, A. E.; Trimble, M. R. The precuneus: a review of its functional anatomy and behavioural correlates. *Brain* **2006,** 129, 564-583.

73. Fox, N. C.; Warrington, E. K.; Seiffer, A.; Agnew, S.; MN, R. Presymptomatic cognitive deficits in individuals at risk of familial Alzheimer's disease. A longitudinal prospective study. *Brain* **1998,** 121, 1631-1639.

74. Marijuana for Alzheimer's. 2008. [cited Jun 25 2008]. Available from: http://marijuanaforalzheimers.blogspot.com/2007/09/marijuana-may-prevent-alzheimers.html.

75. Thompson, P. M.; Vidal, C.; Giedd, J. N.; Gochman, P.; Blumenthal, J.; Nicolson, R.; Toga, A. W.; Rapoport, J. L. Mapping adolescent brain change reveals dynamic wave of accelerated gray matter loss in very early-onset schizophrenia. *Proc Natl Acad Sci U S A* **2001,** 98, 11650-11655.

76. Thompson, P. M.; Mega, M. S.; Woods, R. P.; Zoumalan, C. I.; Lindshield, C. J.; Blanton, R. E.; Moussai, J.; Holmes, C. J.; Cummings, J. L.; Toga, A. W. Cortical change in Alzheimer's disease detected with a disease-specific population-based brain atlas. *Cereb Cortex* **2001,** 11, 1-16.

77. Thompson, P. M.; Hayashi, K. M.; de Zubicaray, G.; Janke, A. L.; Rose, S. E.; Semple, J.; Herman, D.; Hong, M. S.; Dittmer, S. S.; Doddrell, D. M.; Toga, A. W. Dynamics of gray matter loss in Alzheimer's disease. *J Neurosci* **2003,** 23, 994-1005.

78. Giacobini, E. *Butyrylcholinesterase: Its function and inhibitors*. Martin Dunitz: London, 2003.

79. Geula, C.; Mesulam, M. M. Cortical cholinergic fibers in aging and Alzheimer's disease: a morphometric study. *Neuroscience* **1989,** 33, 469-481.

80. Wright, C. I.; Geula, C.; Mesulam, M. M. Neurological cholinesterases in the normal brain and in Alzheimer's disease: relationship to plaques, tangles, and patterns of selective vulnerability. *Ann Neurol* **1993,** 34, 373-384.

81. Giacobini, E.; DeSarno, P.; Clark, B.; McIlhany, M. The cholinergic receptor system of the human brain: neurochemical and pharmacological aspects in aging and Alzheimer. *Prog Brain Res* **1989,** 79, 335-343.

82. Perry, E. K.; Tomlinson, B. E.; Blessed, G.; Bergmann, K.; Gibson, P. H.; Perry, R. H. Correlation of cholinergic abnormalities with senile plaques and mental test scores in senile dementia. *Br Med J* **1978,** 2, 1457-1459.

83. van Dam, D.; Marescau, B.; Engelborghs, S.; Cremers, T.; Mulder, J.; Staufenbiel, M.; De Deyn, P. P. Analysis of cholinergic markers, biogenic amines, and amino acids in the CNS of two APP overexpression mouse models. *Neurochemistry international* **2005,** 46, 409-422.

84. Abdel Behavioural Neuroscience Lab. 2008. [cited Jul 26 2008]. Available from: http://abdellab.sunderland.ac.uk/lectures/Parmacology/ANSdoc/cholinergic9.html.

85. Geula, C.; Mesulam, M. M. Cholinesterases and the pathology of Alzheimer disease. *Alzheimer Dis Assoc Disord* **1995,** 9 Suppl 2, 23-28.

86. Everitt, B. J.; Robbins, T. W. Central cholinergic systems and cognition. *Annu Rev Psychol* **1997,** 48, 649-684.

87. Cell Science. 2008. [cited Jul 26 2008]. Available from: http://www.cellscience.com/CCA.htm.

88. Mesulam, M. M.; Mash, D.; Hersh, L.; Bothwell, M.; Geula, C. Cholinergic innervation of the human striatum, globus pallidus, subthalamic nucleus, substantia nigra, and red nucleus. *J Comp Neurol* **1992,** 323, 252-268.

89. Watase, K.; Zogjbi, H. Y. Modelling brain diseases in mice: the challenges of design and analysis. *Nature* **2003,** 4, 296-307.

90. Van Dam, D.; De Deyn, P. P. Drug discovery in dementia: the role of rodent models. *Nat Rev: Drug Discov* **2006,** 5, 956-970.

91. Luo L; Craik, F.I. Aging and memory: a cognitive approach. *Can J Psychiatry* **2008,** 53, 346-353.

92. Ingram, D. K.; Spangler, E. L.; Iijima, S.; Ikari, H.; Kuo, H.; Greig, N. H.; London, E. D. Rodent models of memory dysfunction in Alzheimer's disease and normal aging: moving beyond the cholinergic hypothesis. *Life Sci* **1994,** 55, 2037-2049.

93. Erickson, C. A.; Barnes, C. A. The neurobiology of memory changes in normal aging. *Exp Gerontol* **2003,** 38, 61-69.

94. Patat, A.; Klein, M. J.; Surjus, A.; Hucher, M.; Granier, J. RU 41,656 does not reverse the scopolamine-induced cognitive deficit in healthy volunteers. *Eur J Clin Pharmacol* **1991,** 41, 225-231.

95. Ebert, U.; Kirch, W. Scopolamine model of dementia: electroencephalogram findings and cognitive performance. *Eur J Clin Invest* **1998,** 28, 944-949.

96. Bejar, C.; Wang, R. H.; Weinstock, M. Effect of rivastigmine on scopolamine-induced memory impairment in rats. *Eur J Pharmacol* **1999,** 383, 231-240.

97. Chen, J.; Long, Y.; Han, M.; Wang, T.; Chen, Q.; Wang, R. Water-soluble derivative of propolis mitigates scopolamine-induced learning and memory impairment in mice. *Pharmacol Biochem Behav* **2008,** 90, 441-446.

98. Dunnett, S. B.; Everitt, B. J.; Robbins, T. W. The basal forebrain-cortical cholinergic system: interpreting the functional consequences of excitotoxic lesions. *Trends Neurosci* **1991,** 14, 494-501.

99. Wenk, G. L.; Harrington, C. A.; Tucker, D. A.; Rance, N. E.; Walker, L. C. Basal forebrain neurons and memory: a biochemical, histological, and behavioral study of differential vulnerability to ibotenate and quisqualate. *Behav Neurosci* **1992,** 106, 909-923.

100. Shaughnessy, L. W.; Barone, S., Jr.; Mundy, W. R.; Herr, D. W.; Tilson, H. A. Comparison of intracranial infusions of colchicine and ibotenic acid as models of neurodegeneration in the basal forebrain. *Brain Res* **1994,** 637, 15-26.

101. Toledano, A.; Alvarez, M. I. Lesions and dysfunctions of the nucleus basalis as Alzheimer's disease models: general and critical overview and analysis of the long-term changes in several excitotoxic models. *Curr Alzheimer Res* **2004,** 1, 189-214.

102. Duff, K.; Suleman, F. Transgenic mouse models of Alzheimer's disease: how useful have they been for therapeutic development? *Brief Funct Genomic Proteomic* **2004,** 3, 47-59.

103. Lewis, J.; McGowan, E.; Rockwood, J.; Melrose, H.; Nacharaju, P.; Van Slegtenhorst, M.; Gwinn-Hardy, K.; Paul Murphy, M.; Baker, M.; Yu, X.; Duff, K.; Hardy, J.; Corral, A.; Lin, W. L.; Yen, S. H.; Dickson, D. W.; Davies, P.; Hutton, M. Neurofibrillary tangles, amyotrophy and progressive motor disturbance in mice expressing mutant (P301L) tau protein. *Nat Genet* **2000,** 25, 402-405.

104. Schenk, D.; Barbour, R.; Dunn, W.; Gordon, G.; Grajeda, H.; Guido, T.; Hu, K.; Huang, J.; Johnson-Wood, K.; Khan, K.; Kholodenko, D.; Lee, M.; Liao, Z.; Lieberburg, I.; Motter, R.; Mutter, L.; Soriano, F.; Shopp, G.; Vasquez, N.; Vandevert, C.; Walker, S.; Wogulis, M.; Yednock, T.; Games, D.; Seubert, P. Immunization with amyloid-beta attenuates Alzheimer-disease-like pathology in the PDAPP mouse. *Nature* **1999,** 400, 173-177.

105. Calhoun, M. E.; Wiederhold, K. H.; Abramowski, D.; Phinney, A. L.; Probst, A.; Sturchler-Pierrat, C.; Staufenbiel, M.; Sommer, B.; Jucker, M. Neuron loss in APP transgenic mice. *Nature* **1998,** 395, 173-177.

106. Chishti MA; Yang DS; Janus C; Phinney AL; Horne P; Pearson J; Strome R; Zuker N; Loukides J; French J; Turner S; Lozza G; Grilli M; Kunicki S; Morissette C; Paquette J; Gervais F; Bergeron C; Fraser PE; Carlson GA; George-Hyslop PS; D., W. Early-onset amyloid deposition and cognitive deficits in transgenic mice expressing a

double mutant form of amyloid precursor protein 695. *J Biol Chem* **2001,** 276, 21562-21570.

107. Pérez M; Ribe E; Rubio A; Lim F; Morán MA; Ramos PG; Ferrer I; Isla MT; J., A. Characterization of a double (amyloid precursor protein-tau) transgenic: tau phosphorylation and aggregation. *Neuroscience* **2005,** 130, 339-347.

108. Pérez M; Morán MA; Ferrer I; Avila J; P, G.-R. Phosphorylated tau in neuritic plaques of APP(sw)/Tau (vlw) transgenic mice and Alzheimer disease. *Acta Neuropathologica* **2008,** 116, 409-418.

109. Oddo, S.; Caccamo, A.; Kitazawa, M.; Tseng, B. P.; LaFerla, F. M. Amyloid deposition precedes tangle formation in a triple transgenic model of Alzheimer's disease. *Neurobiol Aging* **2003,** 24, 1063-1070.

110. Rodríguez JJ; Jones VC; Tabuchi M; Allan SM; Knight EM; LaFerla FM; Oddo S; A., V. Impaired adult neurogenesis in the dentate gyrus of a triple transgenic mouse model of Alzheimer's disease. *PloS One* **2008,** 3, e2935.

111. Dale, H. H. The action of certain esters of choline and their relation to muscarine. *J Pharmacol Exp Ther* **1914,** 6, 147-190.

112. Stedman, E.; Stedman, E.; White, A. C. A comparison of the choline-esterase activities of the blood-sera from various species. *Biochem J* **1933,** 27, 1055-1060.

113. Mendel, B.; Rudney, H. Studies on cholinesterase: 1. Cholinesterase and pseudo-cholinesterase. *Biochem J* **1943,** 37, 59-63.

114. Robitzki, A.; Mack, A.; Hoppe, U.; Chatonnet, A.; Layer, P. G. Butyrylcholinesterase antisense transfection increases apoptosis in differentiating retinal reaggregates of the chick embryo. *J Neurochem* **1998,** 71, p413-420.

115. Mack, A.; Robitzki, A. The key role of butyrylcholinesterase during neurogenesis and neural disorders: an antisense-5'butyrylcholinesterase-DNA study. *Prog Neurobiol* **2000,** 60, 607-628.

116. Giacobini, E. *Cholinesterases and Cholinesterase Inhibitors*. 1st Edition ed.; Martin Dunitz Ltd.: London, 2000; p 270.

117. Chatonnet, A.; Lockridge, O. Comparison of butyrylcholinesterase and acetylcholinesterase. *Biochem J* **1989,** 260, 625-634.

118. Hartmann, J.; Kiewert, C.; Duysen, E. G.; Lockridge, O.; Greig, N. H.; Klein, J. Excessive hippocampal acetylcholine levels in acetylcholinesterase-deficient mice are moderated by butyrylcholinesterase activity. *J Neurochem* **2007,** 100, 1421-1429.

119. Iwasaki, T.; Yoneda, M.; Nakajima, A.; Terauchi, Y. Serum butyrylcholinesterase is strongly associated with adiposity, the serum lipid profile and insulin resistance. *Intern Med* **2007,** 46, 1633-1639.

120. Silver, A. *The Biology of Cholinesterases*. North-Holland Publishing Company: Oxford, 1974; Vol. 36, p 596.

121. Kalman, J.; Rakonczay, Z.; Abraham, G.; Boda, K.; Farkas, T. Serum butyrylcholinesterase activity in hyperlipidaemia. *Atherosclerosis* **2003,** 173, 145-146.

122. Darvesh, S.; Hopkins, D. A.; Geula, C. Neurobiology of butyrylcholinesterase. *Nat Rev Neurosci* **2003,** 4, 131-138.

123. Millard, C. B.; Broomfield, C. A. A computer model of glycosylated human butyrylcholinesterase. *Biochem Biophys Res Commun* **1992,** 189, 1280-1286.

124. Wikimedia Commons. 2008. [cited Jun 5 2008]. Available from: http://commons.wikimedia.org/wiki/Image:Butyrylcholinesterase_1P0I.png.

125. Lockridge, O.; Bartels, C. F.; Vaughan, T. A.; Wong, C. K.; Norton, S. E.; Johnson, L. L. Complete amino acid sequence of human serum cholinesterase. *J Biol Chem* **1987,** 262, 549-557.

126. Soreq, H.; Seidman, S. Acetylcholinesterase--new roles for an old actor. *Nat Rev Neurosci* **2001,** 2, 294-302.

127. Masson, P.; Xie, W.; Froment, M. T.; Levitsky, V.; Fortier, P. L.; Albaret, C.; Lockridge, O. Interaction between the peripheral site residues of human butyrylcholinesterase, D70 and Y332, in binding and hydrolysis of substrates. *Biochim Biophys Acta* **1999,** 1433, 281-293.

128. Vellom, D. C.; Radic, Z.; Li, Y.; Pickering, N. A.; Camp, S.; Taylor, P. Amino acid residues controlling acetylcholinesterase and butyrylcholinesterase specificity. *Biochemistry* **1993,** 32, 12-17.

129. Lockridge, O.; Eckerson, H. W.; La Du, B. N. Interchain disulfide bonds and subunit organization in human serum cholinesterase. *J Biol Chem* **1979,** 254, 8324-8330.

130. Perrier, A. L.; Massoulie, J.; Krejci, E. PRiMA: the membrane anchor of acetylcholinesterase in the brain. *Neuron* **2002,** 33, 275-285.

131. Feng, G.; Krejci, E.; Molgo, J.; Cunningham, J. M.; Massoulie, J.; Sanes, J. R. Genetic analysis of collagen Q: roles in acetylcholinesterase and butyrylcholinesterase assembly and in synaptic structure and function. *J Cell Biol* **1999,** 144, 1349-1360.

132. Bon, S.; Coussen, F.; Massoulie, J. Quaternary associations of acetylcholinesterase. II. The polyproline attachment domain of the collagen tail. *J Biol Chem* **1997,** 272, 3016-3021.

133. Silk, E.; King, J.; Whittaker, M. Scientific Review No. 5. Assay of cholinesterase in clinical chemistry. *Ann Clin Biochem* **1979,** 16, 57-75.

134. Darvesh, S.; Grantham, D. L.; Hopkins, D. A. Distribution of butyrylcholinesterase in the human amygdala and hippocampal formation. *J Comp Neurol* **1998,** 393, 374-90.

135. Vigny, M.; Gisiger, V.; Massoulie, J. "Nonspecific" cholinesterase and acetylcholinesterase in rat tissues: molecular forms, structural and catalytic properties, and significance of the two enzyme systems. *Proc Natl Acad Sci U S A* **1978,** 75, 2588-2592.

136. Burgen, A.; Chipman, L. Cholinesterase and succinic dehydrogenase in the central nervous system of the dog. *J Physiol* **1951,** 114, 296-305.

137. McTiernan, C.; Adkins, S.; Chatonnet, A.; Vaughan, T. A.; Bartels, C. F.; Kott, M.; Rosenberry, T. L.; La Du, B. N.; Lockridge, O. Brain cDNA clone for human cholinesterase. *Proc Natl Acad Sci U S A* **1987,** 84, 6682-6686.

138. Darvesh, S.; Hopkins, D. A. Differential distribution of butyrylcholinesterase and acetylcholinesterase in the human thalamus. *J Comp Neurol* **2003,** 463, 25-43.

139. Duysen, E. G.; Li, B.; Xie, W.; Schopfer, L. M.; Anderson, R. S.; Broomfield, C. A.; Lockridge, O. Evidence for nonacetylcholinesterase targets of organophosphorus nerve agent: supersensitivity of acetylcholinesterase knockout mouse to VX lethality. *J Pharmacol Exp Ther* **2001,** 299, 528-535.

140. Chatonnet, F.; Boudinot, E.; Chatonnet, A.; Taysse, L.; Daulon, S.; Champagnat, J.; Foutz, A. S. Respiratory survival mechanisms in acetylcholinesterase knockout mouse. *Eur J Neurosci* **2003,** 18, 1419-1427.

141. Li, B.; Duysen, E. G.; Carlson, M.; Lockridge, O. The butyrylcholinesterase knockout mouse as a model for human butyrylcholinesterase deficiency. *J Pharmacol Exp Ther* **2008,** 324, 1146-1154.

142. Sternfeld, M.; Rachmilewitz, J.; Loewenstein-Lichtenstein, Y.; Andres, C.; Timberg, R.; Ben-Ari, S.; Glick, C.; Soreq, H.; Zakut, H. Normal and atypical butyrylcholinesterases in placental development, function, and malfunction. *Cell Mol Neurobiol* **1997,** 17, 315-332.

143. Layer, P. G.; Allebrandt, K.; Andermann, P.; Bodur, E.; Boopathy, R.; Bytyqi, A. H.; Paraoanu, L. E. On the multifunctionality of cholinesterases. *Chem Biol Interact* **2005,** 157-158, 37-41.

144. Xie, W.; Stribley, J. A.; Chatonnet, A.; Wilder, P. J.; Rizzino, A.; McComb, R. D.; Taylor, P.; Hinrichs, S. H.; Lockridge, O. Postnatal developmental delay and supersensitivity to organophosphate in gene-targeted mice lacking acetylcholinesterase. *J Pharmacol Exp Ther* **2000,** 293, 896-902.

145. Brimijoin, S.; Koenigsberger, C. Cholinesterases in neural development: new findings and toxicologic implications. *Environ Health Perspect* **1999,** 107 Suppl 1, 59-64.

146. Behra, M.; Cousin, X.; Bertrand, C.; Vonesch, J. L.; Biellmann, D.; Chatonnet, A.; Strahle, U. Acetylcholinesterase is required for neuronal and muscular development in the zebrafish embryo. *Nat Neurosci* **2002,** 5, 111-118.

147. Kalman, J.; Juhasz, A.; Rakonczay, Z.; Abraham, G.; Zana, M.; Boda, K.; Farkas, T.; Penke, B.; Janka, Z. Increased serum butyrylcholinesterase activity in type IIb hyperlipidaemic patients. *Life Sci* **2004,** 75, 1195-1204.

148. Abbott CA; Mackness MI; Kumar S; Olukoga AO; Gordon C; Arrol S; Bhatnagar D; Boulton AJ; PN., D. Relationship between serum butyrylcholinesterase activity, hypertriglyceridaemia and insulin sensitivity in diabetes mellitus. *Clin Sci* **1993,** 85, 77-81.

149. Rustemeijer, C.; Schouten, J. A.; Voerman, H. J.; Beynen, A. C.; Donker, A. J.; Heine, R. J. Is pseudocholinesterase activity related to markers of triacylglycerol synthesis in Type II diabetes mellitus? *Clin Sci (Lond)* **2001,** 101, 29-35.

150. Sridhar, G. R.; Nirmala, G.; Apparao, A.; Madhavi, A. S.; Sreelatha, S.; Rani, J. S.; Vijayalakshmi, P. Serum butyrylcholinesterase in type 2 diabetes mellitus: a biochemical and bioinformatics approach. *Lipids Health Dis* **2005,** 4, 18.

151. Randell, E. W.; Mathews, M. S.; Zhang, H.; Seraj, J. S.; Sun, G. Relationship between serum butyrylcholinesterase and the metabolic syndrome. *Clin Biochem* **2005,** 38, 799-805.

152. Alcântara VM; Chautard-Freire-Maia EA; Scartezini M, C. M.; Braun-Prado K; G., P. Butyrylcholinesterase activity and risk factors for coronary artery disease. *Scand J Clin Lab Invest* **2002,** 62, 399-404.

153. La Du, B. Plasma esterase activity and the metabolism of drugs with ester groups. *Ann N Y Acad Sci* **1971,** 179, 684-694.

154. Kalow, W.; Genest, K. A method for the detection of atypical forms of human serum cholinesterase; determination of dibucaine numbers. *Can J Biochem Physiol* **1957,** 35, 339-346.

155. Arpagaus, M.; Kott, M.; Vatsis, K. P.; Bartels, C. F.; La Du, B. N.; Lockridge, O. Structure of the gene for human butyrylcholinesterase. Evidence for a single copy. *Biochem* **1990,** 29, 124-131.

156. Neville, L. F.; Gnatt, A.; Padan, R.; Seidman, S.; Soreq, H. Anionic site interactions in human butyrylcholinesterase disrupted by two single point mutations. *J Biol Chem* **1990,** 265, 20735-20738.

157. Bartels, C. F.; Jensen, F. S.; Lockridge, O.; van der Spek, A. F.; Rubinstein, H. M.; Lubrano, T.; La Du, B. N. DNA mutation associated with the human butyrylcholinesterase K-variant and its linkage to the atypical variant mutation and other polymorphic sites. *Am J Hum Genet* **1992,** 50, 1086-1103.

158. Rubinstein, H. M.; Dietz, A. A.; Lubrano, T. E1k, another quantitative variant at cholinesterase locus 1. *J Med Genet* **1978,** 15, 27-29.

159. Evans, R. T.; Wardell, J. On the identification and frequency of the J and K cholinesterase phenotypes in a Caucasian population. *J Med Genet* **1984,** 21, 99-102.

160. Bartels, C. F.; James, K.; La Du, B. N. DNA mutations associated with the human butyrylcholinesterase J-variant. *Am J Hum Genet* **1992,** 50, 1104-1114.

161. Lehmann, D. J.; Johnston, C.; Smith, A. D. Synergy between the genes for butyrylcholinesterase K variant and apolipoprotein E4 in late-onset confirmed Alzheimer's disease. *Hum Mol Genet* **1997,** 6, 1933-1936.

162. Garry, P. J.; Dietz, A. A.; Lubrano, T.; Ford, C.; James, K.; Rubinstein, H. M. New allele at cholinesterase locus 1. *J Med Genet* **1976,** 13, 38-42.

163. Rubinstein, H. M.; Dietz, A. A.; Lubrano, T.; Garry, P. J. E1j, a quantitative variant at cholinesterase locus 1: immunological evidence. *J Med Genet* **1976,** 13, 43-45.

164. Jensen, F. S.; Bartels, C. F.; La Du, B. N. Structural basis of the butyrylcholinesterase H-variant segregating in two Danish families. *Pharmacogenetics* **1992,** 2, 234-240.

165. Whittaker, M.; Britten, J. J. E1h, a new allele at cholinesterase locus 1. *Hum Hered* **1987,** 37, 54-58.

166. Liddell, J.; Lehmann, H.; Silk, E. A 'silent' pseudo-cholinesterase gene. *Nature* **1962,** 193, 561-562.

167. Manoharan, I.; Kuznetsova, A.; Fisk, J. D.; Boopathy, R.; Lockridge, O.; Darvesh, S. Comparison of cognitive functions between people with silent and wild-type butyrylcholinesterase. *J Neural Transm* **2007,** 114, 939-945.

168. Primo-Parmo, S. L.; Bartels, C. F.; Wiersema, B.; van der Spek, A. F.; Innis, J. W.; La Du, B. N. Characterization of 12 silent alleles of the human butyrylcholinesterase (BCHE) gene. *Am J Hum Genet* **1996,** 58, 52-64.

169. Arpagaus, M.; Chatonnet, A.; Masson, P.; Newton, M.; Vaughan, T. A.; Bartels, C. F.; Nogueira, C. P.; La Du, B. N.; Lockridge, O. Use of the polymerase chain reaction for homology probing of butyrylcholinesterase from several vertebrates. *J Biol Chem* **1991,** 266, 6966-6974.

170. Wierdl, M.; Morton, C. L.; Danks, M. K.; Potter, P. M. Isolation and characterization of a cDNA encoding a horse liver butyrylcholinesterase: evidence for CPT-11 drug activation. *Biochem Pharmacol* **2000,** 59, 773-781.

171. Rachinsky, T. L.; Camp, S.; Li, Y.; Ekstrom, T. J.; Newton, M.; Taylor, P. Molecular cloning of mouse acetylcholinesterase: tissue distribution of alternatively spliced mRNA species. *Neuron* **1990,** 5, 317-327.

172. Chung, S. Y.; Moriyama, T.; Uezu, E.; Uezu, K.; Hirata, R.; Yohena, N.; Masuda, Y.; Kokubu, T.; Yamamoto, S. Administration of phosphatidylcholine increases brain acetylcholine concentration and improves memory in mice with dementia. *J Nutr* **1995,** 125, 1484-1489.

173. Higgins, J. P.; Flicker, L. Lecithin for dementia and cognitive impairment. *Cochrane Database Syst Rev* **2003**, CD001015.

174. Fioravanti, M.; Yanagi, M. Cytidinediphosphocholine (CDP-choline) for cognitive and behavioural disturbances associated with chronic cerebral disorders in the elderly. *Cochrane Database Syst Rev* **2005**, CD000269.

175. Secades, J. J.; Lorenzo, J. L. Citicoline: pharmacological and clinical review, 2006 update. *Methods Find Exp Clin Pharmacol* **2006,** 28 Suppl B, 1-56.

176. Parnetti, L.; Amenta, F.; Gallai, V. Choline alphoscerate in cognitive decline and in acute cerebrovascular disease: an analysis of published clinical data. *Mech Ageing Dev* **2001,** 122, 2041-2055.

177. Jossan, S. S.; Adem, A.; Winblad, B.; Oreland, L. Characterisation of dopamine and serotonin uptake inhibitory effects of tetrahydroaminoacridine in rat brain. *Pharmacol Toxicol* **1992,** 71, 213-215.

178. Knapp, M. J.; Knopman, D. S.; Solomon, P. R.; Pendlebury, W. W.; Davis, C. S.; Gracon, S. I. A 30-week randomized controlled trial of high-dose tacrine in patients with Alzheimer's disease. The Tacrine Study Group. *JAMA* **1994,** 271, 985-991.

179. Wong WJ; Liu HC; Fuh JL; Wang SJ; Hsu LC; Wang PN; WY., S. A double-blind, placebo-controlled study of tacrine in Chinese patients with Alzheimer's disease. *Dement Geriatr Cogn Disord* **1999,** 10, 289-294.

180. Maltby, N.; Broe, G. A.; Creasey, H.; Jorm, A. F.; Christensen, H.; Brooks, W. S. Efficacy of tacrine and lecithin in mild to moderate Alzheimer's disease: double blind trial. *BMJ* **1994,** 308, 879-883.

181. Mohs, R. C.; Doody, R. S.; Morris, J. C.; Ieni, J. R.; Rogers, S. L.; Perdomo, C. A.; Pratt, R. D. A 1-year, placebo-controlled preservation of function survival study of donepezil in AD patients. *Neurology* **2001,** 57, 481-488.

182. Seltzer, B.; Zolnouni, P.; Nunez, M.; Goldman, R.; Kumar, D.; Ieni, J.; Richardson, S. Efficacy of donepezil in early-stage Alzheimer disease: a randomized placebo-controlled trial. *Arch Neurol* **2004,** 61, 1852-1856.

183. Winblad, B.; Kilander, L.; Eriksson, S.; Minthon, L.; Batsman, S.; Wetterholm, A. L.; Jansson-Blixt, C.; Haglund, A. Donepezil in patients with severe Alzheimer's disease: double-blind, parallel-group, placebo-controlled study. *Lancet* **2006,** 367, 1057-1065.

184. Raina, P.; Santaguida, P.; Ismaila, A.; Patterson, C.; Cowan, D.; Levine, M.; Booker, L.; Oremus, M. Effectiveness of cholinesterase inhibitors and memantine for treating dementia: evidence review for a clinical practice guideline. *Ann Intern Med* **2008,** 148, 379-397.

185. Forette, F.; Anand, R.; Gharabawi, G. A phase II study in patients with Alzheimer's disease to assess the preliminary efficacy and maximum tolerated dose of rivastigmine (Exelon). *Eur J Neurol* **1999,** 6, 423-429.

186. Figiel, G. S.; Sadowsky, C. H.; Strigas, J.; Koumaras, B.; Meng, X.; Gunay, I. Safety and efficacy of rivastigmine in patients with Alzheimer's disease not responding adequately to donepezil: an open-label study. *Prim Care Companion of J Clin Psychiatry* **2007,** 10, 291-298.

187. Raskind, M. A.; Peskind, E. R.; Wessel, T.; Yuan, W. Galantamine in AD: A 6-month randomized, placebo-controlled trial with a 6-month extension. The Galantamine USA-1 Study Group. *Neurology* **2000,** 54, 2261-2268.

188. Raskind, M. A.; Peskind, E. R.; Truyen, L.; Kershaw, P.; Damaraju, C. V. The cognitive benefits of galantamine are sustained for at least 36 months: a long-term extension trial. *Arch Neurol* **2004,** 61, 252-256.

189. van Dyck, C. H.; Newhouse, P.; Falk, W. E.; Mattes, J. A. Extended-release physostigmine in Alzheimer disease: a multicenter, double-blind, 12-week study with dose enrichment. Physostigmine Study Group. *Arch Gen Psychiatry* **2000,** 57, 157-164.

190. Thal, L. J.; Ferguson, J. M.; Mintzer, J.; Raskin, A.; Targum, S. D. A 24-week randomized trial of controlled-release physostigmine in patients with Alzheimer's disease. *Neurology* **1999,** 52, 1146-1152.

191. Francis, P. T. Glutaminergic systems in Alzheimer's disease. *Int J Geriatr Psychiatry* **2003,** 18, S15-21.

192. Reisberg, B.; Doody, R.; Stoffler, A.; Schmitt, F.; Ferris, S.; Mobius, H. J. Memantine in moderate-to-severe Alzheimer's disease. *N Engl J Med* **2003,** 348, 1333-1341.

193. Orgogozo, J. M.; Rigaud, A. S.; Stoffler, A.; Mobius, H. J.; Forette, F. Efficacy and safety of memantine in patients with mild to moderate vascular dementia: a randomized, placebo-controlled trial (MMM 300). *Stroke* **2002,** 33, 1834-1839.

194. Akiyama, H.; Barger, S.; Barnum, S.; Bradt, B.; Bauer, J.; Cole, G. M.; Cooper, N. R.; Eikelenboom, P.; Emmerling, M.; Fiebich, B. L.; Finch, C. E.; Frautschy, S.; Griffin, W. S.; Hampel, H.; Hull, M.; Landreth, G.; Lue, L.; Mrak, R.; Mackenzie, I. R.; McGeer, P. L.; O'Banion, M. K.; Pachter, J.; Pasinetti, G.; Plata-Salaman, C.; Rogers, J.; Rydel, R.; Shen, Y.; Streit, W.; Strohmeyer, R.; Tooyoma, I.; Van Muiswinkel, F. L.; Veerhuis, R.; Walker, D.; Webster, S.; Wegrzyniak, B.; Wenk, G.; Wyss-Coray, T. Inflammation and Alzheimer's disease. *Neurobiol Aging* **2000,** 21, 383-421.

195. Kitamura, Y.; Shimohama, S.; Koike, H.; Kakimura, J.; Matsuoka, Y.; Nomura, Y.; Gebicke-Haerter, P. J.; Taniguchi, T. Increased expression of cyclooxygenases and peroxisome proliferator-activated receptor-gamma in Alzheimer's disease brains. *Biochem Biophys Res Commun* **1999,** 254, 582-586.

196. Pasinetti, G. M.; Aisen, P. S. Cyclooxygenase-2 expression is increased in frontal cortex of Alzheimer's disease brain. *Neuroscience* **1998,** 87, 319-324.

197. in 't Veld, B. A.; Launer, L. J.; Breteler, M. M.; Hofman, A.; Stricker, B. H. Pharmacologic agents associated with a preventive effect on Alzheimer's disease: a review of the epidemiologic evidence. *Epidemiol Rev* **2002,** 24, 248-268.

198. in 't Veld, B. A.; Launer, L. J.; Hoes, A. W.; Ott, A.; Hofman, A.; Breteler, M. M.; Stricker, B. H. NSAIDs and incident Alzheimer's disease. The Rotterdam Study. *Neurobiol Aging* **1998,** 19, 607-611.

199. Schmiedeskamp, M. Preventing good brains from going bad. *Sci Am* **2004,** 14, 84-91.

200. Waring, S. C.; Rocca, W. A.; Petersen, R. C.; O'Brien, P. C.; Tangalos, E. G.; Kokmen, E. Postmenopausal estrogen replacement therapy and risk of AD: a population-based study. *Neurology* **1999,** 52, 965-970.

201. Mulnard, R. A.; Cotman, C. W.; Kawas, C.; van Dyck, C. H.; Sano, M.; Doody, R.; Koss, E.; Pfeiffer, E.; Jin, S.; Gamst, A.; Grundman, M.; Thomas, R.; Thal, L. J. Estrogen replacement therapy for treatment of mild to moderate Alzheimer disease: a randomized controlled trial. Alzheimer's Disease Cooperative Study. *Jama* **2000,** 283, 1007-1015.

202. Emilien, G.; Beyreuther, K.; Masters, C. L.; Maloteaux, J. M. Prospects for pharmacological intervention in Alzheimer disease. *Arch Neurol* **2000,** 57, 454-459.

203. Gaynor, J. M. Synthesis and testing of a novel class of cholinesterase inhibitors. Athlone, Athlone, 2005.

204. Gilmer, J. F.; Moriarty, L. M.; Lally, M. N.; Clancy, J. M. Isosorbide-based aspirin prodrugs. II. Hydrolysis kinetics of isosorbide diaspirinate. *Eur J Pharm Sci* **2002,** 16, 297-304.

205. Dillon, G. The synthesis and biological evaluation of a novel class of butyrylcholinesterase inhibitors using isosorbide as a building block. Trinity College Dublin, Dublin, 2007.

206. Ecobichon, D. J. Characterization of the esterases of canine serum. *Can J Biochem* **1970,** 48, 1359-1367.

207. Rogers, D. C.; Fisher, E. M.; Brown, S. D.; Peters, J.; Hunter, A. J.; Martin, J. E. Behavioral and functional analysis of mouse phenotype: SHIRPA, a proposed protocol for comprehensive phenotype assessment. *Mamm Genome* **1997,** 8, 711-713.

208. O'Brien, P. J.; Irwin, W.; Diaz, D.; Howard-Cofield, E.; Krejsa, C. M.; Slaughter, M. R.; Gao, B.; Kaludercic, N.; Angeline, A.; Bernardi, P.; Brain, P.; Hougham, C. High concordance of drug-induced human hepatotoxicity with in vitro cytotoxicity measured in a novel cell-based model using high content screening. *Arch Toxicol* **2006,** 80, 580-604.

209. Reddy, G. R.; Kumar, T. P.; Mohan, P. M.; Babu, K. S. Diurnal variations in physiological activities in the garden snail, Cryptozona ligulata. *J Comp Physiol A: Neuroethol Sens Neural Behav Physiol* **1978,** 125, 59-66.

210. Lechin, F.; Pardey-Maldonado, B.; van der Dijs, B.; Benaim, M.; Baez, S.; Orozco, B.; Lechin, A. E. Circulating neurotransmitters during the different wake-sleep stages in normal subjects. *Psychoneuroendocrinology* **2004,** 29, 669-685.

211. Sidell, F. R.; Kaminskis, A. Influence of age, sex and oral contraceptives on human blood cholinesterase activity. *Clin Chem* **1975,** 21, 1393-1395.

212. Roy, C. G., G.; Chamoulaud, S.; Rivière, J. L. Plasma esterase activities in european human raptors. *J Wildl Dis,* **2005,** 41, 184-208.

213. Ecobichon, D. J.; Comeau, A. M. Pseudocholinesterases of mammalian plasma: physicochemical properties and organophosphate inhibition in eleven species. *Toxicol Appl Pharmacol* **1973,** 24, 92-100.

214. Ellman, G. L.; Courtney, K. D.; Andres, V., Jr.; Feather-Stone, R. M. A new and rapid colorimetric determination of acetylcholinesterase activity. *Biochem Pharmacol* **1961,** 7, 88-95.

215. Turner, J. M.; Hall, R. A.; Whittaker, M.; Kricka, L. J. Effects of storage and repeated freezing and thawing on plasma cholinesterase activity. *Ann Clin Biochem* **1984,** 21 (Pt 5), 363-365.

216. Irwin, S. Drug Screening and Evaluative Procedures: Current approaches do not provide the information needed for properly predicting drug effects in man. *Science* **1962,** 136, 123-128.

217. Shaw, G. G. Some shortcomings of direct intraventricular injection in mice. *Br J Pharmacol* **1974,** 50, 603-605.

218. Doyle, K. M. Neurotoxic Effects of the Polyamines. Trinity College Dublin, Dublin, 1993.

219. Bioseb In Vivo Research Instruments. [cited May 16 2008]. Available from: http://www.bioseb.com/bioseb/pages/objets/image/item/GR_it.jpg.

220. Flecknall, P. *Laboratory animal anaesthesia: an introduction for research workers and technicians*. 2nd ed.; Academic Press: London, 1987.

221. Birkett, D. J. *Pharmacokinetics made easy.* 2nd ed.; McGraw-Hill: Sydney, 2002; p 88.

222. Feldmann, D.; Flandrois, C.; Jardel, A.; Phan, T. M.; Aymard, P. Circadian variations and reference intervals for some enzymes in urine of healthy children. *Clin Chem* **1989,** 35, 864-867.

223. Arsaradnam, M. P.; Morgan, L.; Wright, J.; Gama, R. Diurnal variation in lipoprotein lipase activity. *Ann Clin Biochem* **2002,** 39, 136-139.

224. Augustinsson, K. B. Electrophoresis studies on blood plasma esterases. *Acta Chemica Scandinavica* **1959,** 13, 1097-1105.

225. Li, B.; Sedlacek, M.; Manoharan, I.; Boopathy, R.; Duysen, E. G.; Masson, P.; Lockridge, O. Butyrylcholinesterase, paraoxonase, and albumin esterase, but not carboxylesterase, are present in human plasma. *Biochem Pharmacol* **2005,** 70, 1673-1684.

226. Augustinsson, K. B. The normal variation of human blood cholinesterase activity. *Acta Physiol Scand* **1955,** 35, 40-52.

227. Robertson, G. S. Serum protein and cholinesterase changes in association with contraceptive pills. *Lancet* **1967,** 1, 232-235.

228. Lepage, L.; Schiele, F.; Gueguen, R.; Slest, G. Total cholinesterase in plasma: Biological variations and reference limits. *Clin Chem* **1985,** 31, 546-550.

229. Redderson, C. L. Interactions of steroids and serum cholinesterase. *Int J Clin Pharmacol* **1973,** 8, 51-57.

230. Worek, F.; Reiter, G.; Eyer, P.; Szinicz, L. Reactivation kinetics of acetylcholinesterase from different species inhibited by highly toxic organophosphates. *Arch Toxicol* **2002,** 76, 523-529.

231. Weisner, J.; Kriz, Z.; Kuca, K.; Jun, D.; Koca, J. Acetylcholinesterase: the structural similarities and differences. *J Enzyme Inhib Med Chem.* **2007,** 22, 417-424.

232. Satoh, T. Toxicological implications of esterases--from molecular structures to functions. *Toxicol Appl Pharmacol* **2005,** 207, S11-S18.

233. IPHA Medicines Compendium. 2008. [cited Jul 26 2008]. Available in: www.medicines.ie

234. Gugler, R.; Lain, P.; Azarnoff, D. L. Effect of portacaval shunt on the disposition of drugs with and without first-pass effect. *J Pharmacol Exp Ther* **1975,** 195, 416-423.

235. Hirayama, H.; Morgado, J.; Gasinska, I.; Pang, K. S. Estimations of intestinal and liver first-pass metabolism in vivo. Studies on gentisamide conjugation in the rat. . *Drug Metab Dispos* **1990,** 18, 588-594.

236. Kourounakis, P. N.; Rekka, E. *Advanced drug design and development: a medicinal chemistry approach.* Routledge: USA, 1994.

237. Kim, S. G.; Sohn, Y.; Yoo, J. K.; Lee, J. W.; Liem, A.; Miller, J. A. Inhibition of vinyl carbamate-induced hepatotoxicity, mutagenicity, tumorgenicity by isopropyl-2-(1,3-dithietane-2-ylidene)-2-[N-(4-methylthiazol-2-yl)carbamoyl]acetate YH439 *Carcinogenesis* **1998,** 19, 687-690.

238. Bolognesi, M. L.; Bartolini, M.; Cavalli, A.; Andrisano, V.; Rosini, M.; Minarini, A.; Melchiorre, C. Design, synthesis, and biological evaluation of conformationally restricted rivastigmine analogues. *J Med Chem* **2004,** 47, 5945-5952.

239. Greig, N. H.; Yu, Q.; Zhu, X.; Holloway, H. W.; Perry, T.; Lee, B.; Ingram, D. K.; Lahiri, D. K. A new therapeutic target in Alzheimer's disease treatment: attention to butyrylcholinesterase. *Curr Med Res Opin.* **2001,** 17, 159-165.

240. Cahill, A. L.; Ehret, C. F. Circadian variations in the activity of tyrosine hydroxylase, tyrosine aminotransferase, and tryptophan hydroxylase: relationship to catecholamine metabolism. *J Neurochem* **1981,** 37, 1109-1115.

241. Mizuno, T.; Arita, J.; Kimura, F. Spontaneous acetylcholine release in the hippocampus exhibits a diurnal variation in both young and old rats. *Neurosci Lett* **1994,** 178, 271-274.

242. Voshchinina, O. N. [Circadian rhythms in the functional activity of rat brain capillaries]. *Arkh Anat Gistol Embriol* **1978,** 75, 56-59.

243. Lucic Vrdoljak, A.; Bradamante, V.; Radic, B.; Peraica, M.; Fuchs, R.; Reiner, Z. Butyrylcholinesterase activity and plasma lipids in dexamethasone treated rats. *Acta Pharm* **2005,** 55, 177-185.

244. Pearson, R. C.; Gatter, K. C.; Brodal, P.; Powell, T. P. The projection of the basal nucleus of Meynert upon the neocortex in the monkey. *Brain Res* **1983,** 259, 132-136.

245. Whitehouse, P. J.; Price, D. L.; Clark, A. W.; Coyle, J. T.; DeLong, M. R. Alzheimer disease: evidence for selective loss of cholinergic neurons in the nucleus basalis. *Ann Neurol* **1981,** 10, 122-126.

246. Kristt, D. A.; McGowan, R. A., Jr.; Martin-MacKinnon, N.; Solomon, J. Basal forebrain innervation of rodent neocortex: studies using acetylcholinesterase histochemistry, Golgi and lesion strategies. *Brain Res* **1985,** 337, 19-39.

247. Cho, Y. H.; Friedman, E.; Silva, A. J. Ibotenate lesions of the hippocampus impair spatial learning but not contextual fear conditioning in mice. *Behav Brain Res* **1999,** 98, 77-87.

248. Giovannelli, L.; Casamenti, F.; Scali, C.; Bartolini, L.; Pepeu, G. Differential effects of amyloid peptides beta-(1-40) and beta-(25-35) injections into the rat nucleus basalis. *Neuroscience* **1995,** 66, 781-792.

249. Ogawa, M.; Iida, Y.; Nakagawa, M.; Kuge, Y.; Kawashima, H.; Tominaga, A.; Ueda, M.; Magata, Y.; Saji, H. Change of central cholinergic receptors following lesions of nucleus basalis magnocellularis in rats: search for an imaging index suitable for the early detection of Alzheimer's disease. *Nucl Med Biol* **2006,** 33, 249-254.

250. Hohmann, C. F.; Coyle, J. T. Long-term effects of basal forebrain lesions on cholinergic, noradrenergic and serotonergic markers in mouse neocortex. *Brain Res Bull* **1988,** 21, 13-20.

251. Hohmann, C. F.; Berger-Sweeney, J. Sexually dimorphic responses to neonatal basal forebrain lesions in mice: II. Cortical morphology. *J Neurobiol* **1998,** 37, 595-606.

252. Conor, D. J.; Langleis, P. J.; Thal, L. J. Behavioural impairments after lesions of the nucleus basalis by ibotenic acid and quisqualic acid. *Brain Res* **1991,** 555, 84-90.

253. Casamenti, F.; Prosperi, C.; Scali, C.; Giovannelli, L.; Pepeu, G. Morphological, biochemical and behavioural changes induced by neurotoxic and inflammatory insults to the nucleus basalis. *Int J Dev Neurosci* **1998,** 16, 705-714.

254. Puolivali, J.; Miettinen, R.; Pradier, L.; Riekkinen, P., Jr. Apolipoprotein E-deficient mice are not more susceptible to the biochemical and memory deficits induced by nucleus basalis lesion. *Neuroscience* **2000,** 96, 291-297.

255. Bioresources Unit TCD. 2008. The peri-operative use of NSAID analgesia in rats and mice. [cited May 15 2008]. Available from: http://www.tcd.ie/BioResources/documents_general/drug_dosage_in_use_in_bru.htm.

256. Chauveau, F.; Celerier, A.; Ognard, R.; Pierard, C.; Beracochea, D. Effects of ibotenic acid lesions of the mediodorsal thalamus on memory: relationship with emotional processes in mice. *Behav Brain Res* **2005,** 156, 215-223.

257. Paxinos, G.; Franklin, K. B. J. *The Mouse Brain in Stereotaxic Coordinates.* 2nd ed.; Academic Press: California, 2004.

258. Morris, R. Spatial localization does not require the presence of local cues. *Learn Motiv* **1981,** 12, 239-260.

259. Sarter, M. Animal cognition: defining the issues. *Neurosci Biobehav Rev* **2004,** 28, 645-650.

260. D'Hooge, R.; De Deyn, P. P. Applications of the Morris water maze in the study of learning and memory. *Brain Res Brain Res Rev* **2001,** 36, 60-90.

261. Maaswinkel, H.; Whishaw, I. Q. Homing with locale, taxon, and dead reckoning strategies by foraging rats: sensory hierarchy in spatial navigation. *Behav Brain Res* **1999,** 99, 143-152.

262. Upchurch, M.; Wehner, J. M. Differences between inbred strains of mice in Morris water maze performance. *Behav Genet* **1988,** 18, 55-68.

263. Petrie, B. F. Learning set spatial navigation performance in three mouse strains. *Psychol Rep* **1995,** 77, 1339-1342.

264. Wahlsten, D.; Cooper, S. F.; Crabbe, J. C. Different rankings of inbred mouse strains on the Morris maze and a refined 4-arm water escape task. *Behav Brain Res* **2005,** 165, 36-51.

265. Wright, J. W.; Alt, J. A.; Turner, G. D.; Krueger, J. M. Differences in spatial learning comparing transgenic p75 knockout, New Zealand Black, C57BL/6, and Swiss Webster mice. *Behav Brain Res* **2004,** 153, 453-458.

266. Van Dam, D.; Lenders, G.; De Deyn, P. P. Effect of Morris water maze diameter on visual-spatial learning in different mouse strains. *Neurobiol Learn Mem* **2006,** 85, 164-172.

267. Random Org. 1998-2008. [cited Jul 30 2008]. Available from: http://www.random.org.

268. Ennaceur, A.; Delacour, J. A new one-trial test for neurobiological studies of memory in rats. 1: Behavioral data. *Behav Brain Res* **1988,** 31, 47-59.

269. Silvers, J. M.; Harrod, S. B.; Mactutus, C. F.; Booze, R. M. Automation of the novel object recognition task for use in adolescent rats. *J Neurosci Methods* **2007,** 166, 99-103.

270. Bevins, R. A.; Besheer, J. Object recognition in rats and mice: a one-trial non-matching-to-sample learning task to study 'recognition memory'. *Nat Protoc* **2006,** 1, 1306-1311.

271. Middei, S.; Daniele, S.; Caprioli, A.; Ghirardi, O.; Ammassari-Teule, M. Progressive cognitive decline in a transgenic mouse model of Alzheimer's disease overexpressing mutant hAPPswe. *Genes Brain Behav* **2006,** 5, 249-256.

272. Wellman, C. L.; Pelleymounter, M. A. Differential effects of nucleus basalis lesions in young adult and aging rats. *Neurobiol Aging* **1999,** 20, 381-393.

273. Ridley, R. M.; Baker, H. F.; Drewett, B.; Johnson, J. A. Effects of ibotenic acid lesions of the basal forebrain on serial reversal learning in marmosets. *Psychopharmacology* **1985,** 86, 438-443.

274. Janas, A. M.; Cunningham, S. C.; Duffy, K. B.; Devan, B. D.; Greig, N. H.; Holloway, H. W.; Yu, Q. S.; Markowska, A. L.; Ingram, D. K.; Spangler, E. L. The cholinesterase inhibitor, phenserine, improves Morris water maze performance of scopolamine-treated rats. *Life Sci* **2005,** 76, 1073-1081.

275. Mandel, R. J.; Thal, L. J. Physostigmine improves Morris water maze performance following nucleus basalis magnocellularis lesions in rats. *Psychopharmacology* **1988,** 96, 421-425.

276. Holmstedt, B. Distribution and determination of cholinesterases in mammals. *Bull World Health Organ* **1971,** 44, 99-107.

277. Pugovkin, A. P.; Artem'eva, A. I.; Lazarev, S. G. [Resistance and capacity function of blood vessels of the brain during activation of its cholinergic mechanisms]. *Biull Eksp Biol Med* **1992,** 113, 3-5.

278. Peruzzi, P.; Borredon, J.; Seylaz, J.; Lacombe, P. Tacrine overcompensates for the decreased blood flow induced by basal forebrain lesion in the rat. *Neuroreport* **1996,** 8, 103-108.

279. Clinton, L. K.; Billings, L. M.; Green, K. N.; Caccamo, A.; Ngo, J.; Oddo, S.; McGaugh, J. L.; LaFerla, F. M. Age-dependent sexual dimorphism in cognition and stress response in the 3xTg-AD mice. *Neurobiol Dis* **2007,** 28, 76-82.

280. Stefansson, H.; Sigurdsson, E.; Steinthorsdottir, V.; Bjornsdottir, S.; Sigmundsson, T.; Ghosh, S.; Brynjolfsson, J.; Gunnarsdottir, S.; Ivarsson, O.; Chou, T. T.; Hjaltason, O.; Birgisdottir, B.; Jonsson, H.; Gudnadottir, V. G.; Gudmundsdottir, E.; Bjornsson, A.; Ingvarsson, B.; Ingason, A.; Sigfusson, S.; Hardardottir, H.; Harvey, R. P.; Lai, D.; Zhou, M.; Brunner, D.; Mutel, V.; Gonzalo, A.; Lemke, G.; Sainz, J.; Johannesson, G.; Andresson, T.; Gudbjartsson, D.; Manolescu, A.; Frigge, M. L.; Gurney, M. E.; Kong, A.; Gulcher, J. R.; Petursson, H.; Stefansson, K. Neuregulin 1 and susceptibility to schizophrenia. *Am J Hum Genet* **2002,** 71, 877-892.

281. Rispoli, V.; Rotiroti, D.; Carelli, V.; Liberatore, F.; Scipione, L.; Marra, R.; Giorgioni, G.; Di Stefano, A. Choline pivaloyl esters improve in rats cognitive and memory performances impaired by scopolamine treatment or lesions of the nucleus basalis of Meynert. *Neurosci Lett* **2004,** 356, 199-202.

282. Ballmaier, M.; Casamenti, F.; Scali, C.; Mazzoncini, R.; Zoli, M.; Pepeu, G.; Spano, P. F. Rivastigmine antagonizes deficits in prepulse inhibition induced by selective immunolesioning of cholinergic neurons in nucleus basalis magnocellularis. *Neuroscience* **2002,** 114, 91-98.

283. Lindner, M. D. Reliability, Distribution, and validity of age-related cognitive deficits in the Morris water maze. *Neurobiol Learn Mem* **1997,** 68, 203-220.

284. Oliverio, A.; Bovet, D. Effects of Age on Maze Learning and Avoidance Conditioning in Mice. *Life Sci* **1966**, 1317-1324.

285. Winocur, G.; Moscovitch, M. Hippocampal and prefrontal cortex contributions to learning and memory: analysis of lesion and aging effects on maze learning in rats. *Behav Neurosci* **1990,** 104, 544-551.

286. Chappell, J.; McMahan, R.; Chiba, A.; Gallagher, M. A re-examination of the role of basal forebrain cholinergic neurons in spatial working memory. *Neuropharmacology* **1998,** 37, 481-487.

287. Cerbai, F.; Giovannini, M. G.; Melani, C.; Enz, A.; Pepeu, G. N1phenethyl-norcymserine, a selective butyrylcholinesterase inhibitor, increases acetylcholine release in rat cerebral cortex: a comparison with donepezil and rivastigmine. *Eur J Pharmacol* **2007,** 572, 142-150.

288. Greig, N. H.; Utsuki, T.; Ingram, D. K.; Wang, Y.; Pepeu, G.; Scali, C.; Yu, Q. S.; Mamczarz, J.; Holloway, H. W.; Giordano, T.; Chen, D.; Furukawa, K.; Sambamurti, K.; Brossi, A.; Lahiri, D. K. Selective butyrylcholinesterase inhibition elevates brain acetylcholine, augments learning and lowers Alzheimer beta-amyloid peptide in rodent. *Proc Natl Acad Sci U S A* **2005,** 102, 17213-17218.

289. Braida, D.; Paladini, E.; Griffini, P.; Lamperti, M.; Maggi, A.; Sala, M. An inverted U-shaped curve for heptylphysostigmine on radial maze performance in rats: comparison with other cholinesterase inhibitors. *Eur J Pharmacol* **1996,** 302, 13-20.

290. Sweeney, J. E.; Bachman, E. S.; Coyle, J. T. Effects of different doses of galanthamine, a long-acting acetylcholinesterase inhibitor, on memory in mice. *Psychopharmacology (Berl)* **1990,** 102, 191-200.

291. Clark, M. G.; Sun, W.; Myers, T. M.; Bansal, R.; Doctor, B. P.; Saxena, A. Effects of physostigmine and human butyrylcholinesterase on acoustic startle reflex and prepulse inhibition in C57BL/6J mice. *Pharmacol Biochem Behav* **2005,** 81, 497-505.

292. Rowlatt, C.; Chesterman, F. C.; Sheriff, M. U. Lifespan, age changes and tumour incidence in an ageing C57BL mouse colony. *Lab Anim* **1976,** 10, 419-442.

293. Frye, C. A.; Walf, A. A. Progesterone enhances performance of aged mice in cortical or hippocampal tasks. *Neurosci Lett* **2008,** 437, 116-120.

294. Berstein, D.; Olton, D. S.; Ingram, D. K.; Waller, S. B.; Reynolds, M. A.; London, E. D. Radial maze performance in young and aged mice: neurochemical correlates. *Pharmacol Biochem Behav* **1985,** 22, 301-307.

295. Benice, T. S.; Rizk, A.; Kohama, S.; Pfankuch, T.; Raber, J. Sex-differences in age-related cognitive decline in C57BL/6J mice associated with increased brain microtubule-associated protein 2 and synaptophysin immunoreactivity. *Neuroscience* **2006,** 137, 413-423.

296. Gallagher, M.; Nicolle, M. M. Animal models of normal aging: relationship between cognitive decline and markers in hippocampal circuitry. *Behav Brain Res* **1993,** 57, 155-162.

297. Geinisman, Y.; Doteleddo-Morrell, L.; Morrell, F.; Heller, R. E. Hippocampal markers of aged-related memory dysfunction: behavioural, electrophysiological and morphological perspectives. *Prog Neurobiol* **1995,** 45, 223-252.

298. Wotjak, C. T. Of mice and men: potentials and caveats of behavioural experiments in mice. *BIF Futura* **2004,** 19, 158-169.

299. Olton, D. S.; Samuelson, R. J. Remembrance of places passed: spatial memory in rats. *J Exp Psychol: Anim Behav Process* **1976,** 2, 97-116.

300. Frick, K. M.; Burlingame, L. A.; Arters, J. A.; Berger-Sweeney, J. Reference memory, anxiety and estrous cyclicity in C57BL/6NIA mice are affected by age and sex. *Neuroscience* **2000,** 95, 293-307.

301. Magnusson, K. R.; Scruggs, B.; Zhao, X.; Hammersmark, R. Age-related declines in a two-day reference memory task are associated with changes in NMDA receptor subunits in mice. *BMC Neurosci* **2007,** 8, 43.

302. Magnusson, K. R.; Scruggs, B.; Aniya, J.; Wright, K. C.; Ontl, T.; Xing, Y.; Bai, L. Age-related deficits in mice performing working memory tasks in a water maze. *Behav Neurosci* **2003,** 117, 485-495.

303. Coffey, P. J.; Gias, C.; McDermott, C. J.; Lundh, P.; Pickering, M. C.; Sethi, C.; Bird, A.; Fitzke, F. W.; Maass, A.; Chen, L. L.; Holder, G. E.; Luthert, P. J.; Salt, T. E.; Moss, S. E.; Greenwood, J. Complement factor H deficiency in aged mice causes retinal abnormalities and visual dysfunction. *Proc Natl Acad Sci U S A* **2007,** 104, 16651-16656.

304. Gray, J. A.; McNaughton, N. Comparison between the behavioural effects of septal and hippocampal lesions: a review. *Neurosci Biobehav Rev* **1983,** 7, 119-188.

305. Xavier, G. F.; Stein, C.; Bueno, O. F. Rats with dorsal hippocampal lesions do react to new stimuli but not to spatial changes of known stimuli. *Behav Neural Biol* **1990,** 54, 172-83.

306. Morris, R. G. M. Place navigation impaired rats with hippocampal lesions. *Nature* **1982,** 297, 681-683.

307. Sutherland, R. J.; Whishaw, I. Q.; Kolb, B. A behavioural analysis of spatial localization following electrolytic, kainate- or colchicine-induced damage to the hippocampal formation in the rat. *Behav Brain Res* **1983,** 7, 133-153.

308. Thinus-Blanc, C.; Save, E.; Rossi-Arnaud, C.; Tozzi, A.; Ammassari-Teule, M. The differences shown by C57BL/6 and DBA/2 inbred mice in detecting spatial novelty are subserved by a different hippocampal and parietal cortex interplay. *Behav Brain Res* **1996,** 80, 33-40.

309. de Brabander, J. M.; Kramers, R. J.; Uylings, H. B. Layer specific dendritic regression of pyramidal cells with ageing in the human prefrontal cortex. *Eur J Neurosci* **1998,** 10, 1261-1269.

310. Simic, G.; Kostovic, I.; Winblad, B.; Bogdanovic, N. Volume and number of neurons of the human hippocampal formation in normal aging and Alzheimer's disease. *J Comp Neurol* **1997,** 379, 482-494.

311. Yavich, L.; Sirvio, J.; Haapalinna, A.; Puumala, T.; Koivisto, E.; Heinonen, E.; Riekkinen, P. J. The systemic administration of tacrine or selegiline facilitate spatial learning in aged fisher 344 rats. *J Neural Transm* **1996,** 103, 619-626.

312. Minkeviciene, R.; Banerjee, P.; Tanila, H. Cognition-enhancing and anxiolytic effects of memantine. *Neuropharmacology* **2008,** 54, 1079-1085.

313. Ohsawa, I.; Nishimaki, K.; Murakami, Y.; Suzuki, Y.; Ishikawa, M.; Ohta, S. Age-dependent neurodegeneration accompanying memory loss in transgenic mice defective in mitochondrial aldehyde dehydrogenase 2 activity. *J Neurosci* **2008,** 28, 6239-6249.

314. Frick, K. M.; Gresack, J. E. Sex differences in the behavioral response to spatial and object novelty in adult C57BL/6 mice. *Behav Neurosci* **2003,** 117, 1283-1291.

315. Save, E.; Poucet, B.; Foreman, N.; Buhot, M. C. Object exploration and reactions to spatial and nonspatial changes in hooded rats following damage to parietal cortex or hippocampal formation. *Behav Neurosci* **1992,** 106, 447-456.

316. Driscoll, I.; Hamilton, D. A.; Petropoulos, H.; Yeo, R. A.; Brooks, W. M.; Baumgartner, R. N.; Sutherland, R. J. The aging hippocampus: cognitive, biochemical and structural findings. *Cereb Cortex* **2003,** 13, 1344-1351.

317. Sargolini, F.; Roullet, P.; Oliverio, A.; Mele, A. Effects of intra-accumbens focal administrations of glutamate antagonists on object recognition memory in mice. *Behav Brain Res* **2003,** 138, 153-163.

318. Bertaina-Anglade, V.; Enjuanes, E.; Morillon, D.; Drieu la Rochelle, C. The object recognition task in rats and mice: a simple and rapid model in safety pharmacology to detect amnesic properties of a new chemical entity. *J Pharmacol Toxicol Methods* **2006,** 54, 99-105.

319. Messier, C. Object recognition in mice: improvement of memory by glucose. *Neurobiol Learn Mem* **1997,** 67, 172-175.

320. Mizumori, S. J.; Rosenzweig, M. R.; Kermisch, M. G. Failure of mice to demonstrate spatial memory in the radial maze. *Behav Neural Biol* **1982,** 35, 33-45.

321. Hyde, L. A.; Hoplight, B. J.; Denenberg, V. H. Water version of the radial-arm maze: learning in three inbred strains of mice. *Brain Res* **1998,** 785, 236-244.

322. Harburger, L. L.; Lambert, T. J.; Frick, K. M. Age-dependent effects of environmental enrichment on spatial reference memory in male mice. *Behav Brain Res* **2007,** 185, 43-48.

323. Ingram, D. K.; Spangler, E. L.; Iijima, S.; Kuo, H.; Bresnahan, E. L.; Greig, N. H.; London, E. D. New pharmacological strategies for cognitive enhancement using a rat model of age-related memory impairment. *Ann N Y Acad Sci* **1994,** 717, 16-32.

324. Greig, N. H.; Lahiri, D. K.; Sambamurti, K. Butyrylcholinesterase: an important new target in Alzheimer's disease therapy. *Int Psychogeriatr* **2002,** 14 Suppl 1, 77-91.

325. Bentivoglio, A. R.; Altavista, M. C.; Granata, R.; Albanese, A. Genetically determined cholinergic deficiency in the forebrain of C57BL/6 mice. *Brain Res* **1994,** 637, 181-189.

326. Ison, J. R.; Bowen, G. P.; del Cerro, M. A behavioral study of temporal processing and visual persistence in young and aged rats. *Behav Neurosci* **1998,** 112, 1273-1279.

327. Chapillon, P.; Roullet, P. Use of proximal and distal cues in place navigation by mice changes during ontogeny. *Dev Psychobiol* **1996,** 29, 529-545.

328. Geula, C.; Darvesh, S. Butyrylcholinesterase, cholinergic neurotransmission and the pathology of Alzheimer's disease. *Drugs Today (Barc)* **2004,** 40, 711-721.

329. Fadda, F.; Cocco, S.; Stancampiano, R. Hippocampal acetylcholine release correlates with spatial learning performance in freely moving rats. *Neuroreport* **2000,** 11, 2265-2269.

330. Weingand, K.; Brown, G.; Hall, R.; Davies, D.; Gossett, K.; Neptun, D.; Waner, T.; Matsuzawa, T.; Salemink, P.; Froelke, W.; Provost, J. P.; Negro, G. D.; Batchelor, J.; Nomura, M.; Groetsch, H.; Boink, A.; Kimball, J.; Woodman, D.; York, M.; Fabianson-Johnson, E.; Lupart, M.; Melloni, E. Harmonization of animal clinical pathology testing in toxicity and safety studies. *Fundam Appl Toxicol* **1996,** 29, 198-201.

331. Poucet, B. Object exploration, habituation, and response to a spatial change in rats following septal or medial frontal cortical damage. *Behav Neurosci* **1989,** 103, 1009-1016.

332. Ziabreva, I.; Ballard, C. G.; Aarsland, D.; Larsen, J. P.; McKeith, I. G.; Perry, R. H.; Perry, E. K. Lewy body disease: thalamic cholinergic activity related to dementia and parkinsonism. *Neurobiol Aging* **2006,** 27, 433-438.

333. Frotscher, M.; Schlander, M.; Leranth, C. Cholinergic neurons in the hippocampus. A combined light- and electron-microscopic immunocytochemical study in the rat. *Cell Tissue Res* **1986,** 246, 293-301.

334. Kirby, B. P.; Rawlins, J. N. The role of the septo-hippocampal cholinergic projection in T-maze rewarded alternation. *Behav Brain Res* **2003,** 143, 41-48.

335. Kievit, J.; Kuypers, H. G. Organization of the thalamo-cortical connexions to the frontal lobe in the rhesus monkey. *Exp Brain Res* **1977,** 29, 299-322.

336. Lane, R. M.; Potkin, S. G.; Enz, A. Targeting acetylcholinesterase and butyrylcholinesterase in dementia. *Int J Neuropsychopharmacol* **2006,** 9 101-124.

337. Ozer, J.; Ratner, M.; Shaw, M.; Bailey, W.; Schomaker, S. The current state of serum biomarkers of hepatotoxicity. *Toxicology* **2008,** 245, 194-205.

338. Mouse Genome Informatics. 2008 [cited Sep 3 2008]. Available from: http://www.informatics.jax.org/cookbook/images/60.jpg.

339. O'Brien, P. J.; Slaugher, M. R.; Polley, S. R.; Kramer, K. Advantages of glutamate dehydrogenase as a blood biomarker of acute hepatic injury in rats. *Lab Anim* **2002,** 36, 313-321.

340. Thompson, R. W.; Valentine, H. L.; Valentine, W. M. In vivo and in vitro hepatotoxicity and glutathione interactions of N-methyldithiocarbamate and N,N-dimethyldithiocarbamate in the rat. *Toxicol Sci* **2002,** 70, 269-280.

341. Seong, G. K.; Surh, Y. J.; Yeowon, S.; J.K., Y.; Jong Wook, L.; Liem, A.; Miller, J. A. Inhibition of vinyl carbamate-induced hepatotoxicity, mutagenicity, and tumorigenicity by isopropyl-2-(1,3-dithietane-2-ylidene)-2-[N-(4-methylthiazol-2-yl)carbamoyl]acetate (YH439). *Carcinogenesis* **1998,** 19, 687-690.

342. Gomez, J. L.; Garcia-Ayllon, M. S.; Campoy, F. J.; Vidal, C. J. Muscular dystrophy alters the processing of light acetylcholinesterase but not butyrylcholinesterase forms in liver of Lama2(dy) mice. *J Neurosci Res* **2000,** 62, 134-145.

343. Satoh, T.; Hosokawa, M. Structure, function and regulation of carboxylesterases. *Chem Biol Interact* **2006,** 162, 195-211.

344. Watanabe, K.; Kayano, Y.; Matsunaga, T.; Yamamoto, I.; Yoshimura, H. Purification and characterization of a novel 46.5-kilodalton esterase from mouse hepatic microsomes. *Biochem Mol Biol Int* **1993,** 31, 25-30.

345. Coon, M. J. Cytochrome P450: nature's most versatile biological catalyst. *Annu Rev Pharmacol Toxicol* **2005,** 45, 1-25.

346. Cutler, N. R.; Hossain, M.; McDonald, C.; Pommier, F.; Sedek, G.; Jhee, S. S.; Sramek, J. J. Pharmacokinetics of rivastigmine and its metabolite in patients with Alzheimer's disease. *Biol Psychiatry* **2000,** 47, S161.

Appendix I

Volunteer Information Leaflet and Consent form

Volunteer Information Leaflet

Novel and highly selective butyrylcholinesterase inhibitors (approximately 1,000-fold more selective than iso-OMPA (the prototypical butyrylcholinesterase inhibitor), with the additional advantage of 1,000-fold greater potency) have recently been developed in TCD School of Pharmacy, providing a unique opportunity to explore the physiological and pathological roles of butyrylcholinesterase and the potential of its inhibition as a therapeutic strategy in Alzheimer's disease.
Although Alzheimer's disease has been the subject of extensive research, very few studies have examined the effect of butyrylcholinesterase inhibition on cognitive function. This study will investigate the effect of these novel butyrylcholinesterase inhibitors on human plasma *in vitro*.

You will be asked to do the following:

1. Fill out a volunteer consent form
2. Be present in the College Health Centre at 10.00 a.m. on a given day, where a blood sample will be taken (up to 30 ml). This blood sample will be used for a laboratory assessment of butyrylcholinesterase activity in the presence of novel butyrylcholinesterase inhibitors.

Criteria for volunteers:
In order for volunteers to participate in this study you must be aged between 20 and 40. This is in the interests of good experimental design.

Potential risks involved:
While the donation of blood provides a very low level risk for the donor, it is important to understand that on rare occasions the following adverse events may occur:

Fainting
Infection at the site of needle puncture
Penetration of a nearby artery
Penetration of a nearby nerve

However, as the blood will be drawn by qualified and experienced medical personnel, every effort will be made to ensure the safety of all volunteers.

It is important to note the following:
Participation in this study is entirely voluntary, and you are free to withdraw at any stage without giving an explanation.

Volunteer Consent Form

The volunteer should complete the whole of this page him/herself	**Please circle appropriate answer**
Have you read the volunteer information sheet?	Yes / No
Have you had an opportunity to ask questions and discuss this study?	Yes / No
Have you received satisfactory answers to all of your questions?	Yes / No
Do you agree to take part in this study?	Yes / No
Do you understand that you are free to withdraw from this study: At any time? Without having to give a reason for withdrawing?	 Yes / No Yes / No

Volunteer Signature: _____

Signature of Research Supervisor : _____

Date: _____

Appendix II

Behavioural Profile Score Sheet

Mouse drug screening profile

Date _____

Drug _____

Dose and administration route _____

Sex _____

Weight (grams) _____

A. Undisturbed behaviour (record over 5 minutes). Record bizarre or stereotyped behaviour and convulsions separately in *Table E.*

#	Test	*	0	1	2	3	4	5
1	Body position	Not tested	Completely flat	Lying on side	Lying prone	Sitting or standing	Rearing on hind limbs	Repeated vertical leaping
2	Spontaneous activity	Not tested	None, resting	Casual scratching, grooming, slow movement	Vigorous scratching, grooming, moderate movement	Vigorous, rapid/dart movement	Extremely vigorous, rapid/dart movement	
3	Respiration rate	Not tested	Gasping, irregular	Slow, shallow	Normal	Hyperventilation		
4	Tremor	Not tested	None	Mild	Marked			
5	Defaecation	Not tested	Number of pellets					

#	Test	*	0	1	2	3	4	5
6	Urination	Not tested	None	Present				

B. Active behaviour

#	Test	*	0	1	2	3	4	5	6
7	Time elapsed before the mouse starts to move after dropping onto arena floor	Not tested	Time (seconds)	-	-	-	-	-	-
8	Transfer arousal	Not tested	Coma	Prolonged freeze, then slight movement	Extended freeze, then moderate movement	Brief freeze (few seconds), then active movement	Momentary freeze, then swift movement	No freeze, immediate movement	Extremely excited ("manic")
9	Piloerection	Not tested	Absent	Present	-	-	-	-	-
10	Palpebral closure	Not tested	Wide open	1/2 closed	Closed	-	-	-	-
11	Startle response	Not tested	None	Preyer reflex (backward flick of pinnae)	Jump $\leq$ 1 cm	Jump > 1 cm	-	-	-
12	Gait	Not tested	Normal	Fluid but abnormal	Limited movement only	Incapacity	-	-	-
13	Pelvic elevation	Not tested	Markedly flattened	Barely touching	Normal (3mm elevation)	Elevated (more than 3mm elevation)	-	-	-

#	Test	*	0	1	2	3	4	5	6
14	Tail elevation	Not tested	Dragging	Horizontally extended	Elevated / Straub Tail	-	-	-	-
15	Touch escape	Not tested	No response	Mild (escape response to firm stroke)	Moderate (rapid escape response to light stroke)	Vigorous (escape response to approach)	-	-	-
16	Positional passivity	Not tested	Struggles when held by tail	Struggles when held by neck (finger grip, not scruffed)	Struggles when laid supine (on back)	Struggles when held by hind limbs	No struggle	-	-

C. Restrained behaviour (on/above arena)

#	Test	*	0	1	2	3	4
17	Trunk curl	Not tested	Absent	Present	-	-	-
18	Limb grasping	Not tested	Absent	Present	-	-	-
19	Visual placing	Not tested	None	Upon nose contact	Upon vibrissae contact	Before vibrissae contact (18mm)	Early vigorous extension (25mm)
20	Grip strength	Not tested	None	Slight grip, semi-effective	Moderate grip, effective	Active grip, effective	Unusually effective
21	Body tone	Not tested	Flaccid, no return of cavity to normal	Slight resistance	Extreme resistance, board like	-	-
22	Pinna reflex	Not tested	None	Active retraction, moderately brisk flick	Hyperactive, repetitive flick	-	-
23	Corneal reflex	Not tested	None	Active single eye blinking	Multiple eye blinking	-	-

D. Manipulated behaviour and other tests

#	Test	*	0	1	2	3	4
24	Body length	Not tested	mm	-	-	-	-
25	Tail length	Not tested	mm	-	-	-	-
26	Lacrimation	Not tested	None	Present	-	-	-
27	Provoked biting	Not tested	Absent	Present	-	-	-
28	Salivation	Not tested	None	Slight margin of sub-maxillary area	Wet zone entire sub-maxillary area	-	-
29	Abdominal tone	Not tested	Flaccid, no return of cavity to normal	Slight resistance	Extreme resistance, board like	-	-
30	Skin colour	Not tested	Blanched	Pink	Bright, deep red flush	Dark footpad or pigmentation	-
31	Limb tone	Not tested	No resistance	Slight resistance	Moderate resistance	Marked resistance	Extreme resistance
32	Toe pinch	Not tested	Slight withdrawal	Moderate withdrawal, not brisk	Brisk, rapid withdrawal	Very brisk repeated extension and flexion	-
33	Righting reflex	Not tested	No impairment	Impaired	Fails to right when placed on back		-
34	Negative geotaxis	Not tested	Turns and climbs the grid	Turns but then freezes	Moves, but fails to turn	Does not move within 30 seconds	Falls off

35	Aggression	Not tested	None	Provoked biting or attack	-	-	-
36	Vocalization	Not tested	None	Provoked during handling	-	-	-

E. Bizarre Behaviour and Convulsions

37	Bizarre behaviour	Not tested	
38	Convulsions	Not tested	
39	Other comments		

Bizarre Behaviour

HF	Head flicking or head shaking	UW	Upright walking - hind limbs only
HS	Head searching - repetitive	AW	Aimless wandering - slow plodding around with no apparent purpose
H	Hallucinating-like animal appears to respond to objects not present, e.g. visual tracking or fear withdrawal	C	Circling
B	Compulsive biting - usually of grid floor	W	Waltzing - rapid turning in circles
L	Compulsive licking - usually of glass jar	R	Retropulsion - animal walks backwards
SB	Self destructive biting - usually of toes with bleeding	D	Spatial disorientation - walking or stumbling into objects
P	Prancing forelimbs - shifting from one forelimb to another with slight turn of body from side to side	HB	Head bobbing

Convulsions

Clonic type: alternative contraction and relaxation of the voluntary muscles

C Clonic - co-ordinated, unsymmetrical convulsion and natural, purposeful movements, e.g. running, sometimes preceded by a running excitement (Rn)
Cs Clonic symmetrical - repetitive symmetrical jerks or twitches of the limbs
Rn Running excitement - often accompanied by mild clonus or leading to a severe convulsion
Ch Champing - clonus of the jaws only
P Popcorn - seizure where animal repeatedly "pops" into the air
A Asphyxia - a terminal clonic or clonic-tonic convulsion resulting from respiratory failure.

Tonic type: persistent contraction and spasm of a set of voluntary muscles.

T Tonic - sustained extension of hindlimbs, usually preceded by tonic flexion
Tf This is used if tonic flexation occurs without extension
Op Opisthotonus - head, body and limbs are rigidly extended and arched backwards.
Em Emprosthonus - opposite of Op i.e. extended forward.

Miscellaneous Type

Rr Rock and roll - animal is prostrate on its back and rocks from side to side in a seeming effort to right itself, occasionally rolling over (overshooting) and continuing to rock again.
Su Sitting up - sits upright on hindlimbs during the seizure
Pr Praying - sitting up seizure in which forelimbs are held together or crossed in attitude resembling prayer.

Published Articles

Chemico-Biological Interactions 175 (2008) 231–234

Contents lists available at ScienceDirect

Chemico-Biological Interactions

journal homepage: www.elsevier.com/locate/chembioint

Pharmacological effects of a novel isosorbide-based butyrylcholinesterase inhibitor

D. Khan, J.F. Gilmer, C.G. Carolan, J.M. Gaynor, S.A. Ryder*

School of Pharmacy and Pharmaceutical Sciences, Trinity College Dublin, Dublin 2, Ireland

ARTICLE INFO

Article history:
Available online 23 May 2008

Keywords:
Butyrylcholinesterase
Inhibition
Carboxylesterase
Hydrolysis

ABSTRACT

Isosorbide-2-benzylcarbamate-5-benzoate, a novel butyrylcholinesterase inhibitor, shows interspecies variation in its inhibitory activity (IC_{50} of 4.3 nM for human plasma butyrylcholinesterase, but 1.09 μM for mouse plasma butyrylcholinesterase). Stability studies revealed that this drug is resistant to hydrolysis by human plasma (no degradation in 1 h). However, it was found to undergo rapid degradation when incubated with mouse plasma or mouse liver homogenate, yielding benzyl carbamate and benzoic acid. The addition of the carboxylesterase inhibitor bis-(4-nitrophenyl) phosphate (BNPP) inhibited the degradation of the novel drug, indicating that it may be a substrate for both butyrylcholinesterase and carboxylesterase. The absence of carboxylesterase from human plasma explains the drug's stability in this medium. *In vivo*, pharmacodynamic studies on single doses of 1 mg/kg to naïve male C57BL/6 mice revealed maximal plasma butyrylcholinesterase inhibition 20 min after intraperitoneal administration (~60% inhibition) and 1 h after administration by gavage (~45% inhibition). While this plasma butyrylcholinesterase inhibition was short-lived, the drug also penetrated the blood–brain barrier resulting in a slight (10–15%) but persistent (≥72 h) reduction in brain butyrylcholinesterase activity.

© 2008 Elsevier Ireland Ltd. All rights reserved.

1. Introduction

Butyrylcholinesterase (EC 3.1.1.8, BuChE) is found in neurons and glial cells in the human brain, and peripherally in serum [1]. Although the exact function of BuChE remains unclear, it is responsible for the metabolism of various drugs including the anaesthetic succinylcholine [2], and it efficiently hydrolyses acetylcholine (ACh) at high concentrations [3]. In Alzheimer's disease, BuChE may be increased 40–90% in the brain and high levels of BuChE are found in neuronal plaques [4,5]. Novel and potent inhibitors displaying exceptionally high selectivity for BuChE have been developed in our laboratories, providing a unique pharmacological opportunity to explore the physiological and pathological roles of BuChE and the potential for BuChE inhibition as a therapeutic strategy in Alzheimer's disease [6]. One such compound, isosorbide-2-benzylcarbamate-5-benzoate (compound 51, Fig. 1), which displays >60,000-fold selectivity for BuChE over acetylcholinesterase (AChE), has been tested *in vitro* and *in vivo*. This paper describes studies intended to reconcile the metabolism of compound 51 with its *in vivo* activity.

2. Methods

2.1. In vitro butyrylcholinesterase inhibition

BuChE inhibition was measured *in vitro* using a modification of the Ellman assay [7] employing butyrylthiocholine as substrate [8] and a standardized BuChE concentration (5.88 μmol min^{-1} ml^{-1}). Plasma was removed from fresh blood centrifuged at 3000 rpm for 10 min at 4 °C (Sorvall RT6000B). A stock solution of the drug was prepared in a 1:3 solution of acetonitrile:PBS (phosphate

* Corresponding author. Tel.: +353 1 896 2786; fax: +353 1 896 2524.
E-mail address: sryder@tcd.ie (S.A. Ryder).

0009-2797/$ – see front matter © 2008 Elsevier Ireland Ltd. All rights reserved.
doi:10.1016/j.cbi.2008.05.024

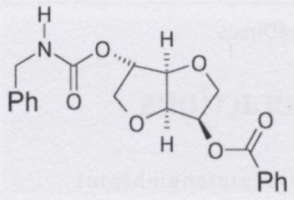

Fig. 1. Compound 51, isosorbide-2-benzylcarbamate-5-benzoate.

buffered saline) pH 8.0 from which serial dilutions (100 μM to 1 nM) were made. The drug and plasma were incubated in 0.1 M PBS (pH 8.0) with 0.3 mM DTNB (5-5′-dithiobis(2-nitrobenzoic) acid) at 37 °C for 30 min. Thereafter 0.5 mM of BTCI (butyrylthiocholine iodide) was added and the absorbance was measured at 405 nm. IC_{50} values were determined from non-linear regression plots using GraphPad Prism 4.0.

2.2. *In vivo butyrylcholinesterase inhibition*

Healthy naïve male C57BL/6 mice (Harlan, UK) were housed singly with *ad libitum* access to food and water under a 12 h light/dark cycle. A single dose of compound 51 (1 mg/kg) was administered intraperitoneally (ip) or orally (po). At various time points ($n=3$ per timepoint) submandibular blood samples were collected in lithium heparinized Microvette tubes and centrifuged at 3000 rpm for 10 min at 4 °C. Plasma BuChE activity was determined using the Ellman assay [7] as previously described. Absorbance values were plotted using GraphPad Prism 4.0.

At the study endpoints, 24, 48 and 72 h post administration of the compound, the level of BuChE inhibition in the brain was assessed. The animals were euthanized by carbon dioxide asphyxiation and the brains were carefully removed and placed on ice until processed. The brain samples were homogenized in physiological saline on ice in three 5-s bursts using an Ultra-turrax T10. The homogenate was centrifuged at 10,000 rpm for 10 min at 4 °C. BuChE activity was analysed using the Ellman assay [7].

2.3. *Hydrolysis studies*

The rate of hydrolysis of compound 51 was determined *in vitro* in human plasma, mouse plasma and mouse liver homogenate using a gradient HPLC method.

2.3.1. *Preparation of plasma samples*

Fresh plasma samples were prepared by centrifugation of heparinized venous human or mouse blood for 10 min at 3000 rpm at 4 °C. One millilitre of plasma was added to 2 ml of PBS pH 7.4 (33% solution).

2.3.2. *Preparation of liver samples*

Mouse liver was homogenized on ice in 10 volumes of PBS pH 7.4 in three 5-s bursts using an Ultra-turrax T-10 (IKA-Werke). The homogenate was then centrifuged for 10 min at 10,000 rpm and 4 °C. Liver homogenate (20 μl) was added to 3 ml of PBS pH 7.4.

2.3.3. *Hydrolysis*

One hundred microlitres of compound 51 (8 μM) in acetonitrile was added to the plasma/buffer or liver/buffer solution and incubated at 37 °C. Aliquots (250 μl) were taken at various time points and transferred to Eppendorfs containing 500 μl of a 2% zinc sulfate solution in acetonitrile (1:1). The Eppendorfs were then centrifuged at 10,000 rpm for 7 min. A 20-μl aliquot of the clear supernatant was analysed by HPLC.

Hydrolysis studies using the carboxylesterase inhibitor, bis-(4-nitrophenyl) phosphate (BNPP), were also carried out to determine if carboxylesterase played a role in the hydrolysis of compound 51. BNPP (100 μM) was incubated at 37 °C with the mouse plasma or liver homogenate for 10 min prior to drug addition.

2.3.4. *Chromatography*

High-performance liquid chromatography was performed using a system consisting of a Waters 600 pump and controller, Waters 717 autosampler and a Waters 2996 photodiode-array (PDA) detector controlled by Empower 2 software (Waters). A Hichrom Nucleosil C18 4.0 mm × 250 mm column was used. The plasma and liver samples were both analysed using a gradient method consisting of a 16 mM phosphate buffer (pH 2.5): acetonitrile 80:20 for the first 10 min, grading to 20:80 for the next 5 min, then 60:40 for the next 2 min and finally returning to 80:20 for the last 3 min of the 20 min run. The flow rate was 1 ml/min and the buffer and acetonitrile were helium sparged at a rate of 20 ml/min. The retention times in this system were 9.5 min for benzyl carbamate, 10.0 for benzoic acid and 15.2 min for compound 51. Peak areas were compared quantitatively with external standards of approximately the same concentration. The gradient method was validated for specificity, sensitivity and precision.

2.4. *Statistical analysis*

BuChE activity data were entered into SPSS v.14 (SPSS Inc., Chicago) for analysis. Standard descriptive parameters were calculated and significant differences were determined using Student's *t*-test where appropriate, taking $p<0.05$ to be significant.

3. Results and discussion

Compound 51 (isosorbide-2-benzylcarbamate-5-benzoate) was synthesised in house as part of an ongoing programme of research into isosorbide-based cholinesterase inhibitors, and has proved to be a potent inhibitor of human plasma BuChE *in vitro*. However, interspecies differences were apparent, its IC_{50} of 4.3 nM in human plasma contrasting with an IC_{50} of 1.09 μM in mouse plasma.

In vivo, a single dose of 1 mg/kg given to male C57BL/6 mice displayed maximal plasma BuChE inhibition 20 min after ip administration (~60% inhibition), and 1 h after administration po (~45% inhibition). However, the duration of action was short-lived by both routes, restoration of BuChE activity being substantially complete

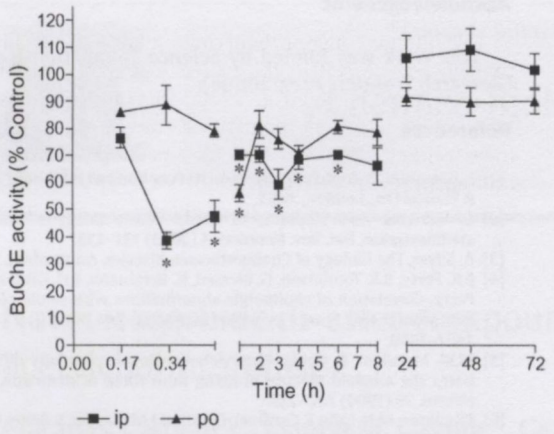

Fig. 2. Mouse plasma BuChE activity following a single intraperitoneal or oral dose (1 mg/kg) of compound 51. (Mean ± standard deviation; $n = 3$.) Asterisks indicate a significant difference in BuChE activity relative to controls ($p < 0.05$, t-test).

within 24 h (Fig. 2). There was a subsequent increase in plasma BuChE activity 24 h after ip administration with a concomitant rise in liver production of the enzyme to 115%. Combined with the fact that repeated dosing (5 mg/kg or 10 mg/kg po daily) over a 1-week period showed an increase in plasma BuChE activity, this suggests the existence of an efficient BuChE homeostatic mechanism.

Single doses of 1 mg/kg of compound 51 by the intraperitoneal and oral routes also caused reductions of ~20 and 15%, respectively in BuChE activity in the brain, indicating the ability of the drug to cross the blood–brain barrier. Furthermore, these reductions persisted for at least 72 h after dosing (Fig. 3). The superior BuChE inhibition achieved by this compound in human plasma, compared with its effects in mice, prompted exploration of the possibility that it is subject to more rapid metabolism in mice.

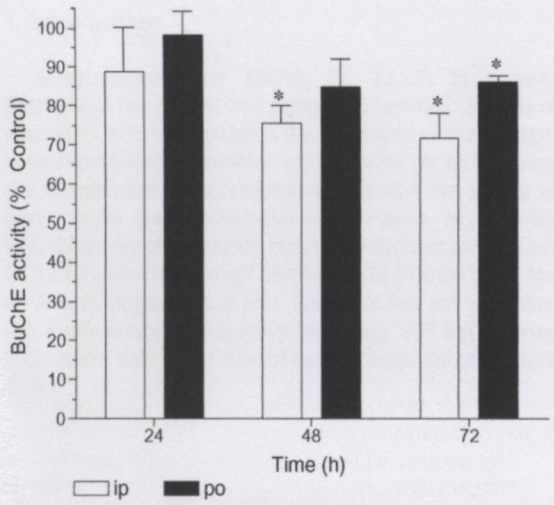

3. Mouse brain BuChE activity following a single intraperitoneal or dose (1 mg/kg) of compound 51. (Mean ± standard deviation; $n = 3$.) sks indicate a significant difference in butyrylcholinesterase activity e to controls ($p < 0.05$, t-test).

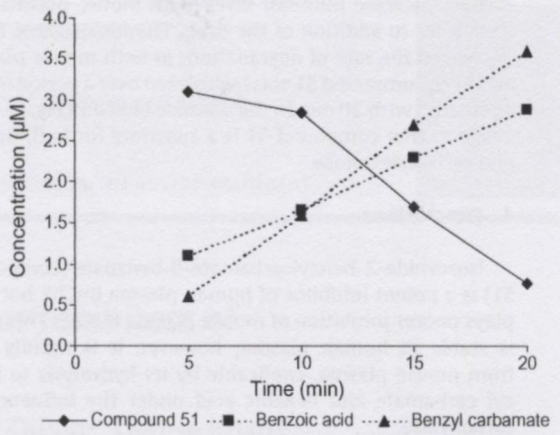

Fig. 4. Hydrolysis of compound 51 in a 33% mouse plasma solution incubated at 37 °C (pH 7.4).

Hydrolysis studies revealed that compound 51 is stable in human plasma: no decrease in drug concentration was seen over a 60-min period. In contrast, rapid hydrolysis was observed in mouse plasma and mouse liver. The concentration of the drug decreased over a period of 20 min with the concomitant formation of the metabolites benzyl carbamate and benzoic acid (Fig. 4).

Human plasma contains almost twice the concentration of BuChE in mouse plasma: 5 and 2.6 mg/l, respectively [9]. Accordingly, if BuChE were responsible for the hydrolysis of compound 51, its disappearance would have been more rapid in human than mouse plasma samples. The instability of compound 51 in mouse plasma and liver, allied with the higher IC_{50} observed in mouse plasma compared to the IC_{50} for human plasma BuChE, suggests that this drug is not a substrate of BuChE alone.

Human and mouse plasma differ insofar as mouse plasma contains an additional enzyme, carboxylesterase [9,10] (EC 3.1.1.1). Despite an abundance of carboxylesterase in human liver and small intestine, none is found in human plasma [9,11]. The hydrolysis of compound 51 by carboxylesterase was confirmed by incubation of the

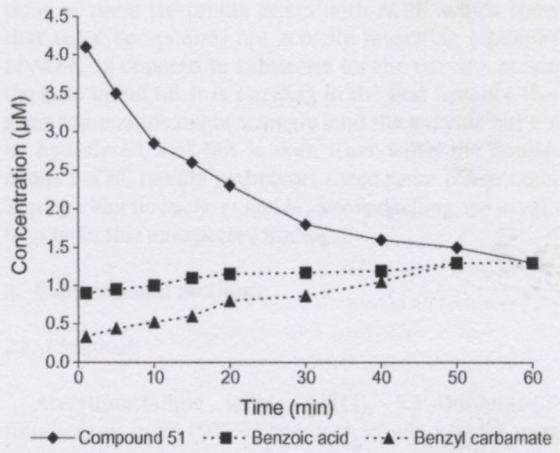

Fig. 5. Hydrolysis of compound 51 in a 33% mouse plasma solution incubated with 100 μM BNPP at 37 °C (pH 7.4).

carboxylesterase inhibitor BNPP with mouse plasma and liver prior to addition of the drug. The inclusion of BNPP decreased the rate of degradation: in both mouse plasma and liver, compound 51 was hydrolysed over a period of 1 h, compared with 20 min in the absence of BNPP (Fig. 5). This suggests that compound 51 is a substrate for both BuChE and carboxylesterase.

4. Conclusions

Isosorbide-2-benzylcarbamate-5-benzoate (compound 51) is a potent inhibitor of human plasma BuChE but displays poorer inhibition of mouse plasma BuChE. This drug is stable in human plasma; however, it is rapidly lost from mouse plasma, explicable by its hydrolysis to benzyl carbamate and benzoic acid under the influence of carboxylase.

Pharmacodynamic studies show decreased plasma and brain BuChE activity following a single intraperitoneal or oral dose of 1 mg/kg. The ability of this novel compound to cross the blood–brain barrier and reduce brain BuChE activity will prove interesting in cognitive tests *in vivo*, as BuChE has gained recognition as a new therapeutic target in Alzheimer's disease (AD). In the healthy brain, AChE is the predominant cholinesterase, with BuChE playing a supporting role. However, AChE levels show a pronounced decline at an early stage of AD whereas BuChE levels increase as the disease progresses [12]. It has been proposed that BuChE may play a key part in compensating for AChE loss [13], limiting the value of selective AChE inhibition as a strategy for cholinergic enhancement in AD. While AChE inhibitors such as donepezil and galantamine have gained a place in the management of AD, the addition of a BuChE inhibitor such as compound 51 could enhance clinical efficacy.

Acknowledgement

This work was funded by Science Foundation Ireland (Research Frontiers Programme).

References

[1] E. Giacobini, Butryrlcholinesterase: Its Function and Inhibitors, Taylor & Francis Ltd., London, 2003.
[2] S. Darvesh, D.A. Hopkins, C. Geula, Neurobiology of butyrylcholinesterase, Nat. Rev. Neurosci. 4 (2003) 131–138.
[3] A. Silver, The Biology of Cholinesterases, Elsevier, Amsterdam, 1974.
[4] E.K. Perry, B.E. Tomlinson, G. Blessed, K. Bergmann, P.H. Gibson, R.H. Perry, Correlation of cholinergic abnormalities with senile plaques and mental test scores in senile dementia, Brit. Med. J. 2 (1978) 1457–1459.
[5] M.M. Mesulam, C. Geula, Butyrylcholinesterase reactivity differentiates the amyloid plaques of aging from those of dementia, Ann. Neurol. 36 (1994) 722–727.
[6] J.F. Gilmer, M.N. Lally, P. Gardiner, G. Dillon, J.M. Gaynor, S. Reidy, Novel isosorbide-based substrates for human butyrylcholinesterase, Chem. Biol. Interact. 157/158 (2005) 317–319.
[7] G.L. Ellman, K.D. Courtney, V. Andres Jr., R.M. Feather-Stone, A new and rapid colorimetric determination of acetylcholinesterase activity, Biochem. Pharmacol. 7 (1961) 88–95.
[8] A. Chatonnet, O. Lockridge, Comparison of butyrylcholinesterase and acetylcholinesterase, Biochem. J. 260 (1989) 625–634.
[9] B. Li, M. Sedlacek, I. Manoharan, R. Boopathy, E.G. Duysen, P. Masson, O. Lockridge, Butyrylcholinesterase, paraoxonase, and albumin esterase, but not carboxylesterase, are present in human plasma, Biochem. Pharmacol. 70 (2005) 1673–1684.
[10] T. Satoh, M. Hosokawa, Structure, function and regulation of carboxylesterases, Chem. Biol. Interact. 162 (2006) 195–211.
[11] M. Taketani, M. Shii, K. Ohura, S. Ninomiya, T. Imai, Carboxylesterase in the liver and small intestine of experimental animals and human, Life Sci. 81 (2007) 924–932.
[12] E. Giacobini, Cholinergic function and Alzheimer's disease, Int. J. Geriatr. Psychiatr. 18 (Suppl. 1) (2003) S1–S5.
[13] N.H. Greig, T. Utsuki, D.K. Ingram, Y. Wang, G. Pepeu, C. Scali, Q.S. Yu, J. Mamczarz, H.W. Holloway, T. Giordano, D. Chen, K. Furukawa, K. Sambamurti, A. Brossi, D.K. Lahiri, Selective butyrylcholinesterase inhibition elevates brain acetylcholine, augments learning and lowers Alzheimer beta-amyloid peptide in rodent, Proc. Natl. Acad. Sci. U.S.A. 102 (2005) 17213–17218.

Chemico-Biological Interactions 175 (2008) 293–297

Contents lists available at ScienceDirect

Chemico-Biological Interactions

journal homepage: www.elsevier.com/locate/chembioint

Novel isosorbide di-ester compounds as inhibitors of acetylcholinesterase

Ciaran G. Carolan[a,*], Joanne M. Gaynor[b], Gerry P. Dillon[a], Denise Khan[a], Sheila A. Ryder[a], Sean Reidy[b], John F. Gilmer[a]

[a] School of Pharmacy and Pharmaceutical Sciences, Trinity College Dublin, College Green, Dublin 2, Ireland
[b] School of Science, Athlone Institute of Technology, Athlone, Ireland

ARTICLE INFO

Article history:
Available online 18 May 2008

Keywords:
Acetylcholinesterase
Butyrylcholinesterase
Isosorbide esters
Inhibitor
Docking

ABSTRACT

We report herein that a variety of isosorbide di-esters, previously reported to be novel substrates for butyrylcholinesterase (BuChE, EC 3.1.1.8), are in fact inhibitors of the homologous enzyme acetylcholinesterase (AChE), with IC_{50} values in the micromolar range. *In vitro* studies show that they are mixed inhibitors of the enzyme, and thus the ternary enzyme-inhibitor–substrate complex can form in acetylcholinesterase. This is rationalised by molecular modelling which shows that the compounds bind in the mid-gorge area. In this position, simultaneous substrate binding might be possible, but the hydrolysis of this substrate is prevented. The di-esters dock within the butyrylcholinesterase gorge in a very different manner, with the ester sidechain at the 5-position occupying the acyl pocket at residues Leu286 and Val288, and the 2-ester binding to Trp82. The carbonyl group of the 2-ester is susceptible to nucleophilic attack by Ser198 of the catalytic triad. The larger residues of the acyl pocket in acetylcholinesterase prevent binding in this manner. The results complement each other and explain the differing behaviours of the esters in the cholinesterase enzymes. These findings may prove very significant for future work.

© 2008 Elsevier Ireland Ltd. All rights reserved.

1. Introduction

Acetylcholinesterase (AChE, EC 3.1.1.7) is present throughout the central and peripheral nervous systems of mammals, where it catalyses the hydrolysis of the endogenous ester neurotransmitter acetylcholine (ACh), allowing the termination of ACh receptor-mediated ion gating at nerve–nerve and neuromuscular junctions. ACh is also hydrolysed by the enzyme butyrylcholinesterase (BuChE, EC 3.1.1.8), which although present in the human body, has no known physiological role. The enzymes are very similar, possessing 53% sequence homology and both having their active sites at the base of an enzymatic gorge of depth 20 Å.

This group previously reported that certain isosorbide esters (Fig. 1) are hydrolysed extremely rapidly by BuChE [1]. Here we report the results of studies on the interactions of these isosorbide esters with AChE, which show that these compounds are actually reversible inhibitors of AChE, as opposed to substrates for the enzyme as was the case in BuChE. It is puzzling in the first instance that ester compounds might strongly bind the enzyme but not be hydrolysed, and this is even truer when the homologous BuChE rapidly hydrolyses these same compounds. Through kinetic analyses and *in silico* modelling, we sought to explain this unexpected finding.

2. Experimental methods

2.1. Chemicals

Acetylthiocholine iodide (ATCI), 5,5′-Dithiobis-(2-nitrobenzoic acid) (DTNB) and acetylcholinesterase were

* Corresponding author. Tel.: +353 1 8962794.
E-mail address: carolanc@tcd.ie (C.G. Carolan).

0009-2797/$ – see front matter © 2008 Elsevier Ireland Ltd. All rights reserved.
doi:10.1016/j.cbi.2008.05.013

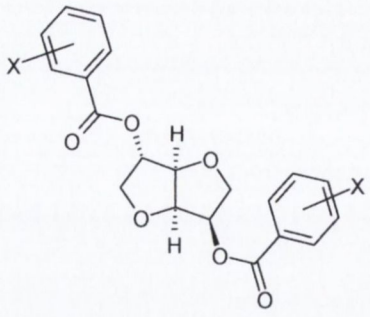

Fig. 1. The structure of the di-benzoate compounds tested. X represents either a chlorine or bromine substituent on the aromatic rings.

purchased from Sigma–Aldrich, Ireland. The acetylcholinesterase used was the Type V-S protein from *Electrophorus electricus* (electric eel), purchased as a lyophilised powder. It was solubilized in 0.02 M phosphate buffer pH 7.0, stabilised by addition of 1 mg/ml bovine serum albumin (BSA), and refrigerated until use.

2.2. Synthesis of isosorbide-based esters

The di-esters were prepared from isosorbide using the appropriate acid chloride in the presence of a tertiary base. They were obtained as crystalline materials following chromatography and characterised by both NMR and MS.

2.3. Inhibition assays

Studies using RP-HPLC showed that the di-esters were not hydrolysed when they were incubated with *E. electricus* AChE; instead, the esters were inhibitors. Inhibition of the *E. electricus* AChE by the di-esters was assayed using the method of Ellman et al. [2], modified to allow the assay to be run in 96-well plate format.

E. electricus AChE and 5,5′-Dithiobis-(2-nitrobenzoic acid), (DTNB) were incubated in phosphate buffer solution pH 8.0 at 37 °C at final concentrations of 0.05 U/ml and 0.3 mM, respectively. Inhibitors were incubated in this enzymatic solution for 30 min at concentrations between 100 nM and 100 μM, prior to addition of the substrate acetylthiocholine iodide; concentrations of ATCI ranged between 100 μM and 5 mM in the final solution. The absorbance of the resulting solutions was monitored at 405 nm. In each resulting plot, data points were obtained on the basis of readings from at least four replicate wells.

Plots of $1/v$ against $[I]$ and s/v against $[I]$ were prepared to examine the nature of the inhibition by each test compound. (v : reaction rate, s, substrate concentration and $[I]$, inhibitor concentration). Values for K_i and K_i' were calculated by plotting K_m/V_{max} and $1/V_{max}$ against $[I]$, where K_m and V_{max} were calculated by fitting data to the Michaelis–Menten equation using non-linear regression. In each case, a straight line was obtained, and the intercept on the $[I]$ axis gave $-K_i$ when K_m/V_{max} was plotted, and $-K_i'$ when $1/V_{max}$ was plotted [3]. All data manipulations and graphing calculations were carried out using GraphPad Prism version 4.03 (GraphPad Software).

2.4. Molecular modelling

The binding of the di-ester compounds to both BuChE and AChE was examined to see whether differential binding to each enzyme could explain the different behaviour of the di-esters in the enzymes. Isosorbide di-(4-chlorobenzoate) was docked to the active sites of both hBuChE and *E. electricus* AChE. Isosorbide di-(4-bromobenzoate) was also docked to AChE.

Docking calculations were carried out using AutoDock version 4.0, with the Lamarckian genetic algorithm (LGA) [4]. The inhibitor was built using the builder function of MOE (Chemical Computing Group, Montreal, Canada) and minimized with MOPAC 7 (PM3 method) interfaced to MOE.

The crystal structure of hBuChE in complex with a choline molecule [5] (PDB code 1P0M) was used as a basis for modelling the interaction with BuChE. The missing sidechain of residue Gln486 was added in Swiss-PDB Viewer version 3.7, and the missing residues 1-3, 378-379 and 455 added using the 'Add residue' command in the same program. These added residues were minimized within MOE, with the rest of the macromolecule held fixed. Of the two conformations of the catalytic serine observed in the crystal structure noted above, the one where it makes the anticipated hydrogen bond with His438 was used. His438 was protonated at the δ position. The substrates and the enzyme were further prepared for the docking calculation using AutoDockTools 1.4.5. Rotation was allowed for all usual bonds in the ligand, but the macromolecule was held rigid. The 3D affinity grid box was designed to include the full active site gorge of human BChE. The number of grid points in the x-, y-, z-axes was 64, 64, and 40 with grid points separated by 0.375 Å. One hundred docking runs were completed, with 25,000,000 energy evaluations allowed as a maximum in each run. The lowest energy result was taken as the correctly docked pose.

An identical approach was undertaken to dock the same ligand to AChE. Since high-resolution crystal structures of *E. electricus* AChE were not available, the 1.8 Å resolution structure of the homologous *Torpedo californica* AChE was used for modelling purposes [6]. (PDB Code 1EA5) The catalytic domains of the two proteins present 68% identity [7], while the residues of the active site gorge are even more closely matched. However, residue Phe330 in the active site gorge of *Torpedo* AChE is replaced by a Tyrosine residue, while Ile439 – also close to the gorge – is replaced by a proline in the protein from the electric eel. In order to take into account these and other differences, a homology model was built for *E. electricus* AChE using the *T. californica* structure as a template.

The homology-model application of MOE was used for this purpose. In building the initial geometry, all coordinates were copied for residues whose identity was conserved in both proteins, while backbone coordinates were copied for others. Loops and missing sidechains were added from generic libraries within MOE to prepare 10 different models. After addition of hydrogen atoms and coarse minimization, the highest scoring protein based on electrostatic solvation energy, calculated using a Generalized Born/Volume Integral (GB/VI) methodology, was taken for-

Table 1
K_i and K_i' values for selected isosorbide di-esters, calculated as described in the text.

Compound name	K_i (μM)	K_i' (μM)
Isosorbide di-(2-chlorobenzoate)	43.31	1286
Isosorbide di-(3-chlorobenzoate)	7.79	50.4
Isosorbide di-(4-chlorobenzoate)	6.60	92.6
Isosorbide di-(4-bromobenzoate)	104.90	4361

ward for final model building. It was minimised to a root mean square gradient of 0.01. This final model was checked for appropriate geometry before use.

The di-benzoate compounds were docked within the active site of the modeled protein. The number of grid points in the *x*-, *y*- and *z*-axes was 54, 58 and 56 in this case, but all other steps were as described for BuChE modelling.

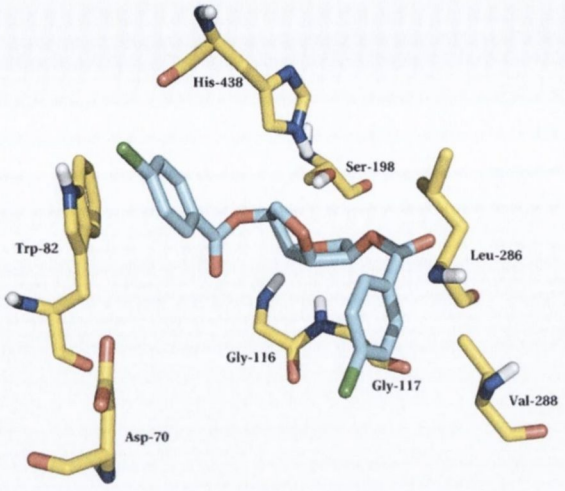

Fig. 2. Isosorbide di-(4-chlorobenzoate) docked to hBuChE.

3. Results

All isosorbide di-ester compounds tested were inhibitors of AChE, with K_i values in the μM range, as shown in Table 1. The most potent inhibitors were isosorbide di-(3-chlorobenzoate) and isosorbide di-(4-chlorobenzoate), with K_i values of 7.79 and 6.60 μM, respectively. The di-(4-bromobenzoate) was significantly less potent.

We subsequently sought to characterise the inhibition of AChE by the isosorbide esters. Plots of $1/v$ against $[I]$ and s/v against $[I]$ together were used to investigate the mode of linear inhibition, as described by Cornish-Bowden. [3] These plots were prepared from data obtained at different substrate and inhibitor concentrations in *E. electricus* AChE. The lines intersected just above the $[I]$ -axis in the Dixon plot and just below the axis in the plot of s/v against $[I]$, indicating mixed inhibition. This type of inhibition would most likely arise in our system if the ternary EIS complex can form but cannot break down to products. We could characterise the K_i value as the dissociation constant of EI and K_i' as the inhibitor dissociation constant of the EIS complex.

Models of isosorbide di-(4-chlorobenzoate) in BuChE and AChE indicated why the isosorbide esters might be substrates in BuChE but inhibitors of AChE. In BuChE, numerous docked poses scored highly, indicating that there are many stable structures formed upon binding, and between which the docked molecule could cycle within the active site gorge of the enzyme. The highest scoring pose, however, sees the di-benzoate lining the base of the gorge, as in Fig. 2. The ester group at the 5-position occupies the acyl pocket between residues Leu286 and Val288, while the 2-ester function is orientated in the direction of Trp82, which normally binds the cationic head of the choline substrate

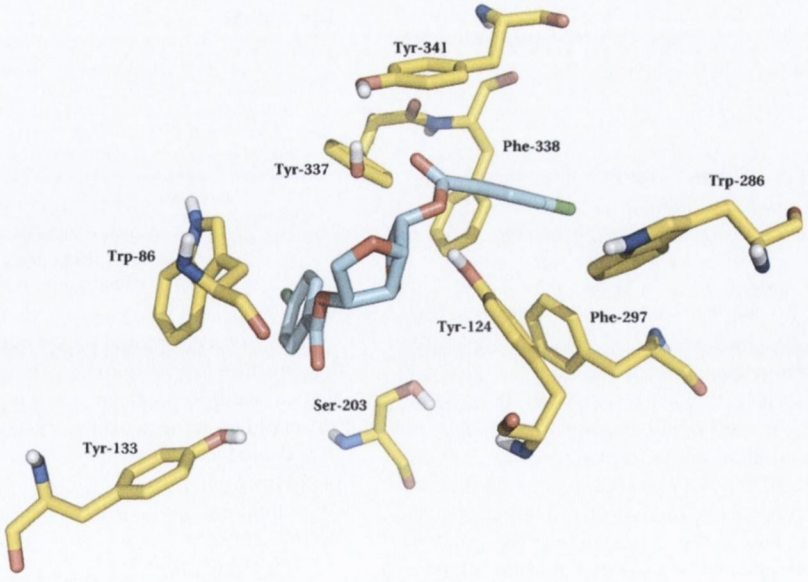

Fig. 3. Isosorbide di-(4-chlorobenzoate) docked to AChE.

through cation–π interactions. The carbonyl carbon at the 2-position is 4.6 Å from the nucleophilic O-γ of Ser198. More importantly, the carbonyl oxygen is directed away from the catalytic serine and towards the oxyanion hole residues Gly116, Gly117 and Ala199. The residue is placed almost optimally for nucleophilic attack of Ser198 at the carbonyl carbon of the 2-ester, which will result in substrate hydrolysis at this position. The ester at the 5-position was not hydrolysed appreciably when tested, and this can also be explained using this same model. The carbonyl group is inappropriately placed for attack. Furthermore, this ester group is *endo* to the V-shaped isosorbide ring, meaning that the approach of the catalytic serine is sterically hindered.

The active site gorge in AChE is more cramped, and this means that a wholly different docking pose is adopted. The acyl pocket is occluded by the presence of residues Phe295 and Phe297 (equivalent to residues Phe288 and Phe290 in *T. californica* enzyme), among others, so that the molecule cannot fit within the gorge in the same manner as in BuChE. The di-ester sits higher up the gorge, as shown in Fig. 3, with the more stable 5-ester group binding to Trp86 and closest to the catalytic triad residues, not withstanding the fact that it is poorly placed for hydrolysis. The carbonyl carbon of the labile 2-benzoate is 10.7 Å from O-γ of Ser198, and is bound in an aromatic pocket formed by residues Phe297, Phe338, Tyr337, Try-341 and Trp286. Thus, the docking is well stabilized, but further descent within the gorge in order to engage the catalytic machinery is not possible, and hence this molecule acts as an inhibitor of AChE.

Isosorbide di-(4-bromobenzoate) was also docked within the active site of *E. electricus* AChE as described above. It docked precisely as described for the chlorobenzoate, and with an almost identical docking score. It was thus puzzling that it was a significantly less potent inhibitor in the *in vitro* tests. We suggest that reduced binding might arise because of the reduced electron density redistribution that occurs in the presence of bromine compared to chlorine substituents—this has been used to explain the improved binding of chlorotacrine to AChE compared to tacrine itself [8]. Otherwise, the increased steric bulk of bromine substituents may mean that the optimal binding pose described above is not as readily achieved.

4. Discussion

The results of the *in vitro* analyses and molecular modelling work described complement each other and reveal much about the nature of the binding of isosorbide di-esters to the cholinesterase enzymes, and the nature of the cholinesterase enzymes themselves. The *in vitro* work showed all di-esters to be mixed inhibitors of moderate potency in AChE, as opposed to extremely good substrates for BuChE, with a similar affinity for the enzyme to the prototypical substrate butyrylcholine [9]. Mixed inhibitors form complexes with their target enzymes so that typically, the ternary EIS complex can be formed, as well as EI and ES complexes. This ternary complex does not break down to form catalytic products. Thus, while the inhibitor is not strictly competitive with the substrate, and the substrate can still bind to the enzyme in the presence of the inhibitor, its presence prevents substrate turnover due to interference with the enzyme's function or with the appropriate binding of the substrate. The molecular docking of isosorbide di-(4-chlorobenzoate) to AChE reveals how this might be better understood. The di-ester cannot bind directly at the active site—if it could, it would be hydrolysed as is the case in BuChE. Instead, it binds within the gorge as depicted. In this orientation, it can be envisaged that the substrate should still be able to enter the active site; however, its binding in an appropriate manner is blocked by the presence of the inhibitor, and hence no substrate turnover is observed in this scenario.

The results of these studies have much significance for future work. These studies have shown that molecules based on the isosorbide template can bind both AChE and BChE, but very different outcomes can arise from their binding in either case. Subsequent studies have begun to examine the binding of isosorbide 2-carbamates to the enzymes. Initial results have shown these compounds to be selective for BuChE in most cases, with strong pseudo-irreversible inhibition observed [10]. In AChE, though inhibition is still apparent, it is only moderate. This might be anticipated from these studies of reversible inhibitors, since the carbamylation reaction should take place more quickly in BuChE if binding occurs in the same way as for the di-esters. Thus, the isosorbide template provides promise for future compounds that might have differential effects in BuChE and AChE.

5. Conclusions

A number of *in vitro* studies have shown that isosorbide di-esters are mixed inhibitors of AChE as opposed to substrates for BuChE as reported previously. Molecular modelling work shows the different binding modes in each enzyme that give rise to these different results. The isosorbide template might be useful for subsequent work where compounds with such contrasting activities in the cholinesterase enzymes are desirable.

References

[1] J.F. Gilmer, M.N. Lally, P. Gardiner, G. Dillon, J.M. Gaynor, S. Reidy, Novel isosorbide-based substrates for human butyrylcholinesterase, Chem. Biol. Interact. 157–158 (2005) 317–319.
[2] G.L. Ellman, K.D. Courtney, V. Andres Jr., R.M. Feather-Stone, A new and rapid colorimetric determination of acetylcholinesterase activity, Biochem. Pharmacol. 7 (1961) 88–95.
[3] A. Cornish-Bowden, Principles of Enzyme Kinetics, first ed., Butterworths, London, 1976.
[4] G.M. Morris, D.S. Goodsell, R.S. Halliday, R. Huey, W.E. Hart, R.K. Belew, A.J. Olson, Automated docking using a Lamarckian genetic algorithm and an empirical binding free energy function, J. Comput. Chem. 19 (1998) 1639–1662.
[5] Y. Nicolet, O. Lockridge, P. Masson, J.C. Fontecilla-Camps, F. Nachon, Crystal structure of human butyrylcholinesterase and of its complexes with substrate and products, J. Biol. Chem. 278 (2003) 41141–41147.
[6] Harel M, Weik M, Silman I, Sussman JL, Native acetylcholinesterase (E.C. 3.1.1.7) from torpedo californica at 1.8 Å resolution, in press (structure available online at http://www.pdb.org).
[7] S. Simon, J. Massoulie, Cloning and expression of acetylcholinesterase from Electrophorus. Splicing pattern of the 3′ exons in vivo and in transfected mammalian cells, J. Biol. Chem. 272 (1997) 33045–33055.
[8] S.T. Wlodek, J. Antosiewicz, J.A. McCammon, T.P. Straatsma, M.K. Gilson, J.M. Briggs, C. Humblet, J.L. Sussman, Binding of tacrine and 6-chlorotacrine by acetylcholinesterase, Biopolymers 38 (1996) 109–117.

[9] W. Xie, C.V. Altamirano, C.F. Bartels, R.J. Speirs, J.R. Cashman, O. Lockridge, An improved cocaine hydrolase: the A328Y mutant of human butyrylcholinesterase is 4-fold more efficient, Mol. Pharmacol. 55 (1999) 83–91.

[10] J.M. Gaynor, G.P. Dillon, S. Reidy, J.F. Gilmer, Synthesis and structure activity relationships (SAR) of a new class of potent and selective butyrylcholinesterase inhibitors, Chem. Biol. Interact. 157–158 (2005) 380–381.

Isosorbide-2-carbamate Esters: Potent and Selective Butyrylcholinesterase Inhibitors

Ciaran G. Carolan,[†] Gerald P. Dillon,[†] Joanne M. Gaynor,[‡] Sean Reidy,[‡] Sheila A. Ryder,[†] Denise Khan,[†] Juan F. Marquez,[†] and John F. Gilmer*[,†]

School of Pharmacy and Pharmaceutical Sciences, Trinity College, Dublin 2, Ireland

Received May 14, 2008

In this study, we report the SAR and characterization of two groups of isosorbide-based cholinesterase inhibitors. The first was based directly on the clinically used nitrate isosorbide mononitrate (ISMN) retention of the 5-nitrate group and introduction of a series of 2-carbamate functionalities. The compounds proved to be potent and selective inhibitors of human plasma butyrylcholinesterase (*hu*BuChE). In the second group, the nitrate ester was removed and replaced with a variety of alkyl and aryl esters. These generally exhibited nanomolar potency with high selectivity for BuChE over acetylcholinesterase (AChE). The most potent and selective compound was isosorbide-2-benzyl carbamate-5-benzoate with an IC_{50} of 4.3 nM for BuChE and >50000 fold selectivity over human erythrocyte AChE. Inhibition with these compounds is time-dependent, competitive, and slowly reversible, indicating active site carbamylation.

Introduction

There are two types of cholinesterase enzymes found in vertebrates: acetylcholinesterase (EC 3.1.1.7; AChE[a]) and butyrylcholinesterase (EC 3.1.1.8; BuChE). These are probably the most widely studied enzymes due to their extraordinary efficiency and the classical relationship between AChE and the neurotransmitter acetylcholine. AChE has been a drug target for the treatment of Alzheimer's disease (AD) since the emergence of the cholinergic hypothesis of AD over 25 years ago. This followed recognition that the cognitive impairments in AD correlated with cholinergic deficits such as reduced synaptic acetylcholine synthesis and choline acetyltransferase (ChAT) activity.[1,2] These observations were made just as the role of the cholinergic system in memory processing and learning began to be more widely appreciated.[3] The introduction of the cholinesterase inhibitors (CHIs), first tacrine then donepezil, rivastigmine, and galantamine, has made an important contribution to the management and well-being of early stage AD patients, although significant scientific and clinical questions about these remain.

In the past few years, CHI medicinal chemistry has diversified from pure AChE inhibitor design into a number of related strategies: (i) dual binding site inhibitors that bind at the active site *and* at the AChE peripheral site, which catalyzes the aggregation of β-amyloid in vitro[4,5] (dual binding site occupancy has also led to the compounds of femtomolar potency[6]); (ii) hybrid compounds that affect both the metabolism of ACh and stimulate its receptor targets;[7] (iii) hybrids that contain CHI functionality and a second noncholinergic modality, e.g., MAO inhibitory activity, melatonin surrogates, or nitric oxide releasing capability.[8−10] A fourth recent strategy (iv) has been to develop selective inhibitors for BuChE. In contrast to AChE, no physiological role has been assigned to BuChE, nor has it a known endogenous substrate; for the present, it takes its name from butyrylcholine, a synthetic substance it hydrolyses exceedingly rapidly (BuChE was historically referred to as pseudocholinesterase, perhaps disparagingly). BuChE is found ubiquitously throughout the human body but is at high concentrations in the lung, liver, and serum. This distribution pattern points to a role in primary metabolism, possibly in protecting the organism from agents that might inhibit the pivotal functions of AChE. Indeed, BuChE has a prominent role in the metabolism of ester drugs and in the activation of ester prodrugs. There are also suggestions that it may be involved in lipoprotein regulation.[11] Evidence for the involvement of BuChE in AD and support for its role as a drug target may be summarized as follows: (i) the nullizygous (AChE −/−) mouse while having a clear phenotype appears to have normal CNS function, indicating at least a compensatory role for BuChE in the CNS;[12] (ii) while synaptic AChE levels decrease to 10−15% of normal during AD progression, BuChE activity is maintained or even increased;[13] (iii) post mortem tissue analysis on AD patients shows a high level of BuChE in the hallmark lesions of AD[14] (although it might well have a protective role here); (iv) in rats, the selective BuChE inhibitor cymserine causes elevation of acetylcholine and augments long-term potentiation and learning.[15] A notable feature of that study was the absence of peripheral side effects that are associated with AChE inhibitors.

We reported previously that isosorbide esters tend to undergo very rapid hydrolysis in the presence of mammalian esterases.[16−18] The aspirin ester of isosorbide mononitrate (ISMNA) is one of the few compounds reported that can act as an aspirin prodrug (at least in rabbit plasma) and it is a potent inhibitor of platelet aggregation.[16] This is because, in the case of ISMNA, hydrolysis at the aspirin ester group proceeds faster than at the neighboring acetyl group. We hypothesized that it might be possible to generate potent and selective inhibitors for the cholinesterases by replacing the aspirin group in ISMNA with a carbamate functionality while retaining the isosorbide-5-nitrate group as illustrated in Figure 1b. The 5-nitrate appeared to us to be an important recognition feature for esterase complementarity. In this paper, we report on the pattern of enzyme inhibition by isosorbide-2-carbamate-5-nitrates and then isosorbide2-carbamate-5-alkyl and -aryl esters. Some of the compounds in the latter

* To whom correspondence should be addressed. Phone: +353-1-896 2795. Fax: +353-1-896 2793. E-mail: gilmerjf@tcd.ie.

[†] School of Pharmacy and Pharmaceutical Sciences, Trinity College.

[‡] School of Science, Athlone Institute of Technology, Westmeath, Ireland.

[a] Abbreviations: AChE, acetylcholinesterase; ATCI, acetylthiocholine iodide; BTCI, butyrylthiocholine iodide; BuChE, butyrylcholinesterase; DCC, dicyclohexylcarbodiimide; DTNB, 5,5′-dithiobis-(2-nitrobenzoic acid); *hu*BuCHE, human butyrylcholinesterase; ISMN, isosorbide-5-mononitrate; ISMNA, isosorbide mononitrate aspirinate; MAO, monoamino oxidase; SAR, structure activity relationship, TBAF, tetrabutylammonium fluoride; TBDMS, tertbutyldimethylsilyl; TMS, tetramethylsilane.

10.1021/jm800564y CCC: $40.75 © 2008 American Chemical Society
Published on Web 09/26/2008

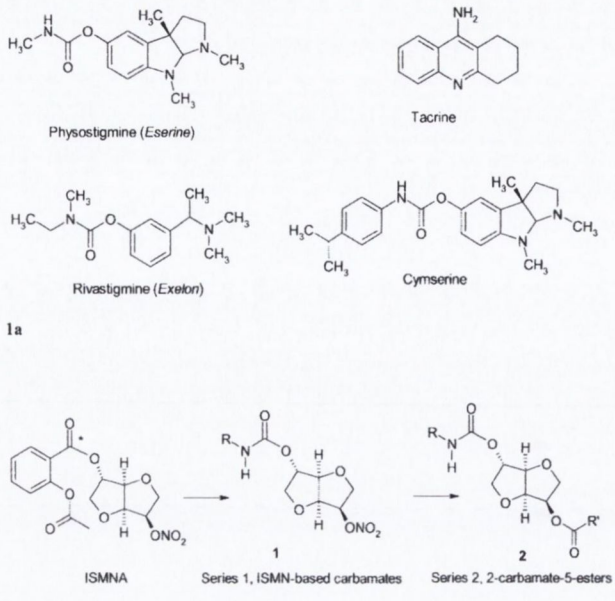

Figure 1. (1a) Carbamate inhibitors of the cholinesterases. (1b) Design strategy behind isosorbide-based carbamates.

group turned out to be among the most selective BuChE inhibitors reported. We also report preliminary kinetic and modeling data that provides an explanation for how these anomalous compounds work.

Chemistry

Isosorbide-2-carbamate-5-nitrates (series **1**, Figure 1b) were obtained by direct carbamylation of ISMN with the appropriate isocyanate in DCM in the presence of a triethylamine. The 2-carbamate-5-ester compounds of series **2** were obtained by removal of the nitrate under reductive conditions (H_2, Pd/C) and esterification with a series of commercially available acid chlorides. Where an acid chloride for a desired ester was not available, the acid itself was used instead with DCC/DMAP coupling (Scheme 1). In a few cases, acylation of the 2-carbamate nitrogen was found to compete with 5-esterification, and it proved difficult to get useful amounts of the target ester. In these cases, the order of carbamylation and esterification was reversed. ISMN was TBDMS-protected, the 5-nitrate removed, and then the 5-position esterified (Scheme 1). The 2-TBDMS group was then removed (TBAF) and the carbamate introduced as described already.

Enzyme Inhibition—SAR. Candidate inhibitors were evaluated using Ellman's spectrophotometric determination of cholinesterase activity with either human plasma or purified BuChE from human plasma.[19] For AChE activity, electric eel enzyme was used because this has quite similar active site structure to the human enzyme. Initially, the assumption was made that the inhibitors would act through carbamylation of the enzymes because their design was based on supersubstrates for *hu*BuChE (Figure 1b). Carbamate inhibition can be considered a two-step process with an initial rapidly established reversible interaction being followed by a slower covalent reaction between enzyme and inhibitor, forming an enzyme carbamate adduct.[20] The carbamate adduct hydrolyses slowly, liberating the free enzyme. The slow recovery of enzyme activity provides the fundamental kinetic distinction between carbamate inhibitors and ester substrates. Each stage of the carbamate inhibition and hydrolysis process can be influenced by structural features of the inhibitor.[20] IC_{50} values determined at a single time point are a composite value, reflecting the initial equilibrium as well as the rates of the carbamylation and decarbamylation steps and they are a generally used global measure of carbamate potency: *E/I* incubation times of 15−30 min are typical in the literature.[21−23] Inhibitory potency was determined in this study following incubation of the enzyme and test compound for 30 min. Several of the more potent compounds were also tested at 60 min with no significant shift in potency. Inhibition was initially evaluated at 100 μM with IC_{50} values estimated only for compounds showing significant inhibition (Table 1). The 5-nitrate compounds (series **1**) generally exhibited low micromolar potency toward BuChE with no significant inhibition of AChE at 100 μM. Potency increased in the series from methyl, ethyl, propyl, to butyl carbamate; the cyclohexyl carbamate had similar potency to the ethyl carbamate. The phenyl carbamates **1 g−k** were moderate inhibitors of both cholinesterases with slight preference in some cases for AChE. The most potent compound in the nitrate series was the 2-benzylcarbamate **1f** with an IC_{50} of 50 nM and >2000 fold selectivity for BuChE. When the benzyl group was maintained but the nitrate removed (leaving the isosorbide-5-position unsubstituted, **3**), there was a 74-fold drop in potency as well as selectivity (3.7 μM) although not because of any significant increase in potency toward AChE. Clearly, the 5-subsituent has a marked effect on inhibitory potency toward BuChE. It was therefore decided to explore 2-benzylcarbamates variously substituted at the 5-position with aryl and alkyl esters. The acetyl, propionyl, valeryl, and cyclopropyl ester compounds (**2a−e**) were moderately potent but selective inhibitors of BuChE. The cyclopentyl ester was the most potent of the alkyl ester compounds with an IC_{50} of 5.8 nM for BuChE and 975-fold selectivity over AChE. The 5-benzoate ester (**2i**) was the most potent compound in this study and the most selective BuChE inhibitor reported with an IC_{50} ratio of >63000 over electric eel AChE (4.3 nM/272 μM). When purified human erythrocyte AChE was used instead, the IC_{50} dropped a little to 221 μM and the selectivity ratio to 51000. The nicotinate esters **2j−k** were prepared as potentially more water soluble analogues, but they were around 20-fold less potent and selective than the corresponding benzoate. The influence of the ionisability of the pyridine ring on BuChE affinity or turnover was evaluated by measuring the IC_{50} at pH values in the range 6−8, the typical Ellman pH. The potency was found to be pH invariant in this range. A number of larger esters were prepared in order to test the hypothesis that in the case of BuChE, the isosorbide-5-ester group is accommodated by a large pocket or possibly back up the main active site channel. It was found that the benzoate ester could be replaced by 1- or 2-naphthoyl or biphenyl esters (**2l−n**) with little loss in potency. The cinnamate (**2o**) and coumarin (**2q**) esters were, however, significantly less potent and the heptyloxybenzoate ester (**2p**) quite inactive (IC_{50} 2.8 μM). Having used the 2-benzyl carbamate to probe for the optimal 5-ester, we now maintained the 5-benzoate group but changed the 2-carbamate group. The 5-benzoate-2-methylcarbamate (**2r**), -2-(3,4-dichlorophenylcarbamate) (**2s**), and 2-butylcarbamate (**2t**) compounds were significantly more potent than their nitrate analogues (**1a**, **1j**, and **1d**) as expected, but clearly in this panel of possible acyl groups, a benzyl carbamate is optimal in the 2-position and a benzoate ester at the 5-position.

Enzyme Inhibition—Mode. The relationship between inhibitory potency and assay substrate concentration was surveyed initially in a classical way in order to determine the mode of inhibition. Substrate hydrolysis velocity was proportional to

Scheme 1. Showing the Synthesis Routes to Candidate Inhibitors[a]

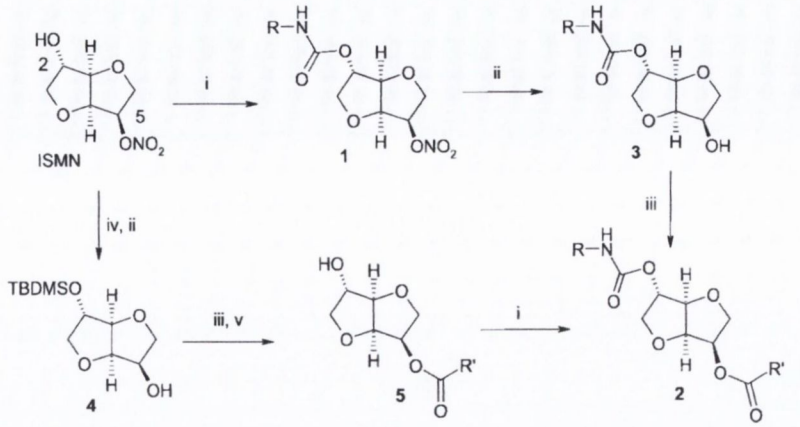

[a] (i) Isocyanate, pyridine or Et_3N/DMAP, DCM, 40 °C, 2 h; (ii) Pd/C, H_2, EtOAc, 12 h, RT; (iii) R′(CO)Cl, DMAP, Et_3N, DCM, RT, 8 h or R′C(O)OH, DCC, DMAP, DCM, RT, 8 h; (iv) TBDMSCl, imidazole, DMAP, DCM, 2 h, RT; (v) TBAF, THF, RT, 15 min.

Table 1. Carbamate Test Compounds along with Inhibition Data and Selectivity for BuChE and AChE[a]

	BuChE		AChE		
compd	%[b]	IC_{50} (μM)[c]	%[b]	IC_{50} (μM)[c]	selectivity[d]
series **1**, R=					
1a −methyl	82	5.1 (2.2−11.8)	67	17.2 (6−31)	
1b −ethyl	73	3.9 (1.6−9.7)	1		
1c −propyl	93	0.639 (0.66−1.2)	1	1520 (1300−1700)	2383
1d −butyl	92	0.894 (0.65−1.23)	32	1440 (1010−3300)	1610
1e−cyclohexyl	99	2.5 (1.7−3.4)	30		>40
1f −benzyl	96	0.051 (0.4−0.7)	35		>2000
1g −(3-trifluormethylphenyl)	10		12		
1h −phenyl	37		23		
1i −(2-chlorophenyl)	11		24		
1j −(3,4-dichlorophenyl)	28		78	9.9 (7.9−12.3)	
1k −(3-chlorophenyl)	11		24		
series **2**, R=Bn, R′=					
2a−acetyl	97	4.1 (3−5)	12		>25
2b−propionyl	97	0.98 (0.8−1.21)	5		>100
2c−valeryl	95	0.7 (0.52−0.94)	4		>142
2d−cyclopropyl	97	0.334 (0.25−0.44)	55		~300
2e−cyclopentyl	99	0.006 (0.001−0.0012)	88	56.3 (29−79)	9383
2f−triflate	85	0.359 (0.15−0.88)	6		>278
2g−mesylate	9.8		3		
2h−tosylate	25		66		
2i−benzoate	99	0.0043 (0.001−0.007)	21	272.5 (210−354)	63,255
2j−nicotinate	99	0.057 (0.049−0.068)	33		1754
2k−isonicotinate	97	0.088 (0.074−0.106)	24		
2l −(1-naphthoyl)	99	0.028 (0.025−0.032)	86	37.6 (21−69)	1342
2m −(2-naphthoyl)	100	0.032 (0.022−0.048)	80	43.4 (26−71)	1367
2n−biphenyl	99	0.012 (0.01−0.015)	89	51.6 (28−75)	4187
2o−cinnamate	96	0.137 (0.103−0.183)	82	55.9 (52−60)	~729
2p−(4-hepyloxy-)benzoate	80	2.8 (2.2−3.2)	21		35
2q−coumarin ester	100	0.073 (0.06−0.08)	81	60.4 (41−81)	821
R′, benzoate, R, carbamate					
2r−2-methycarbamate−	93	0.669 (0.541−0.768)	54		~150
2s −3,4-dichlorphenyl	38		70		
2t−2-butyl	99	0.072 (0.031−0.163)	31		1389
3−2-benzylcarbamate-5-OH	95	3.7 (3.3−4.1)	15		>27
eserine		0.028 (0.011−0.041)		0.103 (0.61−0.17)	3.7
iso-OMPA		0.733 (0.555−0.953)		2.5 (0.9−3.7)	3.41
BW284c51		255 (180−362)		0.063 (0.05−0.09)	2.5e-4

[a] All experiments performed in triplicate. [b] Inhibition % was determined at 100 μM inhibitor concentration. [c] IC_{50} values are expressed with the 95% confidence interval. [d] Selectivity was estimated by dividing the IC_{50} for AChE by the IC_{50} for BuChE. In cases where there was negligible inhibition of AChE at 100 μM and the IC_{50} was not determined, the selectivity is stated to be greater than the value obtained using 100 μM instead of the IC_{50}.

substrate concentration with increasing V_{max} values. Hydrolysis velocity was inversely proportional to inhibitor concentration consistent with a competitive mode of inhibition. However K_M values shifted only slightly. Double reciprocal plots yielded increasing slopes and intercepts, indicating mixed inhibition. Secondary replots of Lineweaver−Burk and Dixon data further indicated a significant amount of noncompetitive inhibition. This pattern can be observed when a reversible model is applied to pseudoirreversible inhibitors, and the assay is to a large extent measuring residual enzyme activity after carbamylation has already occurred. Therefore, the time dependence of inhibition was evaluated by sampling enzyme activity at successive time points immediately after introducing the inhibitor and then substrate. The experiment was performed repeatedly at increas-

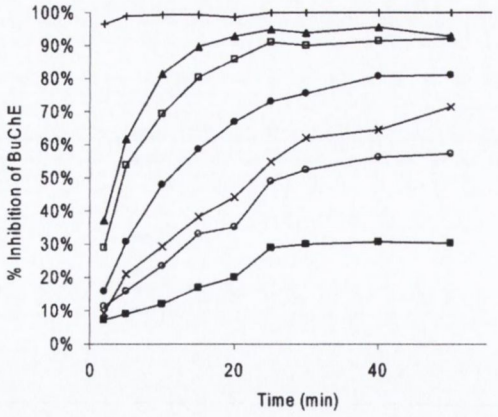

Figure 2. Percentage inhibition of *hu*BuChE by **2i** as a function of time at a BTCI concentration of 0.5 nM and inhibitor concentrations of 1.25 mM (+), 333 nM (▲), 250 nM (□), 125 nM (●), 83 nM (×), 62.5 nM (○), 50 nM (■).

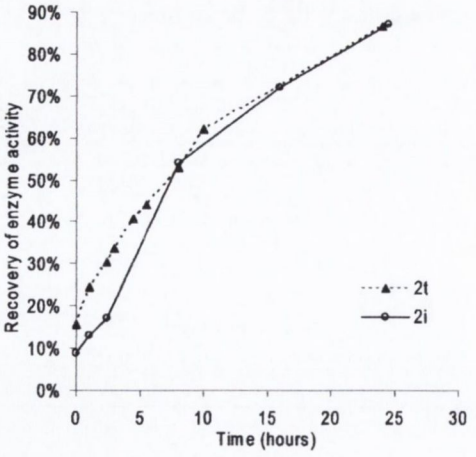

Figure 3. Recovery of purified *hu*BuChE enzyme activity following treatment with compound **2i** and **2t** and dilution.

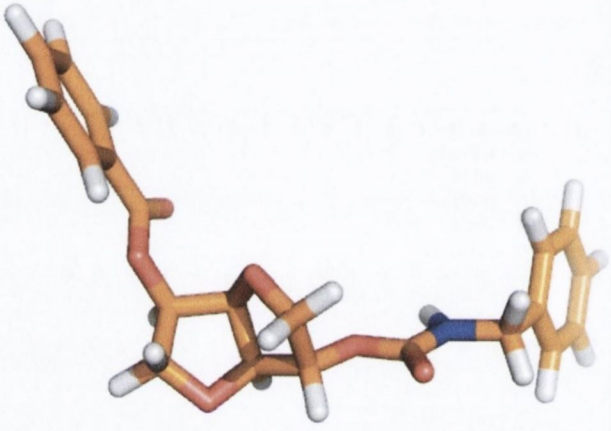

Figure 4. Conformation for compound **2i** produced using a stochastic search procedure followed by energy minimization using the MMFF94s force field in MOE. The 5-ester group is *endo* to the V-shaped ring, whereas the 2-carbamate is *exo*.

ing inhibitor but fixed substrate concentrations. The disappearance of enzyme activity for compounds **1f**, **2i**, and **2t** was time-dependent at low concentration but apparently immediate at high concentration. At intermediate−low concentration, the disappearance was first order and proportional to inhibitor concentration as shown in Figure 2 for **2i**. The IC_{50} values for **2i** determined at 60 min (3.6 nM (1.3−9.7)) was similar to the 30 min value. Further experiments were performed at fixed inhibitor concentration but increasing substrate concentration in the range 0.5−10 mM. The disappearance of enzyme activity was again time-dependent and the extent of inhibition at maximal inhibition was inversely proportional to substrate concentration, indicating competitive inhibition. When the carbamylation experiment was repeated for **2i** in the presence of edrophonium, a reversible active site directed inhibitor, there was a marked reduction in the rate and extent of inhibition.[24] Another relevant kinetic feature of carbamate inhibition is the slow regeneration of enzyme activity as the enzyme−carbamate adduct undergoes turnover. *hu*BuChE solutions were treated with compound **1f**, **2i**, or **2t** at a concentration giving 100% for two hours. Compound **2t** was selected because it gives rise to an enzyme−butyl carbamate adduct, whereas **1f** and **2i** generate enzyme−benzyl carbamates, albeit with different potencies. In the case of inhibitors **2i** and **2t**, the recovery of enzyme activity was measured following dilution to prevent reinhibition. Activity recovered slowly over 24 h but with similar rates (Figure 3). The **1f-E** solution was transferred to a dialysis bag and immersed in a buffered solution, which was then periodically changed as dialysis proceeded. In this case, there was significant residual inhibition up to 32 h.

In summary, the evidence for competitive cholinesterase carbamylation by the isosorbide-based carbamates is: (i) inhibition is time-dependent at low inhibitor concentration but independent of it at high concentration; (ii) the extent and rate of enzyme inhibition is substrate concentration dependent; (iii) inhibition is attenuated in the presence of the active-site dependent reversible inhibitor edrophonium; (iv) inhibition kinetics are first order at low concentration; (v) there is slow recovery of enzyme activity.

Modeling, Stability, and Structural Studies. Carbamate inhibitors of the cholinesterases are generally related to physostigmine, isolated from the *calabar* bean. They usually consist of an alkyl or aryl carbamate of a phenol with a distal amino group that is positively charged at physiological pH (Figure 1a). The compounds described here depart markedly from this pattern in being neutral (nonamino) and because they are derived from the secondary alcohol and pseudosugar, isosorbide. Isosorbide is V-shaped because of its *cis* ring junction with an angle of approximately 120 ° between two planar rigid rings. (Figure 4). The 2-α-OH group lies *exo* to the ring and the 5-*β* group *endo*. *Endo* substituents are directed into the V, *exo* groups outside it. Although this makes the 2-position more sterically accessible, in isosorbide, the 5-OH is activated because of an intramolecular H-bond to one of the ring oxygen atoms. In the 2-carbamate-5-esters, the 5-ester is directed orthogonal to the plane of isosorbide rings, whereas the 2-*exo* group points away from the system (Figure 4). In isosorbide diesters, the 2-group tends to undergo very rapid hydrolysis in human plasma. (This observation was critical to the carbamate design reported here.) The 5-*endo* ester is much less prone to hydrolysis (at least by butyrylcholinesterase) and in human plasma, isosorbide 2,5-diesters undergo hydrolysis almost exclusively at the 2-position, liberating the corresponding 5-monoester. For example, the half-life for isosorbide-2,5-dibenzoate at V_{max} concentration in 50% human plasma is 19 s with the exclusive liberation of isosorbide-5-benzoate.[18] The 5-benzoate product eventually decays with a half-life of 41 min. The dibenzoates do not undergo processing by AChE, indeed, substituted dibenzoates are moderately potent AChE inhibitors.[25]

To confirm the stability of the 5-ester under assay conditions, compound **2i** was incubated in 50% human plasma solution in

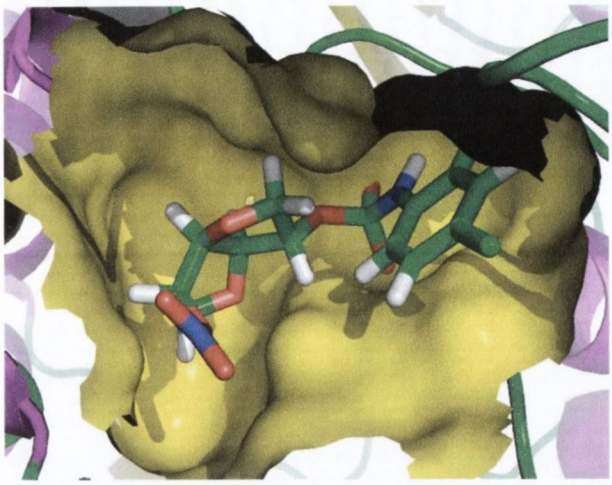

Figure 5. Compound **1f** docked within the active site gorge of *hu*BuChE with Connolly interaction surface in yellow and a Gaussian contact surface as a red mesh.

the range 10−100 μM. No hydrolysis occurred over several hours as measured by HPLC, and there was no apparent formation of either benzoic acid or isosorbide-5-benzoate, the carbamylation product. Enzyme−substrate interactions with the isosorbide-2-carbamate are preferred over enzyme-5-ester and the carbamate interaction is inhibitory, abolishing esterase activity. The failure to detect the carbamylation byproduct in this experiment is probably due to the negligible depletion of inhibitor by the tiny amount of enzyme present (BuChE is present in human plasma at about 5 mg/L with a mass of 86 kD per subunit).[26] Although isosorbide-5-esters are products of the pseudosubstrate carbamate interaction, they do not accumulate sufficiently in the inhibitory period to have influenced the inhibitory data. The isosorbide-5-benzoate ester product of compound **2i** is in any case a weak reversible inhibitor of BuChE (30% at 100 μM). The modeling and kinetic data for series **2** suggest that the 5-ester group promotes carbamylation by binding in the active site in orientations that are productive for enzyme carbamylation but not for 5-ester hydrolysis. BuChE is the most significant esterase in human plasma (at least in terms of activity). We can anticipate problems with the compounds in in vivo models because of nonspecific 5-ester hydrolysis by carboxylesterases present in other tissues that do not possess the same substrate or inhibitor/substrate as BuChE.[27] However, these observations are not relevant to interpretation of the BuChE−ligand interaction data presented here.

A modeling approach was used to further explore the nature of 5-ester interaction, the role of the 5-ester group in determining potency, and the basis for cholinesterase selectivity. Modeling of cholinesterase enzymes and their inhibitors has been aided greatly by the elucidation of the structures of enzyme−ligand complexes for both BuChE and its homologous enzyme, AChE.[28−30] The active sites of both enzymes are at the base of a gorge of some 20 Å depth in both cases.[31,32] On the basis of crystallographic studies, mutagenesis work, and radiolabeling studies, a number of subsites have been identified in the catalytic gorges that are typically involved in binding ligands, both substrates and inhibitors. While the residues that comprise these sites vary between BuChE and AChE, the overall structures are basically similar, and comparisons between the two uncover the origins of binding specificity and the basis of ligand selectivity for one enzyme over the other.

These enzymes are serine hydrolases, and a classic catalytic triad is formed with histidine and glutamate. In *hu*BuChE, these residues are Ser-198, His-438, and Glu-325. Other residues of note in BuChE are Trp-82, the principal residue of the cation-π site where the cationic head of choline substrates bind; the peripheral site residues, Asp-70 and Tyr-332, which bind ligands initially and help to orientate them appropriately to slide down the gorge and interact with the active site, and Glu-116, Glu-117, and Ala-199, which together form the oxyanion hole that stabilizes the negative charge on the carbonyl oxygen that develops subsequent to the nucleophilic attack by O-γ of the catalytic serine. The principal difference between the enzymes is the size of the acyl pocket. In AChE, the pocket is occluded by the aromatic groups of residues Phe-288 and Phe-290 (*Torpedo californica* AChE numbering is used throughout the text when referring to residues of AChE). In the larger BuChE channel, the acyl pocket is lined with the aliphatic residues Leu-286 and Val-288.

Kinetic studies indicated that inhibition by the isosorbide-based carbamates proceeds through serine carbamylation. This involves a tetrahedral intermediate that collapses to the carbamylated drug−enzyme adduct. While the transition state during a reaction process is associated with a first-order saddle point on the potential energy surface, this tetrahedral intermediate is an energy minimum on the overall surface and can thus be modeled using classical force field-based methods as described by Gao et al.[33]

Isosorbide inhibitors of BuChE were modeled in the active site of the enzyme as this tetrahedral intermediate, allowing us to draw structural conclusions regarding the basis of relative inhibitor activity. The approach has the virtue of limiting the potential containment volume of the ligand and has been used to model cholinesterase inhibitors previously.[34] It is structurally very similar to the reversible Michaelis complex formed upon initial binding and will indicate the likelihood of initial binding in a manner that is appropriate for carbamylation.

Modeling of the isosorbide-based inhibitors was based on the 2.0 Å resolution crystal structure of *hu*BuChE. (PDB entry 1p0i).[32] When BuChE was crystallized and its structure established, it was noted that the catalytic Ser-198 was bound to an unidentified moiety that was ultimately modeled as butyrate. Apparently, the presence of this butyrate fragment was essential for crystallization. The butyrate was bound to the serine residue in a tetrahedral configuration, with one oxygen atom orientated toward the oxyanion hole. The second oxygen atom points toward Trp-82, while the butyryl chain points toward the acyl pocket. The butyrate fragment could thus be used as a template for the tetrahedral intermediate involved in carbamylation. The assignment of directionality for the other functional groups was based on the positioning of similar groups in crystal structures of other enzyme−ligand complexes. The bulky isosorbide ester fragment could be orientated toward Trp-82, while the carbamate side chain could be directed toward the acyl pocket; similar placement of side chains could be observed in the crystal structures of rivastigmine and trimethylammonium trifluoroacetophenone with AChE (PDB codes 1gqr and 1amn, respectively).[29,35] The inhibitors were built in situ within the enzyme active site using the butyrate fragment as a template and placing each group at the appropriate binding subsite. A tethered minimization procedure gave rise to the models, two of which are presented in Figures 5 and 6.

The general activity of the inhibitor series could be explained by the fact that the isosorbide moiety, when the attached carbamate is bound by the catalytic serine, closely lines the base of the gorge (Figure 5) while orientating the two groups at the 2- and 5-position toward appropriate pockets. The relative

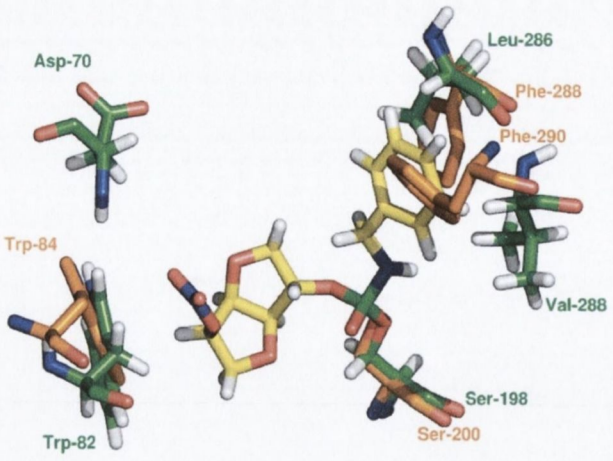

Figure 6. Compound **1f** covalently bound to *hu*BuChE. Residues Ser-200, Trp-84, Phe-288, and Phe-290 of *Tc*AChE are also shown, having been overlaid from the AChE structure from PDB code 1EA5. AChE residues are shown in orange; BuChE residues are green and the ligand yellow.

potencies of the different compounds in Table 1 could be explained by the extent to which the functional groups, permitting interactions with various residues of the active site gorge.

In series **1**, the carbamate group was altered while a nitrate group was maintained at the 5-position of isosorbide. The carbamate function was orientated toward the acyl pocket, and it was the differential interaction of the various groups with the residues at this position that gave rise to the variable potencies of these compounds. Smaller carbamate compounds tended to be poorer inhibitors of BuChE, largely because they failed to fully occupy the large pocket formed by residues Leu286 and Val288. Thus the methyl and ethyl carbamates were relatively poor inhibitors, but potency increased for propyl and butyl carbamates as the longer chains could fit better within the gorge. The phenyl carbamates were also poor inhibitors of BuChE in general because they similarly could not fill the pocket. The extra methylene group in the benzyl carbamate functional group allowed extension of the side chain into the acyl pocket, however, and the formation of $\sigma-\pi$ interactions between the aromatic ring of the ligand and the aliphatic side chains of the surrounding residues. These findings were borne out within the models: the interaction energy between the benzyl carbamate compounds and BuChE was predicted as being almost 8 kcal·mol^{-1} more favorable than the methyl carbamate and 3 kcal·mol^{-1} more favorable than the phenyl carbamate. The acyl pocket of AChE is larger and therefore less able to cope with large carbamate side chains. Phenyl carbamates tend to interact well with the aromatic side chains of Phe288 and Phe290, a fact that has been documented previously for a number of compounds such as phenserine. Extended side chains at this site tend to favor BuChE selectivity, hence the BuChE selectivity of benzyl carbamate compounds. This effect is demonstrated in Figure 6.

Modification of the group at the 5-position (series **2**) gave rise to compounds of variable potency. In the models that were prepared, the fragments at the 5-position pointed upward toward the gorge entrance, aligned with Trp-82 at the so-called cation-π site and toward the peripheral site residues at the lip of the gorge. The 5-nitrate group is relatively small and relatively few interactions were evident between this group and residues of the catalytic gorge. Its presence was still important; compound **1f** is substantially more potent than compound **3**, and this was predicted by quantitative analysis, which suggested a 7 kcal·mol^{-1} difference in binding energy between the two compounds in favor of compound **1f**. However, the incorporation of a variety of ester derivatives served to significantly increase potency. Models suggested that compound **2i** should bind more avidly to BuChE than **1f** by a factor of 8 kcal·mol^{-1}. This is principally due to the increased interaction with Trp82, the principal residue of the cation-π site. Longer chain esters could also be accommodated due to the general orientation of the 5-group pointing upward toward the gorge entrance. The biphenyl ester, for example, can interact not only with Trp82 but also Trp430, compensating for its steric bulk. Its predicted binding energy was then 1 kcal·mol^{-1} less than compound **2i**.

Table 2. Predicted Binding Affinity for a Selected Range of Inhibitors to BuChE Relative to Compound **2i**

compd	affinity (kcal·mol^{-1})
2n	−0.656
2t	−4.39
2j	−0.166
2r	−10.997
1a	−16.212
1h	−10.693
1f	−8.340
3	−14.562

The predicted binding energies of a number of the compounds, relative to the most potent inhibitor in the group, compound **2i**, are shown in Table 2.

Because the models described below are inherently biased toward the starting pose prior to minimization, a covalent docking procedure was also carried out in order to examine whether the placement of the molecules in the active site was optimal. This was achieved using the Autodock 3 program.[36] In this case, the ligand could dock within the gorge in any orientation without bias toward starting structure. Compound **2i** was docked within the active site gorge of *hu*BuChE. When the results were clustered, the largest of only four molecular clusters contained molecules docked in the described orientation. It was satisfying that the docked poses were generally similar to that produced using the minimization protocol despite the fact that the protein was rigid in this protocol. The simple and fast minimization procedure could apparently produce reliable models of the inhibitors that were replicated by the more rigorous docking approach (Figure 7).

Conclusion

Isosorbide-2-carbamate-5-nitrate and -benzoate esters are highly potent and selective inhibitors of *hu*BuChE. They are structurally distinct from established carbamates, being uncharged and derived from a secondary alcohol. Their neutrality is likely to be important to their potential utility. Central and peripheral BuChE have similar structures at the subunit level so that inhibitors of plasma BuChE ought to act as inhibitors of central BuChE, provided they cross the blood−brain barrier. The compounds act as competitive pseudosubstrates with time-dependent but reversible inhibition. Molecular models indicate that they bind with the carbamate functionality pointed into the acyl pocket and the 5-ester group directed back up the cholinesterase channel. The 5-position shows some tolerance to substitution, which might allow for tuning of pharmaceutical characteristics or the introduction of new pharmacological modalities. Compounds **2i** and **2t** are being evaluated in clinically relevant models of learning and memory in aged mice.

Experimental Section

Chemistry. Infrared (IR) spectra were obtained using a Perkin-Elmer 205 FT Infrared Paragon 1000 spectrometer. Band positions

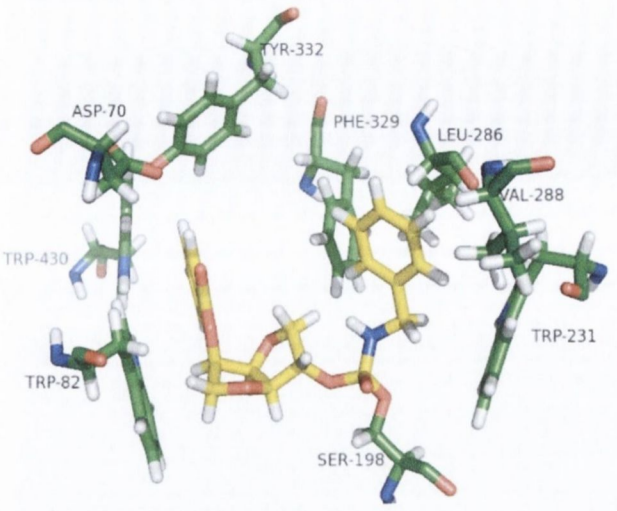

Figure 7. Compound **2i** modeled as the tetrahedral acylation intermediate in the BuChE active site using Autodock 3.

are given in cm^{-1}. Solid samples were obtained by KBr discs, and oils were analyzed as neat films on NaCl plates. ^1H and ^{13}C spectra were recorded at 27 °C on a Brucker DPX 400 MHz FT NMR spectrometer (400.13 MHz ^1H, 100.61 MHz ^{13}C) or a Brucker AV600 (600.13 MHz ^1H, 150.6 MHz ^{13}C) in either $CDCl_3$ or $(CD_3)_2CO$ with TMS as internal standard. In $CDCl_3$, ^1H spectra were assigned relative to the TMS peak at 0.0 ppm, and ^{13}C spectra were assigned relative to the middle $CDCl_3$ triplet at 77.00 ppm. In $(CD_3)_2CO$, ^1H spectra were assigned relative to the $(CD_3)_2CO$ peak at 2.05 ppm, and ^{13}C spectra were assigned relative to the $(CD_3)_2CO$ at 29.5 ppm. Coupling constants were reported in hertz (Hz). HRMS was performed using a Micromass mass spectrophotometer with electrospray ionization at the School of Chemistry, Trinity College Dublin. Elemental analyses were performed at the Microanalytical Laboratory, Department of Chemistry, University College Dublin. Flash chromatography was performed on Merck Kieselgel (particle size: 60 mm).

Isosorbide-2-(butylcarbamate)-5-mononitrate (1d). ISMN (0.7852 g, 4 mmol) was dissolved in dry pyridine (5 mL). Butyl isocyanate (mol wt 99.13 g/mol, $d = 0.880$ g/mL, 8 mmol, 0.79304 g, 0.9 mL) was added and the mixture heated at 100 °C for 1 h. The mixture was cooled and methanol (10 mL) added to remove excess isocyanate. The mixture was then heated for further 10 min at 100 °C, cooled to room temperature, poured into ice−water, and stirred. The precipitate was collected and crystallized from hot methanol to yield 0.69 g of a white crystalline product (59.3%): mp 101.7 °C. ^1H NMR δ ($CDCl_3$): 0.91−0.95 (t, 3H, $J = 7.8$ Hz.), 1.32−1.1.39 (m, 2H), 1.45−1.51 (q, 2H, $J = 7.8$ Hz), 3.16−3.21 (q, 2H, $J = 7$ Hz), 3.88−3.3.92 (m, 1H), 3.96−4.06 (m, 3H), 4.49−4.50 (d, 1H, $J = 5.3$ Hz,), 4.79 (s, 1H), 4.95−4.97 (t, 1H, $J = 5.3$ Hz), 5.17−5.18 (d, 1H, $J = 2.6$ Hz), 5.3−5.35 (m, 1H). ^{13}C NMR ppm ($CDCl_3$): 13.2, 19.39, 31.4, 40.3, 68.7, 73.3, 77.1, 80.9, 80.9, 86.34, 154.6. Anal. ($C_{11}H_{18}N_2O_7$) C, H, N.

Isosorbide-2-(benzylcarbamate)-5-mononitrate (1f). A white crystalline product (47.3%): mp 93.4 °C, $[\alpha]_D$ +99.01 °C. ^1H NMR δ ($CDCl_3$): 3.88−3.91 (m, 1H), 3.96−4.07 (m, 3H), 4.36−4.38 (d, 2H, $J = 6$ Hz), 4.50−4.51 (d, 1H, $J = 4.8$ Hz), 4.94−4.96 (t, 1H, $J = 5.2$ Hz), 5.20−5.21 (d, 1H, $J = 2.8$ Hz), 5.23 (s, 1H), 5.33−5.36 (m, 1H), 7.28−7.38 (m, 5H). ^{13}C NMR ppm ($CDCl_3$): 69.6, 74.1, 77.2, 78.23, 81.76, 81.85, 87.14, 127.95, 128.07, 129.2, 138.42, 155.54. Anal. ($C_{14}H_{16}N_2O_7$) C, H, N.

Isosorbide-2-phenylcarbamate-5-mononitrate (1h). A white crystalline product (22%): mp 156.6 °C, $[\alpha]_D$ +81.0 °. ^1H NMR δ ($CDCl_3$): 3.9 (m, 1H), 4.0 (m, 2H), 4.1 (d, 1H), 4.5 (d, 1H, $J = 4.9$ Hz), 5.0 (t, 1H, $J = 4.9$ Hz), 5.3 (d, 1H, $J = 3$ Hz), 5.4 (m, 1H), 6.7 (s, 1H), 7.1 (t, 1H), 7.3 (m, 4H). ^{13}C NMR ppm ($CDCl_3$): 69.31, 73.59, 78.02, 81.29, 81.53, 86.66, 118.72, 123.93, 129.17, 137.24, 152.05. Anal. ($C_{13}H_{14}N_2O_7$) C, H, N.

Isosorbide-2-benzylcarbamate (3). 2-(Benzylaminocarbonyloxy-)-5-*O*-nitro-1,4:3,6-dianhydro-D-glucitol **1f** (mol wt 324.29 g/mol, 46.25 mmol, 15 g) was dissolved in ethyl acetate:methanol 1:1 (100 mL) in a 250 mL round-bottom flask. A spatula tip-full of 10% palladium on activated carbon was added to the solution. Air was expelled from the flask, and the mixture was kept under an atmosphere of hydrogen gas and stirred for 24 h. The solvent was evaporated under vacuum, and the crude product was dissolved in DCM and filtered through silica. The filtrate was collected and evaporated under vacuum to yield 12.60 g as a white crystalline product (97.5%). mp 76.0 °C. ^1H NMR δ ($CDCl_3$): 2.67 (d, 1H, $J = 7.03$ Hz), 3.57 (dd, 1H, $J = 5.53$, 8.54 Hz), 3.90 (dd, 1H, $J = 6.03$, 9.54 Hz), 4.00 (dd, 1H, $J = 3.51$, 10.54 Hz), 4.10 (d, 1H, $J = 10.45$), 4.31 (m, 1H), 4.38 (d, 2H, $J = 6.03$ Hz), 4.51 (d, 1H, $J = 4.01$ Hz), 4.61 (t, 1H, $J = 4.77$ Hz), 5.17 (m, 1H), 5.22 (d, 1H, $J = 3.01$ Hz), 7.23−7.40 (m, 5H). ^{13}C NMR ppm ($CDCl_3$): 44.70 (CH_2), 71.8, 73.04, 73.38, 78.39, 81.46, 85.25, 127.13, 127.23, 128.30, 137.6, 154.69. Anal. ($C_{14}H_{17}NO_5$) C, H, N.

Isosorbide-2-benzylcarbamate-5-cyclopropanoate (2d). A white crystalline product (265.2 mg, 85.2%): mp 96 °C. ^1H NMR δ ($CDCl_3$): 0.87−0.98 (m, 2H), 1.04 (m, 2H), 1.70 (m, 1H), 3.80 (dd, 1H, $J = 5.52$, 9.54 Hz), 3.95 (dd, 1H, $J = 6.03$, 9.54 Hz), 3.98−4.08 (m, 2H), 4.37 (d, 2H, $J = 6.02$ Hz), 4.52 (d, 1H, $J = 4.51$ Hz), 4.79 (t, 1H, $J = 4.77$ Hz), 5.14 (q, 1H, $J = 5.52$, 11.54 Hz), 5.17−5.27 (m, 2H), 7.22−7.40 (m, 5H). ^{13}C NMR ppm ($CDCl_3$): 44.64, 69.74, 73.25, 73.48, 78.09, 80.27, 85.52, 127.10, 127.17, 128.3, 137.65, 154.81, 173.93. Anal. ($C_{18}H_{21}NO_6$) C, H, N.

Isosorbide-2-benzylcarbamate-5-cyclopentanoate (2e). A white crystalline compound (81.9%): mp 94 °C. ^1H NMR δ ($CDCl_3$): 1.53−2.00 (m, 8H), 2.83 (m, 1H), 3.73 (dd, 1H, $J = 5.02$ and 10.03 Hz), 3.89−4.06 (m, 3H), 4.39 (d, 2H, $J = 6.02$ Hz), 4.50 (d, 1H, $J = 4.51$ Hz), 4.81 (t, 1H, $J = 5.02$ Hz), 5.08−5.18 (m, 2H), 5.20 (d, 1H, $J = 3.01$ Hz), 7.22−7.40 (m, 5H). ^{13}C NMR ppm ($CDCl_3$): 25.35, 25.37, 29.43, 29.73, 43.04, 44.65, 70.12, 73.05, 73.21, 78.06, 80.29, 85.62, 127.10, 127.19, 128.28, 137.61, 154.79, 175.78. Anal. ($C_{20}H_{25}NO_6$) C, H, N.

Isosorbide-2-(benzylcarbamate)-5-benzoate (2i). Compound **3** (0.6027 g, 2 mmol) was dissolved in dry pyridine (5 mL), and the solution was cooled to −5 °C using a salt/water bath. Benzoyl chloride (mol wt 140.57 g/mol, $d = 1.211$ g/mL, 5 mmol, 0.56 mL) was added. The mixture was allowed to come to room temperature, and stirring was continued for 22 h. The mixture was added to ice−water (approx 200 mL), and the precipitated solid was filtered. The resultant solid was taken up in chloroform (15 mL) washed first with water (10 mL) then with saturated brine solution (10 mL), dried with anhydrous sodium sulfate (10 g), filtered into a round-bottomed flask, and evaporated under reduced pressure. The resultant semisolid was recrystallized from hot ethanol to yield 0.74 g of a white crystalline product (96.1%): mp 76.0 °C, $[\alpha]_D$ +13.45 °C. ^1H NMR δ (DMSO): 3.84−3.85 (s, 2H), 3.85−3.97 (m, 2H), 4.18−4.20 (d, 2H, $J = 6.4$ Hz), 4.45−4.46 (d, 1H, $J = 5.2$ Hz), 4.88−4.91 (t, 1H, $J = 5.6$ Hz), 5.03 (s, 1H), 5.36−5.38 (t, 1H), 7.23−7.33 (m 5H), 7.53−7.57 (m, 2H), 7.66−7.70 (m, 1H), 7.97−8.01 (m, 3H). ^{13}C NMR ppm (DMSO): 44.10, 70.89, 73.08, 74.79, 77.86, 81.04, 86.29, 127.16−127.37, 128.63, 129.19, 129.56−129.65, 133.86, 139.89, 155.8, 165.30. Anal. ($C_{21}H_{21}NO_6$) C, H, N.

Isosorbide-2-benzylcarbamate-5-nicotinate (2j). To a solution of 2-*O*-(*t*-(butyl)-dimethylsilyl-)-1,4:3,6-dianhydro-D-glucitol **4** (mol wt 260.40 g/mol, 1.1521 mmol, 300 mg) in dry THF (50 mL) was added 1.25 mol equiv of anhydrous nicotinoyl chloride hydrochloride (mol wt 178.05 g/mol, 1.4400 mmol, 256.4 mg). The mixture was kept under an atmosphere of nitrogen and stirred at room temperature for 15 min. To the mixture was added four mol equiv of triethylamine, and stirring was continued for a further 24 h. The solvent was evaporated under vacuum to give a white residue, which was dissolved in a saturated aqueous solution of Na_2CO_3 (25 mL) and extracted with DCM (3 × 25 mL). The collected organic portions were dried over anhydrous sodium sulfate (5 g) and evaporated to dryness to give a clear oil. The oil was diluted with

THF (10 mL) and 1.1 mol equiv of TBAF (mol wt 261.47 g/mol, 0.7524 mmol, 196.7 mg, 0.7524 mL of a 1 M solution) was added, and the mixture was stirred at room temperature for 15 min. The solution was evaporated to dryness under vacuum giving a brown oil. DCM (10 mL) was added to the reaction vessel, and the solution was stirred at room temperature. To the mixture was added triethylamine (mol wt 101 g/mol, d 0.726 g/mL, 0.7515 mmol, 75.9 mg, 0.1047 mL), benzyl isocyanate (mol wt 133.15 g/mol, d 1.078 g/mL, 0.7515 mmol, 100.2 mg, 0.0929 mL), and DMAP (mol wt 122.17 g/mol, 0.2456 mmol, 30 mg). The mixture was heated to 105 °C for two hours. The mixture was cooled upon completion of the reaction, and methanol (10 mL) was added to remove excess isocyanate. The mixture was heated for a further 15 min at 105 °C and cooled to room temperature. All organic solvent was removed under vacuum giving a clear oil to which was added DCM (20 mL) and washed with 1 M HCl (20 mL), 5% $NaHCO_3$ (20 mL), and saturated brine solution (20 mL) and dried over anhydrous sodium sulfate (2 g). The solution was filtered into a round-bottomed flask, which was evaporated under vacuum to give a white crystalline compound. Purification by column chromatography using hexane and ethyl acetate (3:1 and 1:1) as eluent afforded **2j** as a white crystalline compound (187.7 mg, 42.3%): mp 136 °C, mol. ^{1}H NMR δ ($CDCl_3$): 3.93−4.07 (m, 4H), 4.37 (d, 2H, J = 6.03 Hz), 4.55 (d, 1H, J = 4.52 Hz, IsH-3), 4.94 (t, 1H, J = 5.02 Hz), 5.22 (d, 1H, J = 2.01 Hz), 5.39 (m, 2H), 7.20−7.37 (m, 5H), 7.38−7.48 (s, 1H), 8.32 (d, 1H, J = 7.53 Hz) 8.80 (s, 1H), 9.35 (s, 1H). ^{13}C NMR ppm ($CDCl_3$): 44.64, 70.17, 73.18, 74.50, 77.85, 80.44, 85.82, 123.12, 126.78, 127.0, 127.15, 128.25, 136.74, 137.65, 150.47, 153.23, 154.81, 165.36. Anal. ($C_{20}H_{20}N_2O_6$) C, H, N.

2-(Benzylaminocarbonyloxy-)-5-*O*-(1-naphthoyl)-1,4:3,6-dianhydro-D-glucitol (2l). A white crystalline product (86.8%): mp 126 °C. ^{1}H NMR δ ($CDCl_3$): 4.01−4.16 (m, 4H), 4.38 (d, 2H, J = 6.03 Hz), 4.61 (d, 1H, J = 4.52 Hz), 5.03 (t, 1H, J = 5.02 Hz), 5.11 (s, 1H), 5.26 (s, 1H), 5.51 (q, 1H, J = 5.53, 11.05 Hz), 7.23−7.40 (m, 5H), 7.50−7.60 (m, 2H), 7.65 (t, 1H, J = 7.28 Hz), 7.92 (d, 1H, J = 8.03 Hz), 8.07 (d, 1H, J = 8.03 Hz), 8.25 (d, 1H, J = 7.72 Hz), 8.96 (d, 1H, J = 8.53 Hz). ^{13}C NMR ppm ($CDCl_3$): 44.69, 70.23, 73.2, 74.11, 78.14, 80.56, 85.80, 124.06, 125.31, 125.85, 125.90, 127.11, 127.21, 127.47, 128.11, 128.30, 130.01, 130.95, 133.30, 133.36, 137.54, 154.77, 166.33. Anal. ($C_{25}H_{23}NO_6$) C, H, N.

Isosorbide-2-(methylcarbamate)-5-benzoate (2r). Colorless gum (0.52 g, 65%). ^{1}H NMR δ ($CDCl_3$): 8.02 (2H, d, J = 8.03 Hz), 7.55 (1H, t, J = 7.53 Hz), 7.42 (2H, t, J = 8.03 Hz), 5.36 (1H, d, J = 5.52 Hz), 5.15 (1H, s), 4.91 (1H, t, J = 5.02 Hz), 4.51 (1H, d, J = 5.02 Hz), 3.91 (4H, m,), 2.75 (3H, d, J = 4.52 Hz). ^{13}C NMR δ ($CDCl_3$): 165.45, 155.22, 132.85, 129.24, 128.96, 128.01, 86.29, 80.96, 80.49, 77.21, 73.13, 68.70, 27.00. HRMS: found, $(M - Na)^+$ = 330.0946; required, $(M - Na)^+$ = 330.0954.

Isosorbide-2-(butylcarbamate)-5-benzoate (2t). A white crystalline product; (10.2%): mp 81.7 °C, mol. ^{1}H NMR δ (DMSO): 0.8−0.9 (t, 3H), 1.2−1.3 (q, 2H), 1.33−1.38 (q, J = 2.4 Hz), 2.96−2.99 (q, 2H, J = 6.4 Hz), 3.82−3.83 (s, 2H), 3.89−3.97 (m, 2H), 4.41−4.43 (d, 1H, J = 5.2 Hz), 4.86−4.89 (t, 1H, J = 5.2 Hz), 4.99 (s, 1H), 5.36−5.39 (q, 1H, J = 4 Hz), 7.35−7.38 (t, 1H, J = 5.6 Hz), 7.53−7.57 (m, 2H), 7.66 (m, 1H), 7.9−8 (d, 2H). ^{13}C NMR ppm (DMSO): 13.97, 19.74, 31.75, 40.0, 70.87, 73.08, 74.79, 77.55, 81.02, 86.31, 129.18, 129.55, 129.6, 133.84, 155.53, 165.28. Anal. ($C_{18}H_{23}O_6N$) C, H, N.

Enzyme Studies. Cholinesterase activity was measured using the Ellman spectrophotometric method. *Hu*BuChE activity was measured in replicate samples using a 96-well plate reader. The total volume of test solution in each well was 250 μL. This consisted of 25 μL of plasma solution, 150 μL of phosphate buffer pH 8.0, 25 μL of DTNB solution (0.5 mM), and 25 μL of acetonitrile: distilled water (1:1). The 96-well plate was incubated for 30 min before 25 μL of BTCI solution (0.5 mM) was added, and the reaction was measured at 405 nm over 5 min using an Anthos bt2 plate reader. For the determination of AChE activity, 25 μL of electric eel AChE solution and 25 μL of ATCI solution were used instead of the plasma solution and BTCI solution. For determination of enzyme inhibition, 25 μL of an inhibitor solution was added to the test solution instead of the acetonitrile:water (1:1) solution. Inhibitors were added 30 min before determination of remaining enzyme activity. IC_{50} values were calculated using xlfit 4.0 software and GraphPad Prism 4.02 software. For carbamylation studies with compounds **2i** and **2t**, initial testing involved measuring cholinesterase activity at various [I] and [S] while incubating the enzyme and inhibitor over a 1 h period. Readings were obtained at 0, 5, 10, 20, 30, 40, 50, and 60 min with [E] = 1.2×10^{-3} mg/mL purifed *hu*BuChE, [DTNB] = 0.3 mM, [S] and [I] varied. The relevant amounts of buffer, inhibitor, and enzyme were mixed in a cuvette and allowed to incubate for the various time intervals. Once incubation was complete, the DTNB and substrate were added and the reaction was measured at 412 nm for 5 min. After completion of the above, the data was transformed so as to plot ln E/E_T versus time. The carbamylation experiments were repeated using compound **2t** at 1 mM (giving 100% inhibition) in the presence of the edrophonium (5 mM). The reversibility of carbamate inhibitors was determined by using dialysis or by dilution of the enzyme carbamate adduct and monitoring for recovery of activity. The dialysis experiments were performed using Visking dialysis tubing (Medicell International Ltd. supplied from Lennox Laboratory Supplies Ltd., Dublin) with an exclusion limit of 12000−14000 Da. The enzyme was mixed with inhibitor at a concentration giving 100% inhibition. Each experiment was performed in triplicate. Tubing was sealed at both ends using dialysis clips (Lennox Laboratory Supplies Ltd., Dublin). The samples were dialysed against buffer (1 L) at 37 °C, with samples being removed and assayed at intervals. The buffer was renewed at 4−6 h intervals. A control containing no inhibitor was treated and sampled in parallel with the samples. In the dilution experiments (compounds **2i** and **2t**), enzyme was incubated with sufficient inhibitor for at least 2 h to effect at least 90% inhibition. The mixture was then diluted 1000-fold in order to minimize the possibility of reinhibition by excess inhibitor. This dilution was made using phosphate buffer pH 8.0. The diluted sample was kept at 37 °C for the duration of the analysis, with aliquots being taken at defined time intervals and checked for BChE activity as described previously.

Stability Studies. Pooled plasma solutions (4 mL, 50%) were prepared by centrifugation of citrated human venous blood and dilution of the resultant supernatant with pH 7.4 phosphate buffer (2 mL). The pooled plasma sample gave normal adult BuChE activity. A 100 μL aliquot of compound **2i** in acetonitrile was added to plasma solution and then incubated (37 °C). Aliquots (250 μL) of the incubated mixture were withdrawn at appropriate intervals and transferred to 1.5 mL Eppendorf tubes containing 500 μL of 2% $ZnSO4 \cdot 7H_2O$ in MeCN−H_2O (1:1) solution and 250 μL of acetonitrile. Samples were then vortexed for 30 s and centrifuged for 3 min at 10000 rpm. A 20 μL aliquot of the clear supernatant was analyzed by HPLC. A gradient method was used with a Waters ODS2 4.6 mm × 250 mm column and mobile phase consisting of phosphate buffer (pH 2.5):acetonitrile, 50:50, grading to 20:80 over 20 min. External standards of isorobide-5-benzoate, benzoic acid, and compound **2i** were used to confirm specificity. The eluent was monitored at 230 nm and peak identity and homogeneity confirmed by PDA analysis. The experiment was repeated five times in the range 1−100 μM.

Docking Studies. The atomic coordinates of the crystal structure of BuChE with bound butyrate (PDB code 1p0i) were used. All molecules of water were removed, along with other heteroatoms, to leave only the bound butyrate and the enzyme itself. Residues 1−3, 378−379, and 455, all of which were missing in the original crystal structure, were added using Swiss PDB Viewer v3.7. The added residues were briefly minimized within MOE (Chemical Computing Group, Montreal, Canada) using a sequence of SD, CG, and Truncated Newton algorithms; the AMBER99 force field and atom charges were used to model the protein throughout. Each inhibitor was rehybridized to sp^3 at the carbonyl carbon. The fragments distal to the carbamate were energy minimized using the MM94s force field.[37,38] The carbonyl oxygen was assigned a formal charge of −1. Inhibitor molecules were manually superim-

posed onto the butyrate fragment in the appropriate orientation, as carried out by Luo et al. in AChE.[34] The butyrate fragment was deleted and the inhibitor molecule covalently joined to O-χ of the active site serine, forming the desired intermediate. To prepare the complex for minimization, partial atomic charges for the nonstandard ligand atoms were calculated using MOPAC 7 (AM1-BCC method)[39] interfaced to MOE in a simplified system with the oxyanion hole residues removed. Because the total charge calculated for the inhibitor atoms was not an integer due to charge transfer between the inhibitor and Ser-198 during the reaction, the charge was altered on O-χ of the serine to give an overall charge of -1 on the inhibitor and Ser-198 atoms. AMBER 99 charges were calculated for the remaining protein atoms. The system was optimized for hydrogen bonding and protonation states for each residue in the protein were assigned using PDB2PQR[40] and Propka;[41] it was always ensured that Glu-325 and His-438 were appropriately protonated, such that the important hydrogen-bonding network of the catalytic triad was maintained. Subsequently, the whole system was energy minimized in MOE using sequential SD (100 steps) and TN (1000 steps or to an rms gradient of <0.01 kcal/(mol·A)) algorithms. The distances between the negatively charged carbonyl oxygen and the backbone nitrogens of the oxyanion hole residues were constrained, along with the distances between the hydrogen-bonding atoms of the catalytic triad. Generalized Born solvation was used with an interior dielectric constant of 20 and an exterior dielectric of 80. A nonbonded cutoff was applied, with a smoothing function applied between 12 and 15 Å. A second iteration of charge calculation and energy minimization was performed in an identical manner to arrive at the final models of the protein−carbamate adducts shown.

The interaction energies of the enzyme−ligand complexes were calculated using MOE. The interaction energies reported are the pairwise atomic interaction energies between the atoms of the ligand and all other atoms in the system. A reaction field model was used to describe electrostatic interactions, while all other parameters described for the minimization procedure were maintained when calculating these energies.

For the covalent docking procedure, the protein−ligand adduct was set up using Michel Sanner's Autodock Tools version 1.4.6, (http://autodock.scripps.edu/resources/adt), the graphical user interface to Autodock. The tetrahedral ligand of **2i** that had been produced using the procedures described above was extracted from the complex and set up for docking; eight rotable bonds were set in the ligand. The O-χ of serine in the adduct was changed to a covalent-binding atom type. The structure of *hu*BuChE with butyrate described above was used once again for docking, but in this case, the butyrate fragment was removed to leave only the protein itself. The protein was modified by deleting the side chain oxygen from Ser-198. Atomic affinity maps, an electrostatic potential map, and a covalent affinity map were computed using AutoGrid 3. The covalent affinity map was calculated using a spherically symmetric inverted Gaussian-shaped potential energy with a half-width of 5.0 Å and an energy penalty of 1000.0 kcal·mol^{-1}, with the minimum energy value centered on the coordinates of the χ-oxygen atom. In subsequent dockings, the covalently binding atom type in the adduct sought out this position, effectively binding the ligand to the protein. Autodock 3 was used to perform 50 independent dockings using the Lamarckian genetic algorithm, each starting from random initial positions. A population size of 300 was used for the search, with a maximum of 2.5 million energy evaluations. The results of these dockings were clustered using an rmsd tolerance of 3.0 Å. The highest scoring results were taken as indicative of the most appropriate binding mode for the ligand.

Acknowledgment. This work was supported by Science Foundation Ireland (05/RFP/CHE0046), Enterprise Ireland (BRGS2002), and IRCSET (Ciaran Carolan). We are grateful to Schwarz-Pharma, Shannon, Co. Clare for a gift of ISMN.

Supporting Information Available: Characterization data for compounds **1a**, **1b**, **1c**, **1e**, **1g**, **1i**, **1j**, **1k**, **21**, **2b**, **2c**, **2f**, **2g**, **2h**, **2k**, **2m**, **2n**, **2o**, **2p**, **2q**, **2s**, **4**; elemental analysis data, purity data by HPLC. This material is available free of charge via the Internet at http://pubs.acs.org.

References

(1) Francis, P. T.; Palmer, A. M.; Snape, M.; Wilcock, G. K. The cholinergic hypothesis of Alzheimer's disease: a review of progress. *J. Neurol. Neurosurg. Psychiatry* **1999**, *66*, 137–147.

(2) Bartus, R. T.; Dean, R. L.; Beer, B.; Lippa, A. S. The cholinergic hypothesis of geriatric memory dysfunction. *Science* **1982**, *217*, 408–417.

(3) Drachman, D. A.; Leavitt, J. Human memory and the cholinergic system. *Arch. Neurol.* **1974**, *30*, 113–121.

(4) Muñoz-Ruiz, P.; Rubio, L.; García-Palomero, E.; Dorronsoro, I.; del Monte-Millán, M.; Valenzuela, R.; Usán, P.; de Austria, C.; Bartolini, M.; risano, V.; Bidon-Chanal, A.; Orozco, M.; Luque, F. J.; Medina, M.; Martínez, A. Design, synthesis, and biological evaluation of dual binding site acetylcholinesterase inhibitors: new disease-modifying agents for Alzheimer's disease. *J. Med. Chem.* **2005**, *48*, 7223–7233.

(5) Bolognesi, M. L.; Cavalli, A.; Valgimigli, L.; Bartolini, M.; Rosini, M.; risano, V.; Recanatini, M.; Melchiorre, C. Multi-target-directed drug design strategy: from a dual binding site acetylcholinesterase inhibitor to a trifunctional compound against Alzheimer's disease. *J. Med. Chem.* **2007**, *50*, 6446–6449.

(6) Camps, P.; Formosa, X.; Muñoz-Torrero, D.; Petrignet, J.; Badia, A.; Clos, M. V. Synthesis and pharmacological evaluation of huprine−tacrine heterodimers: subnanomolar dual binding site acetylcholinesterase inhibitors. *J. Med. Chem.* **2005**, *48*, 1701–1704.

(7) Elsinghorst, P. W.; Cieslik, J. S.; Mohr, K.; Tränkle, C.; Gütschow, M. First gallamine−tacrine hybrid: design and characterization at cholinesterases and the M2 muscarinic receptor. *J. Med. Chem.* **2007**, *50*, 5685–5695.

(8) Brühlmann, C.; Ooms, F.; Carrupt, P. A.; Testa, B.; Catto, M.; Leonetti, F.; Altomare, C.; Carotti, A. Coumarins derivatives as dual inhibitors of acetylcholinesterase and monoamine oxidase. *J. Med. Chem.* **2001**, *44*, 3195–3198.

(9) Rodríguez-Franco, M. I.; Fernández-Bachiller, M. I.; Pérez, C.; Hernández-Ledesma, B.; Bartolomé, B. Novel tacrine−melatonin hybrids as dual-acting drugs for Alzheimer disease, with improved acetylcholinesterase inhibitory and antioxidant properties. *J. Med. Chem.* **2006**, *49*, 459–462.

(10) Fang, L.; Appenroth, D.; Decker, M.; Kiehntopf, M.; Roegler, C.; Deufel, T.; Fleck, C.; Peng, S.; Zhang, Y.; Lehmann, J. Synthesis and biological evaluation of NO-donor-tacrine hybrids as hepatoprotective anti-Alzheimer drug candidates. *J. Med. Chem.* **2008**, *51*, 713–716.

(11) Iwasaki, T.; Yoneda, M.; Nakajima, A.; Terauchi, Y. Serum butyrylcholinesterase is strongly associated with adiposity, the serum lipid profile and insulin resistance. *Intern. Med.* **2007**, *46*, 1633–1639.

(12) Mesulam, M. M.; Guillozet, A.; Shaw, P.; Levey, A.; Duysen, E. G.; Lockridge, O. Acetylcholinesterase knockouts establish central cholinergic pathways and can use butyrylcholinesterase to hydrolyze acetylcholine. *Neuroscience* **2002**, *110*, 627–639.

(13) Perry, E. K.; Perry, R. H.; Blessed, G.; Tomlinson, B. E. Changes in brain cholinesterases in senile dementia of Alzheimer type. *Neuropathol. Appl. Neurobiol.* **1978**, *4*, 273–277.

(14) Guillozet, A. L.; Smiley, J. F.; Mash, D. C.; Mesulam, M. M. Butyrylcholinesterase in the life cycle of amyloid plaques. *Ann. Neurol.* **1997**, *42*, 909–918.

(15) Greig, N. H.; Utsuki, T.; Ingram, D. K.; Wang, Y.; Pepeu, G.; Scali, C.; Yu, Q. S.; Mamczarz, J.; Holloway, H. W.; Giordano, T.; Chen, D.; Furukawa, K.; Sambamurti, K.; Brossi, A.; Lahiri, D. K. Selective butyrylcholinesterase inhibition elevates brain acetylcholine, augments learning, and lowers Alzheimer beta-amyloid peptide in rodent. *Proc. Natl. Acad. Sci. U.S.A.* **2005**, *102*, 17213–17218.

(16) Gilmer, J. F.; Moriarty, L. M.; McCafferty, D. F.; Clancy, J. M. Synthesis, hydrolysis kinetics and antiplatelet effects of isosorbide mononitrate derivatives of aspirin. *Eur. J. Pharm. Sci* **2001**, *14*, 221–227.

(17) Gilmer, J. F.; Moriarty, L. M.; Lally, M. N.; Clancy, J. M. Isosorbide-based aspirin prodrugs. II. Hydrolysis kinetics of isosorbide diaspirinate. *Eur. J. Pharm. Sci.* **2002**, *16*, 297–304.

(18) Gilmer, J. F.; Lally, M. N.; Gardiner, P.; Dillon, G.; Gaynor, J. M.; Reidy, S. Novel isosorbide-based substrates for human butyrylcholinesterase. *Chem. Biol. Interact.* **2005**, *157−158*, 317–319.

(19) Ellman, G. L.; Courtney, K. D.; Andres, V.; Featherstone, R. M. A New and Rapid Colorimetric Determination of Acetylcholinesterase Activity. *Biochem. Pharmacol.* **1961**, *7*, 88–95.

(20) Groner, E.; Ashani, Y.; Schorer-Apelbaum, D.; Sterling, J.; Herzig, Y.; Weinstock, M. The kinetics of inhibition of human acetylcholinesterase and butyrylcholinesterase by two series of novel carbamates. *Mol. Pharmacol.* **2007**, *71*, 1610–1617.

(21) Bartolucci, C.; Siotto, M.; Ghidini, E.; Amari, G.; Bolzoni, P. T.; Racchi, M.; Villetti, G.; Delcanale, M.; Lamba, D. Structural determinants of *Torpedo californica* acetylcholinesterase inhibition by the novel and orally active carbamate based anti-Alzheimer drug ganstigmine (CHF-2819). *J. Med. Chem.* **2006**, *49*, 5051–5058.

(22) Luo, W.; Yu, Q. S.; Zhan, M.; Parrish, D.; Deschamps, J. R.; Kulkarni, S. S.; Holloway, H. W.; Alley, G. M.; Lahiri, D. K.; Brossi, A. Novel anticholinesterases based on the molecular skeletons of furobenzofuran and methanobenzodioxepine. *J. Med. Chem.* **2005**, *48*, 986–994.

(23) Yu, Q.; Holloway, H. W.; Utsuki, T.; Brossi, A.; Greig, N. H. Synthesis of Novel Phenserine-Based-Selective Inhibitors of Butyrylcholinesterase for Alzheimer's Disease. *J. Med. Chem.* **1999**, *42*, 1855–1861.

(24) Saxena, A.; Redman, A. M.; Jiang, X.; Lockridge, O.; Doctor, B. P. Differences in active site gorge dimensions of cholinesterases revealed by binding of inhibitors to human butyrylcholinesterase. *Biochemistry* **1997**, *36*, 14642–14651.

(25) Carolan, C. G.; Gaynor, J. M.; Dillon, G. P.; Khan, D.; Ryder, S.; Reidy, S. A.; Gilmer, J. F. Novel isosorbide di-ester compounds as inhibitors of acetylcholinesterase. *Chem–Biol. Interact.* **2008**, 18606399. [Epub ahead of print], PMID.

(26) Li, B.; Sedlacek, M.; Manoharan, I.; Boopathy, R.; Duysen, E. G.; Masson, P.; Lockridge, O. Butyrylcholinesterase, paraoxonase, and albumin esterase, but not carboxylesterase, are present in human plasma. *Biochem. Pharmacol.* **2005**, *70*, 1673–1684.

(27) Khan, D.; Gilmer, J. F.; Carolan, C. G.; Gaynor, J. M.; Ryder, S. A. Pharmacological effects of a novel isosorbide-based butyrylcholinesterase inhibitor. *Chem.–Biol. Interact.* **2008**, 18606399. [Epub ahead of print] PMID.

(28) Harel, M.; Kleywegt, G. J.; Ravelli, R. B.; Silman, I.; Sussman, J. L. Crystal structure of an acetylcholinesterase–fasciculin complex: interaction of a three-fingered toxin from snake venom with its target. *Structure* **1995**, *3*, 1355–1366.

(29) Harel, M.; Quinn, D. M.; Nair, H. K.; Silman, I.; Sussman, J. L. The X-ray Structure of a Transition State Analog Complex Reveals the Molecular Origins of the Catalytic Power and Substrate Specificity of Acetylcholinesterase. *J. Am. Chem. Soc.* **1996**, *118*, 2340–2346.

(30) Harel, M.; Schalk, I.; Ehret-Sabatier, L.; Bouet, F.; Goeldner, M.; Hir C.; Axelsen, P. H.; Silman, I.; Sussman, J. L. Quaternary ligand bindi to aromatic residues in the active-site gorge of acetylcholinesteras *Proc. Natl. Acad. Sci. U.S.A.* **1993**, *90*, 9031–9035.

(31) Sussman, J. L.; Harel, M.; Frolow, F.; Oefner, C.; Goldman, A.; Toke L.; Silman, I. Atomic structure of acetylcholinesterase from *Torpea californica*: a prototypic acetylcholine-binding protein. *Science* **199** *253*, 872–879.

(32) Nicolet, Y.; Lockridge, O.; Masson, P.; Fontecilla-Camps, J. C. Nachon, F. Crystal structure of human butyrylcholinesterase and o its complexes with substrate and products. *J. Biol. Chem.* **2003**, *278* 41141–41147.

(33) Gao, D.; Zhan, C. G. Modeling effects of oxyanion hole on the ester hydrolysis catalyzed by human cholinesterases. *J. Phys. Chem. B* **2005**, *109*, 23070–23076.

(34) Luo, W.; Yu, Q. S.; Kulkarni, S. S.; Parrish, D. A.; Holloway, H. W.; Tweedie, D.; Shafferman, A.; Lahiri, D. K.; Brossi, A.; Greig, N. H. Inhibition of human acetyl- and butyrylcholinesterase by novel carbamates of (−)- and (+)-tetrahydrofurobenzofuran and methanobenzodioxepine. *J. Med. Chem.* **2006**, *49*, 2174–2185.

(35) Bar-On, P. M. C.; Harel, M.; Dvir, H.; Enz, A.; Sussman, J. L.; Silman, I. Kinetic and structural studies on the interaction of cholinesterases with the anti-Alzheimer drug rivastigmine. *Biochemistry* **2002**, *41*, 3555–3564.

(36) Morris, G. M.; Goodsell, D. S.; Halliday, R. S.; Huey, R.; Hart, W. E.; Belew, R. K.; Olson, A. J. Automated docking using a Lamarckian genetic algorithm and an empirical binding free energy function. *J. Comput. Chem.* **1998**, *19*, 1639–1662.

(37) Halgren, T. A. Merck molecular force field 0.1. Basis, form, scope, parameterization, and performance of MMFF94. *J. Comput. Chem.* **1996**, *17*, 490–519.

(38) Halgren, T. A. MMFF VII. Characterization of MMFF94, MMFF94s, and other widely available force fields for conformational energies and for intermolecular-interaction energies and geometries. *J. Comput. Chem.* **1999**, *20*, 730–748.

(39) Jakalian, A.; Bush, B. L.; Jack, D. B.; Bayly, C. I. Fast, efficient generation of high-quality atomic charges. AM1-BCC model: I. Method. *J. Comput. Chem.* **2000**, *21*, 132–146.

(40) Dolinsky, T. J.; Nielsen, J. E.; McCammon, J. A.; Baker, N. A. PDB2PQR: an automated pipeline for the setup of Poisson–Boltzmann electrostatics calculations. *Nucleic Acids Res.* **2004**, *32*, W665–W667.

(41) Li, H.; Roberston, A.; Jensen, J. H. Very fast empirical prediction and interpretation of protein pK_a values. *Proteins* **2005**, *61*, 704–721.

JM800564Y